

UNIVERSITÉ BLAISE PASCAL
(U.F.R. de Recherche Scientifique et Technique)

ÉCOLE DOCTORALE DES SCIENCES FONDAMENTALES
N°448

THÈSE

Pour l'obtention du grade de
Docteur de l'Université Blaise Pascal

Présentée et soutenue publiquement le 2 Juin 2005 par

Fabrice P. LAUSSY

Diplômé d'Études Approfondies en Physique Corpusculaire

QUANTUM DYNAMICS
OF MICROCAVITY POLARITONS

(Dynamique Quantique des Polaritons de Microcavité)

Jury:

Dr. Jacqueline BLOCH

Pr. Alexey KAVOKIN

Pr. Stephan KOCH

Dr. Guillaume MALPUECH

Pr. Paolo SCWHENDIMANN

Pr. Carlos TEJEDOR

Dr. David WHITTAKER

Examineur.

Directeur de Thèse.

Examineur.

Invité.

Président.

Rapporteur.

Rapporteur.

Моему учителю Алексею Кавокину
в знак большого уважения и признательности.

Preface

This text exposes some of the work which I have performed as a Ph. D. aspirant in theoretical physics during the years 2002–2005 in the group of Pr. Alexey Kavokin at the *Laboratoire des Sciences des Matériaux Électronique et d'Automatique* (LASMEA) of Université Blaise Pascal in Clermont–Ferrand, France. It has four chapters, the first provides some introductory material and reviews the state of the art, the three others report original research published in peer reviewed international journals (my list of publication is given on page 125). In more details: the first chapter contains a condensed exposition of the basics of light-matter interaction in microcavities—the physics the present work belongs with—and an account of the considerable amount of work performed and results obtained since the field was started in 1992. In the textbook written on this topic by my Ph. D. advisors, Kavokin & Malpuech (2003), the introduction starts stating that “*The decade from 1992 to 2002 in semiconductor optics can be called the ‘decade of microcavities’*”. It indeed has been a period full of daring proposals, enthusiastic and intense activities, some of which have been hotly debated and remain controversial to this day. The prospects for technology as well as for fundamental physics cannot be underestimated, from the realization of very low threshold light source to quantum light emitters. In the first chapter in which these various aspects are presented, I have tried to convey some of the atmosphere which has accompanied, put to the front or conversely quickly smothered many of the great results obtained with microcavity polaritons. The field is so active, though, that this is the work for a professional historian of science to cover it properly. Selecting what seemed to me the most important publications, I tried nevertheless to attempt an historical essay of the polariton physics, which however is outrageously limited as the expert will immediately observe. The experimental and theoretical parts have been separated in that attempt.

The second chapter is the most important in volume and results. It was my first field of investigation and the one to which I devoted most of the time, starting in July 2002 and culminating with a letter submitted to the Physical Review on September, 17 in 2003 and published on June, 29 in 2004, along with a couple of other more detailed publications. It extends previous efforts by many groups, including ours, to describe relaxation of polaritons to include quantum features of interest, mainly those pertaining to the ground state.

Taking advantage of the spin degree of freedom, a new realm of manipulation and control of light through matter and vice-versa, coined “spinoptronics” (in reference to the popular “spintronics” which does not involve light), has been proposed and extensively studied by our group. A very small account is given in third chapter where polarisation of emitted light stemming from the spin-configuration of polaritons is used to characterise coherent properties of the ground state, and assert to which extent they resemble a Bose condensate.

Fourth and last chapter departs slightly from polariton physics to focus on strong light-matter coupling in quantum dots embedded in microcavities. The experimental realization is recent and this is one topic which we are still investigating, of which I report only work

which has been submitted for publication. A short introduction gives the broad outlines without formalism nor mathematics, and present the scientific content of these four chapters.

The theoretical notions and formalism we shall need are well covered in the literature and presented or referenced as we go along. I have followed most standards usages, may be departing slightly by using consistently the elegant notation ∂_x either for the partial derivative $\partial/\partial x$ and the full derivative d/dx (for all variables), which in the confine of this text will never need be accurately distinguished. Operators are not, in principle, demarked by the use of a carret, $\hat{\Omega}$, except in a few places where this distinction has been thought necessary. Since we shall often refer to polaritons with zero wavevector, for ease of notations it is understood that $\mathbf{k}_0 \equiv \mathbf{0}$. In addition of the bibliography, most important references and especially those directly connected to this text appear at the bottom of each page whenever they are mentioned.

Working in the group of Alexey Kavokin was a one-time experience in my life which has shaped my views and ways of thinking much beyond the scientific scope. Alexey has continuously inspired me with his unusual ways and thoughts which have been a constant delight and sources of personal enlightenment. He has also implicated me fully in his team, in which I have for instance served as the scientific secretary for three international conferences. He had me attend the CL and CLI Fermi schools, present our work in such highly regarded meetings as the NOEKS, EQUONT, PLMCN, CoPhen and ICSCCE conferences and give two research seminars, first one in Ioffe (Russia), and then in CIE (Mexico) where I had the pleasure to meet again our long time collaborator Dr. Yuri Rubo whose inputs were so central in the developments of our models. In all, I had the opportunity to find myself in presence of, and often talk to, an important fraction of the living scientists mentioned in this text, some of them of the highest standard in the history of science.

My work has been carried out mainly with Dr. Guillaume Malpuech, who taught me efficiency, pragmatism and rapidity of action, and seconded Alexey's teaching on the all-important intuition in physics and how this can save time and troubles when formal approach and blind confidence in theoretical constructs start getting weird. On many occasions Guillaume was able to show me wrong with simple counter-examples; much results of this text owe to his guesses which we have subsequently refined. I also have enjoyed my collaboration with Dr. Ivan Shelykh, who made his Post-Doctoral researches in LASMEA on spin dynamics of polaritons and has brought and unequalled amount of results. I had a small scientific activity with him, but this already provided enough results as to constitute one chapter of this work, which fits as a small part of his activity and for which he properly ranks as the main contributor. I had little opportunities to express to him my admiration for the deepness, freedom and originality of his character, culture and intellect. I hope I will be excused doing so now, taking advantage of the special atmosphere which embraces one when crossing the boundary between two important eras of one's life. I also want to acknowledge help from Mikhail Glazov, to which I am indebted among many other things for the corrections and remarks he made to this text in a very limited time. More importantly, thanks to him, I was able while I was writing this thesis to keep thinking on physical problems and not to cut myself apart to solve merely technical and editing ones. Mikhail motivated microscopic foundations for σ_N of fourth chapter, which are currently under investigation. I am sorry that time and memory will not serve me to do full justice to the many people I have met during this time. Still I would like to thank especially Yuri Rubo, Pierre Bigenwald, Monsieur Vasson, Riana Andrieux, Fabien Courtine and Arnaud Robert for the valuable inputs, albeit in very different respects, they brought in these years that I will remember as the best in my student life.

As a final tribute to Alexey and the many extraneous topics he introduced or entertained me with, I like to remember one of the numerous chess puzzles he concocted. Not surprisingly, most were like nothing one is used to, with some beautiful patterns in the disposition of the material, but one of the most interesting is rather innocent looking at first sight. It dates back to April 2002 when I was still a visiting student in his group: it is a mate-in-four combination in what Alexey termed the battle of Waterloo, where Napoleon as Black gets mated starting from the following progression of the battle:

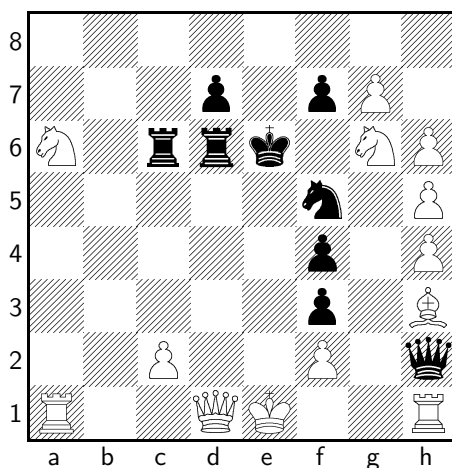


Figure 1: Waterloo battle: White (Anglo-allied and Prussian) to play and mate Black (French) in four moves.

The solution would readily be found as 1 ♔×d6+!! ♕×d6 2 O-O-O+ ♕e6 3 ♖he1+ ♔f6 4 g8♘#. The interesting feature of this problem, beside the sack of the Queen and the mate by under-promotion, is that on closer inspection one realises the castling is not legal since the rook on a1 must have moved previously in this game, and thus the problem has no solution in four moves (making it more interesting: as a problem “White to play and move” the solution is a mate in six). This is, at this time of contemplating my collaboration with this unusual, and in my limited view, I would say exceptional man of science, a good allegory of our intellectual relationship. I have often turned down many ideas without good alternatives, and of course physics is a field of an altogether different complexity than chess, so that in the confine of a few years this has given less frequent clear cuts agreement as those involving pieces on a board to merely end up in dead-ends. But out of my many rebuttals of results he laid down for me to unravel and complete, I actually learned a great deal and I still entertain many problems he has presented me with as promising future directions. The most important one relates to the lifetime of condensed polaritons. I hope that ending my days as a beginning scientist under his guidance, I will always remember his optimistic and creative views about physics, life and everything else, and that I am entering science with some fractions of these—his—qualities. In appreciation of all he has brought to me, I humbly but heartfully dedicate this work to him. As for the proof of the claims regarding the chess problem, I leave them to the reader’s own enjoyment.

Fabrice P. Laussy,
Aubière, April 10, 2005

Preface to revised version

This version essentially corrects various misprints and some inconsistencies in the notations. It also contains, along with a few changes taking into account remarks issues about the manuscript, some results on the statistics of excitons in large quantum dots obtained between the handing over of the manuscript to the jury and the defence where they have been presented. The multiplet structure is in press in Solid State Communications and some outlines of the microscopic derivation along with the structure of Dicke realisation are in press in Physica Status Solidi.

I also want to cite here the work by Stenius (1999) which was unfortunately brought to my attention after completion of this work. This unnoticed paper (unquoted as of June 2005 in the American Physical Society database) extends previous work by İmamoğlu to open systems and therefore bears much relevance to the present approach. In this connection, one will also find the paper by Stenius & Ivanov (1998) of interest. I refer interested readers to these important papers, which are not discussed in this text.

Being honoured with the congratulations of a jury which gathered leading expert of the field, I feel obliged now that I am starting my Post-Doctoral research—with Dr. David Whittaker in the group of Pr. Maurice Skolnick in the University of Sheffield—to make mine the motto of a wise doctor, «*nul n'est digne de posséder un diplôme s'il n'est pas capable de le gagner tous les jours*».

Dr. Fabrice P. Laussy,
Sheffield, June 30, 2005

Contents

1	Exciton–Polaritons in Microcavities (Review)	7
1.1	Photons and Excitons	8
1.1.1	Classical Radiation Field	8
1.1.2	Quantized Radiation Field	13
1.1.3	Quantized Matter field	20
1.2	Main Theoretical Results on Exciton–Polaritons	28
1.2.1	Photon–Exciton Coupling; Polaritons	28
1.2.2	Dynamics of Polaritons	33
1.3	Main Experimental Results on Exciton–Polaritons	38
1.3.1	Polaritons	38
1.3.2	Dynamics of Polaritons	40
1.3.3	Bosonic Behaviours	41
1.4	Conclusions and Perspectives	46
2	Coherence in Polariton Systems	47
2.1	Quantum Kinetics of Polariton Relaxation in Microcavities	48
2.1.1	Semi-classical picture	48
2.1.2	Quantum dynamics of ground state polaritons	49
2.2	Spontaneous Coherence Buildup	65
2.2.1	Bose condensation of conserved particles	65
2.2.2	Two oscillators toy theory	66
2.2.3	Polariton laser	76
2.3	Conclusions and Perspectives	82
3	Order Parameter of Polariton Condensates	83
3.1	Polariton spin	83
3.1.1	Spin and polarisation	83
3.1.2	Self-interaction and beats of polarisation	84
3.1.3	Interaction between condensate and upper polariton states	86
3.2	Polarisation as an order parameter for polaritons BEC	89
3.2.1	The problem of the phase	89
3.2.2	Stimulated random walk	89
3.2.3	Formalism	90
3.2.4	Spontaneous buildup of the polarisation	92
3.3	Determination of the degree of coherence through polarisation	95
3.3.1	Correlations	95

3.3.2	Formalism	96
3.3.3	Polarisation dynamics and measure of the coherence degree	98
3.4	Conclusions and Perspectives	100
4	Exciton–Polaritons in Microcavities with Quantum Dots	103
4.1	The dawn of Cavity QED in semiconductors	103
4.2	Microscopic Foundations	104
4.3	Large Quantum Dots	107
4.4	Bare and Dressed states basis	109
4.5	Spectra of Optical Emission	112
4.6	Conclusions and Perspectives	113
A	Details of Some Auxiliary Calculations	117
A.1	Microscopic Derivation of the Master Equation	117
A.2	Brute Force Verification of the Fokker-Planck Equation	121
A.3	Derivation of the Analytical Expression for the Pseudospin	122

Introduction

A *polariton* is a particle which arises in the solid state when a photon (particle of light) interacts with an elementary excitation of the solid. As quantum mechanics shows, such an excitation is also describable as a particle, and in fact this is why it is qualified as “elementary”. Which kind of excitations exist in the solid depends on which type of system is at stand. All solids propagate sound which, at the quantum level, is described in terms of phonons. A popular type of polariton is therefore the phonon-polariton, also the first kind to have been introduced, by Fano (1956).

In this work, the solid state is an engineered semiconductor heterostructure, i.e., a human-made (by crystal growth) structure assembling various types of semiconductors. The design of this assembly imposes constraints on the excitations which, however, remain essentially that of the semiconductor. In the optical region, an important elementary excitation of a semiconductor is the exciton, an atomlike Coulomb correlated bound state of an electron with a hole. See for instance Haug & Koch’s (1990) textbook which covers a vast gamut of the physics of light-matter interaction in semiconductors.

The *exciton-polariton*—which from now on we will call simply *polariton* since we will consider no other types—arises as the coupling of a photon with an exciton. The concept has been introduced in bulk semiconductors by Hopfield (1958) with “*a general mathematical approach[...] the same as that of Fano (1956)*”[1]. It was independently proposed by Agranovich (1959) (see also Agranovich & Ginsburg (1966)).

But this is in reduced dimensionality, such as is allowed by heterostructures, that polaritons prove to be a most fruitful concept. The formidable impact and powerful abilities of heterostructures in both physics and technology can hardly be exaggerated, see for instance Alferov’s (2000) Nobel lecture for an account. In this work we pay attention mostly to *microcavities*. These are heterostructures made up from superimposed layers of semiconductors. A Bragg mirror is obtained from multiple-quarter-wave layers alternating their refractive index. Facing two such mirrors effectively amounts to a microscopic Fabry-Pérot cavity in which a photon can be trapped (vividly pictured as bouncing back and forth between the two mirrors). One or many Quantum Well (QW) can be embedded in between the mirrors, forming the so-called *active* part of the cavity. This small part is the bed for excitons, to which photons can couple to form the polaritons. A Surface Electron Micrography (SEM) picture of a microcavity is shown on fig. 2, where one can observe the two mirrors (here composed of alternating AlAs and AlGaAs layers) sandwiching the cavity spacer in which the photon is trapped.

With the observations of vacuum Rabi splitting and anticrossing of the photon and exciton dips in reflection spectra (see fig. 3), Weisbuch, Nishioka, Ishikawa & Arakawa (1992) [2]

[1] J. J. Hopfield, Phys. Rev. **112**, 1555 (1958).

[2] C. Weisbuch, M. Nishioka, A. Ishikawa, and Y. Arakawa, Phys. Rev. Lett. **69**, 3314 (1992).

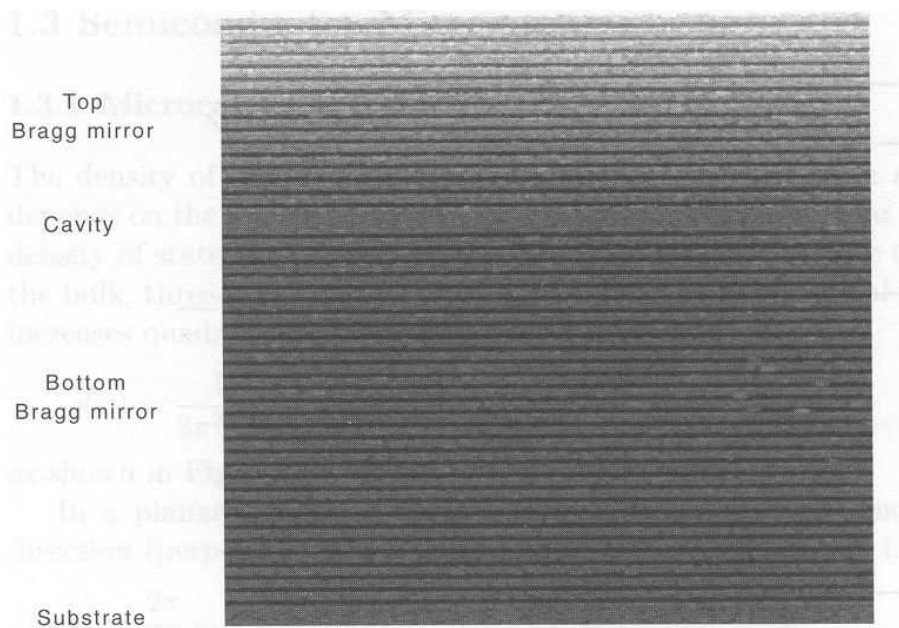


Figure 2: A Scanning Electron Microscopy (SEM) picture [from Yamamoto et al. (2000)] of a typical microcavity, with growth axis in the vertical direction. Two Bragg mirrors made up of alternating semiconductors (AlAs and $\text{Al}_{0.15}\text{Ga}_{0.85}\text{As}$) layers surround the cavity spacer, in which a QW can be embedded to provide an active (nonlinear) medium to the cavity. See also fig. 1.7 (b) on page 42 for an artist's view or fig. 1.2 on page 21 for a schematic view detailing an heterostructure including QWs.

launched the new field of semiconductor physics today known as that of *microcavity-polaritons*. Ironically their interpretation borrowed more to cavity Quantum Electrodynamics than to the polaritonic picture. The physics of cavity polaritons is now endowed with a whole literature of its own. In addition to most of the bibliography, we refer among many other references to the textbook recently published by Kavokin & Malpuech (2003) or the one by Yamamoto et al. (2000); a detailed review has been given by Khitrova, Gibbs, Jahnke, Kira & Koch (1999) and a shorter treatment was provided by Skolnick, Fisher & Whittaker (1998).

A noteworthy feature of polaritons is that they are massive bosons, which entitles them in principle to undergo Bose-Einstein condensation (BEC) [3] at low enough temperatures. BEC has been actively sought experimentally since its daring prediction by Einstein (1925). It was observed experimentally for ultra-cold atomic gases only recently (Anderson, Ensher, Matthews, Wieman & Cornell 1995, Davis, Mewes, Andrews, van Druten, Durfee, Kurn & Ketterle 1995), for which discovery Cornell & Wieman (2001) and Ketterle (2001) have been awarded the Nobel prize. Its experimental evidence has boosted the interest for this physical phenomenon which now stands among the deepest and most fundamentals. In condensed matter, BEC has been actively pursued both for its fundamental and practical importance. From a fundamental point of view, BEC is a subtle transition (except for the ideal gas) which raises many theoretical challenges. From a practical point of view, BEC is a generator of coherent particles stored in a state usually easy to access. A promising candidate to display Bose condensation has been the exciton, but without success (see Griffin, Snoke & Stringari (1996) for a review).

[3] A. Einstein, Sitzungber. Preuss. Akad. Wiss. **1925**, 3 (1925).

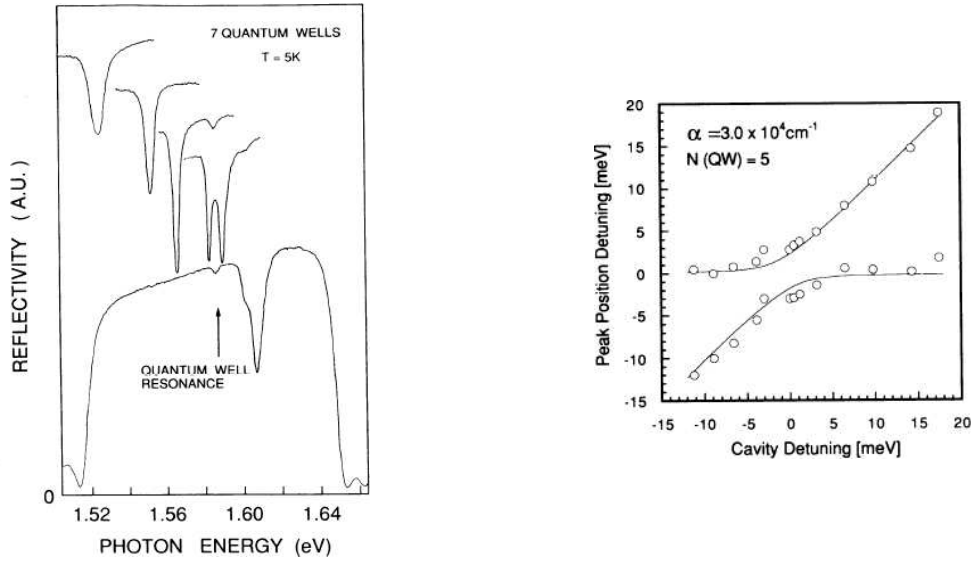


Figure 3: The seminal observation by Weisbuch et al. (1992) of strong coupling in a microcavity, which launched the new field of semiconductor physics known as *microcavity polaritons* physics. Left figure displays reflectivity spectra at 5K of a 7QW GaAs based cavity: the difference in energy between the bare cavity and exciton modes (so-called *detuning*) is varied from top to bottom; at resonance (zero detuning), a splitting is observed about the QW resonance (fourth curve). Past the resonance (negative detuning), the strong coupling is lost again (fifth curve, displayed complete). Right figure gives the splitting between dips as a function of this detuning on a similar structure: the anticrossing at zero detuning is manifest. A more detailed discussion of these figures and the associated experiment is given in section 1.3.1.

On the other hand, microcavities endow polaritons with many features prone to make them the heroes of BEC, such as a mass so small that their critical temperature for condensation is as high as room temperature (to be compared with the nK required in the case of atoms). Along with the prospect of BEC, Īmamođlu proposed a thresholdless laser without population inversion. All this motivated a feverous quest for BEC of polaritons. But despite promising hints of bosonic behaviours from nonlinear emission rates and energy shift in PL spectra reported by Le Si Dang, Heger, Andr e, Boeuf & Romestain (1998) and Senellart & Bloch (1999), the enterprise was met with many difficulties and confusion. The finite lifetime and two-dimensional character of polaritons suggested to drop BEC in favor of a quasi-condensate, a laser, a superfluid or other trends of macroscopic Bose coherence never quite exactly the Bose condensation. Moreover spurious coherence (as that introduced by the pump, or that attributed to other constituents than the polaritons) manifests itself easily in such an optical structure—conversely to cold-atoms where the slightest shadow of coherence is a signature. This added tremendous difficulties and suspicions in all observations. This may be best illustrated by the report of polariton lasing by Pau, Cao, Jacobson, Bj ork, Yamamoto & Īmamođlu (1996), a claim later retracted by the authors (Cao, Pau, Jacobson, Bj ork, Yamamoto & Īmamođlu 1997) in favor of a more conventional photon laser of the VCSEL type. The idea of a *polariton laser* however remained, and a breakthrough was made in this direction with the unambiguous observation by Savvidis, Baumberg, Stevenson, Skolnick, Whittaker & Roberts (2000) of stimulated scattering of polaritons in a pump probe experiment. A gain of up to 70 of a weak probe was observed through a polariton-polariton scattering, cf. fig. 4, which renewed the confidence in microcavity systems towards physics paramount to BEC, if not exactly it. Another major step was taken by Deng, Weihs, Santori, Bloch & Yamamoto’s (2002) observation of second or-

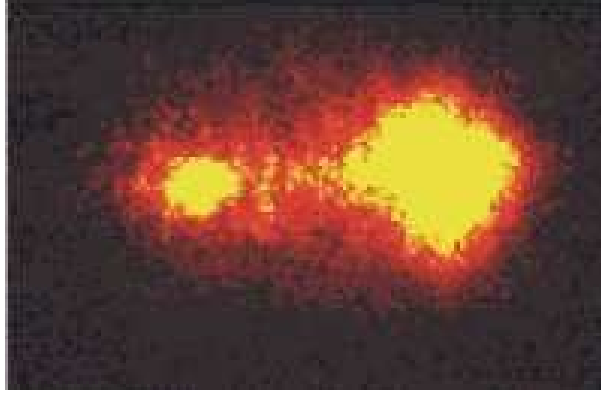


Figure 4: Real space image of PL of a microcavity pumped resonantly at the angle (so-called *magic angle*) where two pump polaritons can elastically scatter one to the ground state, the other to a higher lying energy-momentum state, while satisfying the energy-momentum conservation. A weak probe was previously injected into the ground state which results in giant amplification of its emission (spot on the left). The spot on the right is the reflection from the pump and is thus much more intense as it originates from an externally coherent field. This experiment demonstrates the transfer of a macroscopic number of pump polaritons into the ground state, thanks to boson stimulation.

der coherence from light emitted by a microcavity ground state, which the authors reported to approach the value expected of a condensate [4].

The central problem addressed by this thesis is whether coherence of microcavity polaritons akin to that of a Bose–Einstein condensate is possible. We review the state of the art of the research in this direction in sections 1.2 (theoretically) and 1.3 (experimentally), covering many side issues from weak/strong coupling to nonlinear effects. We also consider at depth the strong coupling without dispersion, typical of cavity QED, which bears strong relationships with polaritons, though we report this discussion to fourth chapter. This journey will show us a lot of the polariton physics but to the extents of our needs it will also leave aside many interesting phenomena, such as the so-called motional narrowing, effects of disorder, most of the polaritons spin-dynamics, parametric amplification and so on. . .

Prior to that historical review of the field, section 1.1 presents a brief reminder of the theoretical notions and formalisms we shall need. Speaking repeatedly of polaritons in terms of particles, we make a prejudice to classical physics which also fathoms the polariton concept in term of a resonance in the dielectric response function of Maxwell equations. One should be careful to keep the classical picture in mind, mainly because it is needed for the canonical quantization of fields but also not to attribute lightheartedly some effects to quantum physics when it is accounted for equally well with classical physics, as has been done for instance with the polariton doublet once explained in terms of quantum anticrossing (in fact deviations between quantum and classical physics are expected in the nonlinear regime only, where quantum physics provides the appropriate description). The classical picture will not be used in the remaining of the text so to the extent that the quantum picture does not harm when it does not add, we will not bother presenting the classical description as well. We also put forward the idea of the polariton laser, the device reminiscent of İmamođlu’s proposal which lurks behind the successful formation of a condensate of polaritons and which was one of the main motivations for this work. The historical character of sections 1.2 and 1.3 is kept throughout this

[4] H. Deng, G. Weihs, C. Santori, J. Bloch, and Y. Yamamoto, *Science* **298**, 199 (2002).

introductory chapter, which hopefully makes the well known aspects more entertaining to read. After this introductory and review chapter, we turn to the original developments of this text.

A condensate is usually studied in its equilibrium phase, and such has been done for polaritons, thereby neglecting one of their most important features: their very short lifetime (of the order of ps). To study a realistic condensate one need therefore either to study its transients, that is, the dynamics of its formation, or to study a steady-state regime where a pumping process replenishes the condensate to compensate for the continuously lost particles. In chapter II we address the problem from the kinetic point of view. In section 2.1 we extend Boltzmann equations to allow them to describe quantum features of particles in the ground state, like their coherence degree. In section 2.2 we show that particles number correlations are needed to be taken into account to properly describe coherence buildup in the system, leading us to a *Quantum Boltzmann Master Equation*. In chapter III we address the problem from the steady-state point of view, taking advantage of the spin degree of freedom of polaritons. We show that the polarisation of the emitted light is an order parameter for BEC in such a system, and that pumping the structure with light of a given circular polarisation, one can accurately deduce from the decay of the polarisation the coherence degree of the condensate.

Cavity Quantum Electrodynamics—which has been hiding behind cavity polaritons since the field was inaugurated by Weisbuch et al. (1992)—is now duly in the realm of solid state physics. The more accurately analogous situation of strong coupling between a mode of the radiation field and an atomiclike system has indeed been recently obtained by Reithmaier, Sek, Löffler, Hofmann, Kuhn, Reitzenstein, Keldysh, Kulakovskii, Reinecker & Forchel (2004) [5] in quantum well width fluctuations, and simultaneously by Yoshie, Scherer, Heindrickson, Khitrova, Gibbs, Rupper, Ell, Shchekin & Deppe (2004) in photonic crystals (see also Peter, Senellart, Martrou, Lemaître, Hours, Gérard & Bloch (2005)). In both case the atomiclike system is a Quantum Dot (QD). This is not to say that cavity QED in solid states brings no specificity of its own. We devote fourth and last chapter to the motivation of the opposite, predicting multiplets in emission spectra.

[5] J. P. Reithmaier *et al.*, Nature **432**, 197 (2004).

Chapter 1

Exciton–Polaritons in Microcavities (Review)

Contents

1.1	Photons and Excitons	8
1.1.1	Classical Radiation Field	8
	Maxwell Equations	8
	Transverse Fields in Reciprocal Space	10
1.1.2	Quantized Radiation Field	13
	Canonical Quantization	13
	Quantum Harmonic Oscillator and States of the field	14
	Coherence of the fields	17
	Microcavities	20
1.1.3	Quantized Matter field	20
	Second quantization of Schrödinger equation	20
	Bosonic stimulation	24
	Phonons, Electrons, Holes and Excitons	25
1.2	Main Theoretical Results on Exciton–Polaritons	28
1.2.1	Photon–Exciton Coupling; Polaritons	28
	Mixed state of light and matter	28
	Dispersion of polaritons	29
	İmamoğlu’s boson	30
	Kira <i>et al.</i> ’s refutations	32
1.2.2	Dynamics of Polaritons	33
	Simple rate equations	33
	Boltzmann equations: Tassone, Malpuech and Porras	35
	Polariton lasers	37
1.3	Main Experimental Results on Exciton–Polaritons	38

1.3.1	Polaritons	38
	Vacuum-field Rabi splitting	38
	Dispersion	39
1.3.2	Dynamics of Polaritons	40
	Bottleneck effect	40
1.3.3	Bosonic Behaviours	41
	Laserlike stimulation	41
	Savidis experiment	41
	Earlier work: Yamamoto, Bloch, Le Si Dang and Kira	42
	Later work: Le Si Dang, Skolnick, Bloch and Yamamoto	44
1.4	Conclusions and Perspectives	46

1.1 Photons and Excitons

1.1.1 Classical Radiation Field

Maxwell Equations

Light was understood as a field on a firm theoretical basis as early as the XIXth century, culminating with Maxwell's (1865) equations

$$\nabla \cdot \mathbf{E}(\mathbf{r}, t) = \frac{1}{\epsilon_0} \rho(\mathbf{r}, t), \quad (1.1a)$$

$$\nabla \cdot \mathbf{B}(\mathbf{r}, t) = 0, \quad (1.1b)$$

$$\nabla \times \mathbf{E}(\mathbf{r}, t) = -\partial_t \mathbf{B}(\mathbf{r}, t), \quad (1.1c)$$

$$\nabla \times \mathbf{B}(\mathbf{r}, t) = \frac{1}{c^2} \partial_t \mathbf{E}(\mathbf{r}, t) + \frac{1}{\epsilon_0 c^2} \mathbf{J}(\mathbf{r}, t). \quad (1.1d)$$

In terms of the *electric field* \mathbf{E} and the *magnetic field* \mathbf{B} (with usual notations), they account for all classical electromagnetic phenomena, covering special relativity as well, which they helped to unveil. This is a precece achievement since our deepest understanding of physical reality as a whole is currently in terms of fields, and was already captured by the theory of electromagnetism. It, moreover, still provides foundations for most quantization schemes.

The connection between fields and matter has been realized much later, arguably satisfactorily for the first time by Schrödinger (1926), and drawing inspirations from familiar light behaviours after the inspiring work of De Broglie. Matter is much more problematic in the classical picture and has no such all-encompassing theory in the classical limit as that provided by eqs. (1.1) for light. One has to resort to simplified model which give good account, even quantitatively, of observed phenomena, but often have feeble connection with reality. One compelling feature of matter is its discreteness, reflecting the quantization of the electric charge as realized by Millikan (1924). The most basic modelling is thus in terms of an assembly of point

particles. This discussion of matter arises because light interacts with matter, and Maxwell equations must reflect this if they really are to provide a full picture of the classical limit. They do so at a fundamental level through the distribution of electric charges ρ and of electric currents \mathbf{J} caused by material media. In terms of point particles of charge q_i for the i th particle which masse is q_i and coordinates in position-momentum phase space is $(\mathbf{r}_i, \partial_t \mathbf{r}_i/m)$, these are expressed as follows:

$$\rho(\mathbf{r}, t) = \sum_i q_i \delta(\mathbf{r} - \mathbf{r}_i(t)) \quad (1.2a)$$

$$\mathbf{J}(\mathbf{r}, t) = \sum_i q_i \partial_t \mathbf{r}_i(t) \delta(\mathbf{r} - \mathbf{r}_i(t)) \quad (1.2b)$$

The link with Newton mechanics is completed with Lorentz expression for the force exerted by the electromagnetic field on a point particle of mass m and charge q located at \mathbf{r} :

$$m \partial_t^2 \mathbf{r} = q(\mathbf{E}(\mathbf{r}, t) + \partial_t \mathbf{r} \times \mathbf{B}(\mathbf{r}, t)) \quad (1.3)$$

Anoter illustration of the limitations of the theories which relate to matter is that (1.3) does not cover relativistic regime, conversely to Maxwell equations.

We take concern in the interaction of light with matter in its condensed form (and ultimately for very specific condensed-matter systems). In a system such as a crystal where a fraction of the charges is bound to, say, molecules, and the other fraction is left free to wander in the solid, the charge density can profitably be split between two contributions,

$$\rho = \sum_i q_i \delta(\mathbf{r} - \mathbf{r}_i(t)) + \sum_{\mu} \sum_{j(\mu)} q_{j(\mu)} \delta(\mathbf{r} - \mathbf{r}_{j(\mu)}(t)) \quad (1.4)$$

where the first summation is over all free charges and the other over the $j(\mu)$ th charge bound to the μ th center (molecule). See for instance Jackson (1975, §4) for a detailed discussion. The benefice of this approach is that since a condensed system involves a tremendous amount of point particles (of the order $10^{23 \pm 5}$), it is illusory to pursue their description taking them all into account. Instead one grants the many point particles as a whole and introduce smooth (continuous) fields for (1.2). Such terms as the second summand in (1.4) become encapsulated in new quantities like the polarisation \mathbf{P} or the magnetization \mathbf{M} of the material. These in turn serve to define new material fields,

$$\mathbf{D} \equiv \epsilon \mathbf{E} + \mathbf{P} \quad (1.5a)$$

$$\mathbf{H} \equiv \frac{1}{\mu} \mathbf{B} - \mathbf{M} \quad (1.5b)$$

for which Maxwell equations turn into a form reminiscent of the original ones:

$$\nabla \cdot \mathbf{D}(\mathbf{r}, t) = \rho_f(\mathbf{r}, t) \quad (1.6a)$$

$$\nabla \cdot \mathbf{B}(\mathbf{r}, t) = 0 \quad (1.6b)$$

$$\nabla \times \mathbf{E}(\mathbf{r}, t) = -\partial_t \mathbf{B}(\mathbf{r}, t) \quad (1.6c)$$

$$\nabla \times \mathbf{H}(\mathbf{r}, t) = \frac{1}{c^2} \partial_t \mathbf{D}(\mathbf{r}, t) + \mathbf{J}_f(\mathbf{r}, t) \quad (1.6d)$$

with introduction of straightforward counterparts to the fundamental case, namely the distribution of *free* charges ρ_f and currents \mathbf{J}_f . Now the description of matter can be made through new concepts as the polarisation \mathbf{P} , which we shall see to be the most significant term in our case, where no free charges or currents exist.

The most powerful extension which builds upon the classical point-particle model, as well as a very simple one, is that of an elastically bound state between a heavy nucleus (atom or molecule) and a light electron, tied to the former like a spring. This is the celebrated *Lorentz oscillator*. Note that such oscillators are included in the new set of equations (1.6)—called *macroscopic* Maxwell equations—as a special form for the polarisation \mathbf{P} .

Transverse Fields in Reciprocal Space

Once a suitable model to describe matter has been found, one has to solve the equations. Formulating them in the *reciprocal space* where fields are expressed as a function of wavevector instead of position, helps laying down a simpler mathematical structure (Cohen-Tannoudji, Dupont-Roc & Grynberg 2001). The link between the field as we introduced it $\mathbf{E}(\mathbf{r}, t)$ and its weight $\mathcal{E}(\mathbf{k}, t)$ in the plane wave basis $e^{i\mathbf{k}\cdot\mathbf{r}}$ is assured by Fourier transforms (we consider here the 3D case):

$$\mathbf{E}(\mathbf{r}, t) = \frac{1}{(2\pi)^{3/2}} \int \mathcal{E}(\mathbf{k}, t) e^{i\mathbf{k}\cdot\mathbf{r}} d\mathbf{k}, \quad (1.7a)$$

$$\mathcal{E}(\mathbf{k}, t) = \frac{1}{(2\pi)^{3/2}} \int \mathbf{E}(\mathbf{r}, t) e^{-i\mathbf{k}\cdot\mathbf{r}} d\mathbf{r}. \quad (1.7b)$$

The properties of differential operators through the Fourier transform translate Maxwell equations (1.1) into the set of *local equations*:

$$i\mathbf{k} \cdot \mathcal{E}(\mathbf{k}, t) = \frac{1}{\epsilon_0} \rho(\mathbf{k}, t), \quad (1.8a)$$

$$i\mathbf{k} \cdot \mathcal{B}(\mathbf{k}, t) = 0, \quad (1.8b)$$

$$i\mathbf{k} \times \mathcal{E}(\mathbf{k}, t) = -\partial_t \mathcal{B}(\mathbf{k}, t) \quad (1.8c)$$

$$i\mathbf{k} \times \mathcal{B}(\mathbf{k}, t) = \frac{1}{c^2} \partial_t \mathcal{E}(\mathbf{k}, t) + \frac{1}{\epsilon_0 c^2} \mathcal{J}(\mathbf{k}, t). \quad (1.8d)$$

(with obvious notations: the cursive letter and its straight counterpart are Fourier transform pairs related the one to the other like (1.7)).

The locality is a first appealing feature, as opposed to real space equations (1.1) where the value of a field at a point depends on other fields values in an entire neighbourhood of this point. The picture clarifies further still by separation between the transverse \perp and longitudinal \parallel components of the field,

$$\mathcal{E}(\mathbf{k}, t) = \mathcal{E}_\perp(\mathbf{k}, t) + \mathcal{E}_\parallel(\mathbf{k}, t), \quad (1.9)$$

(with likewise definitions for other fields), the longitudinal component at point \mathbf{k} being the projection on the unit vector $\mathbf{e}_\mathbf{k} \equiv \mathbf{k}/k$,

$$\mathcal{E}_\parallel(\mathbf{k}, t) = (\mathbf{e}_\mathbf{k} \cdot \mathcal{E}(\mathbf{k}, t)) \mathbf{e}_\mathbf{k} \quad (1.10)$$

and the transverse component is the projection on the perpendicular plane. By definition:

$$\mathcal{E}_\perp(\mathbf{k}, t) \equiv \mathcal{E}(\mathbf{k}, t) - \mathcal{E}_\parallel(\mathbf{k}, t) \quad (1.11)$$

Back in real space, $\mathbf{E}_\perp(\mathbf{r}, t)$ and $\mathbf{E}_\parallel(\mathbf{r}, t)$ are obtained respectively by Fourier transform of (1.9) and (1.10) and correspond to the divergence-free and the curl-free components of the field. That such a decomposition exist is assured by Helmholtz's theorem. The benefits of this decomposition comes from the clear separation it makes between the dynamics of the field arising from the interplay between its electric and magnetic components (the transverse part) and the dynamics created by the sources (thus responsible for the static field if they are at rest). For instance, dotting (1.8a) with \mathbf{k}/k^2 one gets by (1.10) $\mathcal{E}_\parallel(\mathbf{k}, t) = -i\rho(\mathbf{k})\mathbf{k}/(\epsilon_0 k^2)$, which, by Fourier transformation of both sides, gives the electric field well known from electrostatic:

$$\mathbf{E}_\parallel(\mathbf{r}, t) = \frac{1}{4\pi\epsilon_0} \int \rho(\mathbf{r}', t) \frac{\mathbf{r} - \mathbf{r}'}{|\mathbf{r} - \mathbf{r}'|^3} d\mathbf{r}' \quad (1.12)$$

The fact that (1.12) is local in time is a mathematical artifice: only the whole field $\mathbf{E}(\mathbf{r}, t)$ has a physical significance and other instantaneous effects from the transverse field correct those of the longitudinal field. These claims are limited to the mathematical structure of the field. The magnetic field, owing to absence of magnetic monopoles, is always purely transverse (we will therefore not index it with \perp). In this way one can describe the system only with the transverse components of the fields and the distribution of sources. In absence of sources, $\rho = 0$ and $\mathcal{J} = \mathbf{0}$, the field is transverse (1.8a & 1.8b) and the transverse components obey the set of coupled linear equations (1.8c & 1.8d):

$$\begin{cases} \mathbf{k} \times \mathcal{E}_\perp(\mathbf{k}, t) = -\partial_t \mathcal{B}(\mathbf{k}, t) \\ ic^2 \mathbf{k} \times \mathcal{B}(\mathbf{k}, t) = \partial_t \mathcal{E}_\perp(\mathbf{k}, t) \end{cases} \quad (1.13)$$

The diagonalisation can be made by evaluating the cross product of \mathbf{k} with both sides of first line, yielding on l.h.s. $\mathbf{k} \times (\mathbf{k} \times \mathcal{E}_\perp) = -ik^2 \mathcal{E}_\perp$ since \mathcal{E}_\perp is transverse, and on r.h.s. $-\partial_t (\mathbf{k} \times \mathcal{B})$. Introducing $\omega \equiv ck$, (1.13) reads

$$\begin{cases} i\omega \mathcal{E}_\perp(\mathbf{k}, t) = \partial_t (c\mathbf{e}_\mathbf{k} \times \mathcal{B}(\mathbf{k}, t)) \\ i\omega c\mathbf{e}_\mathbf{k} \times \mathcal{B}(\mathbf{k}, t) = \partial_t \mathcal{E}_\perp(\mathbf{k}, t) \end{cases} \quad (1.14)$$

Summing and subtracting both lines

$$\partial_t (\mathcal{E}_\perp(\mathbf{k}, t) \pm c\mathbf{e}_\mathbf{k} \times \mathcal{B}(\mathbf{k}, t)) = \pm i\omega (\mathcal{E}_\perp(\mathbf{k}, t) \pm c\mathbf{e}_\mathbf{k} \times \mathcal{B}(\mathbf{k}, t)) \quad (1.15)$$

lets appear the new modes of the fields \mathbf{a} and \mathbf{b} :

$$\mathbf{a}(\mathbf{k}, t) \equiv -\frac{i}{2\mathcal{C}(\mathbf{k})} (\mathcal{E}_\perp(\mathbf{k}, t) - c\mathbf{e}_\mathbf{k} \times \mathcal{B}(\mathbf{k}, t)), \quad (1.16a)$$

$$\mathbf{b}(\mathbf{k}, t) \equiv -\frac{i}{2\mathcal{C}(\mathbf{k})} (\mathcal{E}_\perp(\mathbf{k}, t) + c\mathbf{e}_\mathbf{k} \times \mathcal{B}(\mathbf{k}, t)), \quad (1.16b)$$

with \mathcal{C} a real constant as yet undefined, written as such for later convenience. Since \mathbf{E} and \mathbf{B} are real, relation (1.7) implies that $\mathcal{E}(-\mathbf{k}, t)^* = \mathcal{E}(\mathbf{k}, t)$ (the same for \mathcal{B}) which allows to keep

only one variable, e.g., \mathbf{a} , and write $\mathbf{a}(-\mathbf{k}, t)^*$ instead of $\mathbf{b}(\mathbf{k}, t)$. Inverting (1.16), one obtains the expression of the physical fields (in reciprocal space) in terms of its fundamental modes:

$$\mathcal{E}_\perp(\mathbf{k}, t) = i\mathcal{C}(\mathbf{k})(\mathbf{a}(\mathbf{k}, t) - \mathbf{a}^*(-\mathbf{k}, t)) \quad (1.17a)$$

$$\mathcal{B}(\mathbf{k}, t) = \frac{i\mathcal{C}(\mathbf{k})}{c}(\mathbf{e}_\mathbf{k} \times \mathbf{a}(\mathbf{k}, t) + \mathbf{e}_\mathbf{k} \times \mathbf{a}^*(-\mathbf{k}, t)) \quad (1.17b)$$

This mathematical setting has therefore replaced the electric and magnetic fields by a set of complex variables $\mathbf{a}(\mathbf{k}, t)$ (which give the transverse components of the fields) and the phase-space variables of sources $(\mathbf{r}_i, \partial_t \mathbf{r}_i/m)$. All quantities of interest which can be expressed in terms of the fields and the dynamical variables can naturally be written with the new set of variables. For instance the total energy $H = (\epsilon_0/2) \int [\mathbf{E}^2 + \mathbf{B}^2] d\mathbf{r}$ evaluates to

$$H = \sum_i \frac{1}{2} m_i (\partial_t \mathbf{r}_i)^2 + \sum_i \frac{q_i^2}{2\epsilon_0(2\pi)^3} \int \frac{d\mathbf{k}}{k^2} + \frac{1}{8\pi\epsilon_0} \sum_{i \neq j} \frac{q_i q_j}{|\mathbf{r}_i - \mathbf{r}_j|} + H_\perp \quad (1.18)$$

with clear physical meaning for each term: the first one is the kinetic energy of the particles while the second and third terms are the Coulomb energy. The second term actually poses the well known problem of divergence of the self-energy of a particle. The fourth term H_\perp is the energy of the transverse field and the one of most interest to us. Explicitly, it reads:

$$H_\perp = \epsilon_0 \int \mathcal{C}(\mathbf{k})^2 [\mathbf{a}^*(\mathbf{k}) \cdot \mathbf{a}(\mathbf{k}) + \mathbf{a}(-\mathbf{k}) \cdot \mathbf{a}^*(-\mathbf{k})] d\mathbf{k} \quad (1.19)$$

illustrating the foretold connection with \mathbf{a} . In the same way, one can evaluate other quantities of interest like the impulsion or the angular momentum (Cohen-Tannoudji et al. 2001). Two fields of importance in this transverse field representation of the electromagnetic field are the “auxiliary” potential fields \mathbf{A} (so-called *potential vector*) and U (*scalar potential*). They relate to “physical” fields \mathbf{E} and \mathbf{B} as follows:

$$\mathbf{B}(\mathbf{r}, t) = \nabla \times \mathbf{A}(\mathbf{r}, t) \quad (1.20a)$$

$$\mathbf{E}(\mathbf{r}, t) = -\partial_t \mathbf{A}(\mathbf{r}, t) - \nabla U(\mathbf{r}, t). \quad (1.20b)$$

Their existence is respectively ensured by eqs. (1.1b) and (1.1c), which they subsequently compel. Their mathematical preponderance over their physical existence was motivated by the freedom in their definition: various different fields \mathbf{A} and U yield the same fields \mathbf{E} and \mathbf{B} . For any well-behaved scalar field $F(\mathbf{r}, t)$, the so-called *gauge transformation*

$$\mathbf{A}(\mathbf{r}, t) \rightarrow \mathbf{A}(\mathbf{r}, t) + \nabla F(\mathbf{r}, t) \quad (1.21a)$$

$$U(\mathbf{r}, t) \rightarrow U(\mathbf{r}, t) - \partial_t F(\mathbf{r}, t) \quad (1.21b)$$

leaves the physics unchanged. This is a point of considerable theoretical implications which we shall encounter again later. The gauge of predilection is the so-called *Coulomb gauge* which fixes F by demanding

$$\nabla \cdot \mathbf{A} = 0. \quad (1.22)$$

That is, the potential vector is made purely transverse, like the magnetic field (its transverse component is moreover gauge invariant). The potential vector is more convenient than the

magnetic field for various reasons, one being that it does not require the cross product with \mathbf{k} :

$$\mathbf{a}(\mathbf{k}, t) = \mathcal{C}(\mathbf{k})(\mathcal{A}(\mathbf{k}, t) - \frac{i}{\omega} \mathcal{E}_{\perp}(\mathbf{k}, t)) \quad (1.23a)$$

$$\mathcal{A}(\mathbf{k}, t) = \frac{\mathcal{C}(\mathbf{k})}{\omega} (\mathbf{a}(\mathbf{k}, t) + \mathbf{a}^*(-\mathbf{k}, t)) \quad (1.23b)$$

to be compared respectively with (1.16a) and (1.17b).

Now that Maxwell equations have been reset in terms of these transverse mode amplitudes \mathbf{a} , they need be solved. In absence of sources, the equation of motion (1.15) for \mathbf{a}

$$\partial_t \mathbf{a}(\mathbf{k}, t) = -i\omega \mathbf{a}(\mathbf{k}, t) \quad (1.24)$$

is that of an oscillator, which readily integrates to

$$\mathbf{a}(\mathbf{k}, t) = \mathbf{a}(\mathbf{k}, 0) e^{-i\omega t} \quad (1.25)$$

The solution in real space is only a Fourier transform away, e.g.,

$$\mathbf{E}_{\perp}(\mathbf{r}, t) = i \int (\mathbf{a}(\mathbf{k}) e^{i(\mathbf{k}\cdot\mathbf{r} - \omega t)} + \text{c.c.}) d\mathbf{k} \quad (1.26)$$

(where we called $\mathbf{a}(\mathbf{k})$ the zero time amplitude).

Inserting back (1.16) in Maxwell equations but now keeping the sources, the equations of motion become

$$\partial_t \mathbf{a}(\mathbf{k}, t) = -i\omega \mathbf{a}(\mathbf{k}, t) + \frac{i}{2\epsilon_0 \mathcal{C}(\mathbf{k})} \mathcal{J}_{\perp}(\mathbf{k}, t) \quad (1.27)$$

Generally $\mathcal{J}_{\perp}(\mathbf{k}, t)$ depends nonlocally on \mathbf{a} . Interactions with sources couple together the various modes of the fields which are otherwise independent. We do not go further at this stage, and proceed to quantize the electromagnetic field which we have presented in a form most adapted to that purpose.

1.1.2 Quantized Radiation Field

Canonical Quantization

A rather straightforward quantization of the classical electromagnetic field is afforded by the so-called *canonical quantization* [Dirac (1927), Fermi (1932) or, e.g., Loudon (2000) for a textbook coverage]. It was shown in the previous section how the free electromagnetic field could be reduced to a set of variables $\mathbf{a}(\mathbf{k}, t)$ which were undergoing harmonic motion (1.25). For convenience we now further decompose the transverse vector variable \mathbf{a} in an orthogonal 2D basis in the transverse \mathbf{k} plane:

$$\mathbf{a}(\mathbf{k}, t) = a_{\uparrow}(\mathbf{k}, t) \mathbf{e}_{\uparrow}(\mathbf{k}) + a_{\downarrow}(\mathbf{k}, t) \mathbf{e}_{\downarrow}(\mathbf{k}) \quad (1.28)$$

where $(\mathbf{e}_{\uparrow}(\mathbf{k}), \mathbf{e}_{\downarrow}(\mathbf{k}), \mathbf{k})$ form an orthogonal basis of unit vectors. When need will arise we will use the full vector expression, but without limitation we now focus on one projection only, say a_{\downarrow} , which for brevity we shall note a .

The free field can therefore formally be understood as a set of independent harmonic oscillators, which couple the one to the others through source terms as in (1.27). The canonical

quantization promotes independent variables a and a^* to ladder operators \hat{a} and \hat{a}^\dagger for the harmonic oscillators (Dirac 1967).

Note that strictly speaking this approach lacks a rigorous derivation; even if one is ready to accept as reasonable the replacement by quantum harmonic oscillators of the oscillating classical variables, there is no guarantee of the well-behaved conjugations relations between \hat{a} and \hat{a}^\dagger or $\hat{\mathbf{r}}$ and $\hat{\mathbf{p}}$ with respect to an hamiltonian which is also essentially postulated in the theory. This is a refinement which needs not concern us here, see, e.g. Cohen-Tannoudji et al. (2001) for a detailed discussion.

A point on notations: throughout this text we shall stick to the same notations and conventions, even when otherwise quoting verbatim from others (thus substituting our notations for theirs). As we quantize more fields, we introduce new particle operators which notations we retain throughout. Taken in isolations, many notations might then appear unusual, more conventional letters having already been assigned to more popular excitations. For instance the photon field normal mode annihilation operators in reciprocal space we shall from now on call B and save a for polaritons, b for phonons, etc... (with little risk for confusion, we also use a for the harmonic oscillator). In real space, however, we shall denote all field operators Ψ , specifying each time which one is under consideration.

Quantum Harmonic Oscillator and States of the field

We give a brief reminder of most important results of the quantum harmonic oscillator to settle notations and introduce more sophisticated notions like the Glauber representation of the density matrix.

We write the hamiltonian $H = p^2/(2m) + \kappa q^2/2$ of an harmonic oscillator of mass m and force constant κ in phase-space of position-momentum (q, p) in terms of dimensionless variables X and P :

$$H = \frac{1}{2}\omega(X^2 + P^2), \quad (1.29)$$

(with change of variables $P = (\kappa m)^{-1/4}p$, $X = (\kappa m)^{1/4}x$ and $\omega \equiv \sqrt{\kappa/m}$, which is readily checked to be a canonical transformation, i.e., $[X, P] = [x, p] = i\hbar$). This hamiltonian can be solved elegantly introducing the *ladder operators*

$$a = \frac{1}{\sqrt{2\hbar}}(X + iP), \quad a^\dagger = \frac{1}{\sqrt{2\hbar}}(X - iP) \quad (1.30)$$

which diagonalise (1.29) as:

$$H = \hbar\omega(a^\dagger a + \frac{1}{2}) \quad (1.31)$$

The fundamental property of these operators is their commutation relation:

$$[a, a^\dagger] = 1 \quad (1.32)$$

from which one can reconstruct the spectrum and eigen-wavefunctions, which we note $|n\rangle$ where n is some positive (or null) integer. We check that they obey:

$$a^\dagger |n\rangle = \sqrt{n+1} |n+1\rangle \quad (1.33a)$$

$$a |n\rangle = \sqrt{n} |n-1\rangle \quad (1.33b)$$

so that especially

$$a^\dagger a |n\rangle = n |n\rangle . \quad (1.34)$$

As for the energy spectrum,

$$E_n = n\hbar\omega + \frac{\hbar\omega}{2}, \quad n \in \mathbb{N} \quad (1.35)$$

This last set of results (1.33–1.35) constitutes the paradigm for so-called *second quantization* formalism, which embeds the essence of many-body quantum mechanics (although it is of course at this level merely elementary quantum mechanics). Naively, relation (1.35) which states that the energy spectrum is equally spaced over a minimum of $\hbar\omega/2$ is read as describing n particles (a “particle” being in this context an entity indistinguishable in some set) each of energy $\hbar\omega$ with a minimum of $\hbar\omega/2$ that represents the energy of the *vacuum*. Owing to their action on a state $|n\rangle$ of n “particles”, a^\dagger (1.33a) is called the *creation operator* (adding one particle to the system) and a (1.33b) the *annihilation operator*. Owing to its eigenvalue, $a^\dagger a$ (1.34) is called the *number operator*.

In a proper theoretical construction, along the lines previously introduced for the light field or as we shall encounter briefly in section 1.1.3, these states $|n\rangle$ —which are called *Fock state*—describe a state with a definite number of particles, e.g., photons in the case of the light field. They are of considerable mathematical importance, corresponding to the eigenstates of what corresponds to the non-interacting part of the hamiltonian, but their physical realisation is difficult when it is at all achievable, in which case it is generally restricted to a small numbers of particles, $n \approx 1$.

One other very important quantum state is the so-called *coherent state* $|\alpha\rangle$, introduced by Schrödinger as the quantum state of the harmonic oscillator which minimises the uncertainty relation:

$$\text{Var}(A) \text{Var}(B) \geq \left(\frac{i}{2} \langle [A, B] \rangle \right)^2, \quad (1.36)$$

between two observables A and B , the averages being taken on the given state $|\alpha\rangle$ of the field. Eq. (1.36) being Schwarz relation in disguise applied on vectors

$$(A - \langle A \rangle) |\alpha\rangle \quad \text{and} \quad (B - \langle B \rangle) |\alpha\rangle, \quad (1.37)$$

it is minimised when these vectors are aligned. In our case of the harmonic oscillator with uncertainty equally distributed in both position P and impulsion X

$$(P - \langle P \rangle) |\alpha\rangle = i(X - \langle X \rangle) |\alpha\rangle \quad (1.38)$$

which, written back in terms of a, a^\dagger , becomes:

$$a |\alpha\rangle = \frac{1}{\sqrt{2\hbar}} (\langle X \rangle + i\langle P \rangle) |\alpha\rangle \quad (1.39)$$

so that the coherent state is the eigenstate of the annihilation operator (if the uncertainty is not equally distributed, the state is a *squeezed coherent state*, a quantum state of major importance also in the case of polaritons).

It was expected that α could be complex (a not being hermitian) and from (1.41) it is seen that it actually spans the whole complex space. The phase associated with this complex number in the sense of a polar angle in Argand space maps to the physical notion of phase. The

physical meaning of the (unsqueezed) coherent state is that of the most classical state allowed by quantum physics, since it has lowest uncertainty in its conjugate variables, and it can be located in the complex plane as the position in the phase space of the quantum oscillator, with position on real axis and momentum on imaginary axis. The hamiltonian being time independent, the evolution of $|\alpha\rangle$ is obtained straightforwardly from the propagator:

$$\begin{aligned} |\alpha(t)\rangle &= e^{-i\omega(a^\dagger a + 1/2)(t-t_0)} |\alpha(t_0)\rangle \\ &= e^{-i\omega(t-t_0)/2} \left| e^{-i\omega(t-t_0)} \alpha(t_0) \right\rangle \end{aligned} \quad (1.40)$$

so that the free propagation of the coherent state is harmonic oscillation in Argand space. Definitely it is a state of well defined phase.

In terms of Fock states, it reads:

$$|\alpha\rangle = \exp(-|\alpha|^2/2) \sum_{n=0}^{\infty} \frac{\alpha^n}{\sqrt{n!}} |n\rangle \quad \alpha \in \mathbb{C}. \quad (1.41)$$

Coherent states are normalised though not orthogonal:

$$\langle \beta | \alpha \rangle = \exp\left(-\frac{1}{2}(|\alpha|^2 + |\beta|^2 - 2\alpha\beta^*)\right) \quad (1.42)$$

with indeed $\langle \alpha | \alpha \rangle = 1$ but $\langle \beta | \alpha \rangle \neq \delta(\alpha - \beta)$, being smaller the farther apart α, β in \mathbb{C} .

These states have been introduced in Quantum Field Theory (QFT) and especially quantum optics by Glauber (1963) in his investigation of quantum optical coherence.

Eventually, another useful quantum state of the field is the so-called thermal state, obtained from quantum statistical theory as:

$$\rho = \exp(-\beta \hbar \omega (a^\dagger a + 1/2)) / Z \quad (1.43)$$

where Z the partition function (trace of the numerator) normalises the density matrix ρ and β is the inverse temperature. It is not a pure state and has only an expression for its density matrix. In the basis of Fock states, it is diagonal with Bose-Einstein distribution, that is, with $\langle n \rangle \equiv \text{Tr}(\rho a^\dagger a)$, the thermal density matrix reads:

$$\rho = \sum_{n=0}^{\infty} \frac{\langle n \rangle^n}{(1 + \langle n \rangle)^{n+1}} |n\rangle \langle n|. \quad (1.44)$$

Glauber also pioneered a representation P for the density matrix ρ akin to Wigner's characteristic function (to which it relates as being the *normal-ordered* characteristic function; "normal order" being defined in the usual sense of all annihilation operators acting first before creation operators):

$$\rho(t) \equiv \int P(\alpha, \alpha^*, t) |\alpha\rangle \langle \alpha| d^2\alpha \quad (1.45)$$

This expression is very helpful to get a physical intuition of coherence, being the weighting factor of ρ in the (overcomplete) basis of coherent states $|\alpha\rangle$ (the overcompleteness allows the diagonal decomposition, which can fail for some cases which we shall not encounter). In

Argand space, the P functions for the three quantum states we have just introduced, namely the Fock state $|n\rangle$, coherent state $|\alpha_0\rangle$ and thermal state (1.43), are given by:

$$P_{\text{Fock}}(\alpha, \alpha^*) = \frac{\exp(-|\alpha|^2)}{n!} \partial_{\alpha^n, \alpha^{*n}}^{2n} \delta(\alpha) \quad (1.46a)$$

$$P_{\text{coh}}(\alpha, \alpha^*) = \delta(\alpha - \alpha_0) \quad (1.46b)$$

$$P_{\text{th}}(\alpha, \alpha^*) = \frac{1}{\pi \langle n \rangle} \exp(-|\alpha|^2 / \langle n \rangle) \quad (1.46c)$$

The expression for a Fock state, as the $2n$ th derivative of a delta function, is not especially agreeable, but we shall be more concerned with the cases of coherent and thermal states or of their combination.

Coherence of the fields

Glauber's main contribution was the introduction of correlators $g^{(n)}$ which he showed were related to optical coherence. We shall be mainly concerned with single mode coherence, for which the first order correlator, defined as

$$g^{(1)}(t, t') \equiv \frac{\langle a^\dagger(t+t')a(t) \rangle}{\sqrt{\langle a^\dagger(t+t')a(t+t') \rangle \langle a^\dagger(t)a(t) \rangle}} \quad (1.47)$$

has limited interest, since it is largely unrelated to the structure of the density matrix, being independent for non-interacting field.

In this case a more relevant quantity is the second order correlator

$$g^{(2)}(t, t') \equiv \frac{\langle a^\dagger(t)a^\dagger(t+t')a(t+t')a(t) \rangle}{\langle a^\dagger(t)a(t) \rangle \langle a^\dagger(t+t')a(t+t') \rangle} \quad (1.48)$$

with higher still orders defined in a similar way, though we shall not need them.

In both cases, t dependence matters for the out-of-equilibrium, regime while t' dependence, which samples the time correlations in the field, can be computed from the knowledge of single-time density matrix with quantum regression theorem, but we shall not use it and restrict our considerations to $g^{(2)}(t, 0)$ since this is for zero delay that the coherent properties are the most imprinted in this quantity. As usual, we will not always let appear explicitly the time dependence and merely write $g^{(2)}(t')$ and $g^{(2)}(0)$ for zero delay or even in this case simply $g^{(2)}$. At infinite time delay $g^{(2)}(t')$ is always equal to one, regardless of the underlying quantum state, two photons detected with infinite delay being completely uncorrelated:

$$g^{(2)}(t' \rightarrow \infty) = 1 \quad (1.49)$$

At zero delay, however, $g^{(2)}$ equals 1 only for the case of a coherent state, while it grows to 2 for thermal states, exhibiting the bunching effect typical of incoherent light, see Glauber (1962). $g^{(2)}$ is generally measured by Hanbury Brown–Twiss experiments, a photon counting experiment set up by Hanbury Brown & Twiss (1957) which is quantum optical in nature: it requires single photon detections at the same time, from which one infers the statistical correlations measured by (1.48). This is a rather delicate experimental measure, but from the mathematical point of view, $g^{(2)}(0)$ is merely computed from diagonal elements of the density matrix:

$$g^{(2)}(0) = \frac{\sum_{n=0}^{\infty} n(n-1)p(n)}{(\sum_{n=0}^{\infty} np(n))^2} \quad (1.50)$$

where $p(n)$, the so-called *statistics* of the state, reads

$$p(n) \equiv \langle n | \rho | n \rangle. \quad (1.51)$$

Two limiting cases of interests are of course provided by the coherent and the thermal case (again, Fock states are usually relevant from a mathematical point of view but in our case will seldom refer to physical reality). The coherent case $|\alpha\rangle$ has Poisson statistics:

$$p_{\text{coh}}(n) = e^{-\langle n \rangle} \frac{\langle n \rangle^n}{n!}, \quad (1.52)$$

with $\langle n \rangle = \langle a^\dagger a \rangle = |\alpha|^2$. The distribution is sharply peaked about its mean, with small fluctuations $\sigma = \langle n \rangle$ in particle number corresponding to the smallest quantum uncertainty allowed for a state without amplitude squeezing. It is at the same time the more classical state of the quantum realm (mapping as closely as allowed by quantum mechanics to a monochromatic wave). This would be the state emitted by an ideal, noiseless laser far above its threshold.

On the opposite, the thermal state, with a $g^{(2)}(0)$ of 2, has exponentially decreasing statistics:

$$p_{\text{th}}(n) = \frac{\langle n \rangle^n}{(1 + \langle n \rangle)^n} \quad (1.53)$$

Now $\sigma = \langle n \rangle^2 + \langle n \rangle$ and particles fluctuate wildly in the system which is most of the time empty (highest probability is for zero particle). For temperatures at which microcavities are operated, this precludes high occupancy numbers, whereas we will mostly investigate condensates which imply such high populations in a single state. This minor point is already a convincing argument that coherency is obtained whenever high occupancy is; a more refined analysis along similar lines is given by Anderson in the proceedings edited by Pitaevskii & Stringari (2003). We shall therefore consider highly populated thermal states as limiting case of mathematical interest but bear in mind that they are not realistic. When there is a large number of particles, the physically relevant case is that of an essentially coherent state, with, say, n_c particles, to which is superimposed a fraction of a thermal state, with n_t particles. Such a state is obtained in the optical field by interfering an ideal coherent radiation with one emitted by a black body. In the resulting field, we will conveniently refer to such particles as coherent and incoherent respectively, though of course once the two fields are merged, a particle does not belong any longer to a part of this decomposition but is indistinguishable from any other. This is just a vivid picture to describe a collective state which has some phase and amplitude spreading. We define the *second order coherence degree* χ as the ratio of the number of coherent particles over the total number of particles:

$$\chi \equiv \frac{n_c}{n_c + n_t} \quad (1.54)$$

with $n_c + n_t = \langle n \rangle$. The density matrix of such a state is easily built from Glauber's P representation of the density matrix (1.45) after the property of P functions for superposition of two uncorrelated fields to be obtained by the convolution of their P functions; this is proved for instance in Mandel & Wolf (1995). From the expressions (1.46b) and (1.46c) one readily gets for such an admixture of coherent and thermal states (which we shall subscript with *coth*):

$$P_{\text{coth}}(\alpha, \alpha^*) = \frac{1}{\pi n_t} e^{-|\alpha - n_c e^{i\varphi}|^2 / n_t}. \quad (1.55)$$

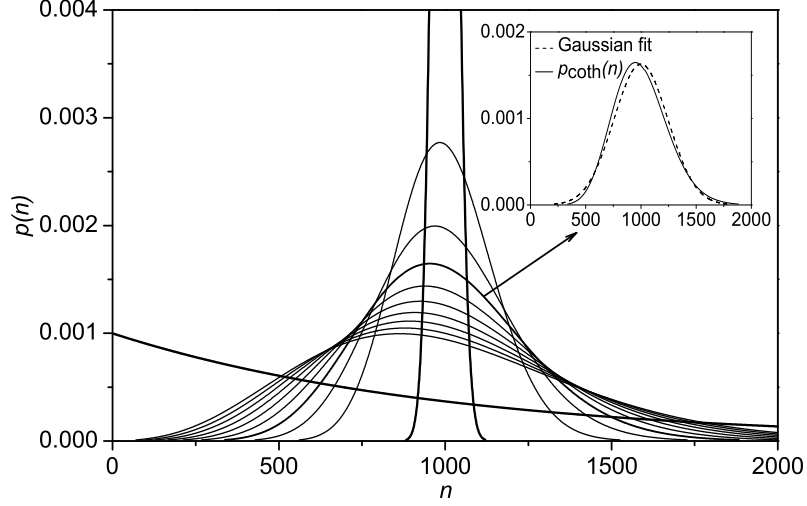


Figure 1.1: Probability distributions $p_{\text{coth}}(n)$ with $\langle n \rangle = 10^3$ and with various degree of coherence, namely with χ running from 99% (sharper thin curve) to 91% (flatter thin curve) together with limiting cases of coherent (100%) and thermal (0%) states, in thick lines. The Poisson distribution of the coherent state assumes maximum value $p_{\text{coh}}(10^3) \approx 0.013$, more than three times higher than is visible. When χ is close to 1, the distribution can be approximated by a Gaussian, as shown in inset for $\chi = 97\%$. The approximation is better for higher χ .

A whole gamut of states with some degree χ of coherence is thus modelled after off-centered Gaussians, which mean yields the coherent fraction $n_c/\langle n \rangle$ and spread the thermal fraction $n_t/\langle n \rangle$. Here φ is the mean phase of the condensate, which is also its order parameter. It is zero if $n_c = 0$ which is the thermal case. The mean of P_{coth} is of course $\langle n \rangle$. The variance is computed as:

$$\text{Var}(P_{\text{coth}}) = \langle n \rangle + n_t^2 + 2n_cn_t, \quad (1.56)$$

and allows to link χ and $g^{(2)}(0)$ as:

$$g^{(2)}(0) = 2 - \chi^2. \quad (1.57)$$

From the above expression, it is straightforward to express $g^{(2)}(0)$ as a function of the first two moments of $p(n)$, the mean $\langle n \rangle$ and the variance $\text{Var}(n) = \sigma^2$:

$$g^{(2)}(0) = 1 + \frac{\sigma^2 - \langle n \rangle}{\langle n \rangle^2}. \quad (1.58)$$

In next section we shall see that to a very good approximation, (3.46) is also a function of the first two moments of $p(n)$ and thus a function of $g^{(2)}$.

As for the statistics, it is obtained evaluating

$$p_{\text{coth}}(n) = \int_{\mathbb{C}} P_{\text{coth}}(\alpha, \alpha^*) |\langle n | \alpha \rangle|^2 d^2\alpha d^2\alpha^*, \quad (1.59)$$

which gives:

$$p_{\text{coth}}(n) = \exp\left(-\frac{\langle n \rangle \chi}{1 + \langle n \rangle (1 - \chi)}\right) \frac{1}{1 + \langle n \rangle (1 + \chi)} L_n\left(-\frac{\chi}{(1 - \chi)(1 + \langle n \rangle (1 - \chi))}\right), \quad (1.60)$$

where L_n is the n^{th} Laguerre polynomial (which has the n dependence of left hand size, $\langle n \rangle$ is constant). This distribution is plotted in fig. 1.1 for values of χ ranging from 0.91 to 0.99 by step of 1%, also with the two limiting cases of the pure coherent state ($\chi = 1$) and the thermal state ($\chi = 0$). As one can see, this distribution very quickly broadens for small deviations from the coherent state, and becomes thermal-like, with huge fluctuations of particle numbers, even for a neatly dominant proportion of coherent particles.

Microcavities

MBE growth technics have made it possible to engineer cavities on the length-scale of the wavelength of light, $\approx \mu\text{m}$, using distributed Bragg reflectors (DBRs). It consists of alternating layers of semiconductors satisfying Bragg condition. The dispersion relation of a photon in a dielectric of refractive index n

$$E_\gamma(\mathbf{k}) = \hbar c |\mathbf{k}| / n \quad (1.61)$$

becomes as a result of the quantization of light on the growth axis of the structure

$$E_\gamma(\mathbf{k}) = \frac{\hbar c}{n} \sqrt{\left(\frac{2\pi}{L}\right)^2 + k_\parallel^2}, \quad (1.62)$$

with c the speed of light, L the cavity effective length yielding the momentum $k_\perp = 2\pi/L$ along the growth axis and k_\parallel the in-plane momentum,

$$\mathbf{k} = (k_\perp, k_\parallel). \quad (1.63)$$

The linear dispersion (1.61) has acquired a parabolic curvature about zero momentum which results in an effective mass for cavity photons,

$$m_\gamma = \frac{2\pi n}{L\hbar c}. \quad (1.64)$$

The hamiltonian for photons in the cavity is, along the same lines as in previous section,

$$H = \sum_{\mathbf{k}} E_\gamma(\mathbf{k}) B_{\mathbf{k}}^\dagger B_{\mathbf{k}} \quad (1.65)$$

where the sum is over $\mathbf{k} = (2\pi/L, k_\parallel)$, with k_\parallel the “variable”.

1.1.3 Quantized Matter field

Second quantization of Schrödinger equation

Second quantization is the name commonly given to procedures tantamount to porting canonical quantization of the electromagnetic field to the Schrödinger wavefunction $\psi(\mathbf{r}, t)$, itself already a field, describing the system at the so-called “first-quantization” level which is ruled by Schrödinger equation:

$$i\hbar \partial_t \psi(\mathbf{r}, t) = \left(-\frac{\hbar^2}{2m} \nabla^2 + V(\mathbf{r}) \right) \psi(\mathbf{r}, t) \quad (1.66)$$

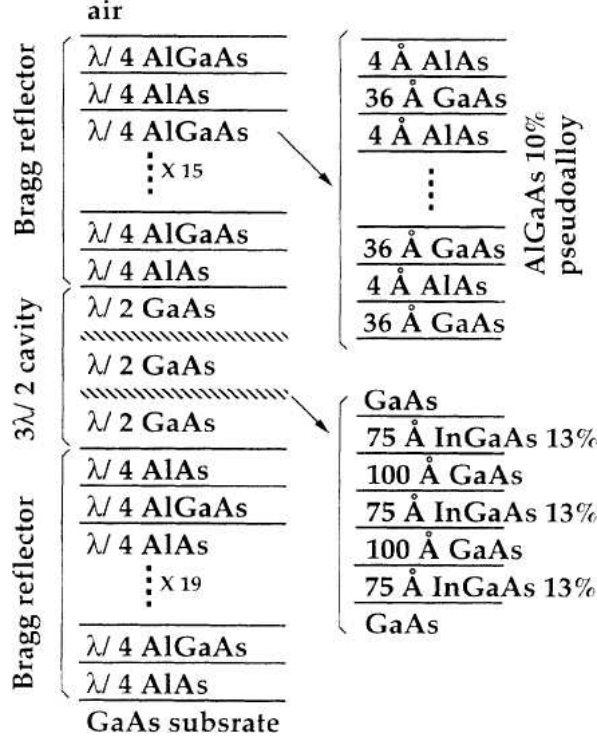


Figure 1.2: Schematic representation of a typical *active* (with QWs) microcavity [from Houdré, Weisbuch, Stanley, Oesterle, Pellandin & Ilegems (1994) and Houdré, Stanley, Oesterle, Ilegems & Weisbuch (1994); this is the structure where room temperature vacuum field Rabi splitting was first observed, cf. section 1.3.1 on page 38]. Each mirror consists in alternating λ -quarter layers of AlAs and AlGaAs (the latter being $\text{Al}_{0.1}\text{Ga}_{0.9}\text{As}$ obtained by alternating 10% of AlAs and 90% of GaAs on $40 \times 10^{-10}\text{m}$). In this structure, the QW is merely a layer of $\text{In}_{0.13}\text{Ga}_{0.87}\text{As}$. There are two sets of three QWs located at the nodes of the field for maximum coupling.

In this way we will be able to delineate the concept of particle and build an efficient formalism, though at a fundamental level it is in fact inescapable (say when relativity is included, or more closely related to our concerns, for gauge particles like photons or phonons which are not conserved).

Eq. (1.66) is termed the *single-particle wavefunction* and $H_0 = -(\hbar^2/2m)\nabla^2 + V(\mathbf{r})$ its *free propagation hamiltonian*. Let us denote $\varphi_\lambda(\mathbf{r})$ a basis of eigenstates of H_0

$$H_0\varphi_\lambda = E_\lambda\varphi_\lambda \quad (1.67)$$

with E_λ the energy spectrum (λ can be taken discrete for some suitable shape of the confining potential V). We call \mathcal{H}_1 the hilbert space spanned by φ_λ and write formally $|\varphi_\lambda\rangle$ by $|\lambda\rangle$. With this notation, the most general single-particle state reads:

$$|\Psi\rangle = \sum_i c_i |\lambda_i\rangle \quad (1.68)$$

for some coefficients c_i .

We introduce the space of N particles as the tensor product

$$\mathcal{H}_N = \bigotimes_{n=1}^N \mathcal{H}_1 \quad (1.69)$$

A basis state of \mathcal{H}_N is of the type

$$|\lambda_{i_1}\rangle \otimes |\lambda_{i_2}\rangle \otimes \cdots \otimes |\lambda_{i_N}\rangle \quad (1.70)$$

Since φ_{λ_i} are orthogonal, we can abbreviate the general state (1.70) by

$$|n_{\lambda_{i_1}} n_{\lambda_{i_2}} \cdots n_{\lambda_{i_k}}\rangle \quad (1.71)$$

with $n_{\lambda_i} \in \mathbb{N}$ the number of times λ_i intervenes in (1.70); this is known as the *occupation number formalism*. Of course

$$\sum_j n_{\lambda_j} = N \quad (1.72)$$

the sum being over the basis states of \mathcal{H}_1 (typically $j \in \mathbb{N}$).

This is a postulate of quantum mechanics that identical particles are indistinguishable: permuting two particles in the system must not have consequences on physically observable quantities, i.e., on their probability to be observed. The wavefunction satisfies this desiderata if it is left unchanged or changes sign upon permutation of two particles, which can be obtained by symmetric (wavefunction unchanged) or antisymmetric (wavefunction sign toggled) linear combinations of (1.70). This is an intrinsic property of the particles at hand, which can be related to their spin in QFT. *Fermions* (half-integer spin particles) have antisymmetric wavefunction while *Bosons* have symmetric wavefunction. The wavefunction of (1.70) projected, say, on real space coordinates \mathbf{r}_i gives

$$\psi_B(\mathbf{r}_1, \cdots, \mathbf{r}_N) = \frac{1}{\sqrt{N! \prod_{i=1}^N n_{\lambda_i}!}} \sum_{\sigma \in \mathfrak{S}(N)} \varphi_{\lambda_{i_1}}(\mathbf{r}_{\sigma(1)}) \cdots \varphi_{\lambda_{i_N}}(\mathbf{r}_{\sigma(N)}) \quad (1.73)$$

for bosonic symmetry, and

$$\psi_F(\mathbf{r}_1, \cdots, \mathbf{r}_N) = \frac{1}{\sqrt{N!}} \sum_{\sigma \in \mathfrak{S}(N)} \zeta^\sigma \varphi_{\lambda_{i_1}}(\mathbf{r}_{\sigma(1)}) \cdots \varphi_{\lambda_{i_N}}(\mathbf{r}_{\sigma(N)}) \quad (1.74)$$

for fermionic symmetry, in which case $\mathfrak{S}(N)$ is the set of permutations of $[1, N]$ and $\zeta^\sigma = \pm 1$ the signature of σ . Up to the normalisation constant, the structure of expression (1.73), resp. (1.74), is that of the permanent, resp. determinant, of the matrix Ψ which elements are given by

$$\Psi_{ij} \equiv \langle \mathbf{r}_j | \lambda_i \rangle = \varphi_{\lambda_i}(\mathbf{r}_j) \quad (1.75)$$

One capital advantage of the occupation number formalism is its ability to embed in a transparent way the proper symmetrization of the state, along with the normalisation constant. Although most of what follows extends or conversely contrasts in a way which can be made systematic for both bosons and fermions by proper notations, we shall focus in the remaining to the bosonic case, as this is the case of our main interest.

We introduce creation operators c_λ^\dagger as follows:

$$b_\lambda^\dagger : \mathcal{H}_N \longrightarrow \mathcal{H}_{N+1} \quad (1.76)$$

$$|n_{\lambda_{i_1}}, \cdots, n_\lambda, \cdots, n_{\lambda_{i_k}}\rangle \longmapsto \sqrt{n_\lambda + 1} |n_{\lambda_{i_1}}, \cdots, n_\lambda + 1, \cdots, n_{\lambda_{i_k}}\rangle \quad (1.77)$$

The sum in (1.72) is now $N + 1$ and application of this operator indeed amounts to adding one particle. For instance, with our initial notations, $c_\lambda^\dagger |\lambda_i\rangle \mapsto \sqrt{n_\lambda + 1} |\lambda \lambda_i\rangle$ again with $n_\lambda = 1$ if $|\lambda\rangle = |\lambda_i\rangle$ and zero otherwise.

The corresponding annihilation operator is as follows:

$$b_\lambda : \mathcal{H}_N \longrightarrow \mathcal{H}_{N-1} \quad (1.78)$$

$$|n_{\lambda_{i_1}}, \dots, n_\lambda, \dots, n_{\lambda_{i_k}}\rangle \mapsto \sqrt{n_\lambda} |n_{\lambda_{i_1}}, \dots, n_\lambda - 1, \dots, n_{\lambda_{i_k}}\rangle \quad (1.79)$$

If initially the space belongs to \mathcal{H}_0 , by definition it is the vacuum $|0\rangle$ which obeys

$$b_\lambda |0\rangle = 0 \quad (1.80)$$

for all λ (the same holds if b_λ acts on some state which has no projection on $|\lambda\rangle$).

The field operator $\Psi(\mathbf{r})$, resp. $\Psi^\dagger(\mathbf{r})$, are defined in terms of creation and annihilation of eigenstates of the system as

$$\Psi(\mathbf{r}) = \sum_\lambda \varphi_\lambda(\mathbf{r}) b_\lambda \quad (1.81a)$$

$$\Psi(\mathbf{r})^\dagger = \sum_\lambda \varphi_\lambda^*(\mathbf{r}) b_\lambda^\dagger \quad (1.81b)$$

As \mathbf{r} is typically a continuous variable, the reverse relations involve integrals. The second-quantised hamiltonian for free propagation (kinetic energy plus confining potential),

$$H = \int \Psi(\mathbf{r})^\dagger \left(-\frac{\hbar^2}{2m} \nabla^2 + V(\mathbf{r}) \right) \Psi(\mathbf{r}) \, d\mathbf{r}, \quad (1.82)$$

becomes in terms of annihilation and creation operators, after substituting (1.81) into (1.82)

$$H = \sum_\lambda E_\lambda b_\lambda^\dagger b_\lambda \quad (1.83)$$

The commutation algebra for Bosonic field can be shown to be

$$\text{(Bosons)} \quad (1.84)$$

$$[\Psi(\mathbf{r}), \Psi(\mathbf{r}')] = [\Psi^\dagger(\mathbf{r}), \Psi^\dagger(\mathbf{r}')] = 0 \quad (1.85)$$

$$[\Psi(\mathbf{r}), \Psi^\dagger(\mathbf{r}')] = \delta(\mathbf{r} - \mathbf{r}') \quad (1.86)$$

or, in reciprocal space, cf. (1.32):

$$[b_\lambda, b_\nu] = [b_\lambda^\dagger, b_\nu^\dagger] = 0 \quad (1.87)$$

$$[b_\lambda, b_\nu^\dagger] = \delta_{\lambda, \nu} \quad (1.88)$$

Likewise relations hold for fermions but for anticommutators of the variables:

$$\text{(Fermions)} \quad (1.89)$$

$$\{\Psi(\mathbf{r}), \Psi(\mathbf{r}')\} = \{\Psi^\dagger(\mathbf{r}), \Psi^\dagger(\mathbf{r}')\} = 0 \quad (1.90)$$

$$\{\Psi(\mathbf{r}), \Psi^\dagger(\mathbf{r}')\} = \delta(\mathbf{r} - \mathbf{r}') \quad (1.91)$$

Symmetry of quantum particles result in striking effects. For fermions it is responsible for Pauli exclusion principle, which forbids particles to occupy the same state (because two lines of matrix Ψ in (1.75) would be identical, thus canceling the determinant). For bosons, it results in the important effect of stimulation which on the opposite tends to attract particles. Since it is central to the effects we shall investigate, we now look at it in further details.

Bosonic stimulation

The symmetry of the bosonic wavefunction results in a tendency for particles to occupy together the same states. It is worth delving into this rather vague statement by explicating the effect on some specific case, more profitably the simplest one, which requires two particles.

Let us consider these two particles in states $|\psi_a\rangle$ and $|\psi_b\rangle$. If they are distinguishable particles, the total wavefunction is

$$\Psi_C = |\psi_a\rangle |\psi_b\rangle \quad (1.92)$$

(subscript C referring to “classical” particles which one can monitor all along and tell apart). If they are bosons, however

$$\Psi_B = \frac{1}{\sqrt{2}}(|\psi_a\rangle |\psi_b\rangle + |\psi_b\rangle |\psi_a\rangle) \quad (1.93)$$

cf. (1.73). Let us consider the single-particle observable Ω_i acting on \mathcal{H}_i , where the subscript distinction is to remind to which Hilbert space Ω_i refers, otherwise, these operators are the same: for instance they both are position, or both momentum operator; again, the index is not to consider two different observables but same observable evaluated on different subspaces (that is, on various particles). Also for simplicity, we assume the states are orthogonal, $\langle \psi_a | \psi_b \rangle = 0$. Therefore, we shall write $\langle \Omega \rangle_{ij}$ (without subscript on Ω) the average $\langle \psi_k | \langle \psi_i | \Omega_1 | \psi_j \rangle | \psi_k \rangle = \langle \psi_i | \langle \psi_k | \Omega_2 | \psi_k \rangle | \psi_j \rangle$ with $i, j, k \in \{a, b\}$, and also write $\langle \Omega \rangle_i = \langle \Omega \rangle_{ii}$ (not repeating the subscript).

We compare the magnitude of the difference between observables for each particle for both cases (distinguishable and symmetrically indistinguishable), that is, we evaluate the mean difference

$$\Delta \equiv \langle (\Omega_1 - \Omega_2)^2 \rangle = \langle \Omega_1^2 \rangle + \langle \Omega_2^2 \rangle - \langle \Omega_1 \Omega_2 \rangle - \langle \Omega_2 \Omega_1 \rangle \quad (1.94)$$

For distinguishable particles,

$$\Delta_C = \langle \Omega^2 \rangle_a + \langle \Omega^2 \rangle_b - 2\langle \Omega \rangle_a \langle \Omega \rangle_b \quad (1.95)$$

while for indistinguishable particles

$$\Delta_B = \Delta_C - 2|\langle \Omega \rangle_{ab}|^2. \quad (1.96)$$

The additional integral in (1.96) arises from $\langle \Omega \rangle_{ab} \langle \Omega \rangle_{ba} = \langle \psi_a | \Omega | \psi_b \rangle \langle \psi_b | \Omega | \psi_a \rangle$ where we used $\Omega^\dagger = \Omega$. Obviously, $\Delta_B \leq \Delta_C$ and the difference is sensitive to the *overlap* of the two wavefunctions in a basis where Ω is diagonal, since in this case, calling $\omega_\xi \delta(\xi - \zeta) = \langle \xi | \Omega | \zeta \rangle$

$$\langle \Omega \rangle_{ab} = \int \omega_\xi \psi_b(\xi)^* \psi_a(\xi) d\xi \quad (1.97)$$

is zero if $\psi_a(\xi)$ and $\psi_b(\xi)$ are not simultaneously nonzero, i.e., if the probability is not null that both particles assume same observable ω_ξ (be found in the “same” state). If this probability is nonzero, bosonic symmetry brings closer the observed values.

For many particles, this statement can be made more precise: *the probability that N bosons be found in the same quantum state is $N!$ times the probability that distinguishable particles be found in the same state.* The proof is instructive and goes as follows, let $|\Psi\rangle$ the wavefunction of the state be developed on a basis ϕ_i of $\mathcal{H}^{\otimes N}$, first in case of distinguishability,

$$|\Psi\rangle_C = \sum_{i_1, \dots, i_N} \alpha_{i_1, \dots, i_N} |\phi_{i_1}\rangle \cdots |\phi_{i_N}\rangle \quad (1.98)$$

then symmetrizing the state to ensure bosonic indistinguishability

$$|\Psi\rangle_B = \frac{1}{\sqrt{N!}} \sum_{i_1, \dots, i_N} \sum_{\sigma \in \mathcal{G}} \alpha_{i_1, \dots, i_N} |\phi_{\sigma(i_1)}\rangle \otimes \dots \otimes |\phi_{\sigma(i_N)}\rangle \quad (1.99)$$

The probability amplitude that all distinguishable particles (resp. indistinguishable) be in the same quantum state, say $|\phi_1\rangle$, is

$$\langle \phi_1^{\otimes N} | \Psi \rangle_C = \alpha_{1, \dots, 1} \quad (1.100a)$$

$$\text{(resp. } \langle \phi_1^{\otimes N} | \Psi \rangle_B = \frac{N!}{\sqrt{N!}} \alpha_{1, \dots, 1}) \quad (1.100b)$$

The ratio of these probabilities is $N!$, especially it is independent of α (which should be nonzero, meaning that one cannot find all particles in the same state if they do not all have a projection in this state). This ratio is therefore independent of any linear combination of the α and thereby of any state of the system, thus showing that the probability to find all particles in the same state if they are indistinguishable (and bosons) is $N!$ this probability for distinguishable particles. A more familiar statement is that if N particles are in the same state, the probability for the $N + 1$ th to be found also in this same state is $N + 1$ times this probability for distinguishable particles. It is proved with conditional probabilities, if “ A ” is the statement “the $N + 1$ th is in some given state $|\varphi\rangle$ ” while “ B ” is the statement “the n th other bosons already are in state $|\varphi\rangle$ ”, thus the probability (with respect to distinguishable particles) that “ A ” is realised given than “ B ” is $\mathbb{P}(A \cap B)/\mathbb{P}(B)$, that is $(N + 1)!/N!$. This $N + 1$ coefficient is usually called the *bosonic stimulation*. It will play a key role in our investigations of polaritons kinetics.

Phonons, Electrons, Holes and Excitons

Various types of excitations can thus be included in this second-quantisation formalism. A popular “quantum” excitation of the solid state is the so-called *phonon*, or quantum of vibration energy. The quantization has much resemblance with that of the electromagnetic field, departing on technical issues only (quantization of a scalar field instead of a vector field, different conservation rules as a result of the crystal symmetry, etc. . .) The procedure will therefore not bring much insights and we refer to the vast literature existing on that topic (a short and good coverage can be found in Kittel’s (1996) textbook). The same is for all important “fundamental” excitations, namely for the semiconductor, electrons and holes.

Here we content to settle notations; we will use $b_{\mathbf{k}}$ for the annihilation Bose operator of an optical phonon of momentum \mathbf{k} and $c_{i,\mathbf{k}}$ for the annihilation Fermi operator for electrons in the i th band, that is in a two-bands model, $i = 1$ (or v) for the valence band and $i = 2$ (or c) the conduction band, or simply $c_{\mathbf{k}}$ for electrons when holes will have been introduced.

The associated dispersion relations are $\hbar\omega_{\mathbf{k}}$ (phonons) and parabolic with effective mass m_e for electrons (with further indices if required to distinguish the various semiconductor bands).

In occupation number formalism, cf. (1.71), the Hilbert spaces for these particles we write as:

$$\mathcal{H}_{\text{phonons}} = \bigcup_{i=0}^{\infty} \bigcup_{\theta_{\mathbf{k}_i}=0}^{\infty} \{ \bigotimes_{j=0}^{\infty} |\theta_{\mathbf{k}_j}\rangle \} \quad (1.101)$$

$$\mathcal{H}_{\text{electrons}} = \bigcup_{i=0}^{\infty} \bigcup_{c_{\mathbf{k}_i}=0}^1 \{ \bigotimes_{j=0}^{\infty} |f_{\mathbf{k}_j}\rangle \} \quad (1.102)$$

We will formally identify the excitation with this notation, namely it will be understood that phonons are identified by the variable θ and electrons by f . A proper but heavy notation would be to index the ket in some way, e.g., to write $|n_{\mathbf{k}_1}\rangle_{\text{ph}}|m_{\mathbf{k}_2}\rangle_{\text{el}}$ for the state with $n_{\mathbf{k}_1}$ phonons in state $|\mathbf{k}_1\rangle$ and $m_{\mathbf{k}_2}$ electrons in state $|\mathbf{k}_2\rangle$, whereas we shall prefer to write $|\theta_{\mathbf{k}_1} = n\rangle|f_{\mathbf{k}_2} = m\rangle$; we will see this shortcut to be always clear from context.

Another fundamental excitation in semiconductors, *the exciton* (in our case, the Wannier exciton), has a much richer structure. It arises as the binding of one electron-hole pair by Coulomb interaction, both particles (of opposite charges) being embedded in the solid as free particles able to wander around (as an ionised electron-hole pair) or orbiting around each-other and moving together as if it was an atom (for that matter the hydrogen or positronium atom).

The second-quantized hamiltonian of a semiconductor at the fermionic level reads, in real space

$$H = \int \Psi(\mathbf{r})^\dagger \left(-\frac{\hbar^2}{2m} \nabla^2 + V(\mathbf{r}) \right) \Psi(\mathbf{r}) d\mathbf{r} \quad (1.103a)$$

$$+ \frac{1}{2} \int \int \Psi(\mathbf{r})^\dagger \Psi(\mathbf{r}')^\dagger \frac{e^2}{|\mathbf{r} - \mathbf{r}'|} \Psi(\mathbf{r}') \Psi(\mathbf{r}) d\mathbf{r} d\mathbf{r}' \quad (1.103b)$$

cf. (1.82), with $\Psi(\mathbf{r})$ the electron annihilation field operator, that we expand in terms of $\varphi_{i,\mathbf{k}}(\mathbf{r}) = \langle \mathbf{r} | i, \mathbf{k} \rangle$ the single-particle wavefunction labelled by the quantum number \mathbf{k} in the i th semiconductor band, cf. (1.81):

$$\Psi(\mathbf{r}) = \sum_{i \in \{c,v\}} \sum_{\mathbf{k}} \varphi_{i,\mathbf{k}}(\mathbf{r}) c_{i,\mathbf{k}} \quad (1.104)$$

Because of interactions and correlations, the determination of $\varphi_{i,\mathbf{k}}(\mathbf{r})$ is a difficult task, typically solved numerically. The full many-body problem (1.103) can be approximated to an effective single-body problem through the so-called Hartree-Fock approximation, which introduces an effective potential V_{eff} . The resulting ‘‘Schrödinger’’ equation with hamiltonian $H_{\text{HF}} = -\hbar^2 \nabla^2 / 2m + V_{\text{eff}}$ is nonlinear since the potential depends on the wavefunction φ , and so the problem remains one of considerable difficulty. Bloch theorem however allows a statement of general validity:

$$\varphi_{i,\mathbf{k}}(\mathbf{r}) \propto e^{i\mathbf{k} \cdot \mathbf{r}} u_{i,\mathbf{k}}(\mathbf{r}) \quad (1.105)$$

with u having the same translational symmetry as the crystal.

Once all the algebra has been gone through, the semiconductor hamiltonian (1.103) becomes in reciprocal space :

$$H = \sum_{i \in \{c,v\}} \sum_{\mathbf{k}} E_i(\mathbf{k}) c_{i,\mathbf{k}}^\dagger c_{i,\mathbf{k}} \quad (1.106a)$$

$$+ \frac{1}{2} \sum_{i \in \{c,v\}} \sum_{\mathbf{k}, \mathbf{p}, \mathbf{q} \neq \mathbf{0}} V(\mathbf{q}) c_{i,\mathbf{k}+\mathbf{q}}^\dagger c_{i,\mathbf{p}-\mathbf{q}}^\dagger c_{i,\mathbf{p}} c_{i,\mathbf{k}} \quad (1.106b)$$

$$+ \sum_{\mathbf{k}, \mathbf{p}, \mathbf{q} \neq \mathbf{0}} V(\mathbf{q}) c_{c,\mathbf{k}+\mathbf{q}}^\dagger c_{v,\mathbf{p}-\mathbf{q}}^\dagger c_{v,\mathbf{p}} c_{c,\mathbf{k}} \quad (1.106c)$$

with E_i the dispersion relation for the i th band and $V(\mathbf{q})$ the Fourier transform of interaction.

The limit of very low density (in fact in the limit where the ground state is devoid of conduction band electron) allows some analytical solutions to be obtained after performing some

approximations. One simplification, both conceptual and from the point of view of the formalism, is the introduction of the hole (fermionic) operator h as

$$h_{\mathbf{k}} = c_{v,-\mathbf{k}}^\dagger \quad (1.107)$$

(spin is also reversed if granted). This allows to get rid of the negative effective mass of valence electrons and deal with an excitation as an “addition” of a particle rather than annihilation (in terms of valence electrons, the ground state is full of electrons and gets depleted by excitations). Conceptually it replaces a sea of valence electrons by a single particle, making it easier to conceive the exciton as a bound state. In terms of electrons $c_{\mathbf{k}}$ and hole $h_{\mathbf{k}}$, (1.106) now reads

$$H = \sum_{\mathbf{k}} [E_e(\mathbf{k})c_{\mathbf{k}}^\dagger c_{\mathbf{k}} + E_h(\mathbf{k})h_{\mathbf{k}}^\dagger h_{\mathbf{k}}] \quad (1.108a)$$

$$+ \frac{1}{2} \sum_{\mathbf{k},\mathbf{p},\mathbf{q} \neq \mathbf{0}} V(\mathbf{q}) [c_{\mathbf{k}+\mathbf{q}}^\dagger c_{\mathbf{p}-\mathbf{q}}^\dagger c_{\mathbf{p}} c_{\mathbf{k}} + h_{\mathbf{k}+\mathbf{q}}^\dagger h_{\mathbf{p}-\mathbf{q}}^\dagger h_{\mathbf{p}} h_{\mathbf{k}}] \quad (1.108b)$$

$$- \sum_{\mathbf{k},\mathbf{p},\mathbf{q} \neq \mathbf{0}} V(\mathbf{q}) c_{\mathbf{k}+\mathbf{q}}^\dagger h_{\mathbf{p}-\mathbf{q}}^\dagger h_{\mathbf{p}} c_{\mathbf{k}} \quad (1.108c)$$

With explicit expression for electron and hole dispersion (as a function of their effective mass):

$$E_e(\mathbf{k}) = E_{\text{gap}} + \frac{\hbar \mathbf{k}^2}{2m_e^*} \quad (1.109a)$$

$$E_h(\mathbf{k}) = \frac{\hbar \mathbf{k}^2}{2m_h^*}. \quad (1.109b)$$

In the low density limit, if one neglects line (1.108b) in the hamiltonian, it can be diagonalised by introducing the *exciton operator*

$$X_v(\mathbf{k}) \equiv \sum_{\mathbf{p}} \varphi_v(\mathbf{p}) h_{\mathbf{k}/2-\mathbf{p}} c_{\mathbf{k}/2+\mathbf{p}}, \quad (1.110)$$

with $\varphi_v(\mathbf{p})$ the Fourier transform of Wannier equation eigenstates (with v the quantum numbers, same as for the hydrogen atom; the spectrum of energy we call E_v).

The exciton hamiltonian becomes:

$$H = \sum_{v,\mathbf{k}} E_X^v(\mathbf{k}) X_v^\dagger(\mathbf{k}) X_v(\mathbf{k}) \quad (1.111)$$

with

$$E_X^v(\mathbf{k}) = E_v + E_e(\mathbf{k}) + E_h(\mathbf{k}) \quad (1.112)$$

This concludes our overview of elementary solid-state QFT. In the text we shall mostly deal with polaritons, the coupling of excitons with photons. The remaining of this chapter is devoted to an elementary description of their properties.

1.2 Main Theoretical Results on Exciton–Polaritons

1.2.1 Photon–Exciton Coupling; Polaritons

Mixed state of light and matter

The polariton can be seen in a simplified but very accurate model as the new eigenstates which arise from the coupling of two oscillators, to wit, the photon and the exciton. Vividly, the polariton is then seen as the chain process where the exciton annihilates, emitting a photon with same energy E and momentum \mathbf{k} , which is later re-absorbed by the medium, creating a new exciton with same (E, \mathbf{k}) , and so on until the excitation finds its way out of the cavity (resulting in the annihilation of the polariton).

In this part we neglect for brevity spins and other states than $1s$ for the exciton. The dipole moment $-e\mathbf{r}$ of the electron-hole pair couples to the light field \mathbf{E} and adds the following coupling hamiltonian to (1.103):

$$H_{\gamma X} = \int \Psi^\dagger(\mathbf{r})[-e\mathbf{r} \cdot \mathbf{E}(\mathbf{r})]\Psi(\mathbf{r}) d\mathbf{r} \quad (1.113)$$

The same procedure to obtain (1.108) from (1.103) including (1.113) leads to the following exciton-photon coupling hamiltonian:

$$H = \sum_{\mathbf{k}} E_\gamma(\mathbf{k}) B_{\mathbf{k}}^\dagger B_{\mathbf{k}} + \sum_{\mathbf{k}} E_X(\mathbf{k}) X_{\mathbf{k}}^\dagger X_{\mathbf{k}} + i \sum_{\mathbf{k}} \hbar g(\mathbf{k}) (C_{\mathbf{k}}^\dagger a_{\mathbf{k}} - C_{\mathbf{k}} a_{\mathbf{k}}^\dagger) \quad (1.114)$$

with $\hbar g(\mathbf{k}) = \mu_{cv} \phi_{1s}(0) \sqrt{E_\gamma(\mathbf{k})/2\varepsilon}$ and μ_{cv} being the dipole matrix element dotted with electron and hole. Hamiltonian (1.114) can be diagonalised provided that X operators obey bosonic algebra $[X_\nu(\mathbf{k}), X_\mu^\dagger(\mathbf{q})] = \delta_{\nu,\mu} \delta_{\mathbf{k},\mathbf{q}}$. Direct evaluation of the commutator with explicit expression (1.110) yields

$$[X_\nu(\mathbf{k}), X_\mu^\dagger(\mathbf{q})] = \delta_{\nu,\mu} \delta_{\mathbf{k},\mathbf{q}} - \sum_{\mathbf{p}} |\phi_{1s}(\mathbf{p})|^2 (c_{\mathbf{k}}^\dagger c_{\mathbf{q}} + h_{-\mathbf{k}}^\dagger h_{-\mathbf{q}}) \quad (1.115)$$

so that the diagonalisation is legitimate at low densities. Especially, $\langle [X_{\mathbf{0}}, X_{\mathbf{0}}^\dagger] \rangle = 1 - O(Na_0^2)$, where N is the density of excitons and a_0 is the Bohr radius associated with ϕ_{1s} . One can therefore treat excitons as bosons with confidence in the limit $Na_0^2 \ll 1$. In such an approximation, the hamiltonian (1.114), bilinear in bosonic operators, is diagonalized with the so-called Hopfield transformation:

$$a_{\mathbf{k}}^L \equiv \mathcal{X}_{\mathbf{k}} X_{\mathbf{k}} - \mathcal{C}_{\mathbf{k}} B_{\mathbf{k}}, \quad (1.116)$$

$$a_{\mathbf{k}}^U \equiv \mathcal{C}_{\mathbf{k}} X_{\mathbf{k}} + \mathcal{X}_{\mathbf{k}} B_{\mathbf{k}}, \quad (1.117)$$

where the so-called *Hopfield coefficients* $\mathcal{C}_{\mathbf{k}}$ and $\mathcal{X}_{\mathbf{k}}$ satisfy $\mathcal{C}_{\mathbf{k}}^2 + \mathcal{X}_{\mathbf{k}}^2 = 1$, so that the transformation is canonical and a operators follow the bosonic algebra as well. As previously with excitons, hamiltonian (1.114) reduces to free propagation terms only

$$H = \sum_{\mathbf{k}} E_U(\mathbf{k}) a_{\mathbf{k}}^{U\dagger} a_{\mathbf{k}}^U + \sum_{\mathbf{k}} E_L(\mathbf{k}) a_{\mathbf{k}}^{L\dagger} a_{\mathbf{k}}^L \quad (1.118)$$

for *upper* and *lower polariton branches*, with second quantized annihilation operators a^U and a^L , respectively. The dispersion relations for these branches are:

$$E_{\mathbf{L}}(\mathbf{k}) = \frac{1}{2}(E_X(\mathbf{k}) + E_\gamma(\mathbf{k})) \pm \frac{1}{2} \sqrt{\delta_{\mathbf{k}}^2 + 4\hbar^2 g(\mathbf{k})^2} \quad (1.119)$$

(the U subscript is associated with the plus sign, L with minus), where E_γ is given by expression (1.62) and E_X by (1.112), and $\delta_{\mathbf{k}}$ is the energy mismatch, or *detuning*, between the cavity and exciton modes:

$$\delta_{\mathbf{k}} \equiv E_\gamma(\mathbf{k}) - E_X(\mathbf{k}) \quad (1.120)$$

The Hopfield coefficients used to diagonalise this hamiltonian are most simply expressed as a function of upper polariton dispersion relation (1.119):

$$\mathcal{C}_{\mathbf{k}} = \frac{\hbar\Omega_{\mathbf{R}}}{\sqrt{(E_{\mathbf{U}}(\mathbf{k}) - E_X(\mathbf{k}))^2 + \hbar^2\Omega_{\mathbf{R}}^2}}, \quad (1.121)$$

$$\mathcal{X}_{\mathbf{k}} = \frac{E_{\mathbf{U}}(\mathbf{k}) - E_X(\mathbf{k})}{\sqrt{(E_{\mathbf{U}}(\mathbf{k}) - E_X(\mathbf{k}))^2 + \hbar^2\Omega_{\mathbf{R}}^2}}. \quad (1.122)$$

where we introduced the *Rabi frequency* $\Omega_{\mathbf{R}} = 2g(\mathbf{k})$.

Dispersion of polaritons

Eq. (1.119) is one of the major results of microcavity polaritons physics for the various consequences this relation bears on many key issues that we are going to address in next chapter. It is plotted in solid lines on page 40 on figs. 1.5 (b) & 1.6 (b) and on page 42 on fig. 1.7 (a) where are also plotted in dashed lines the dispersions for the exciton, eq. (1.112), and the photon, eq. (1.62). The first couple of figures display negative (where bare dispersions cross each other) and positive (where they do not) detunings, while the third figure displays zero detuning (resonance at $\mathbf{k} = \mathbf{0}$).

As the result of the exciton-photon interaction, there is an avoided crossing (anticrossing) of energies. The polariton arises as a coherent mixture of the photon and exciton states which fractions are given by Hopfield coefficients (1.121). As already said, the polariton is the true eigenstate of the system, whereas photon and exciton modes are transient states, exchanging the energy at the Rabi frequency $\Omega_{\mathbf{R}}$. In this simple picture the anticrossing appears however weak the interaction. This can be made more realistic, taking into account the broadening of exciton and photon resonances, by adding to eqs. (1.112) and (1.62) imaginary components $-i\Gamma_X$ and $-i\Gamma_\gamma$ respectively. Γ_X is the broadening caused by excitons interactions (inter-particles or with phonons), while Γ_γ reflects the finite reflectivity which is inversely proportional to the quality factor of the cavity. At zero detuning eq. (1.119) then becomes

$$E_{\mathbf{L}}(\mathbf{k}) = \frac{1}{2}(E_X(\mathbf{k}) + E_\gamma(\mathbf{k}) - i\Gamma_X - i\Gamma_\gamma) \pm \frac{1}{2}\sqrt{\hbar^2\Omega_{\mathbf{R}}^2 - (\Gamma_X - \Gamma_\gamma)^2}. \quad (1.123)$$

This expression depends crucially on the sign of the expression below the radical, demonstrating that the physical behaviour of the system depends on the interrelation between the strength of the exciton-photon coupling and dissipation. If $\hbar\Omega_{\mathbf{R}} > (\Gamma_X - \Gamma_\gamma)$, $E_{\mathbf{L}}$ exhibits the energy splitting already encountered, so-called *Rabi splitting* which corresponds to the *strong coupling* regime, where the correlations between exciton and photon are important and their interaction cannot be dealt with in a perturbative way. An altogether new behaviour of the system is expected and should be described in terms of *polaritons*. The term *vacuum Rabi splitting* has been introduced by Sanchez-Mondragon, Narozhny & Eberly (1983) to denote from Rabi splitting

when the oscillation is between two populated modes (Mollow 1969) (rather than with the vacuum of the other excitation). This terminology is now generally accepted, though some would prefer refer to “normal mode splitting”. To put an emphasis on the specificity of microcavities, the denominations “dressed exciton splitting” or “polariton splitting” have also been used, but are now encountered only for stylistic purposes.

Note that the splitting presented so far relates to the spectrum of energy and is rather a theoretical notion. Experimentally, this splitting relates in more subtle way to splittings in reflectivity (R), transmission (T), absorption (A) and photoluminescence (PL). Indeed this splitting is in general different in all these cases and is also different from the exciton-photon coupling constant g . Yet it can be shown that the general following relation holds:

$$\Delta E_R \geq \Delta E_T \geq \Delta E_A \quad (1.124)$$

and also $\Omega \geq \Delta E_A$. Only the splitting in absorption unambiguously proves strong coupling, while the splitting in transmission or reflectivity is a necessary but not sufficient condition. It might therefore be the most important experimental expression, which we give here:

$$\Delta E_A = \sqrt{\Omega^2 - \frac{(\Gamma_c^2 + \Gamma_x^2)}{2}} \quad (1.125)$$

along with the PL splitting

$$\Delta E_{PL} = \sqrt{2\Omega_R \sqrt{\Omega_R^2 + 4(\Gamma_X + \Gamma_\gamma)^2} - \Omega_R^2 - 4(\Gamma_X + \Gamma_\gamma)^2} \quad (1.126)$$

so that it is possible that although in strong coupling regime (where the device would exhibit effects expected from polaritons), the splitting cannot be resolved from PL observations. Savona, Piermarocchi, Quattropani, Schwendimann & Tassone (1998) give an excellent and much more detailed discussion on these points.

On the other hand, if $\hbar\Omega_R < (\Gamma_X - \Gamma_\gamma)$, the square root becomes imaginary and thus the (real) energy anticrossing disappears. This is the *weak coupling* regime where the system can be described in terms of weakly interacting photon and exciton. Now the energies are degenerated and the broadenings (imaginary part of (1.123)) do differ. More detailed analyses show that with the reflectivity going to zero, the broadening of the photon mode diverges (the photon does not remain in the cavity) and the broadening of the exciton mode approaches the bare QW spontaneous emission rate, describing in effect weakly-interacting photons and excitons.

İmamoğlu’s boson

A capital idea which has been a continual source of inspiration for experimentalists and theoreticians alike is to Bose condense polaritons. In the literature this idea originates in late 1995 with Ataç İmamoğlu, then a proficient young professor at the University of California (in the masterpiece of scientific literature “Quantum Optics” by Mandel & Wolf (1995), he is cited as a contributor to the concept of lasing without population inversion, though via the single-particle coherence effect and not for the work of present concern). Although the historical seed of polariton lasers, the first published proposal by İmamoğlu & Ram (1996) is that of an exciton laser, with authors being even cautious to “ensure that the relevant quasi-particles are excitons rather than polaritons”. A lot of activity had already been carried along excitonic Bose

condensates on the one hand (Griffin et al. 1996) and matter–wave lasers on the other (Wiseman & Collett 1995, Holland, Burnett, Gardiner, Cirac & Zoller 1996). İmamođlu’s insight was to consider the out-of-equilibrium situation and to provide a unifying picture to the case of unstable particles. This led him to gather the main features of a polariton laser: agglomeration in a degenerate mode by stimulated relaxation and emission by spontaneous recombination through coupling to external radiation field. He also proposed the formation of a coherent matter wave by coupling the ground state to another semiconductor and dealing with bose condensed excitons directly, but being technically more difficult this has quickly been put aside; the idea will probably resurface, though, upon completion of the light coherence formation program. He coined in the term *boser* which enjoyed a popular usage in the early developments but has now essentially faded away in favor of the denomination “*polariton laser*”. The main idea, however, has stimulated an instant interest which has remained till our days. The effect is still actively sought with some minute variations and enhancements from other contributors.

The main relaxation mechanism in the early developments was through phonon relaxation, but the final state stimulation was already clearly identified as the key ingredient. The excitonic condensate is built when all exciton-phonon scattering channels involving the ground-state have a population of excitons in excess with respect to the phonon populations:

$$\langle n \rangle_X(\mathbf{k}) > \langle n \rangle_{\text{ph}}(\mathbf{k}) \quad (1.127)$$

for all \mathbf{k} (wavevector), with $\langle n \rangle_{X/\text{ph}}$ the equilibrium number of excitons/phonons in this state. For phonons the equilibrium is the Bose distribution at lattice temperature T_{ph} , while for excitons it is a quasi-equilibrium at a temperature possibly higher. In a bulk microcavity—that is for a structure where the cavity is a bulk layer—integrating over these distributions in 3D yields a minimum exciton density N_X^{min} which ensures (1.127):

$$N_X^{\text{min}} \approx \frac{2.62}{\lambda_{T_{\text{ph}}}^3} \quad (1.128)$$

with $\lambda_{T_{\text{ph}}}$ the thermal de Broglie wavelength of an exciton at temperature T_{ph} . Since in a planar cavity with QWs as the active medium, the exciton is quasi-two dimensional, a cutoff at the minimum energy allowed by phonon scattering is invoked. We refer to the discussion by İmamođlu, Ram, Pau & Yamamoto (1996) for further discussion of these points, including the taking into account in (1.128) of loss rates of phonons and excitons, and improving upon this critical density through efficient LO phonons scatterings. Eq. (1.127) amounts to an inversion population condition, but of an essentially practical character rather than fundamentally needed for stimulation to overcome absorption as is the case in a conventional laser. In fact, the criterion of inversion population by negative value of the state average of the inversion operator $I_{\mathbf{k}}$ of state \mathbf{k} defined by

$$I_{\mathbf{k}} \equiv 1 - n_{e,\mathbf{k}} - n_{h,-\mathbf{k}} \quad (1.129)$$

where $n_{e/h,\mathbf{k}}$ is the number operator for electrons/holes of momentum \mathbf{k} , is not needed for the boser, whence the qualification of lasing without inversion population in this preliminary work. As already noted, this pertains to excitons, that is to polaritons with vanishing Hopfield coefficient for the photon part. When dealing with a polariton proper, the usual stimulation of the photonic fraction comes into play and its increase requires getting closer to an actual electronic inversion population, till the limit of dominant photon fraction where the conventional lasing of an electron-hole plasma is recovered. In the simultaneous publication [6], Quantum Monte–

[6] A. İmamođlu and R. J. Ram, Physics Letter A **214**, 193 (1996).

Carlo simulations through the Quantum State Diffusion formalism were claimed to evidence a Poisson statistics for ground state excitons. We come back to that point in the next chapter of this text.

Kira *et al.*'s refutations

The observations of Pau *et al.* (1996) (cf. 1.3.3) claiming experimental evidence for the Bose action have been reproduced by the group of Khitrova and Gibbs and published with a theoretical model by Kira, Jahnke and Koch [7] in conceptual opposition with that of Īmamoġlu *et al.* The authors criticise the bosonic approximation for approximating “*the full electron-hole Coulomb interaction in the many-body hamiltonian [...] by including only some aspects of the interband attractive part*” and propose instead a full quantum picture starting from a two-band hamiltonian which includes consistently Coulomb interactions and correlations between electrons and holes. They obtain a complex set of coupled equations [their equations 1–3] for the polarisation $P_{\mathbf{k}} \equiv c_{v,\mathbf{k}}^\dagger c_{c,\mathbf{k}}$, the population operators $c_{c,\mathbf{k}}^\dagger c_{c,\mathbf{k}}$ and the photon annihilation operators B_q for photons with zero in-plane wavevector ($\mathbf{q}_{\parallel} = \mathbf{0}, q$). These are a special case of a general theory to describe light-matter interaction in semiconductors developed by the authors, which they call “*semiconductor luminescence equations*”. With the dynamical decoupling scheme (explained in details, e.g., by Binder & Koch (1995))—retaining correlators $\langle B_q^\dagger P_{\mathbf{k}} \rangle$ and $\langle B_q^\dagger b_{q'} \rangle$ and electron $f_{\mathbf{k}}^e \equiv \langle c_{c,\mathbf{k}}^\dagger c_{c,\mathbf{k}} \rangle$, hole $f_{\mathbf{k}}^h \equiv 1 - \langle c_{v,\mathbf{k}}^\dagger c_{v,\mathbf{k}} \rangle$ populations—a closed set of equations is obtained, which however remains very complicated and requires essentially numerical treatment:

$$i\hbar\partial_t \langle B_q^\dagger P_{\mathbf{k}} \rangle = (-E_c(\mathbf{k}) - E_v(\mathbf{k}) - \hbar\omega_q + E_G) \langle B_q^\dagger P_{\mathbf{k}} \rangle \quad (1.130a)$$

$$+ (f_{\mathbf{k}}^e + f_{\mathbf{k}}^h - 1) \Omega(\mathbf{k}, q) \quad (1.130b)$$

$$+ f_{\mathbf{k}}^e f_{\mathbf{k}}^h \Omega_{SE}(\mathbf{k}, q) \quad (1.130c)$$

$$i\hbar\partial_t \langle B_q^\dagger B_{q'} \rangle = \hbar(\omega_{q'} - \omega_q) \langle B_q^\dagger B_{q'} \rangle \quad (1.131a)$$

$$+ i\mathcal{E}_q \tilde{u}_q \langle B_{q'} P_H \rangle + i\mathcal{E}_{q'} \tilde{u}_{q'}^* \langle B_q^\dagger P_H \rangle \quad (1.131b)$$

$$i\hbar\partial_t f_{\mathbf{k}}^{e(h)} = 2i\Im[\mu_{cv}^*(\mathbf{k}) \langle P_{\mathbf{k}} \tilde{D} \rangle] \quad (1.132)$$

The detailed expressions for the various quantities thus involved needs not concern us here, let us content to list the physical meaning of each quantities, which yields the gist of this model: $E_{c,v}(\mathbf{k})$ are the dispersions for conduction/valence electrons (renormalised by interactions and structure details like the QW confinement factor, in a way we do not reproduce), E_G the gap energy, \mathcal{E}_q the radiation field vacuum amplitude, $\tilde{u}(\mathbf{r})$ the effective cavity mode wavefunction and μ_{cv} the dipole matrix element (see [7] for proper discussion). More importantly,

$$\Omega(\mathbf{k}, q) \equiv \mu_{cv}(\mathbf{k}) \langle B_q^\dagger \tilde{E} \rangle + \sum_{\mathbf{k}'} V(\mathbf{k}' - \mathbf{k}) \langle B_q^\dagger P_{\mathbf{k}'} \rangle, \quad (1.133)$$

$$\Omega_{SE}(\mathbf{k}, q) \equiv i\mu_{cv}(\mathbf{k}) \mathcal{E}_q \tilde{u}_q, \quad (1.134)$$

[7] M. Kira *et al.*, Phys. Rev. Lett. **79**, 5170 (1997).

which involve the Coulomb matrix element V and quantised radiation field $\tilde{E} \propto \sum_q B_q u_q$, provide the source for field-particle correlations (cf. (1.130c)). Since $f_{\mathbf{k}}^e f_{\mathbf{k}}^h \Omega_{SE}$ is nonzero in presence of excitations (electrons and holes), it triggers $\langle B_q^\dagger P_{\mathbf{k}} \rangle$ even if they are initially zero. We remind that $P_{\mathbf{k}}$ is the amplitude for an interband transition of the electron, so that $\langle B_q^\dagger P_{\mathbf{k}} \rangle$ is the photon-mediated polarisation. Thus Ω_{SE} , which drives the emission through electron-hole recombination, is interpreted as a *spontaneous emission* term. In the same way, Ω on line (1.130b) provides stimulation (the second term in (1.133) being the renormalisation of stimulation to the first “bare” stimulation term).

From these equations, one can compute the normal incidence luminescence spectrum as the time variation of the light field intensity:

$$I(\mathbf{k}) \propto \partial_t \langle B_{\mathbf{k}}^\dagger B_{\mathbf{k}} \rangle \quad (1.135)$$

This, however, demands numerical simulations, which the authors have performed and found to be in agreement with experimentalists observations. Two appealing features of such numerical approaches are the possibility to artificially neutralise some contributions, e.g., the stimulation term (1.130b), and to gain access to some experimentally awkward or poorly defined quantities, as for instance $\langle [X, X^\dagger] \rangle$. For a true boson, this quantity is exactly one, cf. eq. (1.32). The computations have shown however that this quantity varies from 0.7 down to 0.3 as a function of increasing densities (from $\approx .5$ to $\approx 3 \times 10^{11} \text{cm}^{-2}$), leading to the conclusion that the Boson picture is not valid, and that Pau et al.’s (1996) explanation in terms of close-to-bosons polaritons was mistaken. The more convincing result from this work however comes from the other numerical latitude, namely the artificial switch-off of stimulation, which in effects amounts to discard strong coupling. Doing so, they observed the persistence of the splitting, which was claimed as evidence of strong coupling.

1.2.2 Dynamics of Polaritons

Simple rate equations

Many phenomena involving polaritons derive from their dynamical properties. Even their pre-eminent characteristic—namely their composite nature as the coherent superposition of an exciton and a photon—is intrinsically dynamical, with energy being exchanged back and forth between the two—fields at a rate $\propto \Omega/\hbar$ which falls in the subpicosecond range. In this regard, the anticrossing arises from the change of paradigm through Fourier transform from this temporal picture to its energy counterpart. This is a step of great value since in the linear regime, the temporal behaviour can be dispensed with altogether, establishing the new stationary states (polaritons) as particles as real as their underlying constituents and in many respects even more “real” than coupled excitons-photons.

If the description in term of excitons and photons must be retained, the dynamics comes into play. This is an important aspect of polaritons, since they have finite lifetime through their photon fraction which can tunnel out of the cavity. This results in beats at Rabi frequency. Solving the equation in the exciton–photon basis allows to track the system dynamics in the

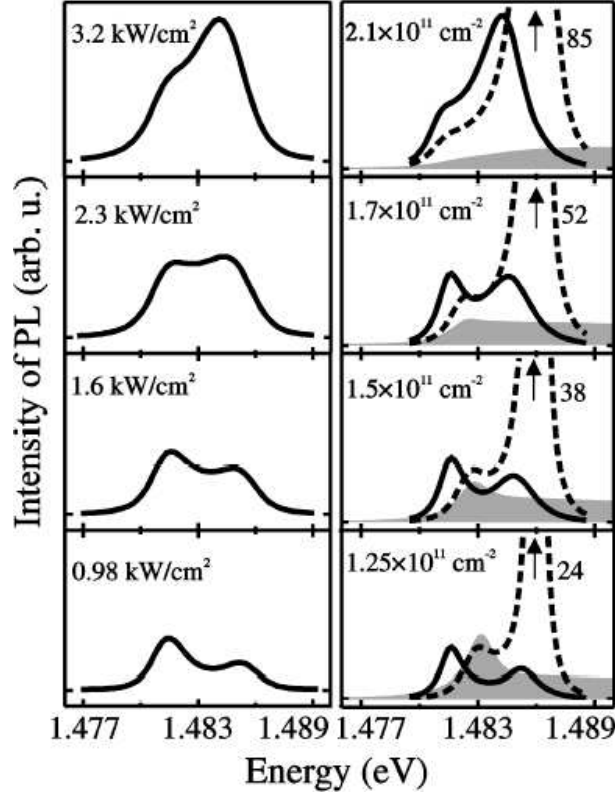


Figure 1.3: PL spectra [from Kira et al. (1997)], experimental (left column) and theoretical as computed with (1.135) solving numerically eqs. (1.130—1.132) (right column). The dashed curves were obtained by discarding line (1.130b) which is responsible for strong coupling, in absence of which the emitted spectra are clearly seen to emit at the bare cavity and “exciton” modes. The cavity detuning of 3meV is ultimately responsible for the observed splitting in the high pumping regime (top of figure) where the upper polariton branch is emitting superlinearly. The shaded curves are the excitonic absorption spectra, the exciton emission is not sensitive to the dressing of the exciton, even when the exciton resonance is bleached.

time domain to account to this cyclic exchange of energy. The hamiltonian reads:

$$H = \hbar\omega_X X^\dagger X + \hbar\omega_p B^\dagger B \quad (1.136a)$$

$$+ \hbar\Omega(B^\dagger X + BX^\dagger) \quad (1.136b)$$

$$+ \sum_k \hbar\omega_X(k) X_k^\dagger X_k + \sum_{k'} \hbar\omega_p(k') B_{k'}^\dagger B_{k'} \quad (1.136c)$$

$$+ \sum_k \hbar g_X(k) (X_k^\dagger X + X_k X^\dagger) + \sum_{k'} \hbar l(k') (B_{k'}^\dagger B + B_{k'} B^\dagger) \quad (1.136d)$$

which can be solved and give for the photon field intensity:

$$I_p(t) = \langle B^\dagger(t) B(t) \rangle = \frac{X_0^2}{\Delta\Delta^*} \Omega^2 4 \exp[-(\gamma_p + \gamma_X)t/2] \sin(\Delta t/2) \sin(\Delta^* t/2) \quad (1.137)$$

This nice analysis was provided by Jacobson, Pau, Cao, Björk & Yamamoto (1995) as a support with exceedingly good agreement to their experimental observation of temporal oscillations of light emitted by a microcavity.

Boltzmann equations: Tassone, Malpuech and Porras

For the followers of the bosonic picture, the experimental failure for Bose action comes from dynamical difficulties: the phonon-aided scattering in the ground state is not efficient because the density of states is small, which—even though it provides polaritons with a small mass and therefore a great de Broglie wavelength—results in inefficient scattering towards the ground state. As polaritons reach the small momenta region of the dispersion, they become more like photons and consequently *i*) their scattering which comes from their excitonic constitution becomes less efficient while *ii*) their lifetime reduces considerably since the leakage of the photon out of the cavity becomes more likely. This results in a *bottleneck* in the relaxation, already known for bulk polaritons (where this effect was thus named), and predicted for microcavities by Tassone, Piermarocchi, Savona, Quattropani & Schwendimann (1997).

The theoretical description of polariton dynamics involve three mechanisms: *i*) an external pumping which initiates the process (continuously or impulsively), *ii*) a relaxation of excitations with the lattice or through interparticles interactions along their dispersion relation which in the case of polaritons is shaped for rich and complicated effects and *iii*) an a radiative recombination which subtract polaritons from the system, part of which is responsible for the luminescence.

A set of Boltzmann equations, that is equations of excitations transfer, captures the interplay of these three competing mechanisms and can decide of the feasibility of a ground state population buildup. In the reciprocal space, for the number $n_{\mathbf{k}}^{\mu}$ of polaritons in state \mathbf{k} and lower/upper branch ($\mu = \text{L, P}$), they are readily written down as

$$\partial_t n_{\mathbf{k}}^{\mu} = \sum_{\nu, \mathbf{k}'} W_{\nu, \mathbf{k}' \rightarrow \mu, \mathbf{k}} n_{\mathbf{k}'}^{\nu} (n_{\mathbf{k}}^{\mu} + 1) \quad (1.138a)$$

$$- \sum_{\nu, \mathbf{k}'} W_{\mu, \mathbf{k} \rightarrow \nu, \mathbf{k}'} n_{\mathbf{k}}^{\mu} (n_{\mathbf{k}'}^{\nu} + 1) \quad (1.138b)$$

$$- \Gamma_{\mathbf{k}}^{\mu} n_{\mathbf{k}}^{\mu} + P_{\mathbf{k}}^{\mu} \quad (1.138c)$$

in the case of phonon scattering alone, as initially considered by Tassone et al. (1997). Each term has a transparent physical meaning: W are rate transfer as computed from Fermi's golden rule, Γ is the inverse lifetime summing contributions from all losses mechanisms and P the pump. The intervention of $n + 1$ expresses as explained in section 1.1.3 the Bose stimulation n in addition of spontaneous scattering $+1$, which for virtually all states is nevertheless close to 1.

The PL spectrum is derived from the numerical solutions of (1.138) in a way similar to (1.135), by relating $\Gamma_{\mathbf{k}}^{\mu} n_{\mathbf{k}}^{\mu}$ to the intensity emitted at angle θ_{PL} , the latter being given by (1.145) and Snell-Descartes relation $n \sin \theta = \sin \theta_{\text{PL}}$ with n the Bragg mirror refraction index (one for air).

Again, the relative importance of these three terms, P , W and Γ , dictates the dynamics and the eventual population buildup in low \mathbf{k} states. Tassone et al. (1997) therefore undergo a systematic study of these quantities.

The pump is intimately associated to the problem of the exciton formation time from excited electron-hole states. Its general expression depends on the injected carriers density n_c as

$$P_{\mathbf{k}} = [\mathcal{C}_{\text{ac}, \mathbf{k}} + \mathcal{C}_{\text{LO}, \mathbf{k}}] n_c, \quad (1.139)$$

where \mathcal{C}_{ac} and \mathcal{C}_{LO} are the formation coefficients for acoustic and optic phonons, respectively. In their simulations, Tassone et al. (1997) assume a thermal distribution of free carriers. After a

common practise to consider only lower branch excitonlike polaritons as created with sufficient effectiveness at a sharp point on the dispersion relation, The constant $C^{(0)}$ has been computed by Piermarocchi, Tassone, Savona, Quattropani & Schwendimann (1997)

Tassone & Yamamoto (1999) extended the previous picture to include interparticles interactions up to binary collisions (polariton-polariton two bodies interactions). This limitation, they comment, has no rigorous basis, and “*the justification is after all phenomenological, in that truncating up to the two-body interaction, we achieve a satisfactory description of the dynamics of the real system*”. This mechanism, analysed in greater details by Ciuti, Schwendimann & Quattropani (2001) for the sake of parametric amplification and providing the interaction strength as

$$V \approx \frac{6xE_b a_B^2}{L^2} \quad (1.140)$$

is later claimed by Porras, Ciuti, Baumberg & Tejedor (2002) to be the most important for relaxation towards the ground state. They limit to lower branch polaritons only where polaritons are created by continuous off-resonant excitation. In this case Eqs. (1.138) upgrade to

$$\partial_t n_i = \sum_{i'} \{W_{i \rightarrow i'} n_i (n_{i'} + 1) - W_{i' \rightarrow i} n_{i'} (n_i + 1)\} \quad (1.141a)$$

$$- \sum_{i_1, i'_1, i''_1} \{W_{i i_1 \rightarrow i'_1 i''_1}^{\text{pol-pol}} n_i n_{i_1} (n_{i_1} + 1) (n_{i'_1} + 1) \quad (1.141b)$$

$$+ W_{i'_1 i''_1 \rightarrow i i_1}^{\text{pol-pol}} n_{i'} n_{i''_1} (n_i + 1) (n_{i_1} + 1)\} \quad (1.141c)$$

$$+ P_i - \Gamma_i n_i. \quad (1.141d)$$

Malpuech, Kavokin, Di Carlo & Baumberg (2002) had previously extended polaritons Boltzmann equations¹ with inclusion of an additional relaxation mechanism to all those already mentioned, namely the electron-polariton scattering (electrons, they propose, are injected either by photoexcitation or by doping). They solve numerically (1.141) but take for the rate transitions W in lines (1.141b & 1.141c):

$$W_{\mathbf{k}_1 \mathbf{k}_2 \rightarrow \mathbf{k}'_1 \mathbf{k}'_2}^{\text{pol-pol}} + W_{\mathbf{k} \rightarrow \mathbf{k}'}^{\text{el}} \quad (1.142)$$

where the electron-aided scattering is computed with Fermi’s golden rule as

$$W_{\mathbf{k} \rightarrow \mathbf{k}'}^{\text{el-pol}} = \frac{2\pi}{\hbar} \sum_{\mathbf{q}} M^2 f_{\mathbf{q}} (1 - f_{\mathbf{q}+\mathbf{k}'-\mathbf{k}}) \delta(E_L(\mathbf{k}') - E_L(\mathbf{k}) - \frac{\hbar^2}{2m_e} (\mathbf{q}^2 - |\mathbf{q} + \mathbf{k} - \mathbf{k}'|^2)) \quad (1.143)$$

with \mathbf{q} the electron wavevector required for resonant scattering, the distribution of electrons $f_{\mathbf{q}}$ following Fermi-Dirac statistics and M the matrix element of interaction between an electron and a polariton. In this way they obtain the important results displayed on fig. 1.4 featuring the bottleneck when exciton-exciton interactions are not allowed (or significant), partial thermalisation when they are, and the efficient thermalisation brought by their additional relaxation with a gas of cold electrons.

¹In their text, Malpuech, Kavokin, Di Carlo & Baumberg (2002) write Eq. (1.141) seemingly like (1.138), with their rate transition $W_{\mathbf{k} \rightarrow \mathbf{k}'}^e$ embedding—not to say hiding—polaritons populations, namely, $W_{\mathbf{k} \rightarrow \mathbf{k}'}^e = W_{\mathbf{k} \rightarrow \mathbf{k}'}^{\text{el-pol}} n_{\mathbf{k}} n_{\mathbf{k}'}$; we shall occasionally also recourse to this practise for its convenience and brevity.)

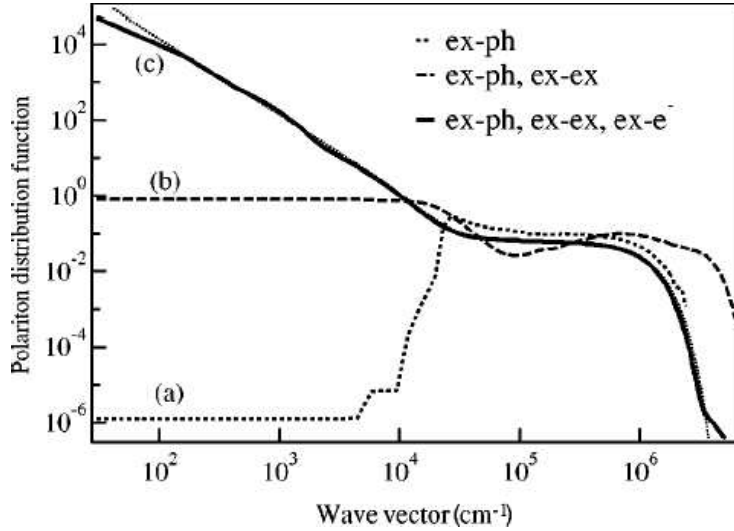


Figure 1.4: Distribution function of polaritons at 10K for a non-resonant pumping of $4.2\text{W}/\text{cm}^2$ as solved numerically by Malpuech, Kavokin, Di Carlo & Baumberg (2002), with various scattering mechanisms granted: (a) exciton-phonon alone, featuring the bottleneck of relaxation (cf. section 1.3.2), (b) exciton-exciton scattering added, providing partial thermalisation (with maximum intensity emitted at lower momenta) and (c) exciton-electron scattering added, this time coming close to full thermalisation; equilibrium Bose distribution is shown dotted for zero chemical potential.

Tassone & Yamamoto (2000) have also solved Boltzmann equations in a micropost, i.e., a microcavity of small ($\approx 2\mu\text{m}$) lateral extension, which allows them to single out a polariton state deep in the minimum and to consider all higher lying momentum states as an excitonic reservoir, which they assume in thermal equilibrium. Their approximations are to neglect the renormalisation of excitation energies and work in the Markov approximation. They limit to densities below $4 \times 10^{10}\text{cm}^{-2}$ to prevent the collapse of Rabi splitting (an assumption which holds for these values in typical GaAs samples). Calling N_i the exciton population of state i (with, in their model, the case $i = 0$ referring to the polariton), they solve a rate equation which includes P_i the pump in state i , Γ_i the rate of losses through various mechanisms such as radiative recombination, $W_{i \rightarrow i'}$ the scattering rate with phonons and $Y_{i_1 \rightarrow i' i_1}$ that with other excitons.

Recently, Cao, Doan, Thoai & Haug (2004) have solved numerically the Boltzmann equations not taking into account exciton-exciton scattering, though still obtaining condensation for some suitable choices of parameters, especially by extension of the density range. This is a result which we shall regard very favourably in next chapter since we shall claim that polariton-polariton scattering is not needed insofar as other relaxation mechanisms exist which are efficient enough to overcome bottleneck or scatter polaritons into the ground state in their radiative lifetime.

Polariton lasers

In the last years, research through Boltzmann equations of polaritons dynamics has developed a strong technological character, seeking best suited structures through heavy and systematic numerical investigations. For instance, Malpuech, Di Carlo, Kavokin, Baumberg, Zamfirescu

& Lugli (2002) have estimated that doped AlGa_N with nine QWs are able to lase in the strong coupling regime at 460K, with a threshold of 100mW on a sample of 50 μ m radius, and soon thereafter, Zamfirescu, Kavokin, Gil, Malpuech & Kaliteevski (2002) have reported that *p*-doped ZnO samples would still operate at temperatures as high as 560K—an absolute record all fields included for a critical temperature associated with BEC—and with low threshold (2mW for a spot of 10 μ m radius), claiming that ZnO is mostly [sic] suited to achieve polariton lasing. To this date it is believed that these structures are the most-promising candidates for tomorrow large scale opto-electronic devices.

In the two following chapters, we leave aside this engineering aspect and come back to the interrogation of the fundamental characteristics of the polaritons in their nonlinear or degenerated phase. The conclusion of this historical review of the field can be put as follows: two schools of thoughts have disputed the theory behind the intriguing phenomena observed in microcavities. On the one hand, that that we might call the “*fermion school*”, led by the models of Kira (for other contributors we might name Littlewood and the work of his coworkers, Keeling, Eastham, Szymanska & Littlewood (2004), or Combescot & Betbeder-Matibet (2002)), insists that a full quantum picture is required to properly take into account electron-hole and radiation field correlations which are built in the system as a result of interactions granted at the most fundamental level. The other trend—aptly called the “*boson school*” and regarded favourably, if not supported entirely, by virtually all other researchers of the field—however contends that the exact fermionic picture is an awkward description of phenomena which are well described in a boson basis, where the main effects can be understood in a simple and effective fashion.

1.3 Main Experimental Results on Exciton–Polaritons

1.3.1 Polaritons

Vacuum-field Rabi splitting

The seminal paper by Weisbuch et al. (1992) [2] was the starting point for the considerable activity to be undertaken with cavity polaritons. This includes the theoretical activity as well, which it has preceded since the main discussions related to exciton-polaritons were essentially related to bulk polaritons. In their paper therefore addressing a virgin field, Weisbuch et al. report the observed vacuum field Rabi splitting in reflectivity measurements at 5K on a GaAs-GaAlAs based cavity with seven QWs (see Fig. 3 on page 3 which is extracted from [2])

Vacuum Rabi splitting has been subsequently observed in a wealth of microcavity structures, starting the following year with the observation at room temperature (300K) by the collaboration surrounding the founding father (Houdré, Stanley, Oesterle, Ilegems & Weisbuch 1994). They measured $\Omega \approx 6.5\text{meV}$ ($\approx 8.8\text{meV}$ at 77K) with the structure displayed on fig. 1.2 on page 21. The nitride based systems have attracted special interest as compared to usual GaN or CdTe cavities for their higher exciton oscillator strength, faster relaxation rates and larger binding energies. This has been indeed confirmed by experiment; let us mention the recent reports of Antoine-Vincent, Natali, Byrne, Vasson, Disseix, Leymarie, Leroux, Semond & Massies (2003) in GaN with $\Omega = 31\text{meV}$ at 5K and that of Tawara, Gotoh, Akasaka, Kobayashi & Saitoh (2004) in InGa_N with Ω from 6 to 17meV at room temperature.

[2] C. Weisbuch, M. Nishioka, A. Ishikawa, and Y. Arakawa, Phys. Rev. Lett. **69**, 3314 (1992).

The Rabi splitting has also been observed in the time domain, the first time by Norris, Rhee, Sung, Arakawa, Nishioka & Weisbuch (1994), where it manifests as a temporal exchange of energy at Rabi frequency between the photon field and the excitonic field. The excitation can be observed in the emission spectrum only when it resides in the cavity field, “*thus the vacuum Rabi oscillation is manifested by oscillatory cavity emission*”, as observed by Norris et al. (1994).

Dispersion

In Weisbuch et al.’s (1992) paper, there is a confusion as to the nature of the observed physical object; the authors call it “*the new system*” which they describe as “*a monolithic solid state replica of the usual atomic system*” and most interestingly, which they oppose to polaritons (in bulk, though). This could have been a matter of pure lexicographic taste, which it partly was on the grounds of available data, but the fact that an energy-momentum dispersion exists compels the quasi-particle picture and thus the description in terms of polaritons, a more complicated system than the dressed state of cavity QED (the picture initially favored by the pioneers of cavity polaritons). This dispersion arises from that of photons and excitons, a situation which does not exist in atomic physics where atoms resonance are isolated and coupled to a single mode of the cavity. It was readily provided by Houdré, Weisbuch, Stanley, Oesterle, Pellandin & Ilegems (1994) after most of this collaboration, (Houdré, Stanley, Oesterle, Ilegems & Weisbuch 1994), had reestablished the polaritonic picture. Both results were made after photoluminescence (PL) experiments, since “*due to the peculiarity of the emission process of the cavity polariton, the position of the PL peaks allows the direct determination of the cavity-polariton dispersion curves*”. Indeed, as observed by the authors, the emitted intensity of photons with momentum \mathbf{k} in solid angle $d\Omega_{\text{out}}$ from polaritons tunnelling out of the cavity from solid angle $d\Omega_{\text{in}}$ (linked to $d\Omega_{\text{out}}$ by Snell-Descartes law) is related to internal polaritons configurations through

$$I(E, \theta_{\text{out}}) d\Omega_{\text{out}} = \sum_{i=L,U} I_i(E, \theta_{\text{in}}) \delta(E - E_i(|\mathbf{k}| \sin(\theta_{\text{out}}))) d\Omega_{\text{in}} \quad (1.144)$$

where $I_i(E, \theta_{\text{in}}) \equiv c_i(E, \theta_{\text{in}}) \rho_i(E) T_i(E, \theta_{\text{in}})$ is the measured PL intensity for $i = U$ (upper branch) polaritons and L (lower branch) polaritons, f is the polariton energy distribution function, ρ the polariton density of state, T the transmission coefficient of polaritons and E_i their dispersion relation (which theoretical expression is given by (1.119)). At a fixed angle θ_{out} one observes two peaks (broadened as Lorentzian or Gaussian functions according to which kind of broadening mechanisms are at work) which one can directly connect to the dispersion relation. The latter can therefore be straightforwardly reconstructed by changing the angle of observation. The ease with which one can monitor and control cavity polaritons by mere angular observations or excitations through the relation

$$\hbar c k_{\parallel} = E_U(\mathbf{k}) \sin \theta \quad (1.145)$$

between in-plane (polariton) wavevector k_{\parallel} of (1.63) and its energy E_U , make them a unique laboratory to investigate light–matter coupling, as opposed to their bulk counterparts which dynamics is hidden inside the system until they reach the surface through complicated random walks. More thorough studies of PL spectra from microcavities have been carried by several groups in 1996, (Stanley, Houdré, Weisbuch, Oesterle & Ilegems 1996, Sermage, Long, Abram, Marzin, Bloch, Planel & Thierry-Mieg 1996, Cao, Pau, Yamamoto & Björk 1996).

1.3.2 Dynamics of Polaritons

Bottleneck effect

The bottleneck has been observed experimentally by Tartakovskii, Emam-Ismaïl, Stevenson, Skolnick, Astratov, Whittaker, Baumberg & Roberts (2000) and Müller, Bleuse & André (2000). The latter work was carried out at 9K on a CdTe-based cavity excited nonresonantly at low exciton densities (below 10^{10}cm^{-2}) so that exciton-exciton scatterings were negligible. The polariton distribution, reconstructed from (1.144) as proportional to the intensity times radiative lifetime, was shown to be markedly out of equilibrium for negative detuning, with a maximum at the crossing point of the photon and exciton dispersions, corresponding to the point where the dispersion-curve slope changes sign. At positive detuning the maximum lies at normal incidence, indicating at least partial thermalization. These results are displayed on figs. 1.5 & 1.6 where the accumulation of polaritons at the bottleneck point is patent for negative detuning.

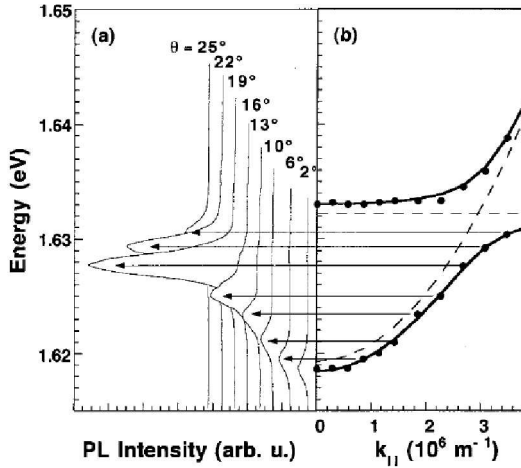


Figure 1.5: (a) Bottleneck effect exhibited for a detuning $\Delta E = -12.9\text{meV}$ as peaked PL intensity about $\theta \approx 20^\circ$. (b) Theoretical polariton dispersions (solid) and bare exciton and photon modes (dashed) superimposed to peaks of emission of fig. a, displaying accumulation of polaritons at the crossing point of the photon-exciton dispersions.

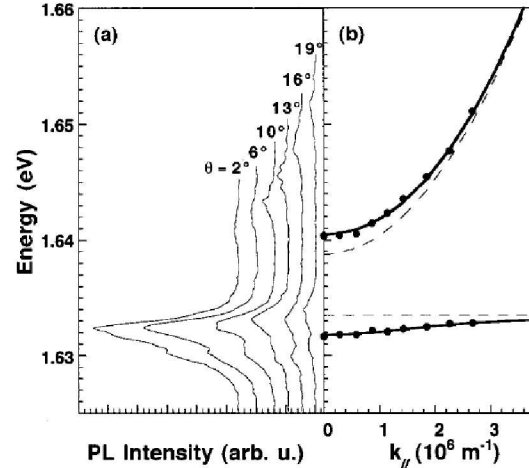


Figure 1.6: (a) Same cavity as for fig. 1.5 sampled at a point where $\Delta = +5.3\text{meV}$, with PL emission now (at least qualitatively) thermalised, with maximum intensity for normal incidence. (b) The corresponding dispersion relations with no crossing point and no change in slope. [Both figures from Müller et al. (2000)].

Tartakovskii et al. (2000) have also observed this bottleneck in a GaAs cavity displaying low k occupancies of about an order of magnitude less than at higher k for small enough excitation, with a PL peak about 16° at $\Delta E = -4.3\text{meV}$, also corresponding to the crossing of the bare exciton and photon dispersions. At zero and positive detuning, they also found the maximum of emission at normal incidence. They were however able to observe the suppression of the bottleneck from exciton-exciton scatterings at negative detuning by increasing the excitation, resulting in maximum of emission from normal incidence also.

1.3.3 Bosonic Behaviours

Laserlike stimulation

Theory once got much ahead of experiment in microcavity polariton physics with a prediction by Īmamođlu & Ram (1996) of strong bosonic manifestation of polaritons in their ground state, resulting through stimulated scattering in an out-of-equilibrium phase akin to a Bose-Einstein condensate (BEC), which the authors believed of general validity and termed the “*boser*” effect [6]. Simultaneously with this theoretical prediction in 1995—which we have already presented in some details in section 1.2.1—the experimental realisation was claimed to have been already observed in unpublished references. The publication appeared a few months later by Pau, Cao, Jacobson, Björk, Yamamoto & Īmamođlu (1996), in which the authors indeed claimed to “*present experimental evidence of spontaneous buildup of coherent exciton polariton population in a microcavity*”. They excited non-resonantly at $0.26\text{mW}/\mu\text{m}^2$ above the threshold a GaAs/Al_xGa_{1-x}As sample at 4.2K, and observed a nonlinear increase of lower and upper branch polaritons with pumping excitation past a threshold before which the increase was linear. The authors were well aware of the necessity to retain strong coupling, and of the importance of this, commenting that “*the polariton still exists, as shown by the anticrossing behavior in the angular resolved PL above threshold.*” (emphasised in italics in their text). It was however realized by the authors that this condition was in fact not met, and that they observed “*a continuous transition directly from the exciton-polariton emission to the bare photon laser without going through the intermediate phase of the exciton-polariton laser*” (Cao et al. 1997). They nevertheless retained the theoretical principle and explained the failure in this experimental attempt by exciton localization on QW interface roughness and impurities, resulting in the extension of the polariton wavefunction smaller than the de Broglie wavelength. Kira et al. (1997) took a different perspective: reporting the same experimental findings as Pau *et al.*, they supported them with a completely different theoretical modelling leaving no room for Boson effects associated with polaritons. Instead, they attribute the observed nonlinear PL in presence of two peaks by many-body correlations between the photon and the electron-hole fields, commenting not without irony that “*boser action is explained [...] without “bosonic effects”*”. They observe in a footnote that while Cao *et al.* retract the boser interpretation, they do not retract the concept of boser, “*making a quantitative theory even more essential*”.

Savvidis experiment

One of the most influential work evidencing the bosonic character of polaritons is that reported by Savvidis et al. (2000) [8]. Pavlos Savvidis, then a Ph. D. student in the group of J. J. Baumberg at Southampton, announced with coworkers observation of low temperature (4K) *stimulated scattering of polaritons* in a pump-probe experiment, “*using two different angles to separately pump and initiate the process*”, as sketched on figure (1.7b). The cavity has a varying length of average $3\lambda/2$ which allows access to different detunings (zero detuning case is shown on fig. a) The lower branch polariton dispersion, shown in solid line, was excited by varying the angle θ of the pump excitation (a 100 fs mode-locked Ti:sapphire laser injecting up to 2 mW pulses of 1.5meV bandwidth). A weak probe (power < 0.3 mW) excites with

[6] A. Īmamođlu and R. J. Ram, Physics Letter A **214**, 193 (1996).

[8] P. G. Savvidis *et al.*, Phys. Rev. Lett. **84**, 1547 (2000).

delay τ the $\mathbf{k} = \mathbf{0}$ state. When the pump is switched off (or cross-circularly polarised) the reflected spectrum displays the two polariton peaks separated by the Rabi splitting $\hbar\Omega \approx 7$ meV. When the pump is switched on and for small delays τ (with a dominant effect for zero delay), an enhancement of the emission is observed from the lower polariton branch with a gain of up to 70 for a pump excitation at angles $\theta = 16.5 \pm 2^\circ$ and with an energy adjusted to excite the lower branch resonantly (see fig. (1.8a)). The nature of the process involved was immediately reckoned: two pump polaritons scatter at the so-called *magic angle* with one polariton relaxing toward the ground state and the other scattered in a higher lying momentum state so as to ensure energy-momentum conservation:

$$E(2\mathbf{k}_p) - E(\mathbf{k}_p) = E(\mathbf{k}_p) - E(\mathbf{0}) \quad (1.146)$$

This process is sketched on fig. (1.7a). It proves the validity of the polaritonic picture since, on the one hand, condition (1.146) is impossible to meet with the quadratic dispersions ω_{cav} or ω_{ex} displayed in dashed line on fig. (1.7a), and because of the matching pump energy with that of the polariton branch on the other hand. The observed exponential gain as a function of pump intensity reported in this paper also second $n + 1$ bosonic stimulation.

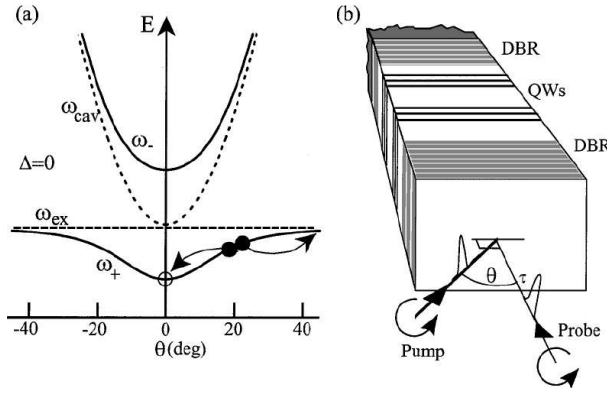


Figure 1.7: (a) Typical dispersion relations (1.119) of upper ω_- and lower ω_+ branch polaritons (solid lines), and in dashed lines the bare exciton ω_{ex} , cf. (1.112), and photon ω_{cav} , cf. (1.62), dispersions. The polariton-polariton stimulated scattering, whereby two pump polaritons $\bullet\bullet$ with momentum \mathbf{k}_p corresponding to $\theta \approx 16.5^\circ$ at zero detuning, scatter into the ground state \circ and a higher lying momentum state to ensure momentum-energy conservation (1.146). The process is stimulated by a weak probe populating the $\mathbf{k} = \mathbf{0}$ state. (b) Sketch of the experiment: the lower branch is excited resonantly by varying the angle θ and matching the energy while a probe of same polarisation is sent with a small time delay τ (positive or negative, with dominant effect at zero delay).

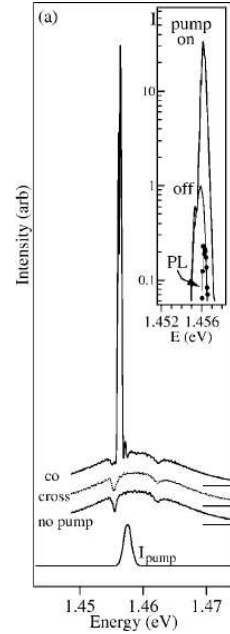


Figure 1.8: The observed considerable enhancement of lower branch polaritons.

The bottleneck and its suppression through exciton-exciton scattering which we have presented in section 1.3.2 has been confirmed by Savvidis, Baumberg, Porras, Whittaker, Skolnick & Roberts (2002) while adding evidence for stimulated scattering, which was obtained by superimposing the magic angle and bottleneck point.

Earlier work: Yamamoto, Bloch, Le Si Dang and Kira

Savvidis' experiment was the crowning achievement to evidence Bosonic stimulation. Prior to or simultaneously with that breakthrough, much activity was conducted around experimental

observation of bosonic behaviours of microcavity polaritons, most of them with the boson effect in sight. In a short and discreet paper in a modest journal, Huang, Tassone & Yamamoto (1999) reported the stimulated scattering of polaritons through a process akin to that of Savvidis but involving polaritons of opposite momenta as initial states (with two pumps exciting the sample at opposite angles). The final states had both zero momentum, thus involving both branches for energy conservation, instead of one polariton gathering all the extra momentum. Also in this experiment a probe in lower-branch $\mathbf{k} = \mathbf{0}$ polaritons was used, but, may be for this reason, the observation was made on the ground state of the *upper-branch*. Although the stimulation was obtained and well accounted for by a simple rate equation model, the effect was never as strong as that of Savvidis et al. (2000). The strong efficiency brought by the nonlinearity at the magic angle was missing. Probably to optimise the scattering efficiency, this unlucky but insightful first attempt was pumping at very high angles ($\approx 51^\circ$) to fall in the exciton-like part of the lower-branch. Moreover, even though polariton-polariton scattering would have been triggered at the magic angle, one might question whether it would not have been missed since its manifestation occurs in the *lower branch* ground state. These results were given more prominence in a rapid communication to volume B of the Physical Review (Huang, Tassone & Yamamoto 2000).

One of the great merits of Savvidis' experiment has been to firmly establish the bosonic character of polaritons, which was left more uncertain after a first erroneous claim to that effect by Pau et al. (1996). This built a tacit and probably founded suspicion that whenever the boson character was invoked in the case of polaritons, it could be more because it was a sought effect than because it was actually needed to explain the observations. The success of polariton parametric amplification, in addition to the beautiful physics it brought forward, was also its necessity of both the polariton picture and the bosonic character of these to fully explain the observations.

Earlier results where bosonic behaviours were at work but in a less transparent fashion, demand our full attention, especially those obtained by Le Si Dang et al. (1998)[9] and Senellart & Bloch (1999)[10]. They reported as early as 1998 stimulation of PL emission. The fact that the stimulation was manifest in the observed spectra rather than in the inner physical mechanism (as is the case in the polariton-polariton scattering of Savvidis) made the authors cautious. For instance Le Si Dang et al. (1998) conclude that although “*it is unambiguously shown that PL of the lower polariton state can be stimulated [...] its physical origin is not identified yet. It could be due to conventional lasing induced by partial saturation of exciton states or to direct stimulation of polariton states via exciton-phonon scattering as discussed by Imamoglu et al.*”. In the same way, Senellart & Bloch (1999) observe that “*new types of experiments [...] should experimentally allow one to unambiguously identify the stimulation process*”. This step was fulfilled by Savvidis *et al.*, hence the importance of their work. But from a fundamental point of view, there is probably equal if not more importance in the non-resonant pumping. This was fully realized by the proponents of boson action, Huang et al. (2000), who in their report of stimulated scattering—the counterpart of the more successful results from Savvidis *et al.*—comment that “*recently, several groups have reported positive results of final state stimulation in microcavity exciton-polariton systems. [...] In the present experiment, we have not achieved a boson, or the spontaneous formation of a lower polariton condensate; rather, we demonstrate that*

[9] D. Le Si Dang, D. Heger, R. André, F. Boeuf, and R. Romestain, Phys. Rev. Lett. **81**, 3920 (1998).

[10] P. Senellart and J. Bloch, Phys. Rev. Lett. **82**, 1233 (1999).

lower polaritons can exhibit final state stimulation in their scattering dynamics". This comment precedes a note added in the proof, that "after submission of this paper [14 January 2000] we became aware of the independent observation of stimulated scattering [by Savvidis *et al.*]"'. One might be tempted to see in this juxtaposition an elaborate polite way to observe that the stimulated scattering of Savvidis *et al.* (and also that of the authors, but which they probably already understood of lesser significance anyway) has little to do with the boson effect. This is indeed the case and especially for Savvidis' configuration, where one almost directly injects LB polaritons into the ground state, whereas the two branches stimulated scattering is markedly less resonant. Among the "several groups mentioned" in this all-important remark by Huang *et al.* are those of Le Si Dang and Bloch, the results of which we now consider in greater details, for they feature or at least claim bosonic behaviours without a resonant external driving.

Observing that the failure of previous attempts was due to the loss of strong coupling by the exciton ionization, Le Si Dang *et al.* opted for wide bandgap semiconductors in the II–VI family (CdTe) offering better stability of excitons. At low temperature (4.2K) they observed a Rabi splitting of about 23meV. Exciting their structure non-resonantly, two thresholds were obtained as a function of pump intensity: first the PL started to increase nonlinearly while remaining, up to a small blueshift, centered on the lower polariton resonance. At higher intensity, the PL broadened and shifted continuously towards the cavity mode, reflecting the loss of strong coupling (see Fig. 1.9 on the next page).

The experiments of Senellart & Bloch were performed in a III–V cavity but also off-resonance and at low temperature (1.4K), with similar results, namely nonlinear variation of lower-branch emission with pump intensity (in this case the upper-branch could be observed as well and seen to vary linearly over the range of pumping powers). In their first report the authors claimed this was an evidence of bosonic stimulation, with support of a three levels rate equation supplied with the experimental findings, allowing them to estimate the onset of non-linearity with a polariton population occupancy factor close to one. This occupancy factor was later experimentally contradicted and the stimulation explanation retracted by Senellart, Bloch, Sermage & Marzin (2000) who showed that the nonlinearity was due to polariton-polariton interactions rather than to some Bose effects.

Later work: Le Si Dang, Skolnick, Bloch and Yamamoto

The research effort after Savvidis *et al.* (2000) experiment was continued toward realization of the boson effect, with renewed enthusiasm and confidence for its basic principle of spontaneous coherence buildup through the formation of a Bose condensate. Boeuf, André, Romestain & Le Si Dang (2000) complemented their results [9] with a study of the impact of *i*) detuning and *ii*) Rabi splitting on the threshold of their stimulation of lower branch PL. The Rabi splitting was tuned through the number of QWs in the cavity, and the independence of threshold for nonlinearity on its value allowed them to rule out an alternative explanation in terms of localized excitons in favor of delocalized polaritons. More interestingly, they observed that the threshold was maximum at zero detuning and displayed a local minimum around -15meV . Both observations strengthen considerably the dynamic picture of relaxation toward the ground state aided by phonon scattering or through a Savvidis/Huang type of polariton-polariton energy/momentum-conserving scattering. Indeed the -15meV detuning was finding, for the structure they considered, the exciton reservoir at the energy/momentum configuration suited for a LO phonon to

[9] D. Le Si Dang, D. Heger, R. André, F. Boeuf, and R. Romestain, Phys. Rev. Lett. **81**, 3920 (1998).

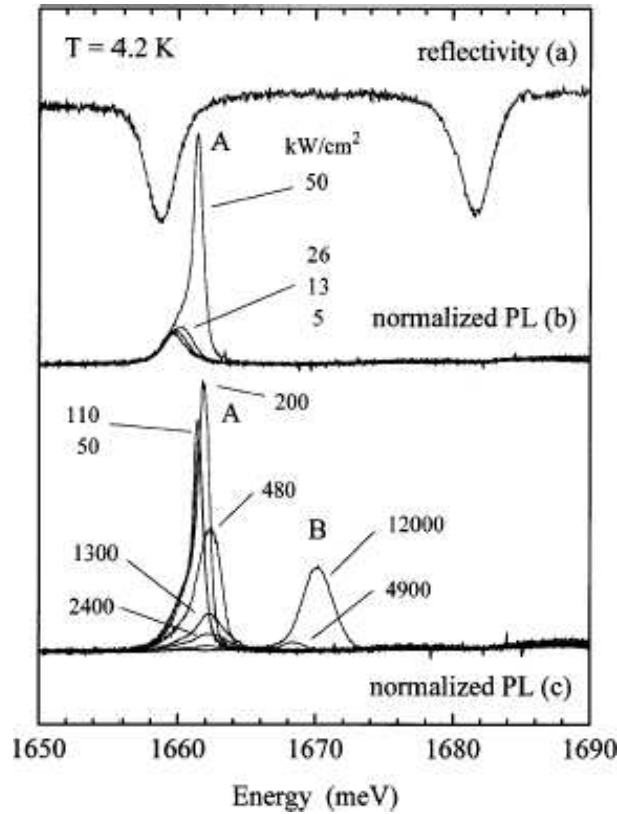


Figure 1.9: Stimulation of lower-polariton branch luminescence as reported in [9]. Upper curve displays the well resolved Rabi splitting which ensures strong coupling. In b) and c), the PL exhibits three regimes, first a linear response to weak pumping (5, 13 and 26kW/cm²) with the normalized spectrum remaining the same, then onset of stimulation yielding curve A (at 50kW/cm², the threshold is at ≈ 40 kW/cm²) which features strong enhancement of PL and a slight blueshift but still about the lower branch polariton resonance, finally for still increasing intensities, the spectrum broadens and centers about the bare cavity resonance (curve B) where it is attributed to conventional lasing of electron-hole plasma population inversion.

resonantly mediate the ground state diffusion.

Soon thereafter, Alexandrou, Bianchi, Péronned, Hallé, Boeuf, André, Romestain & Le Si Dang (2001) also reported probe amplification (though by a factor less than two). Since the off-resonant pumping does not require a good spectral definition of the pump to selectively excite the polariton branch, a good temporal definition is accessible, from which the authors were able to measure the population buildup time in the ground state starting from electron-hole injections above the bandgap energy. They found a time of 4ps. One additional notable positive result of this work is the high temperature (T=80K) at which the effect was observed.

The coherent properties of the field built in this nonlinear regime have been investigated only recently, previous studies focusing on populations only. Messin, Karr, Baas, Khitrova, Houdré, Stanley, Oesterle & Giacobino (2001) have evidenced phase sensitivity of the amplification by homodyne measurement (in the degenerate case where pump, signal and idler are all in the ground state).

1.4 Conclusions and Perspectives

There has been a surge of interest in the past decade for the realisation and understanding for BEC in microcavities. The problem was gradually understood to lie in the dynamics of relaxation of the polaritons, for which a bottleneck exist due to their strongly nonlinear dispersion relation. Although bosonic stimulation has been demonstrated, no clear and satisfying report of BEC has yet been given. Apart from this tendency for agglomeration, the system otherwise remains essentially classical with no need to abandon the paradigm of point particles. However investigations of other quantum effects exhibited by polaritons at a still deeper level is gathering popularity, like squeezing as reported by Karr, Baas, Houdré & Giacobino (2004) or various forms of quantum correlations which could raise the issue of quantum information processing with polaritons, as has been proposed, e.g., by Savasta, Stefano & Girlanda (2003) or Ciuti (2004). Those are topics which might well shape the future of the polariton physics.

For the time being, various questions raised concerning BEC remain opened. The paradigms of Kira *et al.* and Combescot, if inescapable, lead to very deep and fundamental consequences, namely the renunciation of the exciton picture in favor of subtle and complicated electron-hole correlations, and desertion of bosons statistics for all particles with a composite structure. Those are points of crucial importance not only for the specialised field of microcavities, but for solid state and even quantum physics as a whole. The points issued by these theoreticians have certainly not yet received the full attention they deserve, whatever the long term issue. However, the experimental evidence tends to favour the boson picture; such experiments as that of Savvidis fulfil enough support to legitimate continued efforts with polaritons as bose particles which are elicited to Bose condense. In this text, we retain this theme that microcavity physics is intrinsically dynamical and describable in the polariton basis. We will therefore drag with us such weaknesses as the poorly controlled bosonic picture with nonvanishing intensities or in presence of interparticle interactions. Some would argue, however, that this is precisely the point of a physical theory. At least one cannot doom a model in its infancy for such a caveat, which of course has to be fixed when the field grows mature. This reasonable approach allowed for instance Bogoliubov to develop successfully a cornerstone theory for He superfluidity, which described experimentally strongly depleted condensates with theoretical approximations which were requiring the opposite situation. This difficulty occurs in a similar fashion for polaritons, and was raised by Kira *et al.* (1997). Although there is no question of disputing the validity of the objections, we cannot help thinking of tempering them in deference for experimental evidence, as is done for instance by Moskalenko & Snoke (2000) when they observe that “*in the case of superfluid helium, the condition $na^3 \ll 1$ is manifestly not fulfilled, since the size of the helium atoms is comparable with the interparticle spacing in the liquid. Nevertheless, the Bose properties of the system as a whole still dominate the behavior.*”

For the confine of this manuscript, we therefore put aside completely the respectable fermion approach, and take concern in questions such as whether the population buildup observed from lower branch polaritons presents other features more characteristic of a quantum phase than nonlinear intensity of emission. As we have seen, the experimental activity has grown steadily in this direction—taking concern in measure of $g^{(2)}$ or the squeezing degree—but a convincing unified theoretical picture is lacking. Most of the remaining is devoted to fulfill this deficiency.

Chapter 2

Coherence in Polariton Systems

Contents

2.1	Quantum Kinetics of Polariton Relaxation in Microcavities	48
2.1.1	Semi-classical picture	48
2.1.2	Quantum dynamics of ground state polaritons	49
	Microscopic derivation of a ground state polaritons master equation	49
	Qualitative results from the master equation	55
	Analytical solution of the master equation with a seed	57
	Formulation in the Glauber-Sudarshan representation	58
	Numerical simulations	59
	Nonlinear contributions	62
	Anomalous Correlations	64
2.2	Spontaneous Coherence Buildup	65
2.2.1	Bose condensation of conserved particles	65
2.2.2	Two oscillators toy theory	66
	Quantum Boltzmann Master Equation	66
	Growth at equilibrium	71
	Growth out of equilibrium	73
2.2.3	Polariton laser	76
	Numerical simulations	80
2.3	Conclusions and Perspectives	82

2.1 Quantum Kinetics of Polariton Relaxation in Microcavities

2.1.1 Semi-classical picture

We have discussed in the introduction the need for a kinetic description of polaritons which arise from their short lifetime. While one approach, after Kira et al. (1997), advocates the description at the level of an interacting electron-hole-photon system, developing complicated correlations, e.g., between the photon field and polarisation of the electron-hole plasma, another fruitful approach, as asserted by the accord with experiments, grants polaritons as bosons. In this setting, the simplest theoretical description of their dynamics is in term of a Boltzmann equation which in essence reads (cf. eq. (1.141)):

$$\partial_t n_{\mathbf{k}} = (1 + n_{\mathbf{k}}) \sum_{\mathbf{q} \neq \mathbf{k}} W_{\mathbf{q} \rightarrow \mathbf{k}} n_{\mathbf{q}} - n_{\mathbf{k}} \sum_{\mathbf{q} \neq \mathbf{k}} W_{\mathbf{k} \rightarrow \mathbf{q}} (1 + n_{\mathbf{q}}) + P_{\mathbf{k}} - \frac{n_{\mathbf{k}}}{\tau_{\mathbf{k}}}, \quad (2.1)$$

where $n_{\mathbf{k}}$ is the average number of polaritons with wave vector \mathbf{k} , $P_{\mathbf{k}}$ is an external source term (a pump), $1/\tau_{\mathbf{k}}$ is the decay rate (radiative and non-radiative) for a polariton in this state, and $W_{\mathbf{k} \rightarrow \mathbf{q}}$ is the rate of transitions from state \mathbf{k} to state \mathbf{q} . These transitions can be caused by several mechanisms, but especially the phonon-mediated scattering and the polariton-polariton scattering. Matrix elements for these processes have been calculated as explained in the previous chapter. It should be noted that as far as Boltzmann equation is concerned, the explicit expression of these transition rates is relevant only when it comes to simulating a realistic structure, and that otherwise there is no fundamental difference between a relaxation involving a phonon or an elastic scattering with another polariton. If an effect can be evidenced with equation (2.1) it should not be attributed to one peculiar mechanism, e.g., one cannot claim that polariton-polariton interactions are intrinsically required, since identical results can be achieved dispensing from inter-particles interactions by merely promoting another relaxation mechanism (e.g., diffusion with free electrons) to enhance the transition rates.

Eq. (2.1) along with the characteristic dispersion relation of polaritons, eq. (1.62), and with suitable expressions for parameters $W_{\mathbf{k} \rightarrow \mathbf{k}'}$ and $\tau_{\mathbf{k}}$, has proved successful in providing quantitative agreement with photoluminescence experiments. It already contains in effect most of the key ingredients of the polariton physics. There is the stimulation which is embedded in the $(1 + n_{\mathbf{k}})$ expression and that helps the accumulation of polaritons in the ground state on the one hand, and all negative feedback effects which arise from the peculiarity of the dispersion relation and the increasing photon character of polaritons embedded in the transition rates on the other hand. Many results have been obtained by the investigation of the interplay of these competing effects by solving numerically the Boltzmann equation. However, a shortcoming of this formalism is that it is essentially classical. The stimulation is a mere renormalisation of transition rates and most of the important quantities, first of all the coherence, are out of its scope. To remedy to this limitation, while still keeping the full benefit from a successful Boltzmann picture, we now lay down the microscopic theory of the kinetics of ground states polaritons.

2.1.2 Quantum dynamics of ground state polaritons

Microscopic derivation of a ground state polaritons master equation

The most comprehensive microscopy theory provides the wavefunction of the entire system at all times, including electrons and holes, the radiation field, but also atoms from the lattice which vibration provide scatterings with phonons and possible other participants—like additional holes or electrons from doping—and is of course utterly intractable. With our first approximation, the three sets of particles—electrons, holes and photons—recede as polaritons granted as bosons. In the rotating wave approximation, this amounts to perform the Hopfield-Bogoliubov diagonalisation of electron-hole and photons into polaritons for each state \mathbf{k} in the semiconductor hamiltonian. This yields the so-called *polariton hamiltonian*, which reads in the interaction picture:

$$H(t) = \sum_{\mathbf{k}, \mathbf{q} \neq 0} \mathcal{U}_{\mathbf{k}, \mathbf{q}} e^{\frac{i}{\hbar}(E_L(\mathbf{k}) + \hbar\omega_{\mathbf{q}} - E_L(\mathbf{k} + \mathbf{q}))t} a_{\mathbf{k}}^\dagger b_{\mathbf{q}}^\dagger a_{\mathbf{k} + \mathbf{q}} + \text{h.c.} \quad (2.2a)$$

$$+ \sum_{\mathbf{k}, \mathbf{p}, \mathbf{q}} \mathcal{V}_{\mathbf{k}, \mathbf{p}, \mathbf{q}} e^{\frac{i}{\hbar}(E_L(\mathbf{k} + \mathbf{q}) + E_L(\mathbf{p} - \mathbf{q}) - E_L(\mathbf{k}) - E_L(\mathbf{p}))t} a_{\mathbf{k} + \mathbf{q}}^\dagger a_{\mathbf{p} - \mathbf{q}}^\dagger a_{\mathbf{k}} a_{\mathbf{p}} \quad (2.2b)$$

$$+ \sum_{\mathbf{k}, \mathbf{p}, \mathbf{q}} \mathcal{W}_{\mathbf{k}, \mathbf{p}, \mathbf{q}} e^{\frac{i}{\hbar}(E_L(\mathbf{k} + \mathbf{q}) + \frac{\hbar^2}{2m_e}|\mathbf{p} - \mathbf{q}|^2 - E_L(\mathbf{k}) - \frac{\hbar^2}{2m_e}|\mathbf{p}|^2)t} a_{\mathbf{k} + \mathbf{q}}^\dagger c_{\mathbf{p} - \mathbf{q}}^\dagger a_{\mathbf{k}} c_{\mathbf{p}} \quad (2.2c)$$

where the time dependence is shown explicitly everywhere (operators, dispersion relations and matrix elements are time-independent; their definitions have been given in the previous chapter; for convenience we repeat here but without details that a describes polaritons, b phonons and c electrons injected by doping of photoinjections so as to speed up relaxation). Thus first line (2.2a) describes polariton-phonon scattering (the term shown explicitly scatters a polariton off $\mathbf{k} + \mathbf{q}$ state into \mathbf{k} state by emission of a phonon which carries away the momentum difference \mathbf{q}); second line (2.2b) describes polariton-polariton scattering and third line (2.2c) electron-polariton scattering.

Lifetime and pumping are conveniently included at a later stage, though it is possible to include them from the start as conservative processes. For instance the lifetime comes from addition to (2.2) of the coupling of polaritons with the external (outside the cavity) radiation field, which reads:

$$H_{\text{pol-ph}} = \sum_{\mathbf{k}} \int V g(\nu) e^{i(E_L(\mathbf{k}) - \hbar\nu)t} B_{\nu}^\dagger a_{\mathbf{k}} d\nu + \text{h.c.} \quad (2.3)$$

The dissipation occurs when we trace over the external radiation field which being unbounded varies continuously and admit excitations at arbitraries frequencies ν . This approximation to separate the radiation field between a discrete set of modes $B_{\mathbf{k}}$ inside the cavity (hidden in $a_{\mathbf{k}}$ operators in (2.2)) and a continuum field outside is called the *quasi-modes coupling* approximation, it is covered more extensively for instance by Savona et al. (1998). As for the pump, depending on whether it is *i*) a coherent pumping, as is the case of a laser driving resonantly the state, or *ii*) an incoherent pumping, as is the case of a reservoir pouring particles and increasing number state only (not accessing off-diagonal elements), it is modelled by a classical (complex) field $\mathcal{P}_{\mathbf{k}}$ with operators *i*) linear and *ii*) quadratic in polaritons creation operators.

Phonons and electrons can be included as reservoirs with fast enough relaxation to maintain a thermal equilibrium (with Bose-Einstein and Fermi-Dirac distributions, respectively).

Since the density matrix of the system ρ (also in interaction picture) is dealt with partly statistically, we need upgrade Schrödinger equation to Liouville Von Neuman equation:

$$i\hbar\partial_t\rho = [H, \rho]. \quad (2.4)$$

The density matrix ρ describes polaritons of all momenta but also phonons and free electrons. We call ρ_0 the ground state polaritons reduced density matrix which is the part of interest at this stage:

$$\rho_0 \equiv \text{Tr}\rho, \quad (2.5)$$

where the trace is taken over all quantum degrees of freedom except the polariton ground state $\mathbf{k} = \mathbf{0}$. Explicitly:

$$\rho_0 \equiv \sum_{\substack{\mathcal{H}_{\text{polaritons}} \\ \mathbf{k} \neq \mathbf{0}}} \sum_{\mathcal{H}_{\text{phonons}}} \sum_{\mathcal{H}_{\text{electrons}}} \langle n_{\{\mathbf{k}\}} | \langle \theta_{\{\mathbf{k}'\}} | \langle f_{\{\mathbf{k}''\}} | \rho | f_{\{\mathbf{k}''\}} \rangle | \theta_{\{\mathbf{k}'\}} \rangle | n_{\{\mathbf{k}\}} \rangle, \quad (2.6)$$

with, following our previous conventions, n , θ , f the number of polaritons, phonons and electrons, respectively.

In thermal equilibrium, the density matrix for phonons is:

$$\rho_{\text{phonons}} = \bigotimes_{\mathbf{k}} (1 - \exp(-\beta_{\text{ph}}\hbar\omega_{\mathbf{k}})) \sum_{\theta_{\mathbf{k}}=0}^{\infty} \exp(\beta_{\text{ph}}\hbar\omega_{\mathbf{k}}\theta_{\mathbf{k}}) |\theta_{\mathbf{k}}\rangle \langle \theta_{\mathbf{k}}| \quad (2.7)$$

with a likewise expression for electrons but with Fermi-Dirac statistics.

The Boltzmann equation (2.1) is recovered from the microscopic hamiltonian (2.2) by neglecting correlations built between particles as a result of their interaction and evaluating the dynamics to second order. Explicitly, formally integrating eq. (2.4),

$$i\hbar\partial_t\rho(t) = [H(t), \rho(-\infty)] - \frac{i}{\hbar} \int_{-\infty}^t [H(t), [H(\tau), \rho(\tau)]] d\tau. \quad (2.8)$$

this amounts to perform the two following approximations: first *i*) the *Born approximation*, which states that the system does not develop correlations between the reduced density matrices for each species of particles. That is, the total density matrix can be at all times separated in terms of its various particles reduced density matrices as

$$\rho = \rho_0 \rho_{\text{polaritons}} \rho_{\text{phonons}} \rho_{\text{electrons}}, \quad (2.9)$$

with, say, $\rho_{\text{polaritons}}$ the $\mathbf{k} \neq \mathbf{0}$ polaritons states reduced density matrix—that is, $\text{Tr}\rho$ over all states but $|\{n_{\mathbf{k}}\}\rangle$ with $\mathbf{k} \neq \mathbf{0}$, which is traced as well—and obvious similar definitions for other particles. For ease of notations, we shall abbreviate ρ_a the $\mathbf{k} \neq \mathbf{0}$ polaritons density matrix and ρ_b the (time-independent) electrons and phonons density matrix, i.e.,

$$\rho_a \equiv \rho_{\text{polaritons}} \quad (2.10)$$

$$\rho_b \equiv \rho_{\text{electrons}} \rho_{\text{phonons}} \quad (2.11)$$

and

$$\mathcal{E}_{\mathbf{k},\mathbf{q}} \equiv E_L(\mathbf{k}) + \hbar\omega_{\mathbf{q}} - E_L(\mathbf{k} + \mathbf{q}) \quad (2.12)$$

$$\mathcal{E}'_{\mathbf{k},\mathbf{p},\mathbf{q}} \equiv E_L(\mathbf{k} + \mathbf{q}) + \frac{\hbar^2}{2m_e} |\mathbf{p} - \mathbf{q}|^2 - E_L(\mathbf{k}) - \frac{\hbar^2}{2m_e} |\mathbf{p}|^2 \quad (2.13)$$

the coefficients in the time dependent complex exponential, arising from the passage from Schrödinger to Interaction picture (computations with \mathcal{E}' will be found in the appendix).

This separation (2.9) is assumed to hold to first order in Born approximation. In eq. (2.8) this allows to get rid of the initial time commutator $[H(t), \rho(-\infty)]$, and upon substitution of (2.9) into (2.8), to easily evaluate traces of tensor products of operators as products of the traces. In the same spirit all anomalous correlations, i.e., those which have no interpretation in terms of classical quantities like particle numbers, are neglected. Second *ii*) the *Markov approximation*, which assumes a slow time evolution of the system as compared to the typical collision times. That is, in (2.8), $\rho(\tau)$ is replaced with $\rho(t)$, i.e., the system characteristic time of evolution is slow enough as compared to the free propagation dynamics to vary sensibly equally on both time scales, t and τ . Physically this amounts to neglect memory effects, which also amounts to neglect some correlations resulting from interactions. Indeed, Schrödinger equation is markovian. The non markovicity of (2.8) comes from the iteration which physically corresponds to self-interactions of the entire system. When some degree of freedoms are traced over (typically because they are granted as reservoirs), the instantaneous correlations thus built between the system and these reservoirs are explicitly washed out but remain to some extent as a dependency of the system on past states of the reservoirs. If the reservoir has a large band spectrum, as is the case if it has many degrees of freedoms, the correlation time is very short and Markov approximation is a good one: it physically expresses that a small system with few degrees of freedoms (in our case a single harmonic oscillator, the one modelling polaritons ground state) still behaves according to a Schrödinger equation when it is in weak coupling with a big reservoir with many degrees of freedom (in our case the whole bath of phonons).

Carrying out explicitly this procedure—especially the computation of the double commutator $[H(t), [H(\tau), \rho(t)]]$ in (2.8) with expression (2.2) for H —is now detailed for the case of polariton-phonon interaction, (2.2b). The derivation for polariton-electron (with four operators, half of them obeying Fermionic algebra) and polariton-polariton (four identical operators, complicating substantially commutation relations) is reported in appendix A. We shall use similar procedures a few other times and a general way to handle the computation with less heavy algebra will be more detailed in the course of the text for the case where Born approximation is relaxed, cf. section 2.2.3 on page 76. The innermost commutator of eq. (2.8) yields:

$$\begin{aligned} & [H(\tau), \rho(\tau)\rho_a(\tau)\rho_b] = \\ & = \left[\sum_{\mathbf{k},\mathbf{q}} \mathcal{U}_{\mathbf{k},\mathbf{q}} e^{\frac{i}{\hbar}\mathcal{E}_{\mathbf{k},\mathbf{q}}(\tau)} a_{\mathbf{k}}^\dagger b_{\mathbf{q}}^\dagger a_{\mathbf{k}+\mathbf{q}} + \sum_{\mathbf{k},\mathbf{q}} \mathcal{U}_{\mathbf{k},\mathbf{q}}^* e^{-\frac{i}{\hbar}\mathcal{E}_{\mathbf{k},\mathbf{q}}(\tau)} a_{\mathbf{k}} b_{\mathbf{q}} a_{\mathbf{k}+\mathbf{q}}^\dagger, \rho\rho_a\rho_b \right] \\ & = \sum_{\mathbf{k},\mathbf{q}} \mathcal{U}_{\mathbf{k},\mathbf{q}} e^{\frac{i}{\hbar}\mathcal{E}_{\mathbf{k},\mathbf{q}}(\tau)} [a_{\mathbf{k}}^\dagger b_{\mathbf{q}}^\dagger a_{\mathbf{k}+\mathbf{q}}, \rho\rho_a\rho_b] + \sum_{\mathbf{k},\mathbf{q}} \mathcal{U}_{\mathbf{k},\mathbf{q}}^* e^{-\frac{i}{\hbar}\mathcal{E}_{\mathbf{k},\mathbf{q}}(\tau)} [a_{\mathbf{k}} b_{\mathbf{q}} a_{\mathbf{k}+\mathbf{q}}^\dagger, \rho\rho_a\rho_b] \\ & = \sum_{\mathbf{k},\mathbf{q}} \mathcal{U}_{\mathbf{k},\mathbf{q}} e^{\frac{i}{\hbar}\mathcal{E}_{\mathbf{k},\mathbf{q}}(\tau)} (a_{\mathbf{k}}^\dagger b_{\mathbf{q}}^\dagger a_{\mathbf{k}+\mathbf{q}} \rho\rho_a\rho_b - \rho\rho_a\rho_b a_{\mathbf{k}}^\dagger b_{\mathbf{q}}^\dagger a_{\mathbf{k}+\mathbf{q}}) \\ & + \sum_{\mathbf{k},\mathbf{q}} \mathcal{U}_{\mathbf{k},\mathbf{q}}^* e^{-\frac{i}{\hbar}\mathcal{E}_{\mathbf{k},\mathbf{q}}(\tau)} (a_{\mathbf{k}} b_{\mathbf{q}} a_{\mathbf{k}+\mathbf{q}}^\dagger \rho\rho_a\rho_b - \rho\rho_a\rho_b a_{\mathbf{k}} b_{\mathbf{q}} a_{\mathbf{k}+\mathbf{q}}^\dagger) \end{aligned} \quad (2.14)$$

and so the double commutator turns out as:

$$\begin{aligned}
& [H(t), [H(\tau), \rho(\tau)\rho_a(\tau)\rho_b]] = \\
& = \left[\sum_{\mathbf{r}, \mathbf{s}} \mathcal{U}(\mathbf{r}, \mathbf{s}) e^{\frac{i}{\hbar} \mathcal{E}_{\mathbf{k}, \mathbf{q}}(t)} a_{\mathbf{r}}^\dagger b_{\mathbf{s}}^\dagger a_{\mathbf{r}+\mathbf{s}} + \sum_{\mathbf{r}, \mathbf{s}} \mathcal{U}(\mathbf{r}, \mathbf{s})^* e^{-\frac{i}{\hbar} \mathcal{E}_{\mathbf{k}, \mathbf{q}}(t)} a_{\mathbf{r}} b_{\mathbf{s}} a_{\mathbf{r}+\mathbf{s}}^\dagger, \text{“r.h.s. of (2.14)”} \right] \\
& = \sum_{\mathbf{r}, \mathbf{s}} \mathcal{U}(\mathbf{r}, \mathbf{s}) e^{\frac{i}{\hbar} \mathcal{E}_{\mathbf{k}, \mathbf{q}}(t)} \sum_{\mathbf{k}, \mathbf{q}} \mathcal{U}(\mathbf{k}, \mathbf{q}) e^{\frac{i}{\hbar} \mathcal{E}_{\mathbf{k}, \mathbf{q}}(\tau)} [a_{\mathbf{r}}^\dagger b_{\mathbf{s}}^\dagger a_{\mathbf{r}+\mathbf{s}}, a_{\mathbf{k}}^\dagger b_{\mathbf{q}}^\dagger a_{\mathbf{k}+\mathbf{q}} \rho \rho_a \rho_b - \rho \rho_a \rho_b a_{\mathbf{k}}^\dagger b_{\mathbf{q}}^\dagger a_{\mathbf{k}+\mathbf{q}}] \\
& + \sum_{\mathbf{r}, \mathbf{s}} \mathcal{U}(\mathbf{r}, \mathbf{s}) e^{\frac{i}{\hbar} \mathcal{E}_{\mathbf{k}, \mathbf{q}}(t)} \sum_{\mathbf{k}, \mathbf{q}} \mathcal{U}(\mathbf{k}, \mathbf{q})^* e^{-\frac{i}{\hbar} \mathcal{E}_{\mathbf{k}, \mathbf{q}}(\tau)} [a_{\mathbf{r}}^\dagger b_{\mathbf{s}}^\dagger a_{\mathbf{r}+\mathbf{s}}, a_{\mathbf{k}} b_{\mathbf{q}} a_{\mathbf{k}+\mathbf{q}}^\dagger \rho \rho_a \rho_b - \rho \rho_a \rho_b a_{\mathbf{k}} b_{\mathbf{q}} a_{\mathbf{k}+\mathbf{q}}^\dagger] \\
& + \sum_{\mathbf{r}, \mathbf{s}} \mathcal{U}(\mathbf{r}, \mathbf{s})^* e^{-\frac{i}{\hbar} \mathcal{E}_{\mathbf{k}, \mathbf{q}}(t)} \sum_{\mathbf{k}, \mathbf{q}} \mathcal{U}(\mathbf{k}, \mathbf{q}) e^{\frac{i}{\hbar} \mathcal{E}_{\mathbf{k}, \mathbf{q}}(\tau)} [a_{\mathbf{r}} b_{\mathbf{s}} a_{\mathbf{r}+\mathbf{s}}^\dagger, a_{\mathbf{k}}^\dagger b_{\mathbf{q}}^\dagger a_{\mathbf{k}+\mathbf{q}} \rho \rho_a \rho_b - \rho \rho_a \rho_b a_{\mathbf{k}}^\dagger b_{\mathbf{q}}^\dagger a_{\mathbf{k}+\mathbf{q}}] \\
& + \sum_{\mathbf{r}, \mathbf{s}} \mathcal{U}(\mathbf{r}, \mathbf{s})^* e^{-\frac{i}{\hbar} \mathcal{E}_{\mathbf{k}, \mathbf{q}}(t)} \sum_{\mathbf{k}, \mathbf{q}} \mathcal{U}(\mathbf{k}, \mathbf{q})^* e^{-\frac{i}{\hbar} \mathcal{E}_{\mathbf{k}, \mathbf{q}}(\tau)} [a_{\mathbf{r}} b_{\mathbf{s}} a_{\mathbf{r}+\mathbf{s}}^\dagger, a_{\mathbf{k}} b_{\mathbf{q}} a_{\mathbf{k}+\mathbf{q}}^\dagger \rho \rho_a \rho_b - \rho \rho_a \rho_b a_{\mathbf{k}} b_{\mathbf{q}} a_{\mathbf{k}+\mathbf{q}}^\dagger].
\end{aligned} \tag{2.15}$$

With, say, $A_1 \in \mathcal{H}_1$ and $A_2 \in \mathcal{H}_2$, from the tensor product structure of $\Omega = A_1 \otimes A_2$ and $\Upsilon = B_1 \otimes B_2$, we obtain immediately

$$\text{Tr}_{\mathcal{H}_2}[\Omega, \Upsilon] = [A_1, B_1] \text{Tr}_{\mathcal{H}_2}(A_2 B_2). \tag{2.16}$$

The first and fourth lines of (2.15) will not contribute if we neglect off-diagonal correlations of $\mathbf{k} \neq 0$ states. So we are left with:

$$\begin{aligned}
& [H(t), [H(\tau), \rho(\tau)\rho_a(\tau)\rho_b]] = \\
& = \sum_{\mathbf{r}, \mathbf{s}} \mathcal{U}(\mathbf{r}, \mathbf{s}) e^{\frac{i}{\hbar} \mathcal{E}(t)} \sum_{\mathbf{k}, \mathbf{q}} \mathcal{U}(\mathbf{k}, \mathbf{q})^* e^{-\frac{i}{\hbar} \mathcal{E}(\tau)} [a_{\mathbf{r}}^\dagger b_{\mathbf{s}}^\dagger a_{\mathbf{r}+\mathbf{s}}, a_{\mathbf{k}} b_{\mathbf{q}} a_{\mathbf{k}+\mathbf{q}}^\dagger \rho \rho_a \rho_b] \\
& - \sum_{\mathbf{r}, \mathbf{s}} \mathcal{U}(\mathbf{r}, \mathbf{s}) e^{\frac{i}{\hbar} \mathcal{E}(t)} \sum_{\mathbf{k}, \mathbf{q}} \mathcal{U}(\mathbf{k}, \mathbf{q})^* e^{-\frac{i}{\hbar} \mathcal{E}(\tau)} [a_{\mathbf{r}}^\dagger b_{\mathbf{s}}^\dagger a_{\mathbf{r}+\mathbf{s}}, \rho \rho_a \rho_b a_{\mathbf{k}} b_{\mathbf{q}} a_{\mathbf{k}+\mathbf{q}}^\dagger] \\
& + \sum_{\mathbf{r}, \mathbf{s}} \mathcal{U}(\mathbf{r}, \mathbf{s})^* e^{-\frac{i}{\hbar} \mathcal{E}(t)} \sum_{\mathbf{k}, \mathbf{q}} \mathcal{U}(\mathbf{k}, \mathbf{q}) e^{\frac{i}{\hbar} \mathcal{E}(\tau)} [a_{\mathbf{r}} b_{\mathbf{s}} a_{\mathbf{r}+\mathbf{s}}^\dagger, a_{\mathbf{k}}^\dagger b_{\mathbf{q}}^\dagger a_{\mathbf{k}+\mathbf{q}} \rho \rho_a \rho_b] \\
& - \sum_{\mathbf{r}, \mathbf{s}} \mathcal{U}(\mathbf{r}, \mathbf{s})^* e^{-\frac{i}{\hbar} \mathcal{E}(t)} \sum_{\mathbf{k}, \mathbf{q}} \mathcal{U}(\mathbf{k}, \mathbf{q}) e^{\frac{i}{\hbar} \mathcal{E}(\tau)} [a_{\mathbf{r}} b_{\mathbf{s}} a_{\mathbf{r}+\mathbf{s}}^\dagger, \rho \rho_a \rho_b a_{\mathbf{k}}^\dagger b_{\mathbf{q}}^\dagger a_{\mathbf{k}+\mathbf{q}}]
\end{aligned} \tag{2.17}$$

Tracing over phonons:

$$\begin{aligned}
& \text{Tr}_b[H(t), [H(\tau), \rho(\tau)\rho_a(\tau)\rho_b]] = \\
& = \sum_{\mathbf{r}, \mathbf{k}, \mathbf{q} \neq 0} \mathcal{U}(\mathbf{r}, \mathbf{q}) e^{\frac{i}{\hbar} \mathcal{E}(t)} \mathcal{U}(\mathbf{k}, \mathbf{q})^* e^{-\frac{i}{\hbar} \mathcal{E}(\tau)} [a_{\mathbf{r}}^\dagger a_{\mathbf{r}+\mathbf{q}}, a_{\mathbf{k}} a_{\mathbf{k}+\mathbf{q}}^\dagger \rho \rho_a] \theta_{\mathbf{q}} \\
& - \sum_{\mathbf{r}, \mathbf{k}, \mathbf{q} \neq 0} \mathcal{U}(\mathbf{r}, \mathbf{q}) e^{\frac{i}{\hbar} \mathcal{E}(t)} \mathcal{U}(\mathbf{k}, \mathbf{q})^* e^{-\frac{i}{\hbar} \mathcal{E}(\tau)} [a_{\mathbf{r}}^\dagger a_{\mathbf{r}+\mathbf{q}}, \rho \rho_a a_{\mathbf{k}} a_{\mathbf{k}+\mathbf{q}}^\dagger] (1 + \theta_{\mathbf{q}}) \\
& + \sum_{\mathbf{r}, \mathbf{k}, \mathbf{q} \neq 0} \mathcal{U}(\mathbf{r}, \mathbf{q})^* e^{-\frac{i}{\hbar} \mathcal{E}(t)} \mathcal{U}(\mathbf{k}, \mathbf{q}) e^{\frac{i}{\hbar} \mathcal{E}(\tau)} [a_{\mathbf{r}} a_{\mathbf{r}+\mathbf{q}}^\dagger, a_{\mathbf{k}}^\dagger a_{\mathbf{k}+\mathbf{q}} \rho \rho_a] (1 + \theta_{\mathbf{q}}) \\
& - \sum_{\mathbf{r}, \mathbf{k}, \mathbf{q} \neq 0} \mathcal{U}(\mathbf{r}, \mathbf{q})^* e^{-\frac{i}{\hbar} \mathcal{E}(t)} \mathcal{U}(\mathbf{k}, \mathbf{q}) e^{\frac{i}{\hbar} \mathcal{E}(\tau)} [a_{\mathbf{r}} a_{\mathbf{r}+\mathbf{q}}^\dagger, \rho \rho_a a_{\mathbf{k}}^\dagger a_{\mathbf{k}+\mathbf{q}}] \theta_{\mathbf{q}}
\end{aligned} \tag{2.18}$$

Eq. (2.16) implies that only terms containing at least one operator a_0 or a_0^\dagger remain after tracing over $\mathbf{k} \neq \mathbf{0}$ states since $[1, \rho] = 0$. As we neglect off-diagonal correlations, we need in fact keep each time a couple a_0, a_0^\dagger to be averaged with ρ . We further assume the cylindrical symmetry: $n_{-\mathbf{q}} = n_{\mathbf{q}}$, in which case:

$$\begin{aligned}
& \text{Tr}_{ab}[H(t), [H(\tau), \rho(\tau)\rho_a(\tau)\rho_b]] \\
&= \sum_{\mathbf{q} \neq \mathbf{0}} |\mathcal{U}_{\mathbf{0}, \mathbf{q}}|^2 e^{\frac{i}{\hbar}(\mathcal{E}(t) - \mathcal{E}(\tau))} [a_0^\dagger, a_0 \rho] (1 + n_{\mathbf{q}}) \theta_{\mathbf{q}} \\
&+ \sum_{\mathbf{q} \neq \mathbf{0}} |\mathcal{U}_{-\mathbf{q}, \mathbf{q}}|^2 e^{\frac{i}{\hbar}(\mathcal{E}(t) - \mathcal{E}(\tau))} [a_0, a_0^\dagger \rho] n_{\mathbf{q}} \theta_{\mathbf{q}} \\
&- \sum_{\mathbf{q} \neq \mathbf{0}} |\mathcal{U}_{\mathbf{0}, \mathbf{q}}|^2 e^{\frac{i}{\hbar}(\mathcal{E}(t) - \mathcal{E}(\tau))} [a_0^\dagger, \rho a_0] n_{\mathbf{q}} (1 + \theta_{\mathbf{q}}) \\
&- \sum_{\mathbf{q} \neq \mathbf{0}} |\mathcal{U}_{-\mathbf{q}, \mathbf{q}}|^2 e^{\frac{i}{\hbar}(\mathcal{E}(t) - \mathcal{E}(\tau))} [a_0, \rho a_0^\dagger] (1 + n_{\mathbf{q}}) (1 + \theta_{\mathbf{q}}) \\
&+ \sum_{\mathbf{q} \neq \mathbf{0}} |\mathcal{U}_{\mathbf{0}, \mathbf{q}}|^2 e^{\frac{i}{\hbar}(\mathcal{E}(\tau) - \mathcal{E}(t))} [a_0, a_0^\dagger \rho] n_{\mathbf{q}} (1 + \theta_{\mathbf{q}}) \\
&+ \sum_{\mathbf{q} \neq \mathbf{0}} |\mathcal{U}_{-\mathbf{q}, \mathbf{q}}|^2 e^{\frac{i}{\hbar}(\mathcal{E}(\tau) - \mathcal{E}(t))} [a_0^\dagger, a_0 \rho] (1 + n_{\mathbf{q}}) (1 + \theta_{\mathbf{q}}) \\
&- \sum_{\mathbf{q} \neq \mathbf{0}} |\mathcal{U}_{\mathbf{0}, \mathbf{q}}|^2 e^{\frac{i}{\hbar}(\mathcal{E}(\tau) - \mathcal{E}(t))} [a_0, \rho a_0^\dagger] (1 + n_{\mathbf{q}}) \theta_{\mathbf{q}} \\
&- \sum_{\mathbf{q} \neq \mathbf{0}} |\mathcal{U}_{-\mathbf{q}, \mathbf{q}}|^2 e^{\frac{i}{\hbar}(\mathcal{E}(\tau) - \mathcal{E}(t))} [a_0^\dagger, \rho a_0] n_{\mathbf{q}} \theta_{\mathbf{q}}
\end{aligned} \tag{2.19}$$

Finally, grouping terms:

$$\begin{aligned}
& \text{Tr}_{ab}[H(t), [H(\tau), \rho(\tau)\rho_a(\tau)\rho_b]] \\
&= [a_0^\dagger, a_0 \rho] \sum_{\mathbf{q} \neq \mathbf{0}} \left(|\mathcal{U}_{\mathbf{0}, \mathbf{q}}|^2 e^{\frac{i}{\hbar}(\mathcal{E}(t) - \mathcal{E}(\tau))} (1 + n_{\mathbf{q}}(\tau)) \theta_{\mathbf{q}} + |\mathcal{U}(-\mathbf{q}, \mathbf{q})|^2 e^{\frac{i}{\hbar}(\mathcal{E}(\tau) - \mathcal{E}(t))} (1 + n_{\mathbf{q}}(\tau)) (1 + \theta_{\mathbf{q}}) \right) \\
&+ [a_0, a_0^\dagger \rho] \sum_{\mathbf{q} \neq \mathbf{0}} \left(|\mathcal{U}_{-\mathbf{q}, \mathbf{q}}|^2 e^{\frac{i}{\hbar}(\mathcal{E}(t) - \mathcal{E}(\tau))} n_{\mathbf{q}}(\tau) \theta_{\mathbf{q}} + |\mathcal{U}(0, \mathbf{q})|^2 e^{\frac{i}{\hbar}(\mathcal{E}(\tau) - \mathcal{E}(t))} n_{\mathbf{q}}(\tau) (1 + \theta_{\mathbf{q}}) \right) \\
&+ \text{h.c.}
\end{aligned} \tag{2.20}$$

The previous computation was concerned with the commutator only. Back to the full Schrödinger equation (2.8),

$$\begin{aligned}
\partial_t \rho_0 = & - \frac{1}{2} [R_{\text{out}}(t) (a_0^\dagger a_0 \rho_0 - 2a_0 \rho_0 a_0^\dagger + \rho_0 a_0^\dagger a_0) \\
& + R_{\text{in}}(t) (a_0 a_0^\dagger \rho_0 - 2a_0^\dagger \rho_0 a_0 + \rho_0 a_0 a_0^\dagger)],
\end{aligned} \tag{2.21}$$

where $R_{\text{in/out}}$ are eq. (2.20) scalar coefficients integrated over τ , in which the time dependence is shown explicitly everywhere. Markov approximation grants that $n_{\mathbf{k}}(t) \approx n_{\mathbf{k}}(\tau)$, which allows to factor all populations and transitions rates out of the integral in which remain the complex exponentials only. Using the identity

$$\frac{1}{\pi\hbar} \int_{-\infty}^t e^{\pm i\mathcal{E}(t-\tau)/\hbar} d\tau = \delta(\mathcal{E}) \quad (2.22)$$

and discarding terms which do not conserve energy (because of $\delta(E_{\text{pol}}(\mathbf{q}) + \hbar\omega_{\mathbf{q}})$), we find in the case we have just considered (granting polariton-phonon scatterings only):

$$\begin{aligned} R_{\text{in}} &= \frac{2\pi}{\hbar} \sum_{\mathbf{q} \neq 0} |\mathcal{U}_{0,\mathbf{q}}|^2 n_{\mathbf{q}} (1 + \theta_{\mathbf{q}}) \delta(E_{\text{pol}}(\mathbf{q}) - \hbar\omega_{\mathbf{q}}) \\ R_{\text{out}} &= \frac{2\pi}{\hbar} \sum_{\mathbf{q} \neq 0} |\mathcal{U}_{0,\mathbf{q}}|^2 (1 + n_{\mathbf{q}}) \theta_{\mathbf{q}} \delta(E_{\text{pol}}(\mathbf{q}) - \hbar\omega_{\mathbf{q}}) \end{aligned} \quad (2.23)$$

This procedure can be applied along these lines for electron-polariton and polariton-polariton scattering. They both bring specific difficulties, which are more technical than proper to some underlying physics. For this reason we report their treatment to the appendix, and give the result here. In the general case, where R_{out} and R_{in} are time dependent parameters which we can express as

$$R_{\text{in}} = W_{\text{in}}^{\text{pol-ph}} + W_{\text{in}}^{\text{pol-el}} + W_{\text{in}}^{\text{pol-pol}} \quad (2.24a)$$

$$R_{\text{out}} = W_{\text{out}}^{\text{pol-ph}} + W_{\text{out}}^{\text{pol-el}} + W_{\text{out}}^{\text{pol-pol}} + \frac{1}{\tau_0} \quad (2.24b)$$

in terms of the auxiliary variables given by the microscopic derivation:

$$W_{\text{in}}^{\text{pol-ph}}(t) = \frac{2\pi}{\hbar} \sum_{\mathbf{q} \neq 0} |\mathcal{U}_{0,\mathbf{q}}|^2 n_{\mathbf{q}}(t) (1 + \theta_{\mathbf{q}}) \delta(E^{\text{L}}(\mathbf{q}) - \hbar\omega_{\mathbf{q}}) \quad (2.25a)$$

$$W_{\text{out}}^{\text{pol-ph}}(t) = \frac{2\pi}{\hbar} \sum_{\mathbf{q} \neq 0} |\mathcal{U}_{0,\mathbf{q}}|^2 (n_{\mathbf{q}}(t) + 1) \theta_{\mathbf{q}} \delta(E^{\text{L}}(\mathbf{q}) - \hbar\omega_{\mathbf{q}}) \quad (2.25b)$$

$$\begin{aligned} W_{\text{in}}^{\text{pol-el}}(t) &= \frac{2\pi}{\hbar} \sum_{\mathbf{q} \neq 0, \mathbf{s}} |\mathcal{W}_{\mathbf{q},\mathbf{s},-\mathbf{q}}|^2 n_{\mathbf{q}}(t) f_{\mathbf{s}} (1 - f_{\mathbf{q}+\mathbf{s}}) \times \\ &\quad \times \delta(E^{\text{L}}(\mathbf{0}) + \frac{\hbar^2}{2m_e} |\mathbf{q} + \mathbf{s}|^2 - E^{\text{L}}(\mathbf{q}) - \frac{\hbar^2}{2m_e} |\mathbf{s}|^2) \end{aligned} \quad (2.25c)$$

$$\begin{aligned} W_{\text{out}}^{\text{pol-el}}(t) &= \frac{2\pi}{\hbar} \sum_{\mathbf{q} \neq 0, \mathbf{s}} |\mathcal{W}_{\mathbf{q},\mathbf{s},-\mathbf{q}}|^2 (n_{\mathbf{q}}(t) + 1) f_{\mathbf{s}} (1 - f_{\mathbf{s}-\mathbf{q}}) \times \\ &\quad \times \delta(E^{\text{L}}(\mathbf{q}) + \frac{\hbar^2}{2m_e} |\mathbf{s} - \mathbf{q}|^2 - E^{\text{L}}(\mathbf{0}) - \frac{\hbar^2}{2m_e} |\mathbf{s}|^2) \end{aligned} \quad (2.25d)$$

$$\begin{aligned} W_{\text{in}}^{\text{pol-pol}}(t) &= \frac{2\pi}{\hbar} \sum_{\mathbf{q}, \mathbf{s}} |\mathcal{V}_{\mathbf{q},\mathbf{q}+\mathbf{s},\mathbf{s}}|^2 (n_{\mathbf{q}+\mathbf{s}}(t) + 1) n_{\mathbf{q}} n_{\mathbf{s}} \times \\ &\quad \times \delta(E^{\text{L}}(\mathbf{q} + \mathbf{s}) + E^{\text{L}}(\mathbf{0}) - E^{\text{L}}(\mathbf{q}) - E^{\text{L}}(\mathbf{s})) \end{aligned} \quad (2.25e)$$

$$\begin{aligned} W_{\text{out}}^{\text{pol-pol}}(t) &= \frac{2\pi}{\hbar} \sum_{\mathbf{q}, \mathbf{s}} |\mathcal{V}_{\mathbf{q},\mathbf{q}+\mathbf{s},\mathbf{s}}|^2 n_{\mathbf{q}+\mathbf{s}}(t) (n_{\mathbf{q}} + 1) (n_{\mathbf{s}} + 1) \times \\ &\quad \times \delta(E^{\text{L}}(\mathbf{q}) + E^{\text{L}}(\mathbf{s}) - E^{\text{L}}(\mathbf{q} + \mathbf{s}) - E^{\text{L}}(\mathbf{0})). \end{aligned} \quad (2.25f)$$

These turn out to be exactly the rate transitions of the semi-classical Boltzmann equation (2.1). Note that through the time dependence of polariton numbers, these transition rates

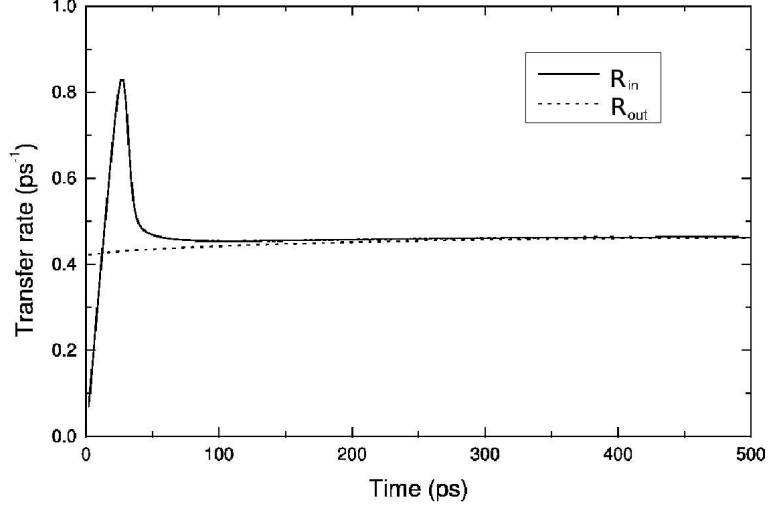


Figure 2.1: Transition rates R_{in} , R_{out} as a function of time, as computed numerically from semi-classical Boltzmann equation for a typical GaAs based cavity and for a strong enough pumping, so that R_{in} overcome significantly R_{out} at an early relaxation stage. In the time domain where $R_{\text{in}} > R_{\text{out}}$, stimulated scattering of polaritons into the ground state flares up, the income rate increases drastically and becomes much greater than the outcome rate. As a result, states with $\langle a_0 \rangle = 0$ are unstable, and a small seed with nonzero order parameter is amplified. In the infinite time limit, $R_{\text{in}} < R_{\text{out}}$ and all the coherence is lost in the system, but can be retained over macroscopic times as the difference is very small. At lower pumping, R_{in} always remains less than R_{out} and the coherence injected into the system is quickly lost.

are also time dependent. They are plotted as a function of time (in a case where parameters allow condensation) on fig. 2.1. As for τ_0 , it corresponds to the lifetime of ground state polaritons (obtained by the perturbation from vacuum fluctuations of the outside radiation field as shown in the appendix). Such an approach has also been used by Glazov, Shelykh, Malpuech, Kavokin, Kavokin & Solnyshkov (2005) to derive polaritons equations of motions including the spin degree of freedom, which is very valuable because one cannot write such equations for the spin from intuition as is conceivable for populations.

Qualitative results from the master equation

Eq. (2.21) provides the equations of motion for any average $A_0 \equiv \langle \hat{A}_0 \rangle$ of a ground state operator \hat{A}_0 , through

$$\partial_t A_0 = \text{Tr}(\hat{A}_0 \partial_t \rho_0) \quad (2.26)$$

$$= -\frac{1}{2} [R_{\text{out}}(t) (\langle \hat{A}_0 a_0^\dagger a_0 \rangle - 2 \langle a_0^\dagger \hat{A}_0 a_0 \rangle + \langle a_0^\dagger a_0 \hat{A}_0 \rangle) + R_{\text{in}}(t) (\langle \hat{A}_0 a_0 a_0^\dagger \rangle - 2 \langle a_0 \hat{A}_0 a_0^\dagger \rangle + \langle a_0 a_0^\dagger \hat{A}_0 \rangle)], \quad (2.27)$$

For instance the equation for $n_0 \equiv \langle a_0^\dagger a_0 \rangle$ is obtained in this way as:

$$\partial_t n_0 = R_{\text{in}} - (R_{\text{out}} - R_{\text{in}}) n_0. \quad (2.28)$$

(the procedure which is here straightforward is detailed in the case of self-interaction in the condensate on page 63.) This fulfills our initial goal to link to the Boltzmann theory since

eq. (2.28)—with rates we have seen to correspond to those obtained by Fermi’s golden rule, used in Boltzmann equation—coincides with the semiclassical kinetic equation, cf. eq. (2.1) without probe:

$$\partial_t n_{\mathbf{0}} = (1 + n_{\mathbf{0}}) \sum_{\mathbf{q} \neq \mathbf{0}} W_{\mathbf{q} \rightarrow \mathbf{0}} n_{\mathbf{q}} - n_{\mathbf{0}} \sum_{\mathbf{q} \neq \mathbf{0}} W_{\mathbf{0} \rightarrow \mathbf{q}} (1 + n_{\mathbf{q}}) - \frac{n_{\mathbf{0}}}{\tau_{\mathbf{0}}}, \quad (2.29)$$

with, again, rate transitions $W_{\mathbf{k} \rightarrow \mathbf{q}}$ given by Fermi’s golden rule. For instance, in the phonon-polariton scattering, they are given by

$$\begin{aligned} W_{\mathbf{q} \rightarrow \mathbf{0}} &= \frac{2\pi}{\hbar} |\mathcal{W}_{\mathbf{0}, \mathbf{q}}|^2 (1 + \theta_{\mathbf{q}}) \delta(E_L(\mathbf{q}) - \hbar\omega_{\mathbf{q}}) \\ W_{\mathbf{0} \rightarrow \mathbf{q}} &= \frac{2\pi}{\hbar} |\mathcal{W}_{\mathbf{0}, \mathbf{q}}|^2 \theta_{\mathbf{q}} \delta(E_L(\mathbf{q}) - \hbar\omega_{\mathbf{q}}) \end{aligned} \quad (2.30)$$

But in addition of these classical quantities which were known from semi-classical equations, we now have access to these variables which characterise the coherent properties of a condensate, as the order parameter $\langle a_{\mathbf{0}} \rangle$,

$$\partial_t \langle a_{\mathbf{0}} \rangle = -\frac{1}{2} (W_{\text{in}} - W_{\text{out}}) \langle a_{\mathbf{0}} \rangle, \quad (2.31)$$

or the second-order correlator, $\langle a_{\mathbf{0}}^\dagger a_{\mathbf{0}}^\dagger a_{\mathbf{0}} a_{\mathbf{0}} \rangle$. The latter is linked to second order coherence measured in two-photon counting experiments, for instance through $g^2(0)$, cf. eq. (1.48). It is convenient to use the *coherence ratio* χ (1.54) related to $g^2(0)$ by

$$\chi \equiv \sqrt{2 - g^2(0)} \quad (2.32)$$

and which corresponds to the ratio of coherent ground state polaritons over total number of ground state polaritons, $\chi = n_c/n_{\mathbf{0}}$, where we remind that $n_{\mathbf{0}} = n_c + n_t$, n_c the number of “coherent polaritons” as explained in first chapter on page 18. In the present setting, this quantity is also expressed by

$$\chi \equiv \frac{\sqrt{2n_{\mathbf{0}}^2 - \langle a_{\mathbf{0}}^\dagger a_{\mathbf{0}}^\dagger a_{\mathbf{0}} a_{\mathbf{0}} \rangle}}{n_{\mathbf{0}}}, \quad (2.33)$$

Often we shall find more convenient to use the so-called *normalised coherence ratio* which we define as :

$$\eta \equiv 2 - g^2(0) \quad (2.34)$$

η varies from 0 for the thermal state to 1 for the coherent state and is directly connected to the important experimental parameter $g^2(0)$, though χ has more physical significance. However, since χ has no relation to the number of condensed polaritons, but only characterise the coherence degree of whatever number is in the ground state (possibly zero), we normalise it to the total population by studying also the evolution of still another quantity, v , defined as the ratio of $\mathbf{k} = \mathbf{0}$ coherent polaritons over the entire polariton population (including all states). This quantity is therefore given by

$$v \equiv \frac{n_{\mathbf{0}} \chi}{\sum_{\mathbf{q}} n_{\mathbf{q}}} \quad (2.35)$$

Initially, while the seed provides maximum coherence for the ground state ($\chi = 1$), this is for a negligible amount $n_{\mathbf{0}}$ as opposed to the total population $\sum_{\mathbf{q}} n_{\mathbf{q}} \gg n_{\mathbf{0}}$ injected incoherently by

off-resonant pumping. Therefore initially ν is essentially zero. As we show below in some regime it can reach values close to 1, meaning that a macroscopic amount of particles have reached the ground state and belong to the coherent fraction in this state. This quantity ν in the confine of the present model is the best representative of Bose condensation, taking into account both the population (classical aspect described by Boltzmann equation) and its coherence degree (quantum aspect). We shall be solving shortly the equations to obtain this quantity but before doing so, another equation is worth considering. Using eq. (2.21), we find

$$\partial_t n_c = -(R_{\text{in}} - R_{\text{out}}) n_c . \quad (2.36)$$

which, may be not surprisingly, has the same shape as the equation for the order parameter (2.31). In fact, the time dependence of χ is proportional to that of $\langle a_0 \rangle / n_0$. Therefore, in our approximations (Born and Markov for a system without inter-particles interactions), the evolution of the order parameter and the number of coherent ground state polaritons are given by homogeneous equations: both the order parameter and the coherence cannot spontaneously build up from an incoherent system. This difficulty is encountered in any theory which deals with average quantities for finite size systems, especially in mean-field theory. The fluctuations, which lead to the spontaneous symmetry breaking when the critical conditions are met, have been systematically traced out, so that a seed must be introduced artificially in order to correctly describe the phase transition process. If we further compare (2.36) with (2.28), we see that, quite naturally, the inhomogeneous part which allows the population buildup comes from the spontaneous diffusion. The stimulated diffusion which will be triggered by this incoherent population will not favor a phase which has not been selected by the spontaneous process, and therefore the amplified population remains incoherent. In this framework, therefore, the fluctuation from spontaneous term cannot serve as a seed for coherence. We bypassed this limitation by considering such a seed modelled by a coherent state. Alternatively, this can also be understood as a weak coherent pulsed probe injected in the ground state.

Analytical solution of the master equation with a seed

While the master equation cannot describe the spontaneous coherence buildup, it is valid to describe dynamics between the condensate if it already exists in the system, and its ‘‘vapour’’. We therefore consider the condensate is present in the system at initial time, which amounts to seed the system with a coherent state (as discussed previously, a population seed is not needed and even if present does not trigger coherence if it is itself devoid of any).

Equation (2.21) is famous as the paradigm master equation for a damped harmonic oscillator. There is an important difference, however, between eq. (2.21) and the equation for an oscillator coupled to a thermal bath: in our case, the coefficients W_{in} and W_{out} depend on time through the occupation numbers $n_q(t)$ of the polaritons which are not in the condensate. They become time independent only when the non-condensed polaritons are thermalized. In the case $\Gamma_0 = 0$, their equilibrium values, \bar{W}_{in} and \bar{W}_{out} are related by:

$$\frac{\bar{W}_{\text{out}}}{\bar{W}_{\text{in}}} = \exp \frac{|\mu|}{k_B T} , \quad (2.37)$$

due to the detailed balance, with μ the small negative chemical potential of the polariton system at equilibrium. The time dependence of rates far from the equilibrium produces, as we show below, nontrivial features in the evolution of ρ_0 .

Using as the condensate seed a coherent state, it is possible to derive the analytical solution for $\rho_0(t)$ if rate transitions $W_{\text{in/out}}$ are known at all times (which is obtained numerically). Indeed, if one solution for the density matrix, let us call it $r_0(t)$, is known, other solutions (for different initial conditions) are obtained from $D(\alpha)r_0D(\alpha)^\dagger$, with D the displacement operator provided that $\partial_t \alpha = (1/2)(W_{\text{in}} - W_{\text{out}})\alpha$. Therefore the problem is reduced to finding the solution $r_0(t)$ with $r_0(0) = |0\rangle\langle 0|$. This particular solution can be written as $r_0(t) = f(a_0^\dagger a_0, t)$ and it follows from eq. (2.21) and the relation

$$a_0 f(a_0^\dagger a_0, t) = f(a_0^\dagger a_0 + 1, t) a_0 \quad (2.38)$$

that $f(z, t)$ satisfies the differential-difference equation

$$\partial_t f = W_{\text{out}}(t)[(z+1)f(z+1, t) - zf(z, t)] \quad (2.39)$$

$$+ W_{\text{in}}(t)[zf(z-1, t) - (z+1)f(z, t)] \quad (2.40)$$

which can be solved by Laplace transform with respect to z , turning eq. (2.39) into a first-order partial differential equation, solvable with the method of characteristics. The final result is:

$$\rho_0(t) = \frac{1}{1+m(t)} D(G(t)\alpha_0) \exp\left\{-\ln\left[\frac{1+m(t)}{m(t)}\right] a_0^\dagger a_0\right\} D(G(t)\alpha_0)^\dagger. \quad (2.41)$$

where intervening parameters are defined as

$$G(t) \equiv \exp\left[\frac{1}{2}\int_0^t (W_{\text{in}}(\tau) - W_{\text{out}}(\tau)) d\tau\right], \quad m(t) \equiv G(t)^2 \int_0^t \frac{W_{\text{in}}(\tau)}{G(\tau)^2} d\tau. \quad (2.42)$$

Formulation in the Glauber-Sudarshan representation

The significance of parameters (2.42) and the physical meaning of the solution is more transparent in the Glauber-Sudarshan representation of the density matrix, cf. (1.45). In this representation, the master equation (2.21) becomes a Fokker-Planck equation

$$\partial_t P = \frac{1}{2}(W_{\text{out}} - W_{\text{in}})(\partial_\alpha \alpha + \partial_{\alpha^*} \alpha^*)P + W_{\text{in}} \partial_{\alpha, \alpha^*}^2 P \quad (2.43)$$

with solution

$$P(\alpha, \alpha^*, t) = \frac{1}{\pi m(t)} \exp\left[-\frac{|\alpha - G(t)\alpha_0|^2}{m(t)}\right] \quad (2.44)$$

This can be deduced from (2.41) or checked by brute force calculation, as is done in appendix (A.2). This is the convolution of a centred gaussian of variance $m(t)$ with a delta function centred about $G(t)\alpha_0$. The former, as a P function, describes a thermal state of mean $m(t)$ while the latter describes a coherent state of mean $G(t)\alpha_0$. Since convolutions of P functions describe superpositions of fields, we have now completed the description of the dynamics of a coherent seed, which can be profitably seen as an input signal to the device: there is a simultaneous coherent amplification of the signal, given by the gain $G(t)$, and an incoherent amplification, attributable to spontaneous diffusion of the order parameter.

Numerical simulations

Exploitation of this formalism requires numerical simulations (needed to calculate the rates in eq. (2.21)), which we have performed and published as Rubo, Laussy, Malpuech, Kavokin & Bigenwald (2003) [11]. They show that in the regime where the dynamics (dictated by semi-classical Boltzmann equations) allows a population buildup in the ground state, the signal retains its shape, especially its phase, over macroscopic time duration. Otherwise it gets quickly damped towards a thermal state again, which is being amplified incoherently.

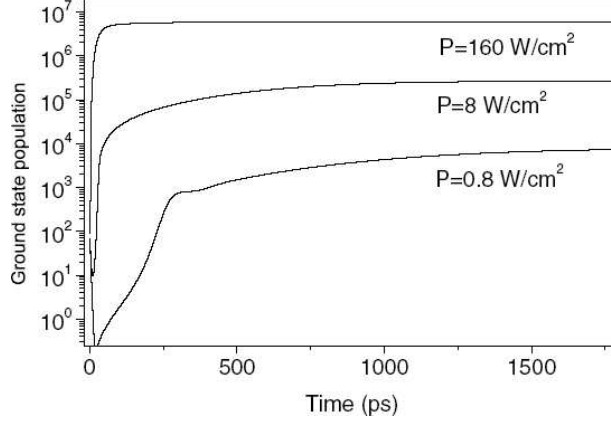


Figure 2.2: Ground state polaritons population $n_0 = \langle a_0^\dagger a_0 \rangle$ as a function of time, for pumping power of .8, 8 and 160W/cm² respectively as reported on the curves. In all case the final occupancy is much higher than one, which has little absolute meaning in a finite size system, although in the kinetic equations, e.g., eq. (2.1), the stimulated term n_0 dominates over 1. Anyway, in this context of Boltzmann equations, this does not presume of the coherent properties, cf. figs 2.3 and table 2.2, which report that for the lowest pumping, near ten thousand polaritons are in the ground state, but have no coherence. At $t = 0$ a seed of 100 polaritons is present (which is seen as the drop of population near initial time which corresponds to $P = .8$ and $P = 8$ W/cm², and not to the higher pumping which rises from the start)

Table 2.1: Parameters used for numerical computations.

Cavity photon lifetime	Non radiative lifetime	Heavy hole exciton mass	Electron mass
8ps	1ns	$0.5m_0$	$0.07m_0$

Table 2.2: Main equilibrium values obtained numerically.

Pumping density (W/cm ²)	N_0	N_0/N_1	N_0/N	$-\mu$ (μ eV)
0.8	7.7×10^3	23.5	0.04	56
8	2.7×10^5	510	0.59	1.6
160	5.8×10^6	5800	0.95	0.07

We consider a GaAs based microcavity containing a single quantum well that we model numerically with the parameters listed in table 2.1. The structure contains an equilibrium free electron gas of density 10^{10} cm⁻² in order to speed up relaxation processes and achieve more

[11] Y. G. Rubo, F. P. Laussy, G. Malpuech, A. Kavokin, and P. Bigenwald, Phys. Rev. Lett. **91**, 156403 (2003).

easily condensation conditions. We also take into account a finite system size R which is assumed to be given by a $100\mu\text{m}$ excitation spot size. This is practically done considering a spacing of $2\pi/R$ between the ground state and the first excited states, whereas the remaining reciprocal space's states are assumed to vary continuously. We model the following experiment: at $t = 0$ an ultrashort laser pulse generates a coherent ground state population containing 100 polaritons, which act as a coherent seed. At the same time, an incoherent non-resonant cw pumping is turned on. The pumping is assumed to give rise to an homogeneous exciton generation rate between states $|\mathbf{k}_1| = 5 \times 10^8 \text{m}^{-1}$ and $7 \times 10^8 \text{m}^{-1}$ which corresponds to an excess energy of 19 and 36 meV. Temperature injection of the exciton gaz is therefore of the order of 300K. Three pumping densities (0.8, 8, and 160W/cm^2) are considered. For all the power used, equilibrium polariton density remains smaller than the oscillator strength bleaching density. This ensures that strong coupling is maintained throughout the experiment. Fig. 2.2 displays the evolution of the ground state population for the pumping densities considered. One can observe that they all achieve values much larger than one. Table 2.2 reports the main equilibrium values obtained, namely, ground state populations, ratio between populations of the ground state and of the first excited state, ratio between ground state populations and total populations, and values of the chemical potential, given by $\mu = k_B T \ln(1 - 1/N_0)$. The distribution functions obtained are all fully thermalized and fit a Bose distribution function.

Figs. 2.3 a, b and c show the evolution of the coherence of the ground state, χ , and of the whole system, v , for the three pumping considered. Three very different behaviors are obtained. In fig. 2.3-a, the coherence injected by the seed disappears on a time scale of a few tens of picoseconds, i.e., before the non resonant pumping generates enough polaritons to substantially populate the ground state. It does not necessarily mean that coherence cannot develop in that case, and a seed introduced after 300ps instead of $t = 0$ results in the buildup of system coherence (not shown). In fig. 2.3-b and 2.3-c, the ground state coherence first decreases more quickly than in fig. 2.3-a, before stabilization. In the same time the whole system coherence strongly increases from 0 to more than 90% as seen on fig. 2.3-c. This behaviour represents, to our knowledge, the first theoretical description of a polariton coherence buildup in a realistic semiconductor microcavity, i.e., including real polariton dispersions and all the major interactions. This coherence buildup is a clear signature of polariton quasi-condensation. On the other hand, the values obtained for coherence degrees in the intermediate regime depend on the seed, namely, the number of polaritons it contains and its time of introduction, an undesirable feature for a seed. In this case, an interpretation in term of a polariton amplifier which amplifies a coherent weak probe and retains its phase over macroscopic duration of time is more relevant [11]. To cover all regimes, a detailed analysis of fluctuations amplitude is needed in order to correctly describe realistic values for coherence degrees, independently of the choice of the seed. The initial decrease of the ground state coherence is due to the flow of incoherent polaritons into the ground state while the ground state population is not yet large enough to ensure phase coherent stimulated scattering. In our case this threshold is about $n_0 = 10^3$. Once the condensation threshold is reached the ground state coherence becomes constant on the time-scale we consider. It slowly decreases with a ms time scale because of the finite size of the system, in accord with the conclusions of Banyai & Gartner (2002).

[11] Y. G. Rubo, F. P. Laussy, G. Malpuech, A. Kavokin, and P. Bigenwald, Phys. Rev. Lett. **91**, 156403 (2003).

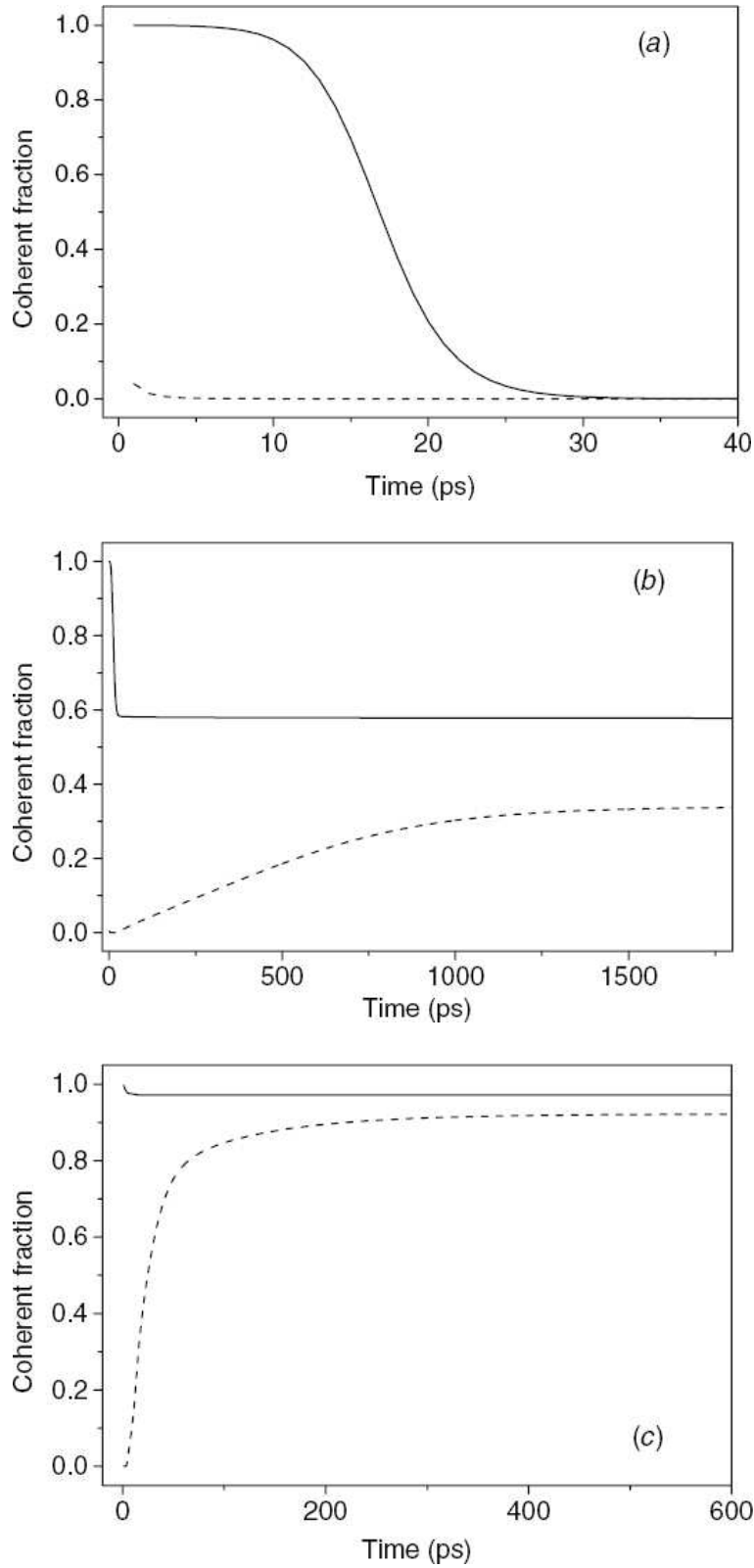


Figure 2.3: Coherent fractions ν (dashed lines) and χ (solid line) for pumping power of .8, 8 and 160W/cm² respectively. ν is defined as the ratio of coherent polaritons in the ground state over the total number of polaritons in the entire system, and χ as the ratio of coherent polaritons in the ground state over the total number of polaritons in the ground state. They are linked by $\nu = \chi n_0 / \sum_{\mathbf{q}} n_{\mathbf{q}}$, eq. (2.35). Ground state coherence χ is maximum at initial time, which corresponds to the introduction “by hand” of a coherent seed. The relevant physical quantity at $t = 0$ is ν , which is vanishingly small. Fig. a is the regime below threshold for coherent amplification, where the seed coherence is rapidly washed out and that of the entire system remains zero. Fig. c on the opposite displays the regime where the coherent seed is coherently amplified: a macroscopic number of particles populate the coherent fraction of the initially small seed. Fig. b displays an intermediate regime.

Nonlinear contributions

The necessity of the seed and to great extent the sensibility of the long time behaviour on its characteristic is a severe limitation of this model, and an immediate goal is to include whatever physics is responsible for the onset of coherence. A successful theory would therefore end up with coherent populations in the ground state but with the vacuum or a thermal state as initial conditions. In their historic publication, İmamoğlu et al. (1996) have claimed such a coherence buildup obtained from Monte Carlo simulations in the quantum state diffusion formalism (this technics is well covered for instance in Yamamoto & İmamoğlu's (1999) textbook). They needed no seed but had taken into account nonlinear quartic terms of the kind $a_0^\dagger a_0^\dagger a_0 a_0$, which, although they claimed were dephasing terms which limits the ground state population and therefore not responsible for this coherence buildup, are the only terms which differ from our case, eq. (2.21). They moreover also identified the source of coherence buildup in bosonic stimulation which is responsible for population buildup, stating that “*the fundamental physical process that results in coherent state formation in a boson is the many-body exciton-phonon interaction*”. Of course the Quantum Monte Carlo simulation itself is merely a numerical method which must recover the same results as an analytical solution if it exists, and which we have provided, eq. (2.41). In this section we investigate the possible impact of nonlinear terms on the spontaneous coherence buildup in the Born-Markov approximation. We therefore consider the most general Lindblad type of master equation:

$$\mathcal{L}\rho = -\frac{i}{\hbar}[H + H_{\text{self}}, \rho] - \frac{1}{\hbar} \sum_{m,m' \in \mathbb{N}} \left[h_{m,m'} [\rho L_m L_{m'} + L_m L_{m'} \rho - 2L_{m'} \rho L_m] + \text{h.c.} \right]. \quad (2.45)$$

In the most general framework, $L_m, L_{m'}$ are any operators pertaining to the ground state—that is, in our case they are combinations of a_0 and a_0^\dagger —while $h_{m,m'}$ are constants provided by a microscopic model as yet unspecified. For instance the linear model studied so far corresponds to $L_0 = a_0, L_1 = a_0^\dagger$ with $h_{0,1} = W_{\text{out}}$ and $h_{1,0} = W_{\text{in}}$, all others $h_{m,m'} = 0$.

First, we grant the self-interacting part (2.2b) which contains the additional terms from İmamoğlu's model. For the condensate it adds to the linear model:

$$H_{\text{self}} = \hbar\chi_0 a_0^\dagger a_0^\dagger a_0 a_0 \quad (2.46)$$

and for interactions with other polariton states:

$$L_2 = a_0 a_0, \quad L_3 = a_0^\dagger a_0^\dagger, \quad L_4 = a_0^\dagger a_0, \quad (2.47a)$$

$$h_{2,3} = \kappa_{e-e}, \quad h_{4,4} = \kappa_{\text{dep}}, \quad (2.47b)$$

still with all others $h_{m,m'} = 0$. We have borrowed the notations from İmamoğlu & Ram (1996) for coupling strength $\hbar\chi_0$ (which they actually write $\hbar\chi$), κ_{e-e} and κ_{dep} , the subscripts for the two latter terms referring to exciton-exciton interactions and dephasing. The polariton-polariton interaction comes from their excitonic fraction and the inter-particles interaction indeed results in some dephasing so the notation is suitable for our concerns and allows direct comparison with their paper (in which they write C for our a_0). Note that in the case (2.47), $L_m L_{m'}$ is hermitean so that the h.c. of eq. (2.45) simply contributes a factor 2 (if κ are real, which can always be made so).

Let us first show that (2.46) merely renormalises eq. (2.31), and thus does not allow spontaneous breaking of the symmetry anymore than phonon-mediated scattering terms. To that

effect we compute its contribution to $\langle a_0 \rangle$ equation of motion, which can be done separately since the trace is linear:

$$\begin{aligned}
\partial_t \langle a_0 \rangle \Big|_{\text{self}} &= \hbar \chi_0 \text{Tr} \left(a_0^\dagger a_0 a_0^\dagger a_0 \rho a_0 - 2 a_0^\dagger a_0 \rho a_0^\dagger a_0^2 + \rho a_0^\dagger a_0 a_0^\dagger a_0^2 \right) \\
&= \hbar \chi_0 \text{Tr} \left(a_0 a_0^\dagger a_0 a_0^\dagger a_0 \rho - 2 a_0^\dagger a_0^2 a_0^\dagger a_0 \rho + a_0^\dagger a_0 a_0^\dagger a_0^2 \rho \right) \\
&= \hbar \chi_0 \text{Tr} \left((a_0 a_0^\dagger a_0 - a_0^\dagger a_0^2) a_0^\dagger a_0 \rho + a_0^\dagger a_0 (a_0^\dagger a_0 - a_0 a_0^\dagger) a_0 \rho \right) \\
&= \hbar \chi_0 \text{Tr} \left([a_0, a_0^\dagger a_0] a_0^\dagger a_0 \rho + a_0^\dagger a_0 [a_0^\dagger, a_0] a_0 \rho \right) \\
&= \hbar \chi_0 \text{Tr} \left(a_0 a_0^\dagger a_0 \rho - a_0^\dagger a_0^2 \rho \right) \\
&= \hbar \chi_0 \text{Tr} \left([a_0, a_0^\dagger a_0] \rho \right) \\
&= \hbar \chi_0 \text{Tr} (a_0 \rho) \\
&= \hbar \chi_0 \langle a_0 \rangle
\end{aligned} \tag{2.48}$$

For the non-unitary evolution, we now show that the result can turn out positive, although none of the terms which allow coherence buildup are included in the analysis of İmamoğlu et al. (1996). It is expected that the terms we are seeking, responsible for the coherence, will also lead to a saturation, so that we can assume the condensate population will not increase indefinitely but will reach a steady value for long times, with the laser operating at equilibrium in continuous pumping. Therefore we look for terms in (2.45) which admit a steady solution and will result in a polariton statistics which is non-thermal. The former condition is not met if the population does not saturate (then the amplification broadens and shifts the mean of $P(\alpha, \alpha^*, t)$ towards infinity) while the latter demands that the peak of $p(n, t) \equiv \langle n | \rho | n \rangle$ is not centred about zero. We limit to next higher order, and this means quartic terms with as many annihilation operators as creation, since otherwise we reach non-diagonal elements. Then we assume that exchanges between ground and other states are dominated by single particle transfers, i.e., that the simultaneous exchange of two or more particles is negligible in comparison. Therefore the number of creation operators minus the number of annihilation operators on one side of ρ must have absolute value which does not exceed 1, so that $|n\rangle, |m\rangle$ are not coupled when $|n - m| > 1$. All terms with two operators on each side of ρ cancel for $p(n)$ dynamics. Therefore only terms with a number imbalance about ρ are relevant and we list them in table 2.3 along with their contribution to $\partial_t p(n)$. As the listing is symbolic with no proper indexing, we replaced $h_{m,m'}$ with constants B_i . Finally we write the detailed balance between neighbour states $|n\rangle$ and $|n \pm 1\rangle$ when $\partial_t p(n) = 0$ and this gives a recurrence relation for the polaritons statistics:

$$\frac{p(n)}{p(n-1)} = \frac{\alpha n + \beta n^2}{\gamma n + \delta n^2} \quad \text{with} \quad \begin{aligned} \alpha &\equiv \bar{W}_{\text{in}} - B_1 + B_3, & \beta &\equiv B_1 + B_2 + B_3 \\ \gamma &\equiv \bar{W}_{\text{out}} - B_6 + B_4, & \delta &\equiv B_4 + B_5 + B_6 \end{aligned} \tag{2.49}$$

with $\bar{W}_{\text{in}}, \bar{W}_{\text{out}}$ the equilibrium values. A mechanism which provides, say, $\alpha \neq 0$ and $\delta \neq 0$ along with $\beta = \gamma = 0$ yields pure poissonian statistics and therefore is one successful in eventually growing from vacuum or thermal state a pure coherent state. Conversely, a mechanism for which $p(n)/p(n-1)$ is a constant yields a geometric distribution characteristic of thermal state. This is the case with the linear model. The more general criterion to tell apart systems

allowing buildup of coherence from vacuum or thermal state to others can therefore be taken as that exhibiting a peak not centred about 0, i.e.,

$$\alpha > \gamma \quad \text{and} \quad \beta < \delta \quad (2.50)$$

and can be readily checked for any hamiltonian or liouvillian identifying coefficients with table 2.3. These results have been presented at the NOEKS7 conference and were published in its proceedings by Laussy, Rubo, Malpuech, Kavokin & Bigenwald (2003) [12].

Anomalous Correlations

Finding out a microscopic hamiltonian or liouvillian which provides coherence buildup with quantitative estimates of the coefficients and thus of the quality of the mechanism to grow coherence is another problem that we will not address. One popular possible cause, the so-called *anomalous correlations*

$$F(\mathbf{k}) = \langle a_{\mathbf{k}} a_{-\mathbf{k}} \rangle, \quad F^*(\mathbf{k}) = \langle a_{\mathbf{k}}^\dagger a_{-\mathbf{k}}^\dagger \rangle, \quad (2.51)$$

developed between the condensate and excited states as a result of interactions, is now shown to fail to fit the previous scheme if the correlations are mediated through phonons scattering, since in this case the master equation extends to (cf. eqs. (A.3) and (A.3)):

$$\begin{aligned} \partial_t \rho_0 = & \mathcal{I}_0 (a_0^\dagger a_0 \rho_0 - 2a_0 \rho_0 a_0^\dagger + \rho_0 a_0^\dagger a_0) \\ & + \hat{\mathcal{I}}_0 (a_0 a_0^\dagger \rho_0 - 2a_0^\dagger \rho_0 a_0 + \rho_0 a_0 a_0^\dagger) \\ & + \mathcal{J} (a_0 a_0 \rho_0 - a_0 \rho_0 a_0 + \rho_0 a_0^\dagger a_0^\dagger - a_0^\dagger \rho_0 a_0^\dagger) \\ & + \mathcal{J}' (a_0^\dagger a_0^\dagger \rho_0 - a_0^\dagger \rho_0 a_0^\dagger + \rho_0 a_0 a_0 - a_0 \rho_0 a_0), \end{aligned} \quad (2.52)$$

with \mathcal{I}_0 , $\hat{\mathcal{I}}_0$, \mathcal{J} , \mathcal{J}' some constants explicited from the microscopic model in the appendix, which actual value currently bears little on our discussion. We pay more attention to the Lindblad operators thus introduced, which are seen not to match the form demanded in table 2.3. Alternatively, one can see that eq. (2.52) gives the order parameter equation of motion as:

$$\partial_t \langle a_0 \rangle = (\mathcal{I}_0 - \hat{\mathcal{I}}_0) \langle a_0 \rangle + (\mathcal{J}' - \mathcal{J}) \langle a_0^\dagger \rangle \quad (2.53)$$

so that it remains ‘‘homogeneous’’ in the sense that if $\langle a_0 \rangle = 0$ initially, so it will remain at later time (since $\langle a_0^\dagger \rangle = \langle a_0 \rangle^*$).

Because using the extended master equation (2.52) would require supplementing Boltzmann equation with equations of motions for anomalous correlations (2.51), we have neglected these terms in our numerical simulations (knowing beforehand this would not favor spontaneous coherence buildup anyway).

We have not investigated how anomalous correlations mediated by polariton-polariton scattering infer on the master equation, since the algebra involved becomes of a considerable complexity. Some attempts in likewise directions have been recently carried out by Sarchi & Savona (2004) but have not yet been published. In the next section, we show how another type of correlations, between particle numbers, allows this coherence buildup without inter-particles interactions.

[12] F. P. Laussy, Y. G. Rubo, G. Malpuech, A. Kavokin, and P. Bigenwald, Phys. Stat. Sol. C **0**, 1476 (2003).

Table 2.3: All terms L_m, L_n (cf. eq. (2.45)) to order 2—and associated coefficients B_i (cf. eq. (2.49))—which directly affect the efficiency of growing a coherent state from vacuum or thermal state because of nonlinear effects.

L_m	$L_{m'}$	$\frac{1}{2}\langle n L_m L_{m'}\rho + \rho L_m L_{m'} - 2L_{m'}\rho L_m n\rangle$	coefficient
$a_0^\dagger a_0 a_0$	a_0^\dagger	$n(n+1)p(n) - (n-1)np(n-1)$	B_1
$a_0 a_0^\dagger a_0$	a_0^\dagger	$(n+1)^2 p(n) - n^2 p(n-1)$	B_2
$a_0 a_0 a_0^\dagger$	a_0^\dagger	$(n+1)(n+2)p(n) - n(n+1)p(n-1)$	B_3
$a_0 a_0^\dagger a_0^\dagger$	a_0	$n(n+1)p(n) - (n+1)(n+2)p(n+1)$	B_4
$a_0^\dagger a_0 a_0^\dagger$	a_0	$n^2 p(n) - (n+1)^2 p(n+1)$	B_5
$a_0^\dagger a_0^\dagger a_0$	a_0	$(n-1)np(n) - n(n+1)p(n+1)$	B_6

2.2 Spontaneous Coherence Buildup

2.2.1 Bose condensation of conserved particles

In this section we investigate how coherence can arise spontaneously in an assembly of bosons accumulating in a single state when their energy dissipation is through scattering to lower energy states, as is the case for polaritons and as is opposed to gauge bosons like photons or phonons where particles can be simply created or annihilated to accommodate the distribution function. The essential difference is that, to the provision that they are unstable, polaritons are conserved particles, i.e., all annihilation operators are matched by a corresponding creation operator. Because of this parity in annihilation/creation, when a polariton leaves one state, it means it has moved to another one. In this regard the lifetime is not a fundamental point, polaritons are unstable particles which can radiatively be removed from the system, but this is qualitatively different from the case of photons, say, which although they are stable (with infinite lifetime), can be annihilated for instance if one lowers the temperature. On the opposite, a massive or conserved particle, or more precisely, a particle with nonzero chemical potential, cannot simply be removed from the system, it must scatter to a lower energy state. This is, in essence, the concept of Bose condensation as laid down by Einstein. As such a polariton laser has much more in common with the BEC of atoms, and thus resembles more to an atom laser than to a conventional laser. However it has also specificities of its own, namely polaritons have a short lifetime and their dispersion relation leads to a bottleneck of relaxation towards ground state for exchange of small momenta. Therefore, although based on macroscopic occupancy of a single state, the dynamics is crucial in this problem and makes it disputable that BEC is involved in microcavities. Also because of the finite lifetime, an hypothetical condensate can be sustained only if the device is operated out of equilibrium. The polariton laser therefore sits between an atom laser and a conventional (photon) laser, the former operating at equilibrium based on BEC, the latter operating far from thermal equilibrium, based on a flux equilibrium. We now show how ensuring this particle number conservation in kinetic equations result in the sought spontaneous coherence buildup. A similar approach has been pioneered by Gardiner & Zoller (1997), precisely for cold atoms and thus without lifetime which is a capital parameter in our approach, and their solutions required heavy Monte Carlo simulations, detailed and carried

out by Jaksch, Gardiner & Zoller (1997), whereas we will motivate approximations to keep the level of complexity of the numerical computation to that of Boltzmann equations.

2.2.2 Two oscillators toy theory

Quantum Boltzmann Master Equation

To gain insights in the mechanisms at work, we first recourse to a toy model which reduces all the relevant physics to its bare minimum. Later we give the full picture suitable to describe a realistic microcavity. The following analysis borrows heavily from the publication by Laussy, Malpuech & Kavokin (2004) [13].

Since dimensionality is not an issue because not the accommodation of a population in phase-space but dynamical effects are responsible for populating the ground state, we describe the system by a zero-dimensional two-oscillators model, one oscillator figuring the ground state, the other an excited state (or assembly of excited states granted as a whole). We also neglect inter-particles interactions, which will clearly show that efficient relaxation is required and such that it conserves particle numbers, but that intrinsic inter-particles interactions are not necessary. The number of polaritons in the entire system fluctuates, but we shall see that the correlations implied by conservation of polaritons in their relaxation is at the heart of our mechanism. One can reconcile the conservation of particles with a fluctuation in their total number with an interpretation as a pulsed experiment, where a laser injects periodically in time a fluctuating number of particles in the system. Each relaxation granted separately involving an exact and constant number of particles, while observed results are averaged over pulses and thus echo an overall fluctuating population.

We label states 1 and 2. There is only one parameter to distinguish them which is the ratio ξ of the rate of transitions $w_{1 \rightarrow 2}$ and $w_{2 \rightarrow 1}$ between these states:

$$\xi \equiv \frac{w_{2 \rightarrow 1}}{w_{1 \rightarrow 2}} \quad (2.54)$$

These w are constants, especially they have no time dependence coming from populations included in these scattering terms, as opposed to such practise introduced in the footnote on page 36 which we shall use later (e.g., 2.116). We assume $\xi > 1$ which identifies state 1 as the ground state (i.e., state of lower energy), since from elementary statistics:

$$\frac{w_{2 \rightarrow 1}}{w_{1 \rightarrow 2}} = e^{(E_2 - E_1)/kT} \quad (2.55)$$

with E_i the energy of state i (by definition of ground state $E_2 > E_1$) and T is the temperature of the system once it has reached equilibrium.

The Hamiltonian for the two-oscillators system coupled through an intermediary oscillator (picturing a phonon) in the rotating wave approximation reads in interaction picture

$$H = V e^{i(\omega_1 - \omega_2 + \omega)t} a_0 a_1^\dagger b + \text{h.c.} \quad (2.56)$$

where a_1 , a_2 and b are (time independent) annihilation operators with bosonic algebra for first oscillator (ground state), second oscillator (excited state) and the ‘‘phonon’’ respectively, with

[13] F. P. Laussy, G. Malpuech, and A. Kavokin, Phys. Stat. Sol. C 1, 1339 (2003).

free propagation energy $\hbar\omega_1$, $\hbar\omega_2$, $\hbar\omega$ and coupling strength V . Carrying the same procedure as previously for ρ , i.e., evaluating the double commutator in (2.8) gives

$$\begin{aligned} \partial_t \rho = & -\frac{1}{2}[w_{1\rightarrow 2}(a_1^\dagger a_1 a_2 a_2^\dagger \rho + \rho a_1^\dagger a_1 a_2 a_2^\dagger - 2a_1 a_2^\dagger \rho a_1^\dagger a_2) \\ & + w_{2\rightarrow 1}(a_1 a_1^\dagger a_2^\dagger a_2 \rho + \rho a_1 a_1^\dagger a_2^\dagger a_2 - 2a_1^\dagger a_2 \rho a_1 a_2^\dagger)], \end{aligned} \quad (2.57)$$

after Markov approximation ($\rho(\tau) \approx \rho(t)$) and factorisation of the entire system density matrix ρ into $\rho\rho_{\text{ph}}$, with ρ , ρ_{ph} the density matrices describing the two oscillators and the phonons respectively. Of course at this stage the whole construct is very close to our previous considerations, but note that no Born approximation is made on ρ so that correlations between the two oscillators are fully taken into account. The transition rates are given by:

$$w_{1\rightarrow 2} = 2\pi|V|^2 \langle b^\dagger b \rangle / (\hbar\omega_2 - \hbar\omega_1) \quad (2.58a)$$

$$w_{2\rightarrow 1} = 2\pi|V|^2 (1 + \langle b^\dagger b \rangle) / (\hbar\omega_2 - \hbar\omega_1) \quad (2.58b)$$

We now obtain from (2.57) the equation for diagonal elements

$$p(n, m) \equiv \langle n, m | \rho | n, m \rangle, \quad (2.59)$$

where $p(n, m)$ is the joint probability distribution to have n particles in state 1 and m in 2. This equation reads

$$\begin{aligned} \partial_t p(n, m) = & (n+1)m[w_{1\rightarrow 2}p(n+1, m-1) - w_{2\rightarrow 1}p(n, m)] \\ & + n(m+1)[w_{2\rightarrow 1}p(n-1, m+1) - w_{1\rightarrow 2}p(n, m)]. \end{aligned} \quad (2.60)$$

This equation for a probability distribution paralleling Boltzmann equation is the QBME for the two-oscillators model. It has a very clear physical significance and one hardly needs to refer to a more general QBME, rigorously derived from a microscopic hamiltonian. For instance the first term on the right hand side expresses that one can increase the probability to have (n, m) particles in states (1, 2) through the process where starting from $(n+1, m-1)$ configuration, one reaches (n, m) by transfer of one particle from state 1 to the other state. This is proportional to $n+1$, the number of particles in state 1 and is stimulated by $m-1$ the number of particles in state 2 to which we add one for spontaneous emission, whence the factor $(n+1)m$. We repeat that $w_{1\rightarrow 2}$ and $w_{2\rightarrow 1}$ are constants and should not be confused with the *bosonic transition rate* defined as $w_{1\rightarrow 2}(1+m)$ and $w_{2\rightarrow 1}(1+n)$ to account in a transparent way for stimulation. Our present discussion will be clarified by expliciting it.

For all quantities Ω which pertain to a single state only, say the ground state (so we can write $\Omega(n)$), it suffices to know the reduced probability distribution for this state, i.e., for ground state:

$$p_1(n) \equiv \sum_{m=0}^{\infty} p(n, m) \quad (2.61)$$

and vice-versa, i.e., for excited state $p_2(m) \equiv \sum_{n=0}^{\infty} p(n, m)$. So that indeed

$$\langle \Omega(n) \rangle = \sum_{n=0}^{\infty} \sum_{m=0}^{\infty} \Omega(n) p(n, m) = \sum_{n=0}^{\infty} \Omega(n) p_1(n) \quad (2.62)$$

We will soon undertake to solve exactly equation (2.60) but to delineate its quality in explaining how coherence arises in the system we first show that if we make the approximation to neglect correlations between the two states, i.e., if we assume the factorisation

$$p(n, m) = p_1(n)p_2(m) \quad (2.63)$$

then the system at equilibrium will never display any coherence, i.e., in accord with our previous discussion, both states will be in a thermal state no matter the initial conditions, the transition rates or any other parameters describing the system. Indeed putting (2.63) into (2.60) and summing over m , we obtain:

$$\begin{aligned} \partial_t p_1(n) = & p_1(n+1)w_{1 \rightarrow 2}(n+1)(\langle m \rangle + 1) \\ & - p_1(n)(w_{2 \rightarrow 1}(n+1)\langle m \rangle + w_{1 \rightarrow 2}n(\langle m \rangle + 1)) \\ & + p_1(n-1)w_{2 \rightarrow 1}n\langle m \rangle \end{aligned} \quad (2.64)$$

with $\langle m \rangle \equiv \sum_m m p_2(m)$ the average number of bosons in state 2. At equilibrium the detailed balance of these two states gives the solution

$$p_1(n+1) = \frac{\langle m \rangle}{\langle m \rangle + 1} \frac{w_{2 \rightarrow 1}}{w_{1 \rightarrow 2}} p_1(n) \quad (2.65)$$

The same procedure for state 2 yields likewise

$$p_2(m+1) = \frac{\langle n \rangle}{\langle n \rangle + 1} \frac{w_{1 \rightarrow 2}}{w_{2 \rightarrow 1}} p_2(m) \quad (2.66)$$

With the notational shortcuts

$$\theta \equiv \frac{\langle n \rangle}{\langle n \rangle + 1}, \quad \nu \equiv \frac{\langle m \rangle}{\langle m \rangle + 1} \quad (2.67)$$

equations (2.65) and (2.66) read after normalisation

$$p_1(n) = (1 - \nu\xi)(\nu\xi)^n \quad (2.68a)$$

$$p_2(m) = (1 - \theta/\xi)(\theta/\xi)^m \quad (2.68b)$$

so that $\langle n \rangle \equiv \sum n p_1(n) = \nu\xi/(1 - \nu\xi)$ which inserted back into (2.67) yields

$$\xi = \frac{\theta}{\nu} \quad (2.69)$$

or, written back in terms of occupancy numbers and transition rates:

$$\frac{w_{2 \rightarrow 1}}{w_{1 \rightarrow 2}} = \frac{\langle n \rangle}{\langle n \rangle + 1} \frac{\langle m \rangle + 1}{\langle m \rangle} \quad (2.70)$$

which give in eq. (2.65), (2.66):

$$p_1(n+1) = \frac{\langle n \rangle}{\langle n \rangle + 1} p_1(n) \quad \text{and} \quad p_2(m+1) = \frac{\langle m \rangle}{\langle m \rangle + 1} p_2(m) \quad (2.71)$$

achieving the proof that both states are (exact) thermal states under the hypothesis (2.63) that we will now relax. This will give rise to a likewise regime where both states are thermal states, but also to another regime where the excited state (state 2) is still in a thermal state, but the ground state (state 1) is non-thermal (and in some limit, has the statistics of a coherent state). This is possible if one takes into account correlations between states. In our case these correlations come from the conservation of particle number, so that the knowledge of particle number in one state determines the number in other state. In fact observe how the QBME connects elements of $p(n, m)$ which lie on antidiagonals of the plane (n, m) . One such antidiagonal obeys equation

$$n + m = N \quad (2.72)$$

where N is a constant, namely, the distance of the antidiagonal to the origin from the geometrical point of view, and the number of particles from the physical point of view. One such antidiagonal is sketched on fig. 2.4. The equation can be readily solved if only one antidiagonal is concerned, i.e., if there are exactly N particles in the system. In case where the particle number in the system is only known with some probability, one can still decouple the equation onto its antidiagonal projections, solve for them individually and add up afterwards weighting each antidiagonal with the probability to have the corresponding particle number. We hence focus on such one antidiagonal N which *conditional* probability distribution is given by $d(n|N) \equiv p(n, N - n)$, with equation of motion given by (2.60) as:

$$\begin{aligned} \partial_t d(n|N) = & (n+1)(N-n)[w_{1 \rightarrow 2} d(n+1|N) - w_{2 \rightarrow 1} d(n|N)] \\ & + n(N-n+1)[w_{2 \rightarrow 1} d(n-1|N) - w_{1 \rightarrow 2} d(n|N)] \end{aligned} \quad (2.73)$$

The equation is well behaved on regard of its domain of definition $0 \leq n \leq N$ since it secures that $d(n|N) = 0$ for $n > N$. This also ensures unicity of solution despite the recurrence solution being of order 2, for $d(1|N)$ is determined uniquely by $d(0|N)$, itself determined by normalisation.

The stationary solution is obtained in this way (or from detailed balance):

$$d(n+1|N) = \frac{w_{2 \rightarrow 1}}{w_{1 \rightarrow 2}} d(n|N), \quad (2.74)$$

with solution

$$d(n|N) = d(0|N) \left(\frac{w_{2 \rightarrow 1}}{w_{1 \rightarrow 2}} \right)^n \quad (2.75)$$

where $d(0|N)$ is defined for normalisation as

$$d(0|N) = \frac{\xi - 1}{\xi^{N+1} - 1}, \quad \xi \equiv \frac{w_{2 \rightarrow 1}}{w_{1 \rightarrow 2}} \quad (2.76)$$

Technically solving for d resembles much the procedure already encountered to solve the equation under assumption (2.63). However we are now paying full attention to correlations between the two states, which turns detailed balancing (2.65) and (2.66) into one of an altogether different type (2.75). This gives by weighting (2.75) the solution to the QBME:

$$p(n, m) = \frac{\xi - 1}{\xi^{n+m+1} - 1} \xi^n P(n+m) \quad (2.77)$$

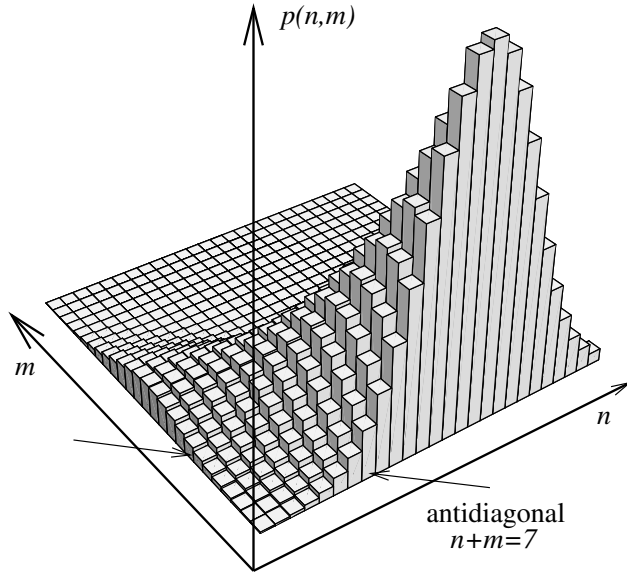


Figure 2.4: $p(n, m)$ steady state solution in case where the distribution function for the number of particles in the entire system $P(N)$ is a gaussian of mean (and variance) 15 and $\xi = 1.2$. One “antidiagonal”, $n + m = 7$, is shown for illustration. The projection on n -axis displays a coherent state whereas the projection on m -axis displays a thermal state.

where

$$P(N) \equiv \sum_{n+m=N} p(n, m) \quad (2.78)$$

is the distribution of total particle number, i.e., the probability to have N particles in the *entire* system. $P(N)$ is time independent since the microscopic mechanism involved conserves particle number for any transition (one can also check that $\partial_t P(N) = 0$). This allows to derive the statistics of separate states:

$$\begin{aligned} p_1(n) &= \xi^n \sum_{N=n}^{\infty} \frac{\xi - 1}{\xi^{N+1} - 1} P(N) \\ p_2(n) &= \xi^{-n} \sum_{N=n}^{\infty} \frac{\xi - 1}{\xi^{N+1} - 1} \xi^N P(N) \end{aligned} \quad (2.79)$$

Observe how the n dependence of the sum index prevents trivial relationship between p_1 and p_2 of the kind $p_1(n) = p_2(N - n)$. Also the asymmetry between ground and excited state is patent from (2.77). It is this feature which allows to have two states with drastic different characteristics, typically a thermal and a coherent state. Indeed, p_1 (resp. p_2) is the product of a sum with an exponentially diverging (resp. converging to zero) function of ξ . In both cases, the sum of positive terms is a decreasing function of n , so that clearly no coherence can ever survive in excited state which fate is always thermal equilibrium, or at least, in accord with our definitions,

$$p_2(n) > p_2(n + n_0) \quad \text{for all } n, n_0 \text{ in } \mathbf{N} \quad (2.80)$$

For p_1 however, ξ^n diverges with n which leaves open the possibility of a peak not centred about zero in this distribution, while it can still be a decreasing function if the sum converges faster still. It is to $P(N)$ to settle this issue, which as a constant of motion is completely determined by the initial condition. The solution for the case where $P(N)$ is a gaussian of mean (and average) 15 is displayed on fig. 2.4. $p(n, m)$ is in this case manifestly not of the type $p_1(n)p_2(m)$ and there is always coherence in the system. In next section we investigate the more interesting situation where coherence is not existing a-priori in the system.

Growth at equilibrium

By growth at equilibrium we mean that, still in the approximation of infinite lifetime, coherence can arise when one lowers temperature, i.e., increases ξ , in a system where initially all states are thermal states. In this case the initial condition for the system is the thermal equilibrium

$$p(n, m) = (1 - \theta)(1 - \nu)\theta^n \nu^m \quad (2.81)$$

where θ , ν are the thermal parameters for ground and excited states respectively. They link to $\langle n \rangle$, the mean number of particles in ground state, through

$$\langle n \rangle = \frac{\theta}{1 - \theta}, \quad (2.82)$$

or, the other way around,

$$\theta = \frac{\langle n \rangle}{1 + \langle n \rangle}. \quad (2.83)$$

Similar relations hold for ν and m . This is one possible steady solution of (2.60) and we discuss how it arises from (2.77) below. For the time being we stress again that a thermal state is essentially empty, as attests its higher probability which is for zero particle. Once in a while, thermal kicks transfer in the state one or many particles, which however do not stay for long before the state is emptied again or replaced by other, unrelated particles. This accounts for the chaotic, or incoherent, properties of such a state. This essentially empty but greatly fluctuating statistics brings no conceptual problem for little populations, but one might enquire whether it is conceivable to have a thermal distribution with high mean number. This is possible for a single state but not for the system as a whole. A macroscopic population can distribute itself in a vast collection of states so that each has thermal statistics, constantly exchanging particles with other states and displaying great fluctuations, but as expected from physical grounds, the whole system does not fluctuate greatly in its number of particles. Therefore we expect $P(N)$, the distribution of particles in the *entire system*, to be peaked about a nonzero value, typically to be a gaussian of mean and variance equal to N . In the pure Boltzmann case, this results from the central limit theorem since the total number of particles is the sum of a large number of uncorrelated random variables, and thus it itself a Gaussian random variable. Reminding our previous definitions, this however does not qualify the system as a coherent emitter, since the statistics must refer to a *single state*, not to a vast assembly of differing emitters. Thus, not surprisingly, coherence arises when a *single* quantum mode models or copy features of a macroscopic system, typically its population distribution. The two-oscillators system which is a rather coarse approximation to a macroscopic system will however display very clearly this mechanism. In the limit where $\xi \gg 1$ it is already visible from (2.79) that $p_1(n) \approx P(n)$, so that

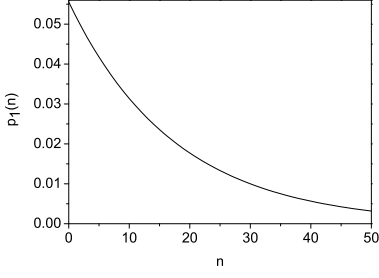


Figure 2.5: Ground state distribution $p_1(n)$ for $\xi = \frac{\theta}{\nu} \approx 1.26$ with 3 particles in excited state and 17 in ground state, both in thermal equilibrium, cf. (2.88), $g^{(2)}(0) = 2$.

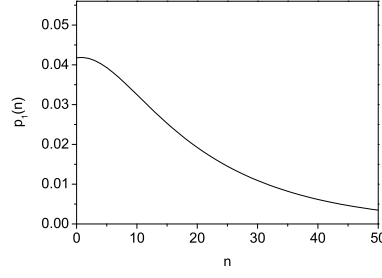


Figure 2.6: Same with ξ raised to 1.5. Distribution is non-thermal, especially $p_1(1) > p_1(0)$, though the distribution is then always decreasing. $g^{(2)}(0) \approx 1.89$.

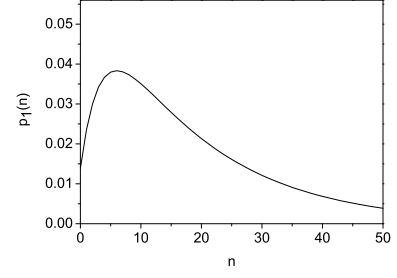


Figure 2.7: Same with $\xi \rightarrow 0$. The distribution is that for the entire system, $p_1(n) = P(N)$, cf. (2.89). Yet it is far from coherent in this model. $g^{(2)}(0) \rightarrow 1.745$.

the statistics of the entire system indeed serves as a blueprint for the ground state (and it alone, excited states being always decreasing as already shown). At equilibrium, with two thermal states, the distribution for the whole system reads:

$$P(N) = \sum_{n+m=N} p(n, m) = (1 - \theta)(1 - \nu) \frac{\theta^{N+1} - \nu^{N+1}}{\theta - \nu} \quad (2.84)$$

This exhibits a peak at a nonzero value provided that

$$\nu + \theta > 1 \quad (2.85)$$

This criterion refers to a first necessary condition: there must be enough particles in the system. The less particles available so that (2.85) is fulfilled, is two. This minimum required to grow coherence fits nicely with the Bose-Einstein condensation picture (one needs at least two bosons to condense). It is not a necessary condition, though; also the dynamical aspect is important as shown by the key role of ξ . Indeed if the system is steady in configuration (2.81), ξ is not a free parameter but is related to θ and ν by:

$$\xi = \frac{\theta}{\nu} \quad (2.86)$$

and in this case the distribution of ground state

$$p_1(n) = (1 - \theta)(1 - \nu) \xi^n \sum_{N=n}^{\infty} \frac{\theta^{N+1} - \nu^{N+1}}{\xi^{N+1} - 1} \frac{\xi - 1}{\theta - \nu} \quad (2.87)$$

reduces by straightforward algebra to

$$p_1(n) = (1 - \theta) \theta^n \quad (2.88)$$

i.e., as should be for consistency, the ground state is in a thermal state, independently of the value of θ (i.e., no matter the number of particles in ground state). This can come as a surprise, but it must be born in mind that this two-oscillators model is an extreme simplification which cannot dispense from some pathological features, namely, the faculty to sustain a thermal macroscopic population, an ability that we understand easily since the ground state

accounts for half of the system! It is expected that with increasing number of states, dimensionality will forbid such an artifact. Also the shape of $P(N)$ hardly resembles a gaussian (see fig. (2.7)) but already in this limiting case it is able to display a peak at a nonzero value provided there are enough particles. With increasing number of states, the central limit theorem will turn this distribution into an actual gaussian. Once again, $P(N)$ is time independent because the relaxation mechanism conserves particle number, which results in correlations between the two states. By increasing ξ to ξ' , one might search new values of θ, ν , say θ', ν' , so that $\theta/(1-\theta) + \nu/(1-\nu) = \theta'/(1-\theta') + \nu'/(1-\nu')$ (conservation of particle number) and $\xi' = \theta'/\nu'$. This is possible if one allows $P(N)$ to change, in which case the two new states are also thermal states. If $P(N)$ is constrained by correlations induced by strict conservation of particle numbers, so that the uncertainty is not shifted as the system evolves, then (2.34) breaks down and this allows (2.77) to grow a coherent state in ground state. This process is illustrated on figures 2.5–2.7, starting from thermal equilibrium and lowering temperatures (increasing ξ). In the two-oscillators model, coherence grown out of thermal states cannot come much closer to a gaussian than illustrated on fig. 2.7 where is displayed the limiting case $\xi \rightarrow 0$ for which the ground state distribution identifies to $P(N)$, cf. (2.84),

$$p_1(n) = (1-\theta)(1-\nu) \frac{\theta^{n+1} - \nu^{n+1}}{\theta - \nu}, \quad (2.89)$$

which is obvious on physical grounding (one particular realisation is that where $w_{1 \rightarrow 2} = 0$ and thus with all particles eventually reaching the ground state) and reinforce our understanding of Bose condensation as the ground state distribution function coming close to the macroscopic distribution, with complete condensation corresponding to identification of $p_1(n)$ with $P(N)$.

Growth out of equilibrium

The previous case holds in an equilibrium picture and for that matter refers to coherence buildup in systems like cold atoms BEC. To address the polariton laser case, it is necessary to extend the two-oscillators model with the additional complication of finite lifetime τ of particles in state 1, with a balance in the total population provided by a pump which inject particles in state 2 at a rate Γ . (We will not crucially need finite lifetime in excited state and thus neglect it, which is good approximation in a typical microcavity where the radiative lifetime drops by a factor of ten to an hundred in the photon-like part of the dispersion.) Although the QBME can be readily extended phenomenologically to take these into account,

$$\begin{aligned} \dot{p}(n, m) = & (n+1)m[w_{1 \rightarrow 2}p(n+1, m-1) - w_{2 \rightarrow 1}p(n, m)] \\ & + n(m+1)[w_{2 \rightarrow 1}p(n-1, m+1) - w_{1 \rightarrow 2}p(n, m)] \\ & + \frac{1}{\tau}(n+1)p(n+1, m) - \frac{1}{\tau}np(n, m) \\ & + \Gamma p(n, m-1) - \Gamma p(n, m) \end{aligned} \quad (2.90)$$

the couplings between different particle numbers forbid to solve this new equation along the same analytical lines as previously, though the numerical solution can be obtained straightforwardly. Introducing $\langle m \rangle_n$ the mean number of polaritons in the excited state given that there are n in the ground state, i.e.,

$$\langle m \rangle_n p_0(n) = \sum_{m=0}^{\infty} mp(n, m) \quad (2.91)$$

with $p_0(n) \equiv \sum_m p(n, m)$ is the reduced ground state statistics, we obtain, by averaging eq. (2.60) over excited states, an equation for the ground state statistics only:

$$\begin{aligned} \partial_t p_1(n) &= (n+1)(w_{1 \rightarrow 2}(\langle m \rangle_{n+1} + 1) + 1/\tau)p_1(n+1) \\ &- \left\{ n((\langle m \rangle_n + 1)w_{1 \rightarrow 2} + 1/\tau) \right. \\ &\quad \left. + (n+1)\langle m \rangle_n w_{2 \rightarrow 1} \right\} p_1(n) \\ &+ n\langle m \rangle_{n-1} w_{2 \rightarrow 1} p_1(n-1), \end{aligned} \quad (2.92)$$

However in this out-of-equilibrium regime, the excited state is not as important as in the equilibrium case where it must be thermal and which configuration is of utmost consequence on the ground state. Thus we can dispense from the actual distribution of excited state and content with the mean $\langle m \rangle_n$ obtained from $\sum_m m p(n, m) = \langle m \rangle_n p_2(n)$. In this case (2.90) can be decoupled to give an equation for $p_1(n)$ alone, and in the ‘‘dynamical’’ steady state, the detailed balance reads:

$$p_1(n+1) = \frac{w_{2 \rightarrow 1} \langle m \rangle_n}{w_{1 \rightarrow 2}(\langle m \rangle_{n+1} + 1) + 1/\tau} p_1(n) \quad (2.93)$$

Up to this point it is still exact, and also in the out-of-equilibrium regime we grant the conservation of particle number as the origin of correlations between the two states, but because of lifetime and pumping, it can now be secured only in the mean, leading us to the following approximation for $\langle m \rangle_n$:

$$\langle m \rangle_n = N - n \quad (2.94)$$

The pump, which has quantitatively disappeared from the formula, is implicitly taken into account through this assumption, since even though particles have a finite lifetime, their number is constant on average. In the coherent case, $p_1(n)$ is a poisson distribution with maximum at $N - N_c$, so that this dependency of N on the pump is in this case $N = \tau P + N_c$.

When the population has stabilised in the ground state by equilibrium of radiative lifetime and pumping, it is found in a coherent state if $N > N_c$ with N_c the critical population defined by:

$$N_c = \frac{1}{\tau(w_{2 \rightarrow 1} - w_{1 \rightarrow 2})} \quad (2.95)$$

and obtained from (2.93) and (2.94) with the requirement that $p_1(1) > p_1(0)$. If this population is exceeded, coherence builds up in the system along with the population, which stabilises at an average given by the maximum of the gaussian-like distribution:

$$\langle n \rangle = n_{\max} = N - N_c \quad (2.96)$$

obtained from $p_1(n) = p_1(n+1)$; so that effectively if $N < N_c$ there is no such gaussian and coherence remains low with a thermal-like state which maximum is for zero occupancy. If $N > N_c$ the state is a gaussian which mean increases with increasing departure of population from the critical population. Thus, the more the particles, the less the particle number fluctuations of the state, and the best its coherence.

On fig. 2.8 is displayed the numerical solution of eq. (2.90) for $p_1(n, t)$, where parameters (see legend) have been chosen so that N exceeds (2.95) and therefore grow some coherence

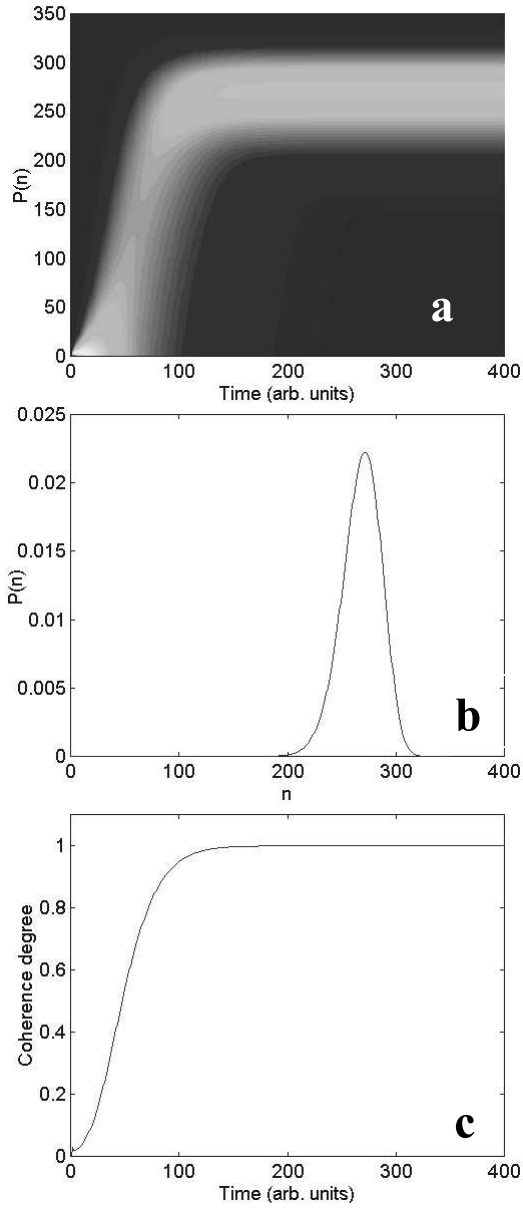


Figure 2.8: System configuration suitable for coherence buildup: $N = 350$, $w_{2 \rightarrow 1} = 10^{-5}$ (arb. units), $w_{1 \rightarrow 2} = 0.75 \times 10^{-5}$ (arb. units) and $1/\tau = 20 \times 10^{-5}$ (arb. units). All units have the same dimension of an inverse time. (a) is a density plot for the time evolution of $p(n)$, starting from vacuum it quickly evolves towards a coherent state. (b) is the projection of $p(n)$ in the steady state. (c) is the time evolution of the normalised coherence degree $\eta = 2 - g^{(2)}(0)$: full coherence is quickly attained.

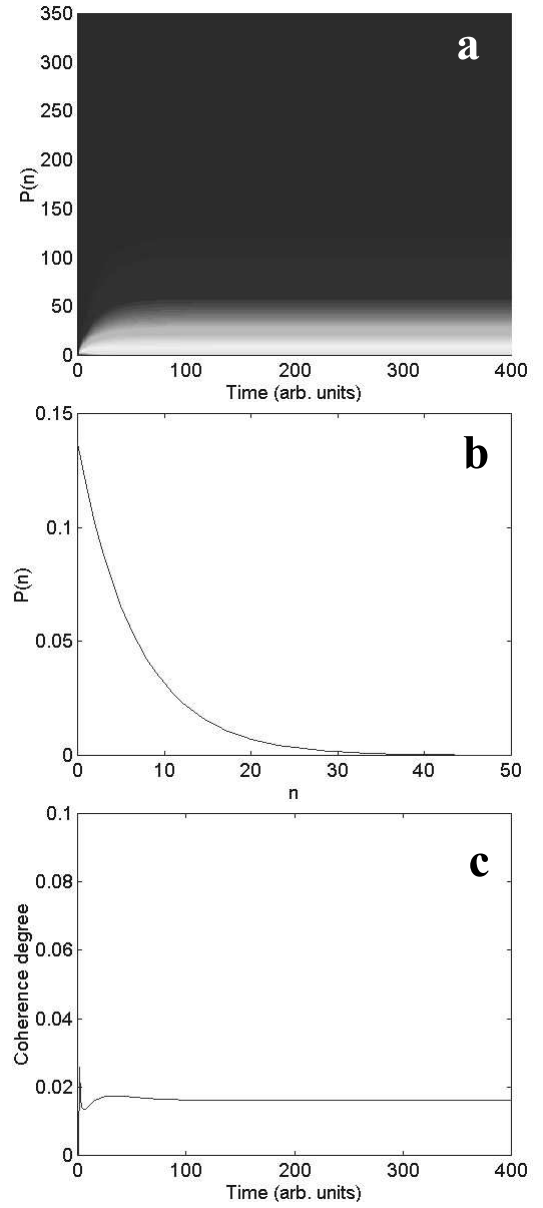


Figure 2.9: System configuration unable to develop coherence. Parameters are the same as for fig. 2.8 except $w_{2 \rightarrow 1} = .95 \times 10^{-5}$ (arb. units) corresponding to a higher temperature. (a) Starting from vacuum the ground state steadies in a thermal state for which a projection (b) is shown. (c) The normalised coherence degree remains low.

from an initially empty ground state (cf. fig. 2.8-a). The coherence is maintained for infinite times and the statistics for the ground state occupancy tends towards a gaussian-like function neatly peaked about a high value (cf. fig. 2.8-b). We define a *coherence degree* equal to $2 - g^{(2)}(0)$, so chosen to be 0 for a genuine thermal state and 1 for a genuine coherent state. In the case where (2.95) is exceeded, the coherence degree of ground state quickly reaches unity (fig. 2.8-c).

On fig. 2.9 is displayed the counterpart situation where parameters (see legend) result in a sub-critical population so that the steady state is thermal, as shown on fig. 2.9-b. The dynamics of $p(n)$, starting from vacuum, is merely to grow this thermal state (cf. fig. 2.9-a) and the coherence degree remains low (cf. fig. 2.9-c).

We have varied the temperature (through $w_{2 \rightarrow 1}$) for simplicity but kept all other parameters constant. This is not very convenient experimentally as this requires adjusting the pumping. The total number of particles N can be expressed as a function of other parameters as follows: the rate equation of particle number in ground and excited state are

$$\partial_t n = -\gamma n - w_{1 \rightarrow 2} n(N - n + 1) + w_{2 \rightarrow 1} (n + 1)(N - n), \quad (2.97a)$$

$$\partial_t (N - n) = P - (n + 1)(N - n)w_{2 \rightarrow 1} + n(N - n + 1)w_{1 \rightarrow 2}. \quad (2.97b)$$

Going to the steady state yields the relation

$$N = \frac{P(\gamma^2 + w_{2 \rightarrow 1}(\gamma - P) + w_{1 \rightarrow 2}(\gamma + P))}{\gamma(w_{1 \rightarrow 2}(\gamma + P) - w_{2 \rightarrow 1}P)} \quad (2.98)$$

which provides an equivalent set of parameters to cross the threshold as a function of P or γ , which is more relevant experimentally.

2.2.3 Polariton laser

The extension from the two oscillators model to a realistic microcavity is straightforward as far as the formalism is concerned, but the resulting equations cannot be tackled directly as previously. Also in this case the pumping and finite lifetime should not be neglected, but for the relaxation, one can still consider phonons mediated scattering only (neglecting polariton-polariton scatterings). Since all these processes are dissipative, we seek a master equation of the Lindblad type for the density matrix ρ of polariton states in the reciprocal space:

$$\partial_t \rho = (\mathcal{L}_{\text{pol-ph}} + \mathcal{L}_\tau + \mathcal{L}_{\text{pump}})\rho \quad (2.99)$$

Here \mathcal{L} are Liouville super-operators which describe respectively scattering (through phonons), lifetime and pumping. The polariton-polariton scattering would add a unitary (non-dissipative) contribution $\mathcal{L}_{\text{pol-pol}} = -\frac{i}{\hbar}[H_{\text{pol-pol}}, \rho]$. In the following we undertake the derivation of $\mathcal{L}_{\text{pol-ph}}$ from the microscopic hamiltonian $H_{\text{pol-ph}}$ for polariton-phonon scattering. Exactly similar procedure can be carried for \mathcal{L}_τ and $\mathcal{L}_{\text{pump}}$ to yield:

$$\mathcal{L}_\tau \rho = -\sum_{\mathbf{k}} \frac{1}{2\tau_{\mathbf{k}}} (a_{\mathbf{k}}^\dagger a_{\mathbf{k}} \rho + \rho a_{\mathbf{k}} a_{\mathbf{k}}^\dagger - 2a_{\mathbf{k}} \rho a_{\mathbf{k}}^\dagger) \quad (2.100a)$$

$$\mathcal{L}_{\text{pump}} \rho = -\sum_{\mathbf{k}} \frac{P_{\mathbf{k}}}{2} (a_{\mathbf{k}} a_{\mathbf{k}}^\dagger \rho + \rho a_{\mathbf{k}}^\dagger a_{\mathbf{k}} - 2a_{\mathbf{k}}^\dagger \rho a_{\mathbf{k}}) \quad (2.100b)$$

with $\tau_{\mathbf{k}}$ the lifetime, $P_{\mathbf{k}}$ the pump intensity in the state with momentum \mathbf{k} and $a_{\mathbf{k}}$ the Bose annihilation operator for a polariton in this state. For instance expression for lifetime comes from the quasi-mode coupling of polaritons with the photon field outside the cavity in the vacuum state (thereby linking spontaneous emission with the perturbation from vacuum fluctuations). We later neglect finite lifetime elsewhere than in ground state, where it is typically several orders of magnitude shorter because of dominant photon fraction. In our simulations, pumping injects excitons 10meV above the bottom of the bare exciton band which we model by nonzero value of $P_{\mathbf{k}}$ for a collection of \mathbf{k} -states normally distributed about a high momentum mean value. Expression (2.100b) describes an incoherent pumping provided by a reservoir which pours particles in the system but does not allow their coming back. Its effect is thus merely to populate the system with incoherent polaritons, which will relax towards the ground state where they might join in a coherent phase before escaping the cavity by spontaneous emission (the light thus emitted retaining this coherence).

We pay special attention to $\mathcal{L}_{\text{pol-ph}}$ which contains the key-ingredients of our results. We repeat here the interaction picture polariton-phonon diffusion term from the polariton hamiltonian (2.2a):

$$H_{\text{pol-ph}} = \sum_{\mathbf{k}, \mathbf{q} \neq \mathbf{0}} \mathcal{V}_{\mathbf{q}} e^{\frac{i}{\hbar}(E_{\text{pol}}(\mathbf{k}+\mathbf{q}) - E_{\text{pol}}(\mathbf{k}) - \hbar\omega_{\mathbf{q}})t} a_{\mathbf{k}+\mathbf{q}} a_{\mathbf{k}}^{\dagger} b_{\mathbf{q}}^{\dagger} + \text{h.c.} \quad (2.101)$$

with $\mathcal{V}_{\mathbf{q}}$ the interaction strength, E_{pol} the lower polariton-branch dispersion, $\hbar\omega_{\mathbf{q}}$ the phonons dispersion and $a_{\mathbf{q}}$, resp. $b_{\mathbf{q}}$, the Bose annihilation operator for a polariton, resp. a phonon, in state \mathbf{q} .

As previously, we compute $\mathcal{L}_{\text{pol-ph}}$ starting with Liouville-Von Neumann equation for polariton-phonon diffusion,

$$\partial_t \rho = -\frac{i}{\hbar} [H_{\text{pol-ph}}, \rho] \quad (2.102)$$

where ρ is the density matrix for polaritons and phonons. Its useful part, namely the polariton density matrix, is obtained by tracing over phonons, $\rho \equiv \text{Tr}_{\text{ph}} \rho$. Density matrix for phonons is granted as a reservoir in equilibrium with no phase coherence nor correlations with ρ . To dispense from this reservoir we write the equation for ρ to order two in the commutator and trace over phonons,

$$\partial_t \rho(t) = -\frac{1}{\hbar^2} \int_{-\infty}^t \text{Tr}_{\text{ph}} [H_{\text{pol-ph}}(t), [H_{\text{pol-ph}}(\tau), \rho]] d\tau \quad (2.103)$$

We define

$$\mathcal{E}_{\mathbf{k}, \mathbf{q}}(t) \equiv \mathcal{V}_{\mathbf{q}} e^{\frac{i}{\hbar}(E_{\text{pol}}(\mathbf{k}+\mathbf{q}) - E_{\text{pol}}(\mathbf{k}) - \hbar\omega_{\mathbf{q}})t} \quad (2.104)$$

and for convenience we write

$$\mathcal{H}(t) \equiv \sum_{\mathbf{k}, \mathbf{q}} \mathcal{E}_{\mathbf{k}, \mathbf{q}}(t) a_{\mathbf{k}+\mathbf{q}} a_{\mathbf{k}}^{\dagger} b_{\mathbf{q}}^{\dagger} \quad (2.105)$$

so that $H_{\text{pol-ph}} = \mathcal{H} + \mathcal{H}^{\dagger}$. Again, operators are time independent. Because the phonons density matrix is diagonal, $[H_{\text{pol-ph}}(t), [H_{\text{pol-ph}}(\tau), \rho]]$ reduces to $[\mathcal{H}(t), [\mathcal{H}^{\dagger}(\tau), \rho(\tau)]] + \text{h.c.}$, which halves the algebra. Also the conjugate hermitian follows straightforwardly, so we are left only with explicit computation of two terms, of which the first reads:

$$[\mathcal{H}(t), \mathcal{H}^{\dagger}(\tau)\rho] = \sum_{\mathbf{k}, \mathbf{q} \neq \mathbf{0}, \mathbf{r} \neq \mathbf{0}} \sum [\mathcal{E}_{\mathbf{k}, \mathbf{q}}(t) a_{\mathbf{k}+\mathbf{q}} a_{\mathbf{k}}^{\dagger} b_{\mathbf{q}}^{\dagger}, \mathcal{E}_{\mathbf{1}, \mathbf{r}}^*(\tau) a_{\mathbf{1}} a_{\mathbf{1}+\mathbf{r}}^{\dagger} b_{\mathbf{r}} \rho(\tau)] \quad (2.106)$$

which, taking the trace over phonons and calling $\theta_{\mathbf{q}}\rho \equiv \text{Tr}_{\text{ph}}(\rho b_{\mathbf{q}}^\dagger b_{\mathbf{q}})$, becomes:

$$\text{Tr}_{\text{ph}}[\mathcal{H}(t), \mathcal{H}^\dagger(\tau)\rho(\tau)] = \sum_{\mathbf{k}, \mathbf{l}, \mathbf{q} \neq \mathbf{0}} \mathcal{E}_{\mathbf{k}, \mathbf{q}}(t) \mathcal{E}_{\mathbf{l}, \mathbf{q}}^*(\tau) \theta_{\mathbf{q}} (a_{\mathbf{k}+\mathbf{q}} a_{\mathbf{k}}^\dagger a_{\mathbf{l}} a_{\mathbf{l}+\mathbf{q}}^\dagger \rho(\tau) - a_{\mathbf{l}} a_{\mathbf{l}+\mathbf{q}}^\dagger \rho(\tau) a_{\mathbf{k}+\mathbf{q}} a_{\mathbf{k}}^\dagger) \quad (2.107)$$

Solving numerically this equation is a considerable task, which however has already been carried out for a similar equation by Jaksch et al. (1997), using Quantum Monte-Carlo simulations. We prefer to make further approximations to reduce its simulation to a level of complexity of the same order as for Boltzmann equations: we take into account correlations between ground state and excited states only, neglecting all correlations between excited states. This is legitimated by the fast particle redistribution between excited states and their rapid loss of phase correlations. Physically this means that if a particle reaches the ground state, its absence is felt to some extent in the collection of excited states in a way which ensures particle number conservation. On the opposite, redistribution of particles between excited states will be seen to obey usual Boltzmann equations which pertain to averages only. Formally, we thus neglect terms like $\langle a_{\mathbf{k}_1} a_{\mathbf{k}_2}^\dagger a_{\mathbf{k}_3} a_{\mathbf{k}_4}^\dagger \rangle$ if \mathbf{k}_i involve nondiagonal elements in the excited state. For nonvanishing terms, we further allow $\langle a_{\mathbf{k}_1} a_{\mathbf{k}_1}^\dagger a_{\mathbf{k}_2} a_{\mathbf{k}_2}^\dagger \rangle = \langle a_{\mathbf{k}_1} a_{\mathbf{k}_1}^\dagger \rangle \langle a_{\mathbf{k}_2} a_{\mathbf{k}_2}^\dagger \rangle$ if neither \mathbf{k}_1 nor \mathbf{k}_2 equal $\mathbf{0}$, for otherwise we retain the unfactored expression. Terms from (2.107) featuring the ground state are:

$$\sum_{\mathbf{k} \neq \mathbf{0}} \mathcal{E}_{\mathbf{k}, -\mathbf{k}}(t) \mathcal{E}_{\mathbf{k}, -\mathbf{k}}^*(\tau) \theta_{\mathbf{k}} (a_0 a_0^\dagger a_{\mathbf{k}}^\dagger a_{\mathbf{k}} \rho(\tau) - a_{\mathbf{k}} a_0^\dagger \rho(\tau) a_0 a_{\mathbf{k}}^\dagger) \quad (2.108a)$$

$$+ \sum_{\mathbf{k} \neq \mathbf{0}} \mathcal{E}_{\mathbf{0}, \mathbf{k}}(t) \mathcal{E}_{\mathbf{0}, \mathbf{k}}^*(\tau) \theta_{\mathbf{k}} (a_0^\dagger a_0 a_{\mathbf{k}} a_{\mathbf{k}}^\dagger \rho(\tau) - a_0 a_{\mathbf{k}}^\dagger \rho(\tau) a_0^\dagger a_{\mathbf{k}}) \quad (2.108b)$$

Recall this expression (2.108) is one part of the term inside the time integral which gives $\partial_t \rho(t)$ evolution. Since $\mathcal{E}_{\mathbf{k}, \mathbf{q}}(t) \mathcal{E}_{\mathbf{k}, \mathbf{q}}^*(\tau) = |\gamma_{\mathbf{q}}|^2 e^{-\frac{i}{\hbar}(E_{\text{pol}}(\mathbf{k}+\mathbf{q}) - E_{\text{pol}}(\mathbf{k}) - \hbar\omega_{\mathbf{q}})(t-\tau)}$, the time integration would yield a delta function of energy (times $-i/\hbar$) if ρ in (2.108) was τ -independent. This delta would itself provide selection rules for allowed scattering processes through the sum over \mathbf{k} . That $\rho(\tau)$ time evolution is slow enough as compared to this exponential to mandate this (Markov) approximation can be checked through evaluation of the phonon reservoir correlation time, which, when the reservoir has a broad-band spectrum as in our case, is short enough to allow the approximation of $\rho(\tau)$ by $\rho(t)$. In this case, (2.108b) vanishes as a non-conserving energy term. Gathering other terms similar to (2.107) eventually gives (from now on we do not write ρ time dependence anymore, which is t everywhere):

$$\partial_t \rho = - \frac{1}{2} \sum_{\mathbf{k} \neq \mathbf{0}} W_{\mathbf{0} \rightarrow \mathbf{k}} (a_0^\dagger a_0 a_{\mathbf{k}} a_{\mathbf{k}}^\dagger \rho + \rho a_0^\dagger a_0 a_{\mathbf{k}} a_{\mathbf{k}}^\dagger - 2a_0 a_{\mathbf{k}}^\dagger \rho a_0^\dagger a_{\mathbf{k}}) \quad (2.109a)$$

$$- \frac{1}{2} \sum_{\mathbf{k} \neq \mathbf{0}} W_{\mathbf{k} \rightarrow \mathbf{0}} (a_0 a_0^\dagger a_{\mathbf{k}} a_{\mathbf{k}}^\dagger \rho + \rho a_0 a_0^\dagger a_{\mathbf{k}} a_{\mathbf{k}}^\dagger - 2a_0^\dagger a_{\mathbf{k}} \rho a_0 a_{\mathbf{k}}^\dagger) \quad (2.109b)$$

where

$$W_{\mathbf{0} \rightarrow \mathbf{k}} \equiv \frac{2\pi}{\hbar} |\gamma_{\mathbf{k}}|^2 \theta_{\mathbf{k}} \delta(E_{\text{pol}}(\mathbf{k}) - E_{\text{pol}}(\mathbf{0}) - \hbar\omega_{\mathbf{k}}) \quad (2.110a)$$

$$W_{\mathbf{k} \rightarrow \mathbf{0}} \equiv \frac{2\pi}{\hbar} |\gamma_{\mathbf{k}}|^2 (1 + \theta_{\mathbf{k}}) \delta(E_{\text{pol}}(\mathbf{k}) - E_{\text{pol}}(\mathbf{0}) - \hbar\omega_{\mathbf{k}}) \quad (2.110b)$$

We call $p(\{n_{\mathbf{k}}\})$ the diagonal of the polariton density matrix, i.e., the dotting of ρ with $|\{n_{\mathbf{k}}\}\rangle = |n_0, n_{\mathbf{k}_1}, \dots, n_{\mathbf{k}_i}, \dots\rangle$ the Fock state with $n_{\mathbf{k}_i}$ polaritons in state \mathbf{k}_i :

$$p(\{n_{\mathbf{k}}\}) \equiv \langle \dots, n_{\mathbf{k}_i}, \dots, n_{\mathbf{k}_1}, n_0 | \rho | n_0, n_{\mathbf{k}_1}, \dots, n_{\mathbf{k}_i}, \dots \rangle \quad (2.111)$$

This is the probability that the system be found in configuration $\{n_{\mathbf{k}}\}$ which equation of motion is the master equation obtained from (2.109) as

$$\begin{aligned} \dot{p}(\{n_{\mathbf{k}}\}) = & - \sum_{\mathbf{k}} (W_{\mathbf{0} \rightarrow \mathbf{k}} n_0 (n_{\mathbf{k}} + 1) + W_{\mathbf{k} \rightarrow \mathbf{0}} (n_0 + 1) n_{\mathbf{k}}) p(\{n_{\mathbf{k}}\}) \\ & + \sum_{\mathbf{k}} W_{\mathbf{0} \rightarrow \mathbf{k}} (n_0 + 1) n_{\mathbf{k}} p(\{n_0 + 1, \dots, n_{\mathbf{k}} - 1, \dots\}) \\ & + \sum_{\mathbf{k}} W_{\mathbf{k} \rightarrow \mathbf{0}} n_0 (n_{\mathbf{k}} + 1) p(\{n_0 - 1, \dots, n_{\mathbf{k}} + 1, \dots\}) \end{aligned} \quad (2.112)$$

This is the counterpart to (2.115), which also parallels closely Boltzmann equation with which it shares the same transition rates (2.110) given by Fermi's golden rule, and so it represents the QBME for polariton lasers. We include back (2.100) in (2.109) (note that we could have done this at any moment) and, following our spirit, we do not solve it for the entire joint probability $p(\{n_{\mathbf{k}}\})$ but average over all excited states to retain the statistical character for the ground state only. Excited states will be described with a Boltzmann equation, thus with thermal statistics. Calling

$$p_0(n_0) \equiv \sum_{i=1}^{\infty} \sum_{n_{\mathbf{k}_i}=0}^{\infty} p(n_0, n_{\mathbf{k}_1}, n_{\mathbf{k}_2}, \dots, n_{\mathbf{k}_j}, \dots) \quad (2.113)$$

the ground state reduced probability (the sum is over all states but the ground state, cf. (2.61)), and

$$\langle n_{\mathbf{k}} \rangle_{n_0} p_0(n_0) \equiv \sum_{n_{\mathbf{k}_1}, n_{\mathbf{k}_2}, \dots} n_{\mathbf{k}} p(\{n_{\mathbf{k}}\}) \quad (2.114)$$

cf. (2.91), we get the ground state QBME equation:

$$\begin{aligned} \dot{p}_0(n_0) = & (n_0 + 1)(W_{\text{out}}^{n_0+1} + 1/\tau_0) p_0(n_0 + 1) \\ & - \left(n_0(W_{\text{out}}^{n_0} + 1/\tau_0) + (n_0 + 1)W_{\text{in}}^{n_0} \right) p_0(n_0) \\ & + n_0 W_{\text{in}}^{n_0-1} p_0(n_0 - 1) \end{aligned} \quad (2.115)$$

with rate transitions now function of the ground state population number n_0 :

$$W_{\text{in}}^{n_0}(t) \equiv \sum_{\mathbf{k}} W_{\mathbf{k} \rightarrow \mathbf{0}} \langle n_{\mathbf{k}}(t) \rangle_{n_0} \quad (2.116a)$$

$$W_{\text{out}}^{n_0}(t) \equiv \sum_{\mathbf{k}} W_{\mathbf{0} \rightarrow \mathbf{k}} (1 + \langle n_{\mathbf{k}}(t) \rangle_{n_0}) \quad (2.116b)$$

while for excited states, in Born-Markov approximation, we indeed recover Boltzmann equations:

$$\langle \dot{n}_{\mathbf{k}} \rangle = \langle n_{\mathbf{k}} \rangle \sum_{\mathbf{q} \neq \mathbf{0}} W_{\mathbf{k} \rightarrow \mathbf{q}} (\langle n_{\mathbf{q}} \rangle + 1) - (\langle n_{\mathbf{k}} \rangle + 1) \sum_{\mathbf{q} \neq \mathbf{0}} W_{\mathbf{q} \rightarrow \mathbf{k}} \langle n_{\mathbf{q}} \rangle, \quad \mathbf{k} \neq \mathbf{0} \quad (2.117)$$

Inclusion of \mathcal{L}_τ and $\mathcal{L}_{\text{pump}}$ for the above adds $-\langle n_{\mathbf{k}} \rangle / \tau_{\mathbf{k}} + P_{\mathbf{k}}$ to this expression. Observe that in this case, transition rates are constants. A concise version of this derivation was published by Laussy, Malpuech, Kavokin & Bigenwald (2005) as [14].

Cast in this form, eq. (2.115) has the same transparent physical meaning in terms of a rate equation for the probability of a given configuration, much like usual rate equations for occupation numbers in the framework of Boltzmann equations. The difference is that transitions from one configuration to a neighbouring one occur at rates which depend on the configuration itself, through the population of the state. $\langle n_{\mathbf{k}} \rangle_{n_0}$ is a function of n_0 that we estimate through a first order expansion about $\langle n_0 \rangle$. This implies that fluctuations of excited states are proportional (with opposite sign) to fluctuations of ground state:

$$\langle n_{\mathbf{k}} \rangle_{n_0} \approx \langle n_{\mathbf{k}} \rangle_{\langle n_0 \rangle} + \left. \frac{\partial \langle n_{\mathbf{k}} \rangle_{n_0}}{\partial n_0} \right|_{\langle n_0 \rangle} (n_0 - \langle n_0 \rangle) \quad (2.118)$$

$\langle n_{\mathbf{k}} \rangle_{\langle n_0 \rangle}$ is given by Boltzmann equation. Since the derivative does not depend on n_0 (it is evaluated at $\langle n_0 \rangle$), we compute it by evaluation of both sides at a known value, for instance $n_0 = N$ with N the total particle number in the entire system, ground and excited states together. This gives

$$\left. \frac{\partial \langle n_{\mathbf{k}} \rangle_{n_0}}{\partial n_0} \right|_{\langle n_0 \rangle} = \frac{\langle n_{\mathbf{k}} \rangle}{\langle n_0 \rangle - N} \quad (2.119)$$

since $\langle n_{\mathbf{k}} \rangle_N = 0$ (no particles are left in excited states when they are all in the ground state). With the knowledge of (2.118) and (2.119) which are known from semi-classical Boltzmann equations, this is now only a matter of numerical simulations.

Numerical simulations

Parameters used are for a CdTe microcavity of $10\mu\text{m}$ lateral size with one QW and a Rabi splitting of 7 meV at zero detuning. The size corresponds to the light spot radius reported by Deng et al. (2002). This is an important parameter as correlations increase with decreasing size of the system. Scattering is mediated by a bath of phonons at a temperature of 6 K and with a thermal gas of electrons of density 10^{11} cm^{-2} accounted for to speed up relaxation. This is below the exciton bleaching density. The cavity is initially empty and pumped non-resonantly from $t = 0$ onwards.

Figure (2.10) displays the ground state population normalised to its steady state value n_{eq} and the coherent fraction χ . Starting from zero for the vacuum state, coherence steadily rises in the system as more polaritons enter the ground state. Interestingly, even though the dynamics can give rise to a temporary decrease in the number of ground state polaritons, the coherence does not drop in echo but continues its ascent. This is better understood with fig. (2.11) where a density plot for $p_0(n_0)$ is shown and where one can observe how the coherent statistics is reached through a tightening of the number of states with high probability of occupancy about the average. The function $p_0(n_0)$, which at first varies wildly, quickly flattens with a large number of particles in a thermal state, then a nonzero maximum appears and the statistics evolves as gaussian-like towards a poisson distribution of mean $\langle n_0 \rangle$ in the steady state. The polariton density of 10^{10} cm^{-2} achieved in the simulation is more than one order of magnitude smaller than

[14] F. P. Laussy, G. Malpuech, A. Kavokin, and P. Bigenwald, *Solid State Commun.* **134**, 121 (2005).

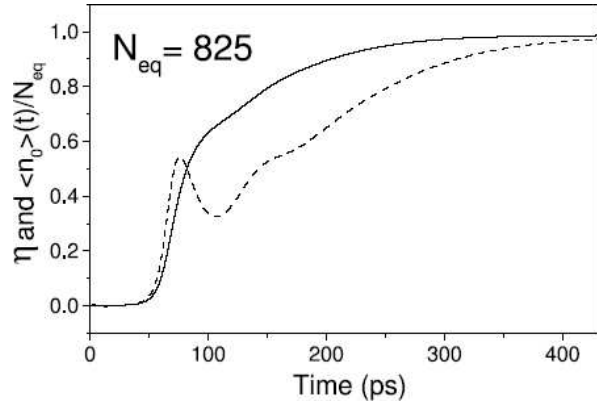


Figure 2.10: Time evolution of normalised ground state population $\langle n_0(t) \rangle / n_{\text{eq}}$ (dotted line) and of normalised coherence ratio $\eta = 2 - g^{(2)}$ (solid line), starting from the vacuum (no coherence): both population and coherence buildup are obtained in the timescale of hundreds of ps.

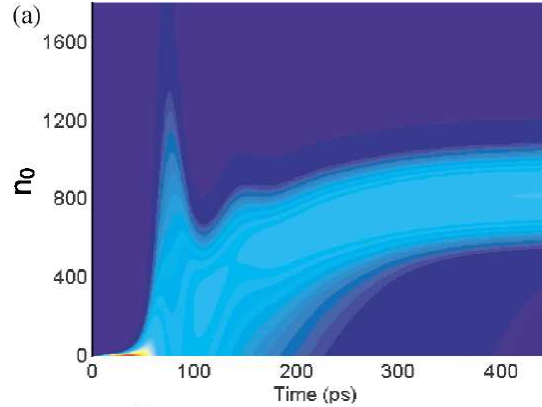


Figure 2.11: Density plot of $p_0(n_0)$ (ground state polaritons distribution) as a function of time for a realistic microcavity (with parameters given in the text). Darker colors correspond to smaller values. Initial state is the vacuum. A coherent state is obtained in the timescale of hundreds of ps.

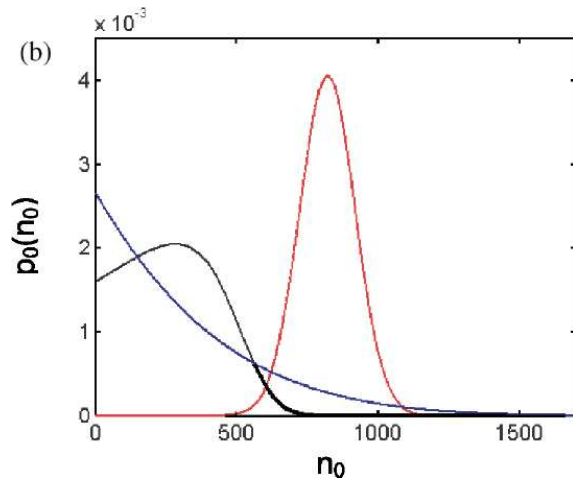


Figure 2.12: Projections of $p_0(n_0)$ of previous figure at three various times: still in a thermal state (exponential decay) close to initial times, ≈ 75 ps; in a fully grown coherent state (Gaussian) in the steady state and in the intermediate region where coherence is building-up, ≈ 100 ps.

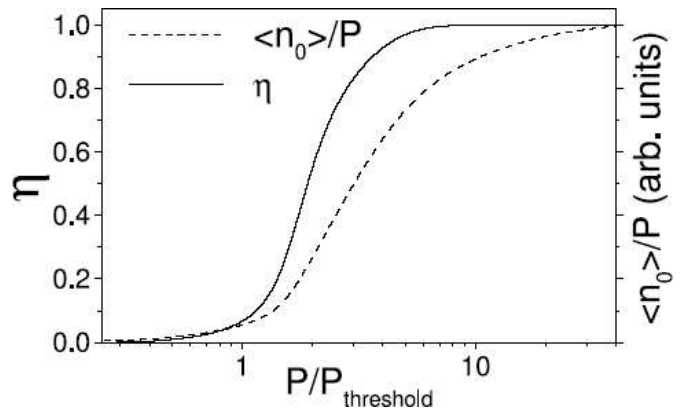


Figure 2.13: Ground state population normalized to pump power $\langle n_0 \rangle / P$ (solid line) and normalised coherence degree η in the steady state (dashed) as a function of the reduced pumping $P/P_{\text{threshold}}$; we find $P_{\text{threshold}} = 26 \text{W/cm}^{-2}$.

the strong/weak coupling transition density in CdTe. In fig. (2.13) is displayed the steady state coherence ratio and population as a function of pumping. It exhibits a clear threshold behavior. These results were published by Laussy, Malpuech, Kavokin & Bigenwald (2004a) as [15], another run of simulations can be found in the publication by Laussy, Malpuech, Kavokin & Bigenwald (2004b) in [16].

2.3 Conclusions and Perspectives

We have extended the semi-classical Boltzmann equations (2.1) to describe the quantum features of interest of the ground state (lasing mode). We obtained an analytical solution for the ground state density matrix (2.41 & 2.43) in the Born-Markov approximation, from which we were able to show that despite coherence cannot appear spontaneously from phonon-mediated relaxation only (even though the latter is able to pour an arbitrary large number of particles in the ground state), if a seed of coherent polaritons is introduced at initial time, it survives for a macroscopic long time in the system. Introduction of inter-particles interactions does not change this picture if one remains at the level of Boltzmann equations, i.e., neglecting anomalous correlations, which might well provide the required nonlinearity. We have shown, however, how anomalous correlations induced by phonons-mediated scatterings do not help in that regard. Then we have relaxed the Born approximation which neglects correlations between particles numbers, and have shown how this allows the spontaneous (without seed) coherence buildup, even in absence of inter-particles interactions, provided that without them the other relaxation mechanisms are still efficient enough to populate the ground state. In this way, coherence builds up with the population, as one might expect. This analysis has been detailed on a toy-model with two oscillators before being extended for a realistic cavity, which has been solved numerically. Extension of this work would include anomalous correlations stemming from polariton-polariton interactions, and a better numerical simulation could be carried out by performing genuine Monte-Carlo computations of eq. (2.107) instead of making the approximation we proposed.

[15] F. P. Laussy, G. Malpuech, A. Kavokin, and P. Bigenwald, *Phys. Rev. Lett.* **93** (2004).

[16] F. P. Laussy, G. Malpuech, A. V. Kavokin, and P. Bigenwald, *J. Phys.: Condens. Matter* **16** (2004).

Chapter 3

Order Parameter of Polariton Condensates

Contents

3.1	Polariton spin	83
3.1.1	Spin and polarisation	83
3.1.2	Self-interaction and beats of polarisation	84
3.1.3	Interaction between condensate and upper polariton states	86
3.2	Polarisation as an order parameter for polaritons BEC	89
3.2.1	The problem of the phase	89
3.2.2	Stimulated random walk	89
3.2.3	Formalism	90
3.2.4	Spontaneous buildup of the polarisation	92
3.3	Determination of the degree of coherence through polarisation	95
3.3.1	Correlations	95
3.3.2	Formalism	96
3.3.3	Polarisation dynamics and measure of the coherence degree	98
3.4	Conclusions and Perspectives	100

3.1 Polariton spin

3.1.1 Spin and polarisation

Polaritons are particles which spin is equal to one—like photons—with two spin projections ± 1 since zero spin does not couple to light. As the photon carries away the spin of its polariton emitter, the polarisation of light emitted by a microcavity is linked to the spin of the polaritons, which we now describe with this further degree of freedom. We shall write $a_{\uparrow\downarrow}$ the annihilation Bose operator for a ground state polariton of spin up \uparrow and down \downarrow . This corresponds to

left-circularly and right-circularly polarised emitted light, respectively. This new degree of freedom adds tremendously to the polariton physics, much of which has been investigated recently by Kavokin, Shelykh, Kavokin, Malpuech & Bigenwald (2004), Shelykh, Kavokin, Kavokin, Malpuech, Bigenwald, Deng, Weihs & Yamamoto (2004) and again Shelykh, Malpuech, Kavokin, Kavokin & Bigenwald (2004). In the polariton laser regime, the laser light polarisation indeed depends on the spin of the polaritons in the condensate, and therefore ultimately on the spin of the seed from which the condensate has been formed, either from a probe or by spontaneous coherence buildup.

In this chapter we take interest in the relationship between polarisation and Bose condensation. This is a specificity of polaritons as it requires bosons which have two projections of spin and which couple irreversibly to the photon light field (for its polarisation to be monitored). One might foresee that if the pump is unpolarised, also would be the emitted light. We shall see in section 3.2 that on the opposite a linear polarisation builds up as a result of coherent superposition of the two spin-projections of the condensate. In 3.3 we further show how the same principles in presence of a polarised pumping allow to deduce $g_2(0)$ from classical optics experiments, without need for quantum optical settings of the HBT type. All these effects are made possible from the interferences between the two spin-components of the condensate, the emitted light carrying away this information through its polarisation.

3.1.2 Self-interaction and beats of polarisation

We first consider the case where two condensates—one for each projection of the spin—coexist and retain their coherent features over appreciable periods (as shown in the previous chapter, typical formation times for polariton condensates belong to the hundred ps range, while spin-lattice relaxation time is much longer). These two phase correlated condensates would spatially be located exactly in the same area of the structure, which is a strong departure of this system from a double-quantum well, proposed for detection of the optical Josephson effect. In the present system the Josephson effect is actually present if any type of interaction between the two condensates exists. Such an interaction must be spin and energy-conserving. The exchange interaction between two spin-polarised exciton condensates has been analyzed by Fernández-Rossier & Tejedor (1997), however, without investigation of the order parameter dynamics of the two condensates. We address here the impact on the polarisation dynamics of cyclic exchange processes between two spin-polarised polariton condensates. We show that characteristic beats in linear polarisation of emitted light appear due to the double spin flip process. Furthermore, we show that besides spin dependent effects, cyclic exchanges influence the coherence of the emitted light, namely, the cyclic processes between a condensate and upper-energy polariton states result in attenuated oscillations of the coherence ratio. To reveal specific effects of the cyclic processes we neglect all other interactions between polaritons, that is we disregard coupling with phonons and also polariton-polariton interaction. Spin-lattice relaxation and all other mechanisms of spin relaxation are neglected as well. We consider again the simplest model of two oscillators, with energies $\hbar\omega_\uparrow$ and $\hbar\omega_\downarrow$, and study the dynamics implied by cyclic interactions, i.e., double spin-flip processes whereby two polaritons, one in each level, simultaneously change their spin. An essential difference between Bose-condensates of simple excitons and exciton-polaritons is that in the latter case, bosonic properties strongly dominate over fermionic interactions of underlying electrons and holes granted separately, so that any electron-electron, hole-hole or electron-hole spin flips can be neglected. Therefore,

in our limitations, with Bose annihilation operators a_\uparrow , a_\downarrow for polaritons of spin -1 and $+1$ respectively, the corresponding model Hamiltonian reduces to:

$$H = \hbar\omega_\uparrow a_\uparrow^\dagger a_\uparrow + \hbar\omega_\downarrow a_\downarrow^\dagger a_\downarrow + \hbar g a_\uparrow^\dagger a_\uparrow a_\downarrow^\dagger a_\downarrow \quad (3.1)$$

with $\hbar g$ the cyclic interaction matrix element. H conserves the total spin and the number of polaritons in both levels so total luminescence as well as intensity of circular polarised components intensity remains constant. Also, two times correlators like $a_i^\dagger(t + \tau)a_j(t)$, $i, j = \uparrow, \downarrow$ or higher orders generalisations have trivial temporal dependence as is to be expected for a single mode (even though it has the additional degree of freedom brought by polarisation). This is readily checked directly in the Heisenberg picture since so simple an Hamiltonian dispenses from quantum regression analysis and the operator solution can be obtained:

$$a_\uparrow(t) = a_\uparrow(0)e^{-i(\omega_\uparrow + g a_\downarrow^\dagger a_\downarrow)t} \quad (3.2a)$$

$$a_\downarrow(t) = a_\downarrow(0)e^{-i(\omega_\downarrow + g a_\uparrow^\dagger a_\uparrow)t} \quad (3.2b)$$

Clearly, optical coherence of fields as defined by Glauber is not affected by these cyclic processes. However, a_\uparrow and a_\downarrow taken independently have nontrivial dynamics, which is also of importance since their quantum average is the BEC order parameter. This dependence means that the effect is linked to field amplitudes rather than to field intensities, and therefore the dynamics of polarisation predominates over fringes making ability (first order coherence) or photons statistics (second order), or indeed, any higher order. The experimental observation comes from the decomposition of the intensity of light emitted in a given linear polarisation I_i as

$$I_i = I_i^c + I_i^{nc} \quad (3.3)$$

with $i = x, y$ the electric field vector direction, I_i^c the coherent fraction and I_i^{nc} the incoherent fraction. Since the incoherent part of emission is largely isotropic (it has a randomly fluctuating linear polarisation) we expect it to give equal contributions to x and y linear polarisations:

$$I_x^{nc} = I_y^{nc} = \frac{1}{2}[\xi^2(N_\uparrow + N_\downarrow) - \varsigma^2(|\alpha_\uparrow|^2 + |\alpha_\downarrow|^2)] \quad (3.4)$$

where $N_{\uparrow,\downarrow}$ are average numbers of polaritons with spin up and down respectively, $\alpha_i \equiv \langle a_i \rangle$, $i = \uparrow, \downarrow$ are corresponding order parameters, and ξ, ς are constants ($\xi \approx \varsigma$). The intensities of coherent components of emitted light are

$$I_{x,y}^c = \frac{\varsigma^2}{2}[|\alpha_\uparrow|^2 + |\alpha_\downarrow|^2 \pm 2|\alpha_\uparrow||\alpha_\downarrow|\cos(\Delta\phi)] \quad (3.5)$$

where \pm correspond to x, y polarisations, respectively. Here $\Delta\phi$ is the phase shift between α_\uparrow and α_\downarrow at $t = 0$. In Eqs. (3.4, 3.5) we supposed that the total emission intensity is determined by the number of polaritons, while the coherent fraction depends on the coherence parameter of the system. If the energies of the two condensates are the same, the phase shift remains constant, and total intensity reads:

$$I_{x,y}(t) = \frac{\xi}{2}(N_\uparrow + N_\downarrow) \pm \varsigma^2 \cos(\Delta\phi)|\alpha_\uparrow||\alpha_\downarrow| \quad (3.6)$$

These formulae show clearly the influence of the order parameter upon the emitted light. Note that $I_x(t) + I_y(t)$ is not affected by the cyclic process and remains constant.

Now for the dynamics of this order parameter. If at $t = 0$ the two states are separated, that is if the total density matrix $\rho_{\uparrow\downarrow}$ can be factored as $\rho_{\uparrow}\rho_{\downarrow}$, eq. (3.2a) reduces to

$$\alpha_{\uparrow}(t) = \alpha_{\uparrow}(0)e^{-i\omega_{\uparrow}t}\text{Tr}(\rho_{\downarrow}e^{-ia_{\downarrow}^{\dagger}a_{\downarrow}t}) \quad (3.7)$$

(corresponding equation for α_{\downarrow} is obtained by interchanging everywhere \uparrow and \downarrow). This assumption can be met experimentally for instance by illuminating the sample with two lasers, each with the polarisation suitable to populate coherently both states, without inducing ab initio correlations. Since $\sum_n \rho_{\downarrow nn} = 1$,

$$\left| \sum_n \rho_{\downarrow nn} e^{-ignt} \right| \leq 1, \quad (3.8)$$

and the equality holds periodically in time, when the exponential argument vanishes. Thus the interaction between the two condensates induces oscillations of the amplitudes of both order parameters. As amplitudes never exceed their initial value, the interaction reduces the temporal averages of the order parameters. Moreover, they oscillate in phase, so that there is no coherence transfer between the two states.

When the system is initially in the coherent state $|\alpha_{\uparrow}\rangle|\alpha_{\downarrow}\rangle$, eq. (3.7) readily evaluates to

$$\alpha_{\uparrow}(t) = \alpha_{\uparrow}(0)e^{-i\omega_{\uparrow}t} \exp[|\alpha_{\downarrow}(0)|^2(e^{igt} - 1)]. \quad (3.9)$$

Since $\hbar g$ varies inversely with the cavity surface, it vanishes in the thermodynamic limit. We assume a lateral size for the system of $1\mu\text{m}$ (pillar) and consider typical parameters for GaAs QWs. The resulting oscillation period is of the order of a hundred picoseconds, which is much shorter than the coherence decay time in a polariton laser operating in its stationary regime, which falls in the μs range. Observe how the larger order parameter amplitude is less modulated than the smaller one. The oscillations of the order parameters of two condensates corresponding to different exciton spin-states result in the oscillations of the linearly polarised emission intensity as fig. 3.3 displays. These oscillations are due to the beats between coherent and incoherent components of the emission, cf. eqs. (3.4—3.6). The coherent component keeps a definite linear polarisation (x -polarisation in fig. 3.3), while the incoherent emission is depolarised thus contributing equally to x - and y -polarisations. These polarisation beats can be considered as a signature of coupling between two spin-polarised condensates being an optical analogy of the Josephson effect.

3.1.3 Interaction between condensate and upper polariton states

The cyclic interaction of the condensate with the higher energy states in polariton lasers reveals essentially the same physics as that already presented in the previous section for spin-polarised interacting condensates, the hamiltonian and its solutions serving as a blueprint. With a more suitable set of notations, cf. (3.1):

$$H = \hbar\omega_0 a_0^{\dagger} a_0 + \hbar\omega_k a_k^{\dagger} a_k + \hbar W a_0^{\dagger} a_0 a_k^{\dagger} a_k \quad (3.10)$$

where subscript 0 pertains to ground state and k to a collective excited states. For cavities with negative detuning the collective- k state would correspond to the bottleneck. We now neglect

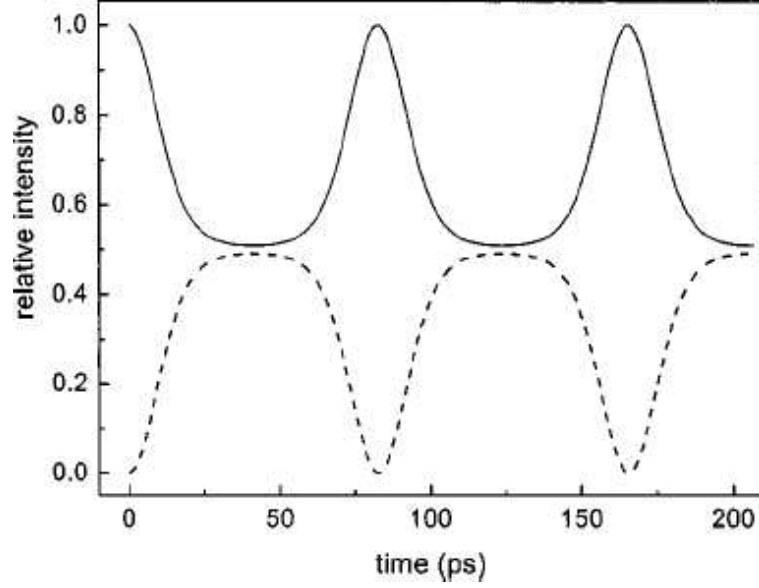


Figure 3.1: Relative intensities of x - (solid lined) and y - (dashed line) polarised components of light emitted by a microcavity where spin flip processes are dominant.

the spin here but we properly take into account the cyclic interaction between the condensate supposed to be in a coherent state at $t = 0$ and the upper energy states supposed to have thermal population.

The density matrix can be separated at $t = 0$ and eq. (3.7) evaluates to:

$$\alpha_0(t) = \alpha_0(0) e^{-i\omega_0 t} \frac{1 - e^{-\beta \hbar \omega_k}}{1 - e^{-\beta \omega_k} e^{-iWt}}, \quad (3.11)$$

so it is seen that the inverse temperature β plays a key role in the amplitude of oscillations. Figure (3.1) shows the oscillating order parameter of a condensate coupled to a single thermalized state calculated for different temperatures. At zero temperature ($\beta \rightarrow \infty$), α_0 remains constant but for increasing temperatures, its oscillations amplitude increases due to the cyclic interaction with higher energy states (with thermal statistics).

This dependency has an important impact on the behavior of condensed exciton polaritons for lasing action. Cyclic processes between polaritons from the condensate and from the reservoir are indeed possible and have the dramatic influence of smothering out the condensate order parameter amplitude. Generalizing eq. (3.11) to the case of a reservoir population distributed in the reciprocal space, we obtain

$$\alpha_0(t) = \alpha_0(0) \exp \left[-i\omega_0 t + \frac{m\mathcal{S}}{2\pi\hbar} \int_{\Delta}^{\infty} \ln \left(\frac{1 - e^{-\beta(\hbar\omega - \mu)}}{1 - e^{-\beta(\hbar\omega - \mu)} e^{-iW(\hbar\omega)t}} \right) d\omega \right] \quad (3.12)$$

where integration is taken over all states occupied by incoherent polaritons which affect order parameter of the ground state with Δ a characteristic energy splitting between the condensate and the reservoir; it depends on the Rabi-splitting and detuning between exciton and photon modes in the microcavity. \mathcal{S} is the area occupied by the polariton condensate and μ is the chemical potential arising from self-interaction in the condensate. Figure (3.2) shows the temporal dynamics of α_0 calculated in this way. For the numerical computation of the integral

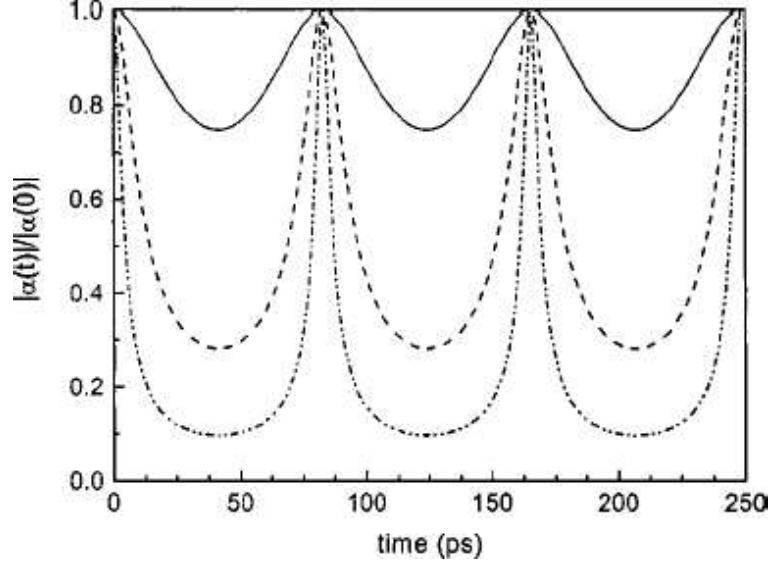


Figure 3.2: Temporal evolution of the amplitude of the order parameter of a pure coherent state coupled to a single thermal state distant by 5meV from the condensate, calculated for different temperatures, $T = 30\text{K}$ (solid line), 100K (dashed) and $T = 300\text{K}$ (dashed-dotted).

in (3.12), a parabolic dispersion of exciton polaritons in the exciton-like part of the lower polariton branch where the reservoir is located has been assumed.

We have further assumed $\Delta = 5\text{meV}$ and temperatures of 100 and 300 K, while the dependence $W(\hbar\omega)$ has been taken of the form

$$W(\hbar\omega) = \frac{W_0}{1 + e^{\hbar(\omega - \omega_0)/\delta}} \quad (3.13)$$

with $W_0 = 50\mu\text{eV}$, $\hbar\omega_0 = 10\text{meV}$ and $\delta = 2\text{meV}$, providing realistic dependence of the matrix element W on energy in a typical GaAs-based microcavity. The energy distribution of W results in an overall decay of the order parameter oscillations.

Back to the experimentally observable quantities, i.e., to the intensities of linearly polarised components of the emitted light: one should pay attention to $\Delta\phi$ which becomes time dependent whenever there is energy imbalance between the two states. This results in an additional modulation of the intensity of the emitted light. In order to avoid these oscillations whose time scale could be as low as a few picoseconds, an equal pumping of both condensates is preferential. Experimentally, an exact period of oscillations of the order parameter $2\pi/W$ can be easily achieved if the structure is pumped at high k with unpolarised light, while the seed of coherent polaritons in the ground state is introduced with a linearly polarised laser. This indeed excites on the average an equal number of spin-up and spin-down excitons. In this case $\alpha_1(0) = \alpha_2(0)$. The spin-lattice relaxation affects both condensates in the same way in this regime, thus it has no impact on the effect we discuss, legitimating us once more in neglecting spin-lattice relaxation in the previous derivation.

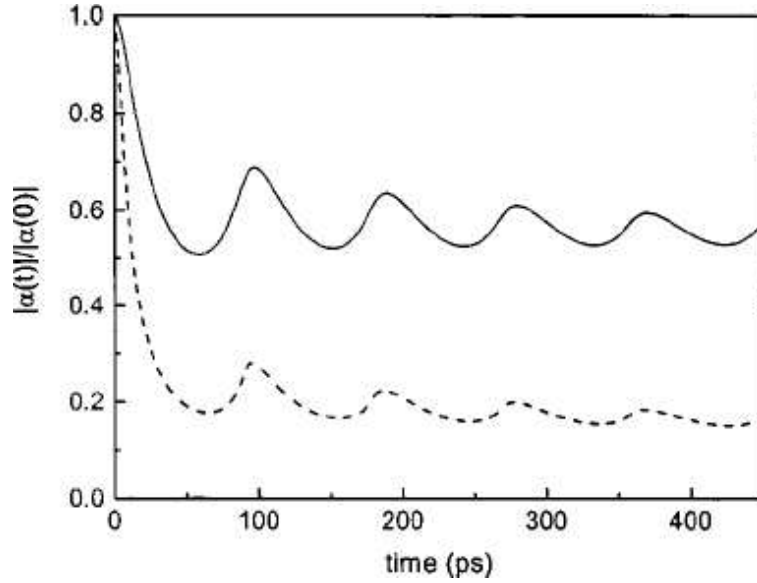


Figure 3.3: Temporal evolution of the order parameter of a Bose condensate of exciton polaritons in a typical polariton laser structure at 100K (solid line) and 300K (dashed). Coupling to the reservoir of incoherent polaritons is taken into account along with eq. (3.12).

3.2 Polarisation as an order parameter for polaritons BEC

3.2.1 The problem of the phase

We now propose a simple experimental method to evidence the appearance (and check the predicted survival) of the order parameter of a condensate made of interacting polaritons. A special difficulty with evidencing whether BEC has indeed occurred in a bosonic system is linked to the problem of its phase. Strictly speaking, BEC is a breaking of the gauge symmetry of the system which results in the appearance of a well defined phase for the condensate wavefunction. The previous considerations with g^2 were pertaining to coherent properties only, that is, that associated to statistics (which depends on diagonal elements of the density matrix) without regard to the phase (which depends on off-diagonal elements). We now show that a spontaneous symmetry breaking (appearance of a well-defined phase) in an ensemble of polaritons manifests itself in a dramatic change of the linear polarisation degree of the light emitted by the cavity and that the lifetime of this polarisation depends strongly on the nature of the polariton state, allowing for a direct evidence of phase effects. From the spin-degeneracy, appearance of the order parameter in the condensate leads to the spontaneous buildup of a linear polarisation whose in-plane orientation is constant in time, though it randomly changes from experiment to experiment in isotropic system. But the spin-degeneracy can also be significantly lifted by fluctuations feeding spin-up and spin-down condensates with unequal populations. The process of building two condensates when Bose stimulation comes into play is now rapidly investigated.

3.2.2 Stimulated random walk

For classical particles, fluctuations would yield a mean imbalance of $\sqrt{n_{0\uparrow} + n_{0\downarrow}}$ particles between the two condensates, with $n_{0\uparrow}$ spin-up and $n_{0\downarrow}$ spin-down particles. Consequently the

circular polarisation degree

$$\rho_c \equiv \frac{n_{0\uparrow} - n_{0\downarrow}}{n_{0\uparrow} + n_{0\downarrow}} \quad (3.14)$$

would vanish like the inverse square root of the occupation number. However, because of stimulation, the probability to reach one condensate or the other depends on respective populations in such a way as to strengthen the more populated state, leading to possibly highly degenerated configurations. The probability for a particle to join the condensate with $n_{0,\uparrow\downarrow}$ particles is

$$p_{\uparrow\downarrow} = \frac{n_{0\uparrow\downarrow} + 1}{n_{0\uparrow} + n_{0\downarrow} + 2}; \quad (3.15)$$

which yields

$$\langle |\rho_c| \rangle = \frac{2 + n_0}{2 + 2n_0} \quad (3.16)$$

that is, approximately 1/2 for large values of the total number of particles $n_0 \equiv n_{0\uparrow} + n_{0\downarrow}$ which corresponds to an elliptically polarised light.

3.2.3 Formalism

We consider an isotropic microcavity pumped out of resonance and incoherently by an unpolarised cw light-source. We do not discuss the dynamics of the polariton condensate formation which was the topic of the previous chapter. Our goal here is to describe the time evolution and dephasing of the condensate (and therefore of the linear polarisation) versus its coherence degree in the stationary regime. In this regime, a balance between incoming and outgoing particles is reached in the ground state, and the energy distribution function of polaritons does not change in time.

The Hamiltonian to describe this system we consider has the general form of the interaction Hamiltonian for spin polarised polaritons. It retains all interactions essential for the effect we discuss and neglects coupling to the excited states, the lifetime, scattering towards spin-forbidden (“dark”) exciton states, radiative decay and spin-lattice relaxation:

$$H = \hbar\omega_0(a_{\uparrow}^{\dagger}a_{\uparrow} + a_{\downarrow}^{\dagger}a_{\downarrow}) + \hbar W_1(a_{\uparrow}^{\dagger}a_{\uparrow}^{\dagger}a_{\uparrow}a_{\uparrow} + a_{\downarrow}^{\dagger}a_{\downarrow}^{\dagger}a_{\downarrow}a_{\downarrow}) + \hbar W_2a_{\uparrow}^{\dagger}a_{\uparrow}^{\dagger}a_{\downarrow}a_{\downarrow} \quad (3.17)$$

where we abbreviate $a_{\uparrow\downarrow}$ for the ground state polariton annihilation operator for spin up and down, respectively, and note $\hbar\omega_0$ the ground state energy, $\hbar W_i$ the interaction constants for polaritons having parallel ($i = 1$) or antiparallel ($i = 2$) spins. This Hamiltonian (3.17) describes dephasing of the polaritons in the condensate caused by their interactions and in this manner is an extension of the hamiltonian (3.1) of the previous section. It neglects however the dephasing induced by spontaneous scattering of exciton-polaritons from the excited states to the condensate.

Intensities I_+ and I_- of the circular polarised components of light emitted by the polariton condensate are proportional to the number operators,

$$I_+ \propto n_{0\uparrow} = \langle a_{\uparrow}^{\dagger}a_{\uparrow} \rangle \quad (3.18a)$$

$$I_- \propto n_{0\downarrow} = \langle a_{\downarrow}^{\dagger}a_{\downarrow} \rangle, \quad (3.18b)$$

while the linear-polarised components of the emitted light $I_{\leftrightarrow}, I_{\uparrow}$ are proportional to

$$I_{\leftrightarrow} \propto \frac{1}{2}(\langle a_{\uparrow}^{\dagger} a_{\uparrow} \rangle + \langle a_{\downarrow}^{\dagger} a_{\downarrow} \rangle) + \Re \langle a_{\uparrow} a_{\downarrow}^{\dagger} \rangle = \frac{1}{2}(n_{0\uparrow} + n_{0\downarrow}) + S_x \quad (3.19a)$$

$$I_{\uparrow} \propto \frac{1}{2}(\langle a_{\uparrow}^{\dagger} a_{\uparrow} \rangle - \langle a_{\downarrow}^{\dagger} a_{\downarrow} \rangle) - \Re \langle a_{\uparrow} a_{\downarrow}^{\dagger} \rangle = \frac{1}{2}(n_{0\uparrow} - n_{0\downarrow}) - S_x \quad (3.19b)$$

The operator of linear polarisation $\hat{S} \equiv a_{\uparrow} a_{\downarrow}^{\dagger}$ determines the in-plane components $S_{x,y}$ of the polariton pseudospin

$$S = \langle \hat{S} \rangle = S_x + iS_y \quad (3.20)$$

and governs the linear polarisation degree of the emitted light through

$$\rho_1 = \frac{2|S|}{n_{0\uparrow} + n_{0\downarrow}}. \quad (3.21)$$

Operator \hat{S} is the ladder operator $S_x + iS_y$ for operators $S_x \equiv \Re a_{\uparrow} a_{\downarrow}^{\dagger}$, $S_y \equiv \Im a_{\uparrow} a_{\downarrow}^{\dagger}$ and $S_z \equiv a_{\uparrow}^{\dagger} a_{\uparrow} - a_{\downarrow}^{\dagger} a_{\downarrow}$ which follow a spin- $\frac{1}{2}$ algebra. For this reason \hat{S} is called the *pseudospin*. It is a powerful representation for two-level systems which allowed many insights into the polaritons spin dynamics.

In Heisenberg representation, the dynamics of \hat{S} is given by

$$\partial_t \hat{S} = \frac{i}{\hbar} [\hat{S}, H] = iV(a_{\uparrow}^{\dagger} a_{\uparrow} - a_{\downarrow}^{\dagger} a_{\downarrow} - 1) \hat{S} \quad (3.22)$$

where we introduced

$$V \equiv 2W_1 - W_2. \quad (3.23)$$

In general, $W_1 \neq W_2$ and often they even have opposite sign, reflecting the fact that while polaritons with parallel spin repel each other, polaritons with opposite spins may form a bound state, called a *bipolariton*. It has been shown theoretically by Ciuti, Savona, Piermarocchi, Quattropani & Schwendimann (1998) that $|W_2| \ll |W_1|$ and confirmed through experiment by Kavokin, Renucci, Amand, Marie, Senellart, Bloch & Sermage (2005) that $|W_2| \approx 0.04|W_1|$. Ciuti et al. (1998) have estimated the exciton-exciton interaction $|W_1|$ as:

$$|W_1| = 6E_b a_B^2 / \mathcal{S} \quad (3.24)$$

where E_b is the exciton binding energy, a_B the exciton Bohr radius and \mathcal{S} the surface of the condensate, given to good approximation by the size of the exciting laser spot. In CdTe microcavities with a lateral size $10\mu\text{m}$, $V \approx 10\text{neV}$.

The pseudospin temporal dependence reads:

$$S(t) = e^{-iVt} \text{Tr} \left[\exp[iVt(a_{\uparrow}^{\dagger} a_{\uparrow} - a_{\downarrow}^{\dagger} a_{\downarrow})] \hat{S}(0) \rho \right] \quad (3.25)$$

where ρ , the density matrix of the system, is time-independent as this analysis holds in Heisenberg representation. $S(t)$ describes variation of the intensity of light emitted by the cavity in a given linear polarisation.

3.2.4 Spontaneous buildup of the polarisation

We now assume that the two condensates are not correlated. This allows to factorise the density matrix as $\rho = \rho_{\uparrow} \otimes \rho_{\downarrow}$, and derive from (3.25)

$$S(t) = e^{-iVt} \text{Tr} \left[\exp[-iVta_{\uparrow}^{\dagger} a_{\uparrow}] a_{\uparrow} \rho_{\uparrow} \right] \text{Tr} \left[\exp[iVta_{\downarrow}^{\dagger} a_{\downarrow}] a_{\downarrow}^{\dagger} \rho_{\downarrow} \right] \quad (3.26)$$

The initial in-plane pseudospin reads

$$S(0) = \alpha_{\uparrow} \alpha_{\downarrow}^* \quad (3.27)$$

with the definition of order parameter for each circularly polarised condensate given, as usual, by $\alpha_{\uparrow\downarrow} \equiv \text{Tr}(a_{\uparrow\downarrow} \rho_{\uparrow\downarrow})$.

From eqs. (3.21) and (3.27) one establishes an explicit connection between the linear polarisation ρ_l and order parameter of BEC defined in the usual way as the quantum average over the Bose annihilation operator. Indeed appearance of the linear polarisation in the condensate is observed only if an order parameter builds up for each of the circularly polarised components. The measurement of the circularly polarised emission gives access to $a_{\uparrow}^{\dagger} a_{\uparrow}$ and $a_{\downarrow}^{\dagger} a_{\downarrow}$ which combined with the measurement of the linear polarisation degree gives a measurement of the order parameter. Note that the superposition of two states with a Poisson distribution but no well defined phase (randomly phased coherent states) does not lead to an in-plane polarisation.

In what follows we compute the time dependence of the in-plane pseudospin versus the coherence degree of the individual condensate using Glauber-Sudarshan representation of the density matrix, upgraded to describe the spin degree of freedom,

$$\rho_{\uparrow\downarrow} = \int |\alpha_{\uparrow\downarrow}\rangle \langle \alpha_{\uparrow\downarrow}| P(\alpha_{\uparrow\downarrow}, \alpha_{\uparrow\downarrow}^*) d\alpha_{\uparrow\downarrow} d\alpha_{\uparrow\downarrow}^* \quad (3.28)$$

with α here characterizing the coherent state $|\alpha\rangle$ (with a given amplitude and phase). From this definition one obtains:

$$S(t) = e^{-iVt} \int P_{\uparrow}(\alpha_{\uparrow}, \alpha_{\uparrow}^*) \langle \alpha_{\uparrow} | e^{-iVta_{\uparrow}^{\dagger} a_{\uparrow}} | \alpha_{\uparrow} \rangle d\alpha_{\uparrow} \int P_{\downarrow}(\alpha_{\downarrow}, \alpha_{\downarrow}^*) \langle \alpha_{\downarrow} | e^{iVta_{\downarrow}^{\dagger} a_{\downarrow}} | \alpha_{\downarrow} \rangle d\alpha_{\downarrow}. \quad (3.29)$$

The initial coherence degree in each of the individual condensates is given by:

$$\chi_{\uparrow\downarrow} = \frac{|\alpha_{\uparrow\downarrow}|^2}{n_{0\uparrow\downarrow}} = \frac{n_{0\uparrow\downarrow, \text{coh}}}{n_{0\uparrow\downarrow, \text{coh}} + n_{0\uparrow\downarrow, \text{th}}} = \sqrt{2 - g_{\uparrow\downarrow}^2(0)}, \quad (3.30)$$

with $g_{\uparrow\downarrow}^2(0)$ the second order coherence of the individual condensates, $n_{0\uparrow\downarrow, \text{th}}$ the average numbers of spin-up and spin-down polaritons in the thermal fraction and $n_{0\uparrow\downarrow, \text{coh}} = |\alpha_{\uparrow\downarrow}|^2$ the average numbers of spin-up and spin-down polaritons in the coherent fraction. The coherence degree varies between 0 (thermal state) and 1 (coherent state). Note, however, that the second order coherence can be related to the order parameter only when one considers a pure coherent state. A measurement of $g^2(0)$ alone does not in general provide full information on the order parameter.

The P function which describes the superposition of the thermal and coherent states reads, cf. eq. (1.55):

$$P_{\uparrow\downarrow}(\alpha, \alpha^*) = \frac{1}{\pi n_{0\uparrow\downarrow, \text{th}}} \exp\left(-\frac{|\alpha - \alpha_{\uparrow\downarrow}|^2}{n_{0\uparrow\downarrow, \text{th}}}\right). \quad (3.31)$$

Using this expression, $S(t)$ evaluates to

$$S(t) = \frac{S(0) \exp\left(-\frac{n_{0\uparrow,\text{coh}}\theta}{n_{0\uparrow,\text{th}}\theta + 1} - \frac{n_{0\downarrow,\text{coh}}\theta^*}{n_{0\downarrow,\text{th}}\theta + 1}\right)}{(n_{0\uparrow,\text{th}}\theta + 1)^2(n_{0\downarrow,\text{th}}\theta^* + 1)^2} \quad (3.32)$$

with $\theta \equiv 1 - \exp[-iVt]$.

We now consider the likely configuration where the coherence degree of spin-up and spin-down condensates are equal and given by χ . In the limit $Vt \ll 1$, expression (3.32) is approximately given by:

$$S(t) = S(0) \frac{e^{-in_0\rho_c\chi Vt} e^{-\frac{1}{2}(n_0 + (1-\chi)(1+\rho_c^2)n_0^2)\chi V^2 t^2}}{(\frac{1}{2}(1-\chi)(1+\rho_c)n_0 iVt + 1)^2 (\frac{1}{2}(1-\chi)(1-\rho_c)n_0 iVt - 1)^2}. \quad (3.33)$$

where $n_0 = n_{0\uparrow} + n_{0\downarrow}$.

The behavior of the pseudospin is dominated by the numerator of (3.33) in the vicinity of the coherent case ($\chi \approx 1$) and by the denominator in the opposite limit, close to the thermal case ($\chi \approx 0$). In a narrow region close to full-coherence, the pseudospin oscillates in time with a period

$$T_0 = \frac{2\pi}{Vn_0\chi|\rho_c|}. \quad (3.34)$$

Conversely to the period of oscillations, the amplitude is very sensitive to the coherence degree. The pseudospin decays like $\exp(-t^2/\tau^2)$ with characteristic time

$$\tau = \frac{\sqrt{2}}{V\sqrt{(n_0 + (1-\chi)(1+\rho_c^2)n_0^2)\chi}}. \quad (3.35)$$

This decay is caused by the energy broadening of the state which is induced by the huge thermal fluctuations in particle number which result in fluctuations of energy and hence on destructively interfering oscillations of the Larmor precessions. For the completely coherent case where the fluctuations in the particle number are as small as allowed without squeezing, the decay time is as high as

$$\tau_{\text{coh}} = \frac{\sqrt{2}}{V\sqrt{n_0}}. \quad (3.36)$$

Note that it increases with L^2 so that the polariton density remains constant, thus the dephasing of a coherent state vanishes in the thermodynamic limit, which fits well with the classical picture of BEC. However, the presence of even a tiny thermal fraction dramatically reduces the decay time. If $(1-\chi)n_0 \gg 1$, the decay times evaluates to

$$\tau = \frac{\sqrt{2}}{Vn_0(1-\chi)} \quad (3.37)$$

and thus almost cancels. Contrary to τ_{coh} , it remains finite in the thermodynamic limit, thus loses the linear polarisation of the condensate no matter how small is the thermal fraction. Thus, only in a narrow region close to full-coherence does the pseudospin exhibit oscillations in time. For values of χ below 85%, there are no observable oscillation and the decay is

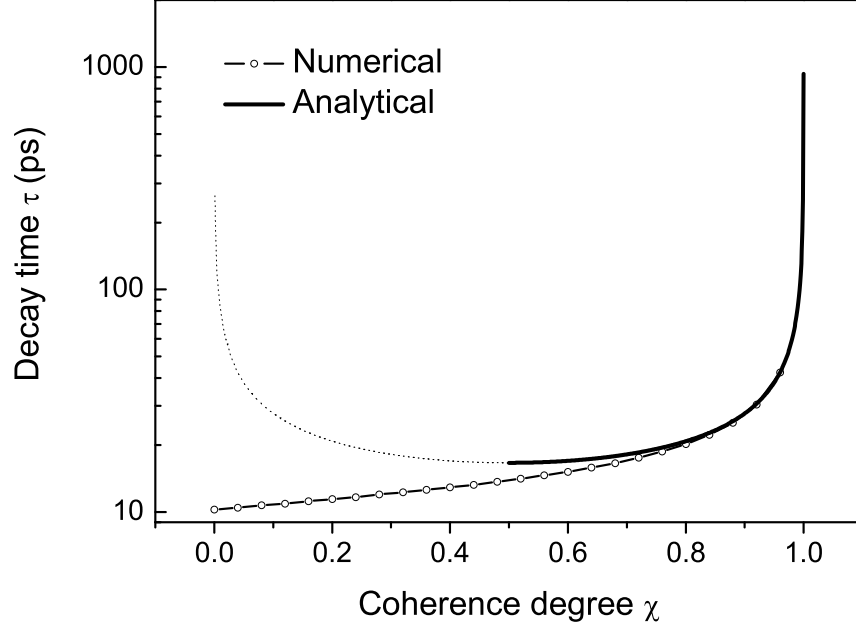


Figure 3.4: Decay time of the polarisation envelope with bullets on numerical points and its analytical approximation (3.33) which holds in the vicinity of coherent cases (solid), here for $\rho_c = 1/2$. The unphysical behaviour of (3.33) is shown dotted.

very fast as well as almost independent on the coherence degree. In the limit of small χ , the pseudospin decays like a Lorentzian:

$$|S(t)| \approx \frac{1}{|1 + 2i(1 - \chi)n_0V|\rho_c|t|} \quad (3.38)$$

On the opposite, close to the coherent limit, the pseudospin oscillates with a period given by the energy splitting between the circularly polarised eigenstates in the coherent fraction.

It also depends on the coherence degree but since the range of validity of this formula is for a small gamut of values of χ , the period of oscillations is essentially independent of the coherent properties of the state. This period is however sensitive to the circular polarisation degree of the condensate which absolute value runs from 0 to 1. The lower limit is reached when the spin-degeneracy is not lifted in which case the polarisation axis does not rotate and only dephasing takes place. The orientation of linear polarisation is random in a system having a perfect in-plane isotropy.

Fig. 3.4 displays the decay time τ as a function of the coherence degree χ . Parameters are those of a CdTe cavity with $n_0 = 10^4$ polaritons in the ground state and $\rho_c = 1/2$. The solid-dotted line results from numerical calculations with (3.33), estimating the typical lifetime as the time it takes for $|S(t)|$ to decrease by a factor e . This is natural in the limit of coherent states where the decay is exponential. The solid line superimposed is the analytical approximation (3.35) which holds over half the defining domain of χ . The curve is displayed dotted below 50% where it loses physical meaning. Past this point, the decay loses its exponential character to behave according to the denominator of (3.38), i.e., approximately like a Lorentzian. Fig. 3.5 shows the decay of the pseudospin in these two opposite regimes. Right hand side displays the pure coherent case, where many oscillations are sustained for as long as several

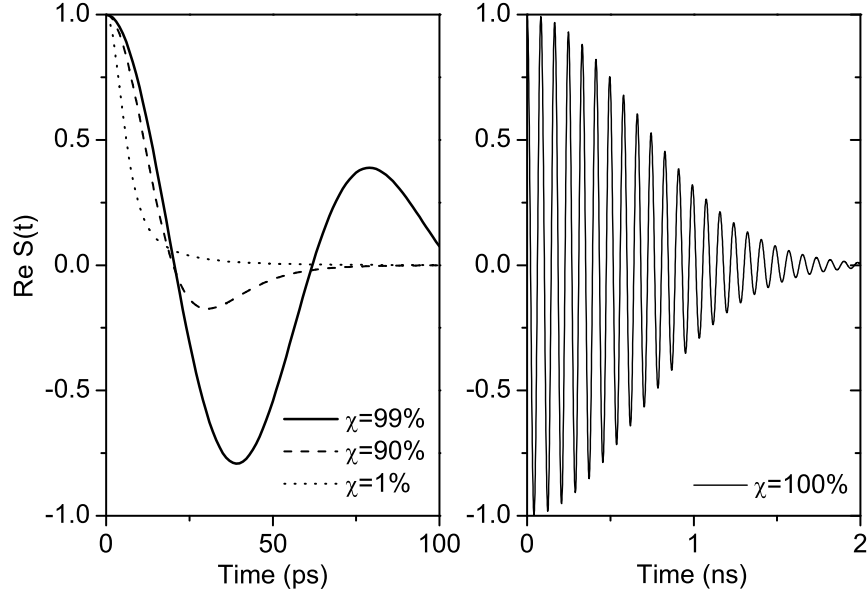


Figure 3.5: Decay of the linear polarisation for the full coherent case ($\chi = 1$) on the right, featuring sustained oscillations, and the impact of thermal contamination ($\chi = .01, .9$ and $.99$) on the left. Note the different timescale (actually the period is the same on both graphics.)

nanoseconds even though there is a very large number of particles. The spontaneous decay time is even longer (few hundreds of nanoseconds in the present case). It is interesting to compare the dephasing time and the typical coherence buildup time, the characteristic time needed for a coherent state to appear after the non-resonant pumping is switched on, which we have found to be, for CdTe microcavities, of the order of few hundreds of picosecconds. This comparison shows that the dephasing induced by the polariton-polariton interaction does not prevent formation of coherent states and therefore symmetry breaking in polariton systems. Left hand side displays two almost coherent cases where the decay time has drastically decreased because of the phase mismatches brought by the thermal fraction. Also displayed is the thermal case, here for $\chi = 10\%$, though this overdamped, non-oscillating decay is characteristic for all cases with $\chi < 85\%$. Since the decay time of $|S(t)|$ is very sensitive to the coherent degree of the condensate, it allows for easy and accurate measurements, a point we shall further investigate in next section. Finally we point out that the dephasing time of a single component condensate can be straightforwardly extracted from the present formalism. We do not address specifically this aspect because this quantity is much harder to measure for a single component condensate than for a superposition of two different one.

3.3 Determination of the degree of coherence through polarisation

3.3.1 Correlations

Light emitted by microcavities can have a nonzero linear polarisation degree without Bose-condensation, for instance if the microcavity is excited by a polarised light. In this case the

pump-induced polarisation can reappear in the ground state. This is the situation we now consider, as opposed to previous section where it was shown that the polarisation builds up from zero along with the condensate and thereby serves as an order parameter for Bose condensation. In presence of preexisting correlations, the polarisation does not depend on the phase relationship between the two populations of spin-up and spin-down polaritons. For instance, thermal light, with no phase whatsoever, can be polarised. We shall suppose here that correlations between the two condensates exist from pumping constrains and thus consider the effect of statistics (or second-order coherence). Again, this is to contrast with previous section where, with the same model hamiltonian but in absence of *ab initio* correlations, the polarisation reflects phase coherency which has appeared in the system. Namely, we now consider an elliptically polarised resonant pump in the more general case—which can degenerate to the cases of linear or circular polarisation—that injects in the system correlated populations of spin-up and spin-down polaritons. We assume they retain their correlations while relaxing toward the ground state, which is the case if the spin-lattice relaxation is negligible. Thus we refer to an experimental geometry close to that described by Shelykh, Kavokin, Kavokin, Malpuech, Bigenwald, Deng, Weihs & Yamamoto (2004) where polarised polaritons are created by resonant pumping at an oblique angle. The non-resonant circularly-polarised pumping, as is the case in the work of Martin, Aichmayr, Viña & André (2002), does not allow for creation of a linearly polarised component of the condensate emission, which is extremely important for characterization of the quantum statistics of polaritons in the condensate, as we show below. We demonstrate theoretically in this paper that the linear polarisation degree of the light emitted by the cavity and especially its lifetime depend sensibly on the statistics of the polariton state, and therefore on $g^2(0)$. Again, it does not depend on the off-diagonal elements of the density matrix, so that a pure coherent state with a well defined phase on the one hand, and a so-called randomly phased coherent state with same statistics (Poissonian) but no phase on the other hand, will display the same linear polarisation.

3.3.2 Formalism

We come back to the couple of energy-degenerated spin-up and spin-down quantum states, occupied by interacting exciton-polaritons granted as ideal bosons. The model hamiltonian remains (3.17). We still focus on the ground state only, thereby neglecting coupling to excited states and thus the dynamics of relaxation, amply covered in the previous chapter. Our point now is to draw the consequences of a condensate already existing in the ground state, not to analyze the dynamics of its formation. On the same basis, we do not need introduce the lifetime in the hamiltonian, which would unnecessarily complicate the analysis, though of course radiative lifetime is mandatory for the effect be observed from the light field emitted by unstable polaritons. This, however, can be accounted for phenomenologically, for instance assuming a continuous pumping holding a balance between polaritons lost by radiative emission and gained from relaxation into the ground state or in pumped regime with lifetime of particles at high momentum much higher than in the ground state so that the former can be considered as a reservoir maintaining constant the population of the latter. The in-plane components of the pseudospin characterize correlations that exist between spin-up and spin-down condensates. We now focus on the case of two initially completely correlated condensates, so that $\langle \hat{S}_x^2 \rangle + \langle \hat{S}_y^2 \rangle + \langle \hat{S}_z^2 \rangle = n_0/2$ with again $n_0 \equiv \langle a_{\uparrow}^{\dagger} a_{\uparrow} \rangle + \langle a_{\downarrow}^{\dagger} a_{\downarrow} \rangle$ as the total number of polaritons in the two condensates. In terms of classical optics, our assumption of complete correlation means that we consider fully

polarised light. We will show that polariton-polariton interactions may provoke depolarisation of light emitted by the cavity (stemming from the decoherence of the polariton condensate). The rate of this depolarisation will be shown to be strongly sensitive to the particles statistics.

The term $V(\langle a_{\downarrow}^{\dagger} a_{\downarrow} \rangle - \langle a_{\uparrow}^{\dagger} a_{\uparrow} \rangle)$ in eq. (3.25) is the energy splitting between right and left-circularly polarised condensates which arises if their populations are not equal. This splitting also referred to as *optically induced Zeeman splitting* has been theoretically analyzed by Fernández-Rossier & Tejedor (1997) and later experimentally observed and reported by Kavokin, Lagoudakis, Malpuech & Baumberg (2003). The pseudospin operator thus rotates at a speed given by the energy splitting between the two condensates. The remarkable feature of this result arises when we move to quantum averages over possible states of the condensate. We show in what follows that $S(t) \equiv \langle \hat{S}(t) \rangle$ depends crucially on the quantum state, specified in its more general form by a density matrix ρ of the spin-degenerated condensate, which is time independent in the Heisenberg picture and thus fully specified by its initial condition. As we investigate the case where the two condensates are correlated from pumping condition, we work in the basis of elliptically polarised states. A polariton with circular polarisation degree given by

$$P \equiv \cos^2 \theta - \sin^2 \theta, \quad (3.39)$$

is the coherent superposition of a spin-up polariton with probability $\cos^2 \theta$ and of a spin-down polariton with probability $\sin^2 \theta$, therefore, its quantum state can be created from the vacuum $|0, 0\rangle$ (zero spin-up and zero spin-down polaritons) by application of the following operator:

$$|1, \theta, \phi\rangle \equiv (\cos \theta a_{\uparrow}^{\dagger} + e^{i\phi} \sin \theta a_{\downarrow}^{\dagger}) |0, 0\rangle. \quad (3.40)$$

Here we also took into account the angle ϕ of in-plane orientation of the axis of the polarisation ellipse, which however plays no role in what follows. This defines $a_{\theta, \phi}^{\dagger}$ the creation operator for an elliptically polarised polariton as

$$a_{\theta, \phi}^{\dagger} \equiv \cos \theta a_{\uparrow}^{\dagger} + e^{i\phi} \sin \theta a_{\downarrow}^{\dagger}. \quad (3.41)$$

The superposition of n such correlated polaritons is obtained by recursive application of the creation operator:

$$|n, \theta, \phi\rangle = a_{\theta, \phi}^{\dagger n} |0\rangle = \frac{1}{\sqrt{n!}} (\cos \theta a_{\uparrow}^{\dagger} + e^{i\phi} \sin \theta a_{\downarrow}^{\dagger})^n |0, 0\rangle, \quad (3.42)$$

which we have normalized (here $|0\rangle$ is the vacuum in the space of elliptically polarised states). Writing the density matrix in this basis, one obtains:

$$S(t) = \sum_{n, n'} \rho_{n, n'} \langle n, \theta, \phi | e^{-iVt/\hbar} \exp\left(\frac{iVt}{\hbar} (a_{\downarrow}^{\dagger} a_{\downarrow} - a_{\uparrow}^{\dagger} a_{\uparrow})\right) \hat{S}(0) | n', \theta, \phi \rangle. \quad (3.43)$$

Simple but lengthy algebra yields for the matrix element (details of the derivation are given in the appendix):

$$\langle n, \theta, \phi | \exp\left(\frac{iVt}{\hbar} (a_{\downarrow}^{\dagger} a_{\downarrow} - a_{\uparrow}^{\dagger} a_{\uparrow})\right) S(0) | n', \theta, \phi \rangle = s_0 n \Theta(t)^{n-1} \delta_{n, n'}, \quad (3.44)$$

with $s_0 = \frac{1}{2} \sin 2\theta e^{-i\phi}$ is the in-plane pseudospin of a single elliptically polarised polariton, and where we introduced as a shortcut:

$$\Theta(t) \equiv \cos^2 \theta e^{-iVt/\hbar} + \sin^2 \theta e^{iVt/\hbar}. \quad (3.45)$$

Whence the direct connection between the pseudospin, or linear polarisation, and the statistics $p(n) \equiv \rho_{n,n}$ of the condensate:

$$S(t) = s_0 \langle n \Theta^{n-1} \rangle, \quad (3.46)$$

where the right-hand side average is over $p(n)$. The two approaches, with or without correlations, differ essentially at this point in the computation of $\langle \hat{S} \rangle$ since in the case of no correlations, the density matrix can be factored and evaluated separately on each spin-projection, cf. (3.26). This results in many differences like the dependency of the decay time of polarisation on the polarisation degree of which we shall see more in what is coming. There is no such influence of the polarisation degree in absence of correlations. Note that $\langle S(t) \rangle$ does not depend on off-diagonal elements of ρ other than for s_0 which is a constant of time. This is also a feature of g_2 , which in this case is defined as:

$$g_2(t, \tau) \equiv \frac{\langle a_{\theta, \phi}^\dagger(t) a_{\theta, \phi}^\dagger(t + \tau) a_{\theta, \phi}(t + \tau) a_{\theta, \phi}(t) \rangle}{|\langle a_{\theta, \phi}^\dagger(t) a_{\theta, \phi}(t) \rangle|^2} \quad (3.47)$$

for spatially homogeneous cases. We consider here the case of $g_2(t, 0)$ only.

3.3.3 Polarisation dynamics and measure of the coherence degree

We now evaluate the in-plane pseudospin with statistics interpolating between thermal and coherent cases, and show results for a typical CdTe microcavity with a lateral size of $60 \mu\text{m}$, $V \approx 10\text{neV}$, exciton binding energy $E_b = 25\text{meV}$, exciton Bohr radius $a_b = 40 \times 10^{-10}\text{m}$ and now $n_0 \approx 10^5$.

In the pure coherent case (1.41), the average pseudospin (3.46) is easily computed as:

$$S(t) = S(0) \exp[n_0(\cos Vt - 1)] \exp[in_0 P \sin Vt] \quad (3.48)$$

with as previously $S(0) = \langle \hat{S}(0) \rangle \equiv s_0 n_0$ the initial in-plane pseudospin and $P \equiv \cos^2 \theta - \sin^2 \theta$ the circular polarisation degree. The in-plane polarisation oscillates with a period

$$T_{\text{coh}} = \frac{2\pi\hbar}{n_0 V P} \quad (3.49)$$

given by the energy splitting between the circularly polarised eigenstates $n_0 V P$. If the spin-degeneracy is not lifted, $\theta = \pi/4$ and the polarisation axis does not rotate, only dephasing takes place. This is the case of a purely linearly polarised condensate made up of two completely correlated spin-up and spin-down condensates of equal populations. If the condensate is elliptically polarised (with different average numbers of particles in its spin-up and spin-down components) the main axis of the ellipse rotates with time: this is self-induced Larmor precession. The projection of the pseudospin on its initial direction oscillates in this case. The amplitude of these oscillations decays with a time constant

$$\tau_{\text{coh}} = \frac{\sqrt{2}\hbar}{\sqrt{n_0 V}}. \quad (3.50)$$

This decay should be followed by a revival after a time $\sqrt{2}\hbar/V$ which for parameters we consider falls in the microsecond range and thus cannot be observed since the polarisation in the

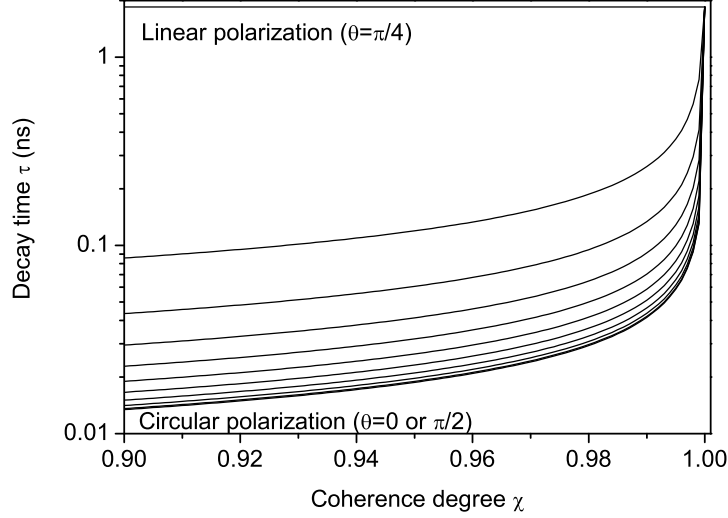


Figure 3.6: Decay time τ of the polarisation as given by eq. (3.55), as a function of the coherence degree χ in a neighborhood of the coherent state, for $P = \cos^2 \theta - \sin^2 \theta$ ranging from 0 (upper envelope) to ± 1 (lower envelope) for θ varying by steps of $1/40$ rad. For a pure coherent state, the lifetime does not depend on the polarisation. By adjusting this polarisation from pumping, one can tune the steepness of decay and therefore the accuracy of the measurement. For the linear polarisation, τ depends on θ on the fourth order of time only, and the change of decay with χ is therefore not experimentally observable in this case. This can be used to measure population or interaction strength, independently of the quantum state of the condensate.

system will be lost because of interactions with polaritons from excited states (which were neglected in this model). In the thermodynamic limit—where $\sqrt{n_0}V$ goes to 0 with \mathcal{S} going to infinity while the polariton density remains constant—the dephasing of the coherent state vanishes, recovering a thermodynamical virtue of BEC in infinite size systems.

In the thermal case (1.53), the average pseudospin (3.46) is computed as:

$$\langle S(t) \rangle = \frac{\langle S(0) \rangle}{(n_0(1 - \Theta(t)) + 1)^2} \quad (3.51)$$

The polarisation decay time is given in this case by

$$\tau_{\text{th}} = \frac{\sqrt{2}\hbar}{n_0V} \quad (3.52)$$

which is about 30ps for the parameters of our model. As the decay time is shorter than the period of the oscillations, none can be observed in this case. Contrary to the coherent case, the broadening does not vanish in the thermodynamic limit. This shows that a linear polarisation in the thermal state is impossible. In reality, a pure thermal state is never realized.

Now we turn to the general case (1.60). In principle one can compute numerically $S(t)$ using the exact formula and in this way extract the period of polarisation oscillation and decay time. We repeat however that the region of interest is close to a coherent state where a minute variation of χ results in important changes of the statistics. Observe also that p_{coth} in this region can be approximated by a Gaussian. The inset in fig. (1.1) shows the quality of this approximation for $\chi = 97\%$ which we will see is already far enough from the coherent states

for interesting effects to have already been observed. We therefore replace the awkward exact distribution (1.60) by a Gaussian which mean and variance are given by the first two moments of (1.60), that is, n_0 and $\sigma^2 = n_0 + n_0^2(1 - \chi^2)$. This allows, evaluating (3.46) in the continuous limit $s_0 \langle x \Theta^{x-1} \rangle$ to obtain an analytical expression in a neighborhood of the coherent state:

$$S(t) = S_0 \exp \left(n_0 \log \Theta(t) + \frac{1}{2} \sigma^2 (\log \Theta(t))^2 \right) \quad (3.53)$$

after neglecting logarithmically small values. Confronting this expression with numerical computations prove it to be sound even far away from the coherent state. In the limit $t \ll \hbar V$, (3.53) reads to order two in time:

$$S(t) \approx S_0 \exp(-t^2/\tau^2) \exp(i2\pi t/T_{\text{coh}}) \quad (3.54)$$

with a decay time τ given by

$$\tau = \frac{\sqrt{2}\hbar}{V \sqrt{n_0 + n_0^2 P^2 (1 - \chi^2)}}, \quad (3.55)$$

while the period of polarisation oscillation keeps the same value (3.49) independently of the coherence degree (close to the pure coherent state, this comes from approximating to n_0 the value at which $p_{\text{coth}}(n)$ is maximum). Most striking effects therefore belong with the lifetime (3.55) which is the central result of this section. Fig. 3.6 shows the decay time of the polarisation versus the coherence degree of the condensate for different linear polarisation degree, for the structure already described. Note the peculiar influence of the polarisation degree P . The decay time τ depends strongly on it once coherence starts to decrease from 1 but is otherwise unaffected in the pure coherent case. This polarisation dependence is not recovered in the limiting thermal case (cf. eq. (3.52)), where (3.55) does not apply anyway and which is not physical. Apart from P , however, the formula is qualitatively right. Pinning the polarisation from pumping one can thus accurately measure $g^2(0)$. This measure requires no quantum optical setup and can be fully realized thanks to time-resolved polarised photo-luminescence. The accuracy is very good thanks to steep variation for well chosen polarisation. The population n_0 can be determined from the linear polarised case, where the coherent degree plays no role. It should be noted, however, that if the number of polaritons in the condensate is small with respect to their number in the excited states, the interactions between the condensate and excited states may dominate over polariton-polariton interactions in the condensate. This is the case, in particular, in systems with a strong relaxation bottleneck effect. This theory does not describe this case.

3.4 Conclusions and Perspectives

We have shown how spin-flip processes result in beats of the polarisation emitted by the condensate of a microcavity (coherent fraction), and predicted periodical modulation of the order parameter arising from cyclic exchanges between ground state and the reservoir of excited states. We have then shown that the spontaneous appearance of linear polarisation in emission of microcavities can be considered as a criterion for Bose-condensation of polaritons, with essential features as follows:

- Spontaneous symmetry breaking in a polariton system which is not fully circularly polarised should be accompanied by a buildup of linear polarisation. Such linear polarisation cannot appear if the system is not coherent or very close to coherent.
- If the polariton condensate is elliptically polarised and in a coherent state, the in-plane component of its pseudospin rotates with a period proportional to the circular polarisation degree of the condensate and to the number of polaritons in the ground state. This results in rotation of the main axis of the polarisation ellipse of the emitted light. This in-plane component decays with a time constant given by the square root of the number of particles in the condensate. The dephasing time becomes longer than the spontaneous dephasing time and goes to infinity in the thermodynamic limit. The typical coherence buildup time is short on this time-scale.
- If the system is in a coherent state and the spin degeneracy is not lifted, the emitted light becomes fully linearly-polarised and its polarisation plane does not rotate in time. The decoherence time is the same as in the previous case. If the structure plane is isotropic, the linear polarisation axis changes randomly from experiment to experiment.

We have also shown how the linear components of polarisation are strongly affected by the coherence degree of a spin-degenerated condensate of polaritons. In particular, we showed that the decay time of the linear polarisation depends strongly on the polarisation degree, which can be tuned experimentally by the polarisation of the pump. In the vicinity of a coherent state with $g_2(0) \approx 1$ the lifetime of the linear polarisation becomes orders of magnitude longer than in thermal or mixed states where $g_2(0) > 1$. This measure therefore allows an accurate, though indirect, determination of the zero delay second order coherence.

Chapter 4

Exciton–Polaritons in Microcavities with Quantum Dots

Contents

4.1	The dawn of Cavity QED in semiconductors	103
4.2	Microscopic Foundations	104
4.3	Large Quantum Dots	107
4.4	Bare and Dressed states basis	109
4.5	Spectra of Optical Emission	112
4.6	Conclusions and Perspectives	113

4.1 The dawn of Cavity QED in semiconductors

Cavity Quantum-Electrodynamics is that branch of Quantum-Electrodynamics which focuses on light-matter interaction within the confines of a cavity. Main effects were pioneered in macroscopic electromagnetic cavities interacting with Rydberg atoms. The first main result was obtained by Purcell, Torrey & Pound (1946) who pointed out the possibility of tuning the spontaneous emission, later to be called the *Purcell effect*. The most popular reference, by Purcell (1946), is in fact a few lines abstract of the American Physical Society 271st meeting reporting that the spontaneous emission time of the nuclear magnetic moment which is about 5×10^{21} s in vacuum (at room temperature) can be reduced to the order of minutes in a cavity. The solid state counterpart was observed by Yamamoto, Machida & Bjork (1992). Rabi oscillations were observed by Raizen, Thompson, Brecha, Kimble & Carmichael (1989) and Zhu, Gauthier, Morin, Wu, Carmichael & Mossberg (1990).

Although very close in principle, cavity QED in atomic cavities and in a solid state system present many differences. In the words of Weisbuch et al. (1992), “*Besides its relying on a much simpler implementation—the solid state system is monolithic—the effect should lead to useful applications.*” A good overview of the cQED with QDs is given by İmamoğlu (2002), which provides in the abstract the main appealing feature of the solid state realisation, namely that “*since quantum dot location inside the cavity is fixed by growth, this system is free of the stringent*

trapping requirements that limit its atomic counterpart” and further comment that “*fabricating photonic nanostructures with ultrasmall cavity-mode volumes enhances the prospects for applications in quantum information processing.*” Recently experimental findings by Reithmaier, Sek, Löffler, Hofmann, Kuhn, Reitzenstein, Keldysh, Kulakovskii, Reinecker & Forchel (2004) and Yoshie, Scherer, Heindrickson, Khitrova, Gibbs, Rupper, Ell, Shchekin & Deppe (2004), published as two consecutive letters to Nature magazine, and that of Peter, Senellart, Martrou, Lemaître, Hours, Gérard & Bloch (2005), have reached the final step of strong coupling. Although the polariton of Weisbuch—observed a long time ago and well understood theoretically as well as finely controlled experimentally—had been initially thought to provide the solid state realisation, we have discussed at length how the polaritons represent in fact a more complicated system. One might think that the delay to strip down this complexity to finally achieve the exact counterpart of one atomic-like system coupled to a mode of radiation without further degrees of freedom was merely a technical problem and that the theory was already laid down in twenty years of literature. We have taken the opposite view that the semiconductor case brings forward many specificities of its own. The most important one, in agreement with İmamoğlu, is that in the solid state case one has a much better control of the atomic-like excitation. A QD stuck in the cavity can be kept immobile while in the atomic cavities case, the excitations are beams of atoms with much difficulties to single out one atom or to deal with it for prolonged periods of time. In the case of semiconductors, for instance, one can expect a much better investigation of coherent exchanges between many QDs through the radiation field, as is modelled by the Dicke model of n two-level atoms interacting through a single mode of radiation. All dispositions from those—phase-mismatched—leading to subradiant configurations where the excitation of two QDs is exchanged back and forth and does not escape, to cooperative one—in-phase—where the excitation is collectively shared leading to superadiant emission, can be obtained by proper identification of the mapping of QDs in the structure and tuning the excitation accordingly.

4.2 Microscopic Foundations

Our consideration towards an understanding of the behaviour of excitons in a large QD starts with the single exciton normalized wavefunction $\varphi(\mathbf{r}_e, \mathbf{r}_h)$ with \mathbf{r}_e and \mathbf{r}_h the position of the electron and hole, respectively. In what follows we restrict to direct band semiconductors with non-degenerate valence band. Such a situation can be experimentally achieved in QDs formed in the quantum well plane of conventional III-V or II-VI semiconductors where the light-hole levels lie far in energy as compared to the heavy-hole ones, due to the size quantization along growth axis, thus we consider only electron-heavy hole excitons. Moreover, we will assume all carriers to be spin polarized and thus we will neglect the spin degree of freedom of the electron-hole pair. This can be realized experimentally by pumping resonantly the structure with circular polarization. or by application of an external magnetic field along the growth axis of the structure.

Expanding the excitonic wavefunction over the independent size-quantization functions of electron $\varphi_{n_e}^e(\mathbf{r}_e)$ and hole $\varphi_{n_h}^h(\mathbf{r}_h)$,

$$\varphi(\mathbf{r}_e, \mathbf{r}_h) = \sum_{n_e, n_h} C_{n_e, n_h} \varphi_{n_e}^e(\mathbf{r}_e) \varphi_{n_h}^h(\mathbf{r}_h), \quad (4.1)$$

one can construct canonically the single exciton creation operator in terms of the creation operators $a_{n_e}^\dagger$ and $b_{n_h}^\dagger$ for electron in the state n_e and hole in the state n_h , respectively:

$$\sigma^\dagger = \sum_{n_e, n_h} C_{n_e, n_h} a_{n_e}^\dagger b_{n_h}^\dagger, \quad (4.2)$$

where electron (hole) creation $a_{n_e}^\dagger$ ($b_{n_h}^\dagger$) and annihilation a_{n_e} (b_{n_h}) operators obey the usual fermionic algebra. Following the standard prescription, the n -excitons state is obtained by repeated applications of the creation operator σ^\dagger on the vacuum state $|0\rangle$,

$$|\Psi_n\rangle = (\sigma^\dagger)^n |0\rangle. \quad (4.3)$$

This wavefunction needs to be normalized. We introduce the unit-norm n -excitons state $|n\rangle$

$$|n\rangle = \frac{1}{\mathcal{N}_n} |\Psi_n\rangle, \quad (4.4)$$

with normalization constant

$$\mathcal{N}_n = \sqrt{\langle \Psi_n | \Psi_n \rangle}. \quad (4.5)$$

The creation operator σ^\dagger can finally be explicated. We call α_n its nonzero matrix elements which lie below the diagonal in the many-excitons representations:

$$\alpha_n = \langle n | \sigma^\dagger | n-1 \rangle, \quad (4.6)$$

which, by confrontations of Eqs. (4.3–4.6) is found to be

$$\alpha_n = \frac{\mathcal{N}_n}{\mathcal{N}_{n-1}}. \quad (4.7)$$

The direct computation of normalization constants according to (4.3) involves complicated algebra. We now return to coordinate representation $\Psi_n(\{\mathbf{r}_{e_i}, \mathbf{r}_{h_j}\})$. It allows to ensure the proper antisymmetry of the excitonic wavefunction imposed by fermionic nature of electrons and holes for the n -excitons wavefunction by writing it as a Slater determinant:

$$\Psi_n(\mathbf{r}_{e_1} \dots \mathbf{r}_{e_n}, \mathbf{r}_{h_1} \dots \mathbf{r}_{h_n}) = \det_{1 \leq i, j \leq n} [\varphi(\mathbf{r}_{e_i}, \mathbf{r}_{h_j})]. \quad (4.8)$$

We found that this arbitrary n -excitons state yields the following recurrent relation for the normalization constants:

$$\mathcal{N}_n^2 = \frac{1}{n} \sum_{k=1}^n (-1)^{k+1} \beta_k \mathcal{N}_{n-k}^2 \prod_{j=0}^{k-1} (n-j)^2, \quad (4.9)$$

with $\mathcal{N}_0 = 1$ and β_k the irreducible k -excitons overlap integrals

$$\beta_k = \int \left(\prod_{i=1}^{k-1} \varphi^*(\mathbf{r}_{e_i}, \mathbf{r}_{h_i}) \varphi(\mathbf{r}_{e_i}, \mathbf{r}_{h_{i+1}}) \right) \varphi^*(\mathbf{r}_{e_k}, \mathbf{r}_{h_k}) \varphi(\mathbf{r}_{e_k}, \mathbf{r}_{h_1}) d\mathbf{r}_{e_1} \dots d\mathbf{r}_{e_k} d\mathbf{r}_{h_1} \dots d\mathbf{r}_{h_k} \quad (4.10)$$

The recurrence equation (4.9) can be solved:

$$\mathcal{N}_n^2 = \sum_{\eta=1}^{p(n)} C_n(\eta) \prod_{k=1}^N \beta_k^{v_\eta(k)} \quad (4.11)$$

where $p(n)$ is the partition function of n (number of ways to write n as a sum of positive integers, i.e., as an integer partition of n) and $v_\eta(i)$ is the number of times $i \in \mathbb{N}$ appears in the η^{th} partition of n . The coefficients C_n of (4.11) read:

$$C_n(\eta) \equiv n!(-1)^{n+\sum_{k=1}^n v_\eta(k)} \prod_{i=1}^k \binom{n - \sum_{j=1}^{i-1} n_j}{n_i} \frac{(n_i - 1)!}{v_\eta(i)!}$$

This completes the general procedure to calculate the matrix elements of the creation operator σ^\dagger . One first needs to specify the envelope function $\varphi(\mathbf{r}_e, \mathbf{r}_h)$ for a single exciton which corresponds to one's specific problem and microscopic implementation, then all β_k should be computed and finally α_n are obtained from (4.9) or (4.11), and (4.7). In particular

$$\alpha_2 = \sqrt{2 - 2\beta_2} \quad (4.12)$$

which is smaller than or equal to $\sqrt{2}$, the corresponding matrix element for the true boson creation operator. This has a very transparent physical meaning: because of Pauli exclusion it is ‘‘harder’’ to create two excitons than two true bosons. We shall consider the cases where this tendency so develops as to ultimately forbid further excitations, i.e., with α_n ultimately vanishing. Clearly realistic modelisations require heavy numerical computations to obtain both φ and β_k . Also, note that φ might be allowed to change with n in the evaluation of (4.8), say for instance if one wants to further refine the modelisation by including bleaching of excitons with density or screening through, e.g., Hulthén potential. Here we do not consider any specific realisations but comment on the general trend of α_n and analyse two limiting ideal cases.

For small quantum dots with size $L \ll a_B$ the exciton Borh radius, Coulomb interaction between electron and hole can be neglected in the lowest order of perturbation theory, as supported by the works of Hu, Koch, Lindberg, Peyghambarian, Pollock & Abraham (1990), Efros, Rosen, Kuno, Nirmal, Norris & Bawendi (1996) and Hawrylak (1999). In this case the ground state wavefunction of the exciton factorises

$$\varphi(\mathbf{r}_e, \mathbf{r}_h) = \varphi_0^e(\mathbf{r}_e) \varphi_0^h(\mathbf{r}_h) \quad (4.13)$$

and overlap integrals $\beta_k = 1$ for all k . Consequently $\mathcal{N}_1 = 1$ and all $\mathcal{N}_k = 0$ for $k \geq 2$. Only a single excitation is allowed since Pauli exclusion results in vanishing wavefunctions for more particles. Therefore, $\alpha_1 = 1$ and all other $\alpha_k = 0$. It is an exact fermionic limit discussed, e.g., in Hawrylak (1999). In a very large quantum dot where $L \gg a_B$, the electron and hole are bound to each other and the wavefunction of the exciton can be written in a form given by, e.g., D’Andrea & Sole (1990) or Que (1992):

$$\varphi(\mathbf{r}_e, \mathbf{r}_h) = \phi(\boldsymbol{\rho}) \Phi(\mathbf{r}), \quad (4.14)$$

where $\boldsymbol{\rho} = \mathbf{r}_e - \mathbf{r}_h$ and $\mathbf{r} = (m_e \mathbf{r}_e + m_h \mathbf{r}_h) / (m_e + m_h)$ with m_e and m_h the effective masses of electron and hole. Functions $\phi(\boldsymbol{\rho})$ and $\Phi(\mathbf{r})$ describe the electron-hole relative motion and center of mass quantization in QD potential, respectively. These functions have drastically different spatial scales: $\phi(\boldsymbol{\rho})$ falls abruptly if $\boldsymbol{\rho} \gg a_B$ and $\Phi(\mathbf{r})$ decreases strongly if $R \gg L$.

Integral (4.10) in this limit gives the probability to find simultaneously the centers of mass of all excitons within a distance of less than a_B from each others. It can be shown that in this large dot limit, overlap integrals β_k have asymptotics decreasing faster than exponentially:

$$\beta_k = f_k \theta^{k-1}, \quad (4.15)$$

where $\theta \sim (a_B/L)^d \ll 1$ with $d = 1, 2, 3$ the effective dimension of the dot, and f_k is some decreasing function of k which is not an exponential. In the case where $f_k = 1$ the solution for \mathcal{N}_k can be found analytically, leading to

$$\alpha_n = \sqrt{n - n(n-1)\theta} \quad (4.16)$$

This corresponds to matrix elements of Dicke (1954) angular momentum creation operator R^+ . Exact algebraic calculations performed with a computer for 2D parabolic QD imply that $f_k \approx 1/k^2$ in which case α_n is comprised between the Dicke and the harmonic oscillator models, displaying an abrupt decay about some value N above which \mathcal{N}_N is vanishingly small, cf. fig. (4.1) on this page.

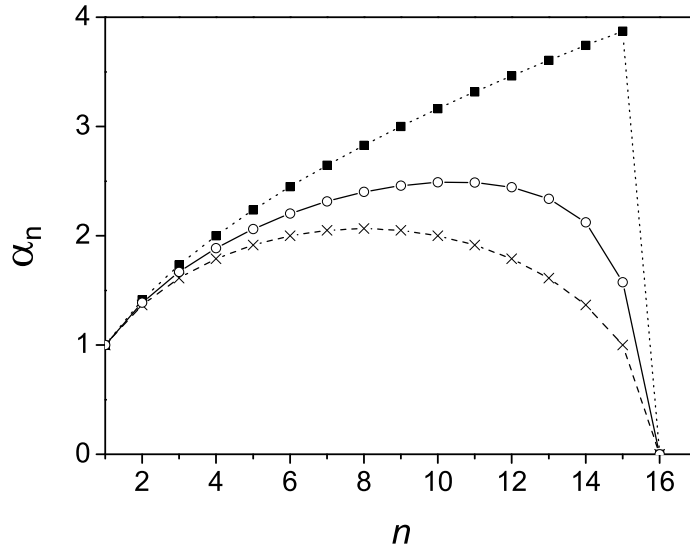


Figure 4.1: α_n matrix elements for σ_{15} , i.e., allowing up to 15 excitations, in three cases of interest: truncated harmonic oscillator (filled boxes) where $\alpha_n = \sqrt{n}$, Dicke states (crosses) where $\alpha_n = \sqrt{n - n(n-N)}/\sqrt{N}$ and general case (empty circles).

As it is expected from physical grounds that Pauli exclusion will eventually forbid more particles, that is, implies a maximum number N of allowed excitations, we consider as another limiting case a truncated harmonic oscillator (THO) where $\alpha_n = \sqrt{n}$ for $n \leq N$ and is zero afterwards. General cases, which are expected to lie in between these two limits, should rely upon numerical evaluations of φ and β_k for the system at hands. In all cases, we call σ_N^\dagger this operator allowing a maximum number of N excitations, $N \approx 1/\theta$. Note that the pure bosonic case where $\alpha_n = \sqrt{n}$ is recovered if β_k becomes zero past $k = 1$ (β_1 is always one).

4.3 Large Quantum Dots

In this chapter, we take concern in this aspect which seems to have precedence experimentally, namely, that of a single QD which size can be controlled in the growth process. Especially in the case of Reithmaier et al. (2004), the QD for small ratio of indium in the InGaAs substrate is effectively a fluctuation of the QW width which can cover an extended area on the surface.

Following the authors, we call these dots *large Quantum Dots*, and we consider that such a large dot can accommodate a limited number of excitons. In this way, such a large dot sits between the fermionic regime where the excitation is a two-level system, which experimental signature is the Mollow triplet, and the bosonic regime of a planar structure where excitations are excitons, able to superimpose without feeling the underlying fermionic structure (but still in the low density limit). From a formal point of view in the purely fermionic case the light mode is coupled to a two-level system, while in the purely bosonic case it is coupled to a harmonic oscillator having an infinite number of equidistant energy levels. Logically, an intermediate case would correspond to the optical mode coupled to a truncated harmonic oscillator, having a finite number, say N , of energy levels.

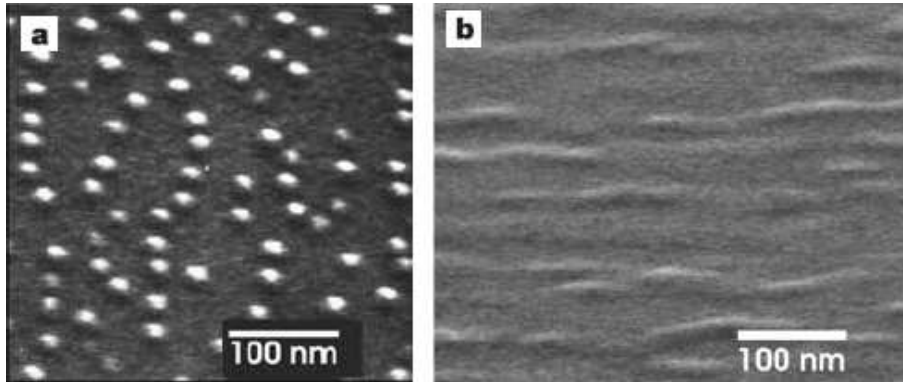


Figure 4.2: SEM of InGaAs QDs [from Reithmaier et al. (2004)] where one can observe the variation in the size of QDs obtained from different In contents in the growth process. For an indium content of 60% (fig. a), the self-assembled dots have characteristic diameter of 15-20nm, while for 30% of indium (fig. b), the dots get elongated with characteristic length of about 100nm for a width of about 30nm.

We therefore study theoretically the emission of light by a QDC using the model of a truncated harmonic oscillator (THO) σ_N . Such oscillators have been used in other contexts and have been popular for the study of fractional statistics, see for instance their use by Ilinskaia & Ilinski (1996) to describe Paulions (operators which follow fermionic algebra on the nodes of a lattice and bosonic one between different nodes). The microscopic foundation for such a model to describe large QDs after the formalism presented in the previous chapter is left for future enquiries, as well as the study of spectra obtained for other limiting cases displayed on fig. 4.1. Of course the exact square root coefficients will not be obtained, but it is our belief that for appropriate choices of parameters, our model will hold to a good approximation and yield good quantitative results (an important *qualitative* departure will be appearance of the multiplet structure below the saturation $n < N$, meaning that excitons feel their underlying fermionic structure before it actually results in the impossibility of further excitations). The advantage of the ideal situation is that it allows for exact analytical solutions.

We hence assume here that the ideal situation of exact bosonic behaviour below the saturation holds, and that a finite number of ideal excitons ($N \geq 1$) can be generated in the quantum state of interest. The value of N scales like $S_{\text{dot}}/\pi a_B^2$ where S_{dot} is the cross-section surface of the dot and a_B the exciton Bohr-radius. The coefficient between the two is expected to be of order between 10^{-1} to 10^{-2} depending on parameters, which is needed first for a single electron-hole pair to bind as an exciton because Coulomb interaction dominates over the confining potential, which requires $R/a_B \gg 1$ (R the radius of the dot) and second, for many

excitons, that the commutator which departs from 1 like Na_B^2/S , cf. (1.115), should ensure $R/a_B \gg (N/\pi)^2$. Physically, it corresponds to the image of a dot much larger than the exciton Bohr radius, so that excitons are confined as whole particles inside it. $N = 1$ recovers the fermionic case. We also assume that the energy separation between quantum confined excitonic states exceeds the vacuum Rabi splitting, so that one can neglect all excitonic states except one, strongly coupled to a single light mode. This latter condition, though very artificial for quantum well microcavities, is easily met in QDC, where typical values of the Rabi splitting are tens of μeV , as reported by experimentalists. Furthermore, we neglect exciton-exciton interactions, which allows us to assume the energy of the excitonic transition to be independent on the number m of excitons already created in a given quantum state if $m < N$. If $m = N$ no more excitons can be created in the quantum state we consider. Again, we assume the exciton-photon system to be fully spin-polarised so that polarisation effects can be neglected.

4.4 Bare and Dressed states basis

The electromagnetic field is modelled in the approximation of the quasi-mode coupling by single mode Bose field annihilation operator a . We introduce for a large quantum dot, able to host N excitons, the operator σ_N which behaves like a Bose field annihilation operator when the number of excitations is less than or equal to N , i.e.,

$$\sigma_N |m\rangle \equiv \sqrt{m} |m-1\rangle \quad (4.17a)$$

$$\sigma_N^\dagger |m\rangle \equiv \sqrt{m+1} |m+1\rangle \theta_{m,N} \quad (4.17b)$$

where $\theta_{m,N}$ is the modified Heaviside step function which is zero if $m \geq N$ and one if $m < N$. In the basis of Fock states

$$|0\rangle = \begin{pmatrix} 1 \\ 0 \\ \vdots \\ 0 \end{pmatrix}, \quad |1\rangle = \begin{pmatrix} 0 \\ 1 \\ \vdots \\ 0 \end{pmatrix}, \quad \dots, \quad |N\rangle = \begin{pmatrix} 0 \\ 0 \\ \vdots \\ 1 \end{pmatrix}, \quad (4.18)$$

its matrix representation is the $N+1$ squared matrix which is a truncation of the annihilation matrix of a Bose field. For instance, for $N=2$,

$$\sigma_2 = \begin{pmatrix} 0 & 1 & 0 \\ 0 & 0 & \sqrt{2} \\ 0 & 0 & 0 \end{pmatrix}, \quad (4.19)$$

or in the general case,

$$\sigma_N = \begin{pmatrix} 0 & 1 & 0 & 0 & \dots & 0 \\ 0 & 0 & \sqrt{2} & 0 & \dots & 0 \\ 0 & 0 & 0 & \sqrt{3} & \dots & 0 \\ \vdots & \vdots & \vdots & \ddots & \ddots & \vdots \\ 0 & 0 & 0 & \dots & 0 & \sqrt{N} \\ 0 & 0 & 0 & \dots & 0 & 0 \end{pmatrix}, \quad (4.20)$$

that is, with zero everywhere except above the diagonal where matrix elements α_n go like the square root, as in the case of the harmonic oscillator (which would be a matrix of “infinite

size”). This representation of course depends on the choice of representation of the canonical basis (4.18); we choose the convention of Merzbacher (1998) to agree with the harmonic oscillator, which corresponds to the limit $\sigma_{N \rightarrow \infty}$. Another limit of interest is $N = 1$ in which case

$$\sigma_1 = \begin{pmatrix} 0 & 1 \\ 0 & 0 \end{pmatrix} \quad (4.21)$$

is the usual two-level system annihilation operator. The algebra for the general operator follows straightforwardly:

$$[\sigma_N, \sigma_N^\dagger] = \mathbf{1}_{N+1} - \lambda_{N+1}, \quad (4.22)$$

where $\mathbf{1}_{N+1}$ is the $N + 1$ squared identity matrix and λ the matrix of same size with zero everywhere except for its lowest-rightmost element which is one, i.e., $(\lambda_{N+1})_{i,j} = (N + 1)\delta_{i,j}\delta_{i,N}$ (with $0 \leq i, j \leq N$).

The hamiltonian for our system is similar to Dicke’s (1954) or Jaynes & Cummings’s (1963) hamiltonian but instead of coupling the field a with a spinor J or a two-level system (fermion) σ_1 , one couples a with this operator σ_N , also in the rotating wave approximation:

$$H = \hbar\omega a^\dagger a + \hbar\omega \sigma_N^\dagger \sigma_N \quad (4.23a)$$

$$+ \hbar g (a^\dagger \sigma_N + a \sigma_N^\dagger). \quad (4.23b)$$

We consider zero detuning for simplicity. Here $\hbar g$ is the coupling constant corresponding to (half) the Rabi splitting in the linear regime. First line (4.23a) describes bare states of photons and excitons, the later being limited to a maximum N . We note eigenstates of this first line alone $|n, m\rangle$ with n the number of photons, any integer number, and m the number of excitons, any integer less than or equal to N . Second line (4.23b) describes the coupling between the two fields which in absence of dissipation will always be “strong” in the quantum mechanical sense. The dissipation is caused by two channels of energy escape included as non-hermitian contributions of the Lindblad type to Von Neumann equation,

$$i\hbar\dot{\rho} = [H, \rho] + \mathcal{L}_a \rho + \mathcal{L}_{\sigma_N} \rho, \quad (4.24)$$

where

$$\mathcal{L}_a \equiv -\frac{\gamma_a}{2} (a^\dagger a \rho - 2a \rho a^\dagger + \rho a^\dagger a) \quad (4.25)$$

describes the photon leakage through the cavity mirror by tunnel effect and

$$\sigma_{\mathcal{N}a} \equiv -\frac{\gamma_{\sigma_N}}{2} (\sigma_N^\dagger \sigma_N \rho - 2\sigma_N \rho \sigma_N^\dagger + \rho \sigma_N^\dagger \sigma_N) \quad (4.26)$$

describes the emission from the active state within the cavity, with associated decay constant γ_a and γ_{σ_N} . The procedure is straightforward in principle: since the number of excitations is conserved by H , one diagonalises it in the subspace of n excitations and thus obtains new eigenstates of the system (so-called *dressed states* in cavity QED terminology). Thus, in the basis

$$\mathcal{H}_n = \{|0, n\rangle, |1, n-1\rangle, \dots, |N, n-N\rangle\} \quad (4.27)$$

(for $n \geq N$), the hamiltonian reduces to:

$$\begin{aligned} H &= \hbar\omega n \mathbf{1}_{N+1} \\ &+ \hbar g \left[\sqrt{i(n-i+1)} \delta_{i,j+1} \right. \\ &\left. + \sqrt{(i+1)(n-i)} \delta_{i,j-1} \right]_{0 \leq i, j \leq N} \end{aligned} \quad (4.28)$$

where the term between square brackets is the generic expression for the interaction matrix (which is zero everywhere but below and above its diagonal). Case $N = 1$ is Jaynes-Cummings model which yields the Mollow triplet. We will deal explicitly with case $N = 2$ which, it is expected, is the case of easiest experimental realization after vacuum Rabi splitting and Mollow triplet:

$$H = \hbar\omega n\mathbf{1}_3 + \hbar g \begin{pmatrix} 0 & \sqrt{n} & 0 \\ \sqrt{n} & 0 & \sqrt{2(n-1)} \\ 0 & \sqrt{2(n-1)} & 0 \end{pmatrix}, \quad (4.29)$$

Cases where n is lower than or equal to N fall into linear regime displaying two peaks, the exciton field never reaching its saturation density. If $n > N$, the new $N + 1$ eigenstates (dressed states) will be denoted, for the manifold n , by $|\nu\rangle_n$ with $\nu = 1, \dots, N + 1$ indexing the state. For $N = 2$,

$$|\nu = 1\rangle_n \equiv \left(\sqrt{\frac{n}{2(3n-2)}}, -\frac{\sqrt{2}}{2}, \sqrt{\frac{n-1}{3n-2}} \right), \quad (4.30a)$$

$$|\nu = 2\rangle_n \equiv \left(-\sqrt{\frac{2(n-1)}{3n-2}}, 0, \sqrt{\frac{n}{3n-2}} \right), \quad (4.30b)$$

$$|\nu = 3\rangle_n \equiv \left(\sqrt{\frac{n}{2(3n-2)}}, \frac{\sqrt{2}}{2}, \sqrt{\frac{n-1}{3n-2}} \right). \quad (4.30c)$$

in the bare states basis \mathcal{H}_2 . The associated eigenvalues are:

$$E_\nu^n \equiv \hbar\omega n + (\nu - 2)\hbar g\sqrt{3n-2} \quad (4.31)$$

The spectrum of emission comes from transitions between manifolds with n and $n - 1$ excitations. One can obtain the exact expression for the luminescence spectrum from (2.4) and quantum regression theorem to evaluate the time correlation function needed for Wiener-Khintchin theorem. We content here with Fermi's golden rule formula for perturbations responsible for (4.25 & 4.26). These perturbations arise from the weak coupling of cavity photons a (resp. excitons σ_N) with the continuum of external modes of the electromagnetic field in vacuum state. Therefore, calling $c_i^{\nu,n}$ the projection of state $|\alpha\rangle_n$ on state $|i, n - i\rangle$ one can obtain the coefficients in (4.30) as:

$$|\nu\rangle_n = \sum_{i=0}^N c_i^{\nu,n} |i, n - i\rangle \quad (4.32)$$

The corresponding transition probabilities between states $|\nu, n\rangle$ and $|\nu', n - 1\rangle$ are obtained as:

$$\begin{aligned} I_{\text{end}} &= |\langle \nu' |_{n-1} a | \nu \rangle_n|^2 = \left| \sum_{i=0}^N (c_i^{\nu',n-1})^* c_i^{\nu,n} \sqrt{n-i} \right|^2 \\ I_{\text{lat}} &= |\langle \nu' |_{n-1} \sigma_N | \nu \rangle_n|^2 = \left| \sum_{i=1}^N (c_{i-1}^{\nu',n-1})^* c_i^{\nu,n} \sqrt{i} \right|^2 \end{aligned} \quad (4.33)$$

In cavity QED terminology, I_{end} and I_{lat} correspond to *end-emission* and *lateral-emission* photo-detection respectively, while in luminescence of a microcavity, one observes the sum of the two contributions $I_{\text{lat}} + I_{\text{end}}$ simultaneously. To detect I_{lat} independently one should use the scattering geometry.

4.5 Spectra of Optical Emission

The main result is the appearance of multiplets in the configuration $n \geq N$. This is in stark contrast with cavity QED where nonlinearity results in apparition of the triplet named after Mollow (1969). Three questions need be solved in the general case: first the number of peaks allowed by the transitions which is of a combinatorial nature, providing the number of transitions between two multiplets taking into account their degeneracy. Second the energy splitting between the various peaks thus obtained which is the eigenvalues problem. Third the strength of transitions which is the eigenvectors problem. If the radiative broadening is so small that all peaks can be discriminated and if no selection rules forbid some transitions, the multiplets structure is that of $2N + 1$ groups of more or less closely packed peaks for a total number of $(N + 1)^2$. We label $\mu = 0$ the group at the centre of the spectrum, and $\mu = \pm 1, \pm 2, \dots$ groups located symmetrically about the central one. The number of peaks is $N + 1 - |\mu|$ in the μ^{th} group. Each peak is identified unambiguously by a couple of integers (k, l) with $0 \leq k, l \leq N$. Peak (k, l) belongs to group $\mu = k - l$ and is the k^{th} (resp. l^{th}) if located at the left (resp. right) of the spectrum, counting as first in each group that of lower energy. The energy of this peak $E(k, l)$ is given by the photon energy released in the transition between two manifolds and is therefore given by the difference of initial and final eigenvalues E_k^n in the dressed states basis:

$$E(k, l) = E_k^n - E_l^{n-1} \quad (4.34)$$

In the case $N = 2$, from (4.31) and (4.34) we get in good approximation (the better the higher n) the mean energy of peak (k, l) as

$$E(k, l) \approx \hbar\omega + (k - l)\hbar g\sqrt{3n} - (2k - 5l + 6)\frac{\hbar g}{2\sqrt{3n}} \quad (4.35)$$

This gives the structure of the multiplet: there is a splitting of magnitude $|v|\hbar g\sqrt{3n}$ between the central ($\mu = 0$) and the v th group of peaks. The central group has a fine structure splitting (between (1,1) and (3,3)) of $\sqrt{3}\hbar g/\sqrt{n}$. At the onset of the nonlinear effect ($n = 3$) the splitting is close to the Rabi splitting $2\sqrt{(\hbar g)^2 - (\gamma_a - \gamma_{\sigma_2})^2}/16$. The fine structure splitting of the groups $\mu = \pm 2$ is half the central one: $\sqrt{3}\hbar g/(2\sqrt{n})$. As n increases, each group of peaks gets farther from the others while inside this group, the fine structure splitting is reduced. This behaviour is seen in fig. 4.4. When the photon field is so intense that for the given broadening γ_{σ_2} the fine splitting is unobservable, the spectra resemble a Mollow triplet. It can be distinguished from it by the splitting which is $\sqrt{3}/2$ times smaller and the presence of additional (small) peaks with a splitting $\sqrt{3}$ larger. Also the ratio between the central peak and its closest satellites is $9/4$ rather than $1/2$ in case of the Mollow triplet, see fig. 4.4c.

This structure applies both for I_{end} and I_{lat} spectra. However, they display two drastically different behaviours. First I_{end} is maximum at the center of the spectrum with peak (2,2) the highest one. The situation is opposite with I_{lat} for which, whatever n , peak (2,2) is an exactly forbidden transition.

The same procedure can be applied to larger values of N , e.g., for $N = 3$ (cf. 4.31):

$$E_v^n = \hbar\omega n + \text{sign}(v - \frac{5}{2})\hbar g\sqrt{(-1)^v\sqrt{2}\sqrt{3n^2 - 9n + 8} + 3n + 4} \quad (4.36)$$

with $1 \leq v \leq 4$, and for $N = 4$:

$$E_v^n = \hbar\omega n + \text{sign}(v - 3)\hbar g\sqrt{\text{sign}(3 - v)(-1)^v\sqrt{2}\sqrt{5n^2 - 25n + 38} + 5n - 10}, \quad (4.37)$$

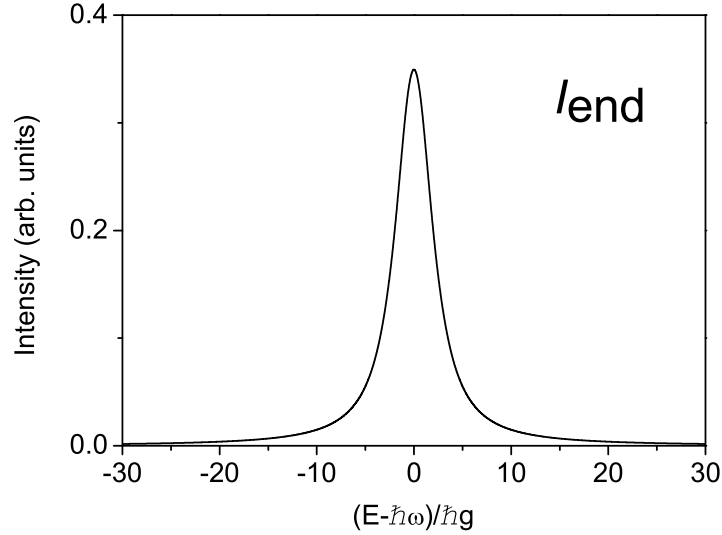


Figure 4.3: Spectra of emission from the cavity mode. All subsequent spectra displayed correspond to “lateral emission” observed in the scattering geometry.

this time with $1 \leq \nu \leq 5$, etc... (where $\text{sign}(x) = 0$ if $x = 0$ and is $x/|x|$ otherwise.) Along the same lines as before, one can derive the structure and splittings of the spectrum of emission in these cases. For instance, for $N = 3$, the (1,1)–(3,3) splitting is $(\sqrt{3} - \sqrt{6})\hbar g / \sqrt{n} \approx 0.74\hbar g / \sqrt{n}$. Note that the difference in energy enters as square roots inside a square root and thus becomes smaller and smaller with increasing N . Figure 4.5c) shows the case of an extremely large dot where satellite peaks become suppressed and the Rabi-like doublet dominates the spectrum. For $N \rightarrow \infty$ the familiar Rabi-doublet seen in the spectra of quantum well cavities is recovered by this model.

4.6 Conclusions and Perspectives

We predicted appearance of multiplets in emission spectra of zero-dimensional photonic cavities containing single large quantum dots. The effect comes from relaxation of the Pauli principle for excitons confined as whole particles in large dots. The effect is strictly nonlinear as it requires the number of photons injected in the cavity to exceed the capacity of the dot. This capacity governs the number of peaks in emission. In the small dot limit, it reduces to three (Mollow triplets). The microscopic motivation for σ_N is the most urgent task of this activity. We are currently investigating numerically the ground state of large quantum dots by variational procedure, which first results give us all reasons to believe the excitation creation operator is indeed close to σ_N .

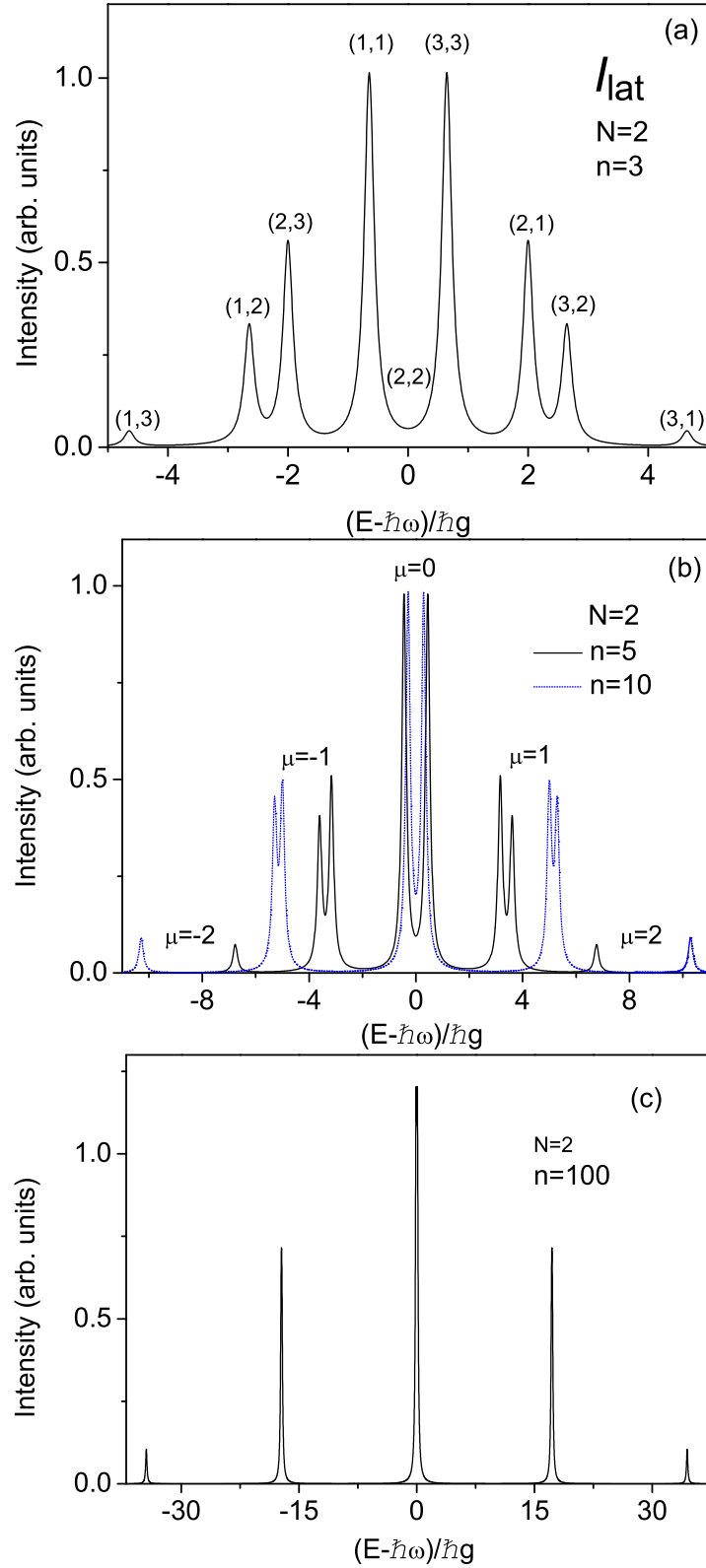


Figure 4.4: Spectra of emission for a dot large enough to accommodate $N = 2$ excitons, with photon field intensity corresponding to a) $n = 3$, b) $n = 5$ (solid) and 10 (dotted) and c) $n = 100$. On fig. a and b, the labelling of multiplets as explained in the text is shown. In the limit of high pumping where the fine structure is lost, c), the three peaks $\mu = 0, \pm 1$ are in the ratio $9/4$ as opposed to Mollow triplet, $1/2$. The splitting between these peaks goes like $\hbar g \sqrt{3n}$ while fine structure splitting goes like $\hbar g \sqrt{3/n}$.

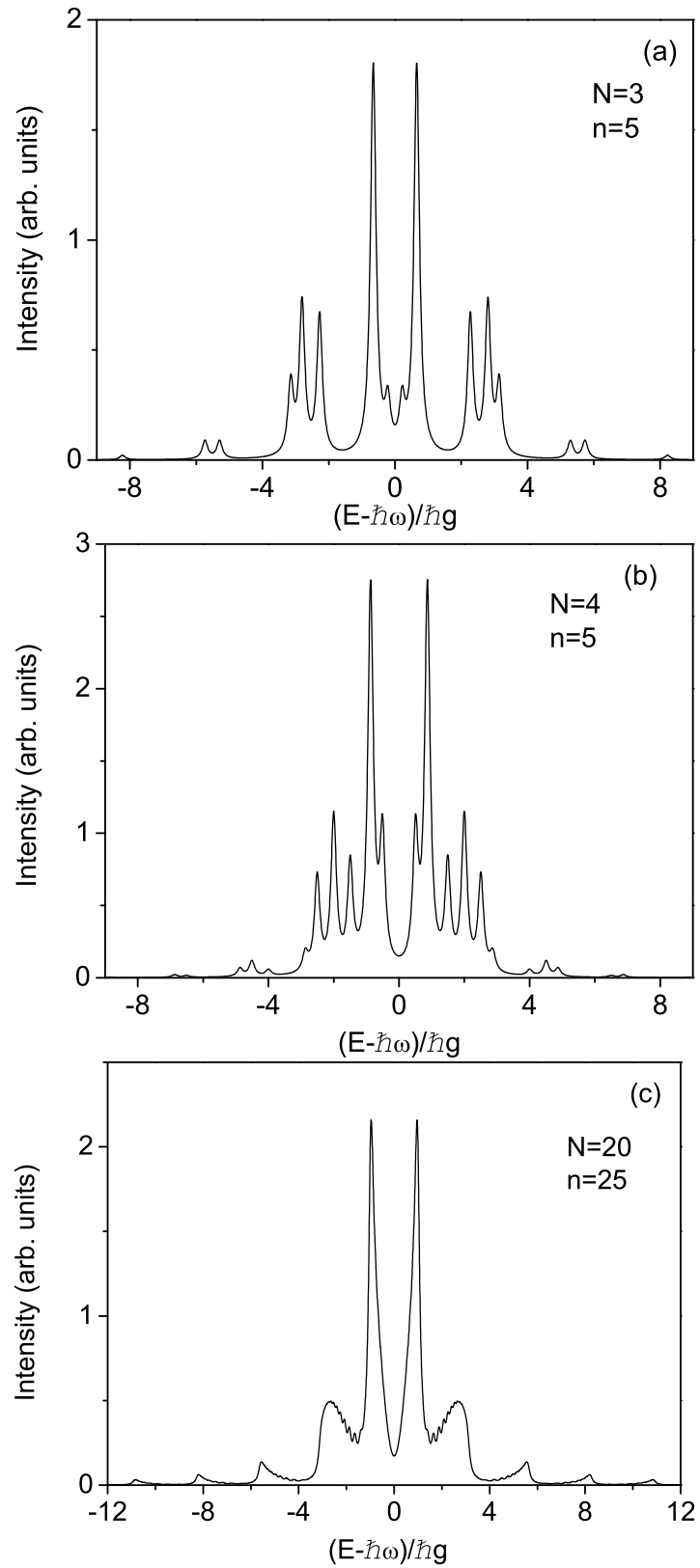


Figure 4.5: Spectra of emission for a dot large enough to accommodate a) $N = 3$, b) $N = 4$ and c) $N = 20$ excitons, with photon field intensity corresponding to $n = 5$ in first two cases and $n = 25$ in the latter. The number of peaks increase like N^2 with N resulting in more complicated fine structures.

Appendix A

Details of Some Auxiliary Calculations

In this appendix we give additional details too cumbersome to appear in the text.

A.1 Microscopic Derivation of the Master Equation

We detail the derivation of master equations like eq. (2.21). The double commutator (2.8) taking into account (2.2b) comes out as:

$$\begin{aligned}
[H(t), [H(\tau), \rho_0(\tau) \rho_k(\tau) \rho_b]] = & \\
& \sum_{\mathbf{r}, \mathbf{s}} \sum_{\mathbf{k}, \mathbf{q}} \mathcal{U}(\mathbf{r}, \mathbf{s}) \mathcal{U}(\mathbf{k}, \mathbf{q}) e^{\frac{i}{\hbar} \mathcal{E}_{\mathbf{r}, \mathbf{s}} t} e^{\frac{i}{\hbar} \mathcal{E}_{\mathbf{k}, \mathbf{q}} \tau} [a_{\mathbf{r}}^\dagger b_{\mathbf{s}}^\dagger a_{\mathbf{r}+\mathbf{s}}, [a_{\mathbf{k}}^\dagger b_{\mathbf{q}}^\dagger a_{\mathbf{k}+\mathbf{q}}, \rho_0(\tau) \rho_k(\tau) \rho_b]] \\
& + \sum_{\mathbf{r}, \mathbf{s}} \sum_{\mathbf{k}, \mathbf{q}} \mathcal{U}(\mathbf{r}, \mathbf{s}) \mathcal{U}(\mathbf{k}, \mathbf{q})^* e^{\frac{i}{\hbar} \mathcal{E}_{\mathbf{r}, \mathbf{s}} t} e^{-\frac{i}{\hbar} \mathcal{E}_{\mathbf{k}, \mathbf{q}} \tau} [a_{\mathbf{r}}^\dagger b_{\mathbf{s}}^\dagger a_{\mathbf{r}+\mathbf{s}}, [a_{\mathbf{k}+\mathbf{q}}^\dagger b_{\mathbf{q}} a_{\mathbf{k}}, \rho_0(\tau) \rho_k(\tau) \rho_b]] \\
& + \frac{1}{2} \sum_{\mathbf{r}, \mathbf{s}} \sum_{\mathbf{k}, \mathbf{p}, \mathbf{q}} \mathcal{U}(\mathbf{r}, \mathbf{s}) \mathcal{V}(\mathbf{k}, \mathbf{p}, \mathbf{q}) e^{\frac{i}{\hbar} \mathcal{E}_{\mathbf{r}, \mathbf{s}} t} e^{i \mathcal{E}_{\mathbf{k}, \mathbf{p}, \mathbf{q}} \tau} [a_{\mathbf{r}}^\dagger b_{\mathbf{s}}^\dagger a_{\mathbf{r}+\mathbf{s}}, [a_{\mathbf{k}+\mathbf{q}}^\dagger a_{\mathbf{p}-\mathbf{q}}^\dagger a_{\mathbf{k}} a_{\mathbf{p}}, \rho_0(\tau) \rho_k(\tau) \rho_b]] \\
& + \sum_{\mathbf{r}, \mathbf{s}} \sum_{\mathbf{k}, \mathbf{q}} \mathcal{U}(\mathbf{r}, \mathbf{s})^* \mathcal{U}(\mathbf{k}, \mathbf{q}) e^{-\frac{i}{\hbar} \mathcal{E}_{\mathbf{r}, \mathbf{s}} t} e^{\frac{i}{\hbar} \mathcal{E}_{\mathbf{k}, \mathbf{q}} \tau} [a_{\mathbf{r}+\mathbf{s}}^\dagger b_{\mathbf{s}} a_{\mathbf{r}}, [a_{\mathbf{k}}^\dagger b_{\mathbf{q}}^\dagger a_{\mathbf{k}+\mathbf{q}}, \rho_0(\tau) \rho_k(\tau) \rho_b]] \\
& + \sum_{\mathbf{r}, \mathbf{s}} \sum_{\mathbf{k}, \mathbf{q}} \mathcal{U}(\mathbf{r}, \mathbf{s})^* \mathcal{U}(\mathbf{k}, \mathbf{q})^* e^{-\frac{i}{\hbar} \mathcal{E}_{\mathbf{r}, \mathbf{s}} t} e^{-\frac{i}{\hbar} \mathcal{E}_{\mathbf{k}, \mathbf{q}} \tau} [a_{\mathbf{r}+\mathbf{s}}^\dagger b_{\mathbf{s}} a_{\mathbf{r}}, [a_{\mathbf{k}+\mathbf{q}}^\dagger b_{\mathbf{q}} a_{\mathbf{k}}, \rho_0(\tau) \rho_k(\tau) \rho_b]] \\
& + \frac{1}{2} \sum_{\mathbf{r}, \mathbf{s}} \sum_{\mathbf{k}, \mathbf{p}, \mathbf{q}} \mathcal{U}(\mathbf{r}, \mathbf{s})^* \mathcal{V}(\mathbf{k}, \mathbf{p}, \mathbf{q}) e^{-\frac{i}{\hbar} \mathcal{E}_{\mathbf{r}, \mathbf{s}} t} e^{i \mathcal{E}_{\mathbf{k}, \mathbf{p}, \mathbf{q}} \tau} [a_{\mathbf{r}+\mathbf{s}}^\dagger b_{\mathbf{s}} a_{\mathbf{r}}, [a_{\mathbf{k}+\mathbf{q}}^\dagger a_{\mathbf{p}-\mathbf{q}}^\dagger a_{\mathbf{k}} a_{\mathbf{p}}, \rho_0(\tau) \rho_k(\tau) \rho_b]] \\
& + \frac{1}{2} \sum_{\mathbf{r}, \mathbf{s}, \mathbf{l}, \mathbf{k}, \mathbf{q}} \mathcal{V}(\mathbf{r}, \mathbf{s}, \mathbf{l}) \mathcal{U}(\mathbf{k}, \mathbf{q}) e^{i \mathcal{E}_{\mathbf{r}, \mathbf{s}, \mathbf{l}} t} e^{\frac{i}{\hbar} \mathcal{E}_{\mathbf{k}, \mathbf{q}} \tau} [a_{\mathbf{r}+\mathbf{l}}^\dagger a_{\mathbf{s}-\mathbf{l}}^\dagger a_{\mathbf{r}} a_{\mathbf{s}}, [a_{\mathbf{k}}^\dagger b_{\mathbf{q}}^\dagger a_{\mathbf{k}+\mathbf{q}}, \rho_0(\tau) \rho_k(\tau) \rho_b]] \\
& + \frac{1}{2} \sum_{\mathbf{r}, \mathbf{s}, \mathbf{l}, \mathbf{k}, \mathbf{q}} \mathcal{V}(\mathbf{r}, \mathbf{s}, \mathbf{l}) \mathcal{U}(\mathbf{k}, \mathbf{q})^* e^{i \mathcal{E}_{\mathbf{r}, \mathbf{s}, \mathbf{l}} t} e^{-\frac{i}{\hbar} \mathcal{E}_{\mathbf{k}, \mathbf{q}} \tau} [a_{\mathbf{r}+\mathbf{l}}^\dagger a_{\mathbf{s}-\mathbf{l}}^\dagger a_{\mathbf{r}} a_{\mathbf{s}}, [a_{\mathbf{k}+\mathbf{q}}^\dagger b_{\mathbf{q}} a_{\mathbf{k}}, \rho_0(\tau) \rho_k(\tau) \rho_b]] \\
& + \frac{1}{4} \sum_{\mathbf{r}, \mathbf{s}, \mathbf{l}, \mathbf{k}, \mathbf{p}, \mathbf{q}} \mathcal{V}(\mathbf{r}, \mathbf{s}, \mathbf{l}) \mathcal{V}(\mathbf{k}, \mathbf{p}, \mathbf{q}) e^{i \mathcal{E}_{\mathbf{r}, \mathbf{s}, \mathbf{l}} t} e^{i \mathcal{E}_{\mathbf{k}, \mathbf{p}, \mathbf{q}} \tau} [a_{\mathbf{r}+\mathbf{l}}^\dagger a_{\mathbf{s}-\mathbf{l}}^\dagger a_{\mathbf{r}} a_{\mathbf{s}}, [a_{\mathbf{k}+\mathbf{q}}^\dagger a_{\mathbf{p}-\mathbf{q}}^\dagger a_{\mathbf{k}} a_{\mathbf{p}}, \rho_0(\tau) \rho_k(\tau) \rho_b]]
\end{aligned} \tag{A.1}$$

Now taking the trace over phonons:

$$\begin{aligned}
\text{Tr}_b[H(t), [H(\tau), \rho_0(\tau)\rho_k(\tau)\rho_b]] = & \\
& \sum_{\mathbf{r}} \sum_{\mathbf{k}, \mathbf{q}} \mathcal{U}(\mathbf{r}, \mathbf{q}) \mathcal{U}(\mathbf{k}, \mathbf{q})^* e^{\frac{i}{\hbar} \mathcal{E}_{\mathbf{r}, \mathbf{q}} t} e^{-\frac{i}{\hbar} \mathcal{E}_{\mathbf{k}, \mathbf{q}} \tau} [a_{\mathbf{r}}^\dagger a_{\mathbf{r}+\mathbf{q}}, a_{\mathbf{k}+\mathbf{q}}^\dagger a_{\mathbf{k}} \rho_0(\tau) \rho_k(\tau)] \langle b_{\mathbf{q}}^\dagger b_{\mathbf{q}} \rangle \\
& - \sum_{\mathbf{r}} \sum_{\mathbf{k}, \mathbf{q}} \mathcal{U}(\mathbf{r}, \mathbf{q}) \mathcal{U}(\mathbf{k}, \mathbf{q})^* e^{\frac{i}{\hbar} \mathcal{E}_{\mathbf{r}, \mathbf{q}} t} e^{-\frac{i}{\hbar} \mathcal{E}_{\mathbf{k}, \mathbf{q}} \tau} [a_{\mathbf{r}}^\dagger a_{\mathbf{r}+\mathbf{q}}, \rho_0(\tau) \rho_k(\tau) a_{\mathbf{k}+\mathbf{q}}^\dagger a_{\mathbf{k}}] \langle b_{\mathbf{q}} b_{\mathbf{q}}^\dagger \rangle \\
& + \sum_{\mathbf{r}} \sum_{\mathbf{k}, \mathbf{q}} \mathcal{U}(\mathbf{r}, \mathbf{q})^* \mathcal{U}(\mathbf{k}, \mathbf{q}) e^{-\frac{i}{\hbar} \mathcal{E}_{\mathbf{r}, \mathbf{q}} t} e^{\frac{i}{\hbar} \mathcal{E}_{\mathbf{k}, \mathbf{q}} \tau} [a_{\mathbf{r}+\mathbf{q}}^\dagger a_{\mathbf{r}}, a_{\mathbf{k}}^\dagger a_{\mathbf{k}+\mathbf{q}} \rho_0(\tau) \rho_k(\tau)] \langle b_{\mathbf{q}} b_{\mathbf{q}}^\dagger \rangle \\
& - \sum_{\mathbf{r}} \sum_{\mathbf{k}, \mathbf{q}} \mathcal{U}(\mathbf{r}, \mathbf{q})^* \mathcal{U}(\mathbf{k}, \mathbf{q}) e^{-\frac{i}{\hbar} \mathcal{E}_{\mathbf{r}, \mathbf{q}} t} e^{\frac{i}{\hbar} \mathcal{E}_{\mathbf{k}, \mathbf{q}} \tau} [a_{\mathbf{r}+\mathbf{q}}^\dagger a_{\mathbf{r}}, \rho_0(\tau) \rho_k(\tau) a_{\mathbf{k}}^\dagger a_{\mathbf{k}+\mathbf{q}}] \langle b_{\mathbf{q}}^\dagger b_{\mathbf{q}} \rangle \\
& + \frac{1}{4} \sum_{\mathbf{r}, \mathbf{s}, \mathbf{l}, \mathbf{k}, \mathbf{p}, \mathbf{q}} \mathcal{V}(\mathbf{r}, \mathbf{s}, \mathbf{l}) \mathcal{V}(\mathbf{k}, \mathbf{p}, \mathbf{q}) e^{i \mathcal{E}'_{\mathbf{r}, \mathbf{s}, \mathbf{l}} t} e^{i \mathcal{E}'_{\mathbf{k}, \mathbf{p}, \mathbf{q}} \tau} [a_{\mathbf{r}+\mathbf{l}}^\dagger a_{\mathbf{s}-\mathbf{l}}^\dagger a_{\mathbf{r}} a_{\mathbf{s}}, a_{\mathbf{k}+\mathbf{q}}^\dagger a_{\mathbf{p}-\mathbf{q}}^\dagger a_{\mathbf{k}} a_{\mathbf{p}} \rho_0(\tau) \rho_k(\tau)] \\
& - \frac{1}{4} \sum_{\mathbf{r}, \mathbf{s}, \mathbf{l}, \mathbf{k}, \mathbf{p}, \mathbf{q}} \mathcal{V}(\mathbf{r}, \mathbf{s}, \mathbf{l}) \mathcal{V}(\mathbf{k}, \mathbf{p}, \mathbf{q}) e^{i \mathcal{E}'_{\mathbf{r}, \mathbf{s}, \mathbf{l}} t} e^{i \mathcal{E}'_{\mathbf{k}, \mathbf{p}, \mathbf{q}} \tau} [a_{\mathbf{r}+\mathbf{l}}^\dagger a_{\mathbf{s}-\mathbf{l}}^\dagger a_{\mathbf{r}} a_{\mathbf{s}}, \rho_0(\tau) \rho_k(\tau) a_{\mathbf{k}+\mathbf{q}}^\dagger a_{\mathbf{p}-\mathbf{q}}^\dagger a_{\mathbf{k}} a_{\mathbf{p}}]
\end{aligned}$$

The first line of which gives

$$\begin{aligned}
\text{Tr}_a \left\{ \sum_{\mathbf{q}} f(\mathbf{0}, \mathbf{q}, \mathbf{0}) [a_{\mathbf{0}}^\dagger a_{\mathbf{q}}, a_{\mathbf{q}}^\dagger a_{\mathbf{0}} \rho_0(\tau) \rho_k(\tau)] \theta_{\mathbf{q}} \right. \\
& + \sum_{\mathbf{q}} f(\mathbf{0}, \mathbf{q}, -\mathbf{q}) [a_{-\mathbf{q}}^\dagger a_{\mathbf{0}}, a_{\mathbf{q}}^\dagger a_{\mathbf{0}} \rho_0(\tau) \rho_k(\tau)] \theta_{\mathbf{q}} \\
& + \sum_{\mathbf{r}} f(\mathbf{0}, -\mathbf{r}, \mathbf{r}) [a_{\mathbf{r}}^\dagger a_{\mathbf{0}}, a_{-\mathbf{r}}^\dagger a_{\mathbf{0}} \rho_0(\tau) \rho_k(\tau)] \theta_{\mathbf{q}} \\
& + \sum_{\mathbf{k}} f(\mathbf{k}, -\mathbf{k}, \mathbf{0}) [a_{\mathbf{0}}^\dagger a_{-\mathbf{k}}, a_{\mathbf{0}}^\dagger a_{\mathbf{k}} \rho_0(\tau) \rho_k(\tau)] \theta_{\mathbf{q}} \\
& \left. + \sum_{\mathbf{q}} f(-\mathbf{q}, \mathbf{q}, \mathbf{0}) [a_{\mathbf{0}}^\dagger a_{\mathbf{q}}, a_{\mathbf{0}}^\dagger a_{-\mathbf{q}} \rho_0(\tau) \rho_k(\tau)] \theta_{\mathbf{q}} \right\} \\
& = \\
& \sum_{\mathbf{q}} f(\mathbf{0}, \mathbf{q}, \mathbf{0}) [a_{\mathbf{0}}^\dagger, a_{\mathbf{0}} \rho_0(\tau)] (1 + n_{\mathbf{q}}) \theta_{\mathbf{q}} \\
& + \sum_{\mathbf{q}} f(\mathbf{0}, \mathbf{q}, -\mathbf{q}) [a_{\mathbf{0}}, a_{\mathbf{0}} \rho_0(\tau)] F^*(\mathbf{q}) \theta_{\mathbf{q}} \\
& + \sum_{\mathbf{r}} f(\mathbf{0}, -\mathbf{r}, \mathbf{r}) [a_{\mathbf{0}}, a_{\mathbf{0}} \rho_0(\tau)] F^*(\mathbf{r}) \theta_{\mathbf{q}} \\
& + \sum_{\mathbf{k}} f(\mathbf{k}, -\mathbf{k}, \mathbf{0}) [a_{\mathbf{0}}^\dagger, a_{\mathbf{0}}^\dagger \rho_0(\tau)] F(\mathbf{k}) \theta_{\mathbf{q}} \\
& + \sum_{\mathbf{q}} f(-\mathbf{q}, \mathbf{q}, \mathbf{0}) [a_{\mathbf{0}}^\dagger, a_{\mathbf{0}}^\dagger \rho_0(\tau)] F(\mathbf{q}) \theta_{\mathbf{q}} \\
& \equiv \\
& I_0 [a_{\mathbf{0}}^\dagger, a_{\mathbf{0}} \rho_0(\tau)] + I_1 [a_{\mathbf{0}}, a_{\mathbf{0}} \rho_0(\tau)] + I_2 [a_{\mathbf{0}}, a_{\mathbf{0}} \rho_0(\tau)] + I_3 [a_{\mathbf{0}}^\dagger, a_{\mathbf{0}}^\dagger \rho_0(\tau)] + I_4 [a_{\mathbf{0}}^\dagger, a_{\mathbf{0}}^\dagger \rho_0(\tau)]
\end{aligned}$$

While the second line gives

$$\begin{aligned}
& \text{Tr}_a \left\{ \sum_{\mathbf{q}} f(\mathbf{0}, \mathbf{q}, \mathbf{0})^* [a_{\mathbf{0}}^\dagger a_{\mathbf{q}}, \rho_0(\tau) \rho_k(\tau) a_{\mathbf{q}}^\dagger a_{\mathbf{0}}] (1 + \theta_{\mathbf{q}}) \right. \\
& \quad + \sum_{\mathbf{q}} f(\mathbf{0}, \mathbf{q}, -\mathbf{q})^* [a_{-\mathbf{q}}^\dagger a_{\mathbf{0}}, \rho_0(\tau) \rho_k(\tau) a_{\mathbf{q}}^\dagger a_{\mathbf{0}}] (1 + \theta_{\mathbf{q}}) \\
& \quad + \sum_{\mathbf{r}} f(\mathbf{0}, -\mathbf{r}, \mathbf{r})^* [a_{\mathbf{r}}^\dagger a_{\mathbf{0}}, \rho_0(\tau) \rho_k(\tau) a_{-\mathbf{r}}^\dagger a_{\mathbf{0}}] (1 + \theta_{\mathbf{q}}) \\
& \quad + \sum_{\mathbf{k}} f(\mathbf{k}, -\mathbf{k}, \mathbf{0})^* [a_{\mathbf{0}}^\dagger a_{-\mathbf{k}}, \rho_0(\tau) \rho_k(\tau) a_{\mathbf{0}}^\dagger a_{\mathbf{k}}] (1 + \theta_{\mathbf{q}}) \\
& \quad \left. + \sum_{\mathbf{q}} f(-\mathbf{q}, \mathbf{q}, \mathbf{0})^* [a_{\mathbf{0}}^\dagger a_{\mathbf{q}}, \rho_0(\tau) \rho_k(\tau) a_{\mathbf{0}}^\dagger a_{-\mathbf{q}}] (1 + \theta_{\mathbf{q}}) \right\} \\
& \quad = \\
& \quad \sum_{\mathbf{q}} f(\mathbf{0}, \mathbf{q}, \mathbf{0})^* [a_{\mathbf{0}}^\dagger, \rho_0(\tau) a_{\mathbf{0}}] n_{\mathbf{q}} (1 + \theta_{\mathbf{q}}) \\
& \quad + \sum_{\mathbf{q}} f(\mathbf{0}, \mathbf{q}, -\mathbf{q})^* [a_{\mathbf{0}}, \rho_0(\tau) a_{\mathbf{0}}] F^*(\mathbf{q}) (1 + \theta_{\mathbf{q}}) \\
& \quad + \sum_{\mathbf{r}} f(\mathbf{0}, -\mathbf{r}, \mathbf{r})^* [a_{\mathbf{0}}, \rho_0(\tau) a_{\mathbf{0}}] F^*(\mathbf{r}) (1 + \theta_{\mathbf{q}}) \\
& \quad + \sum_{\mathbf{k}} f(\mathbf{k}, -\mathbf{k}, \mathbf{0})^* [a_{\mathbf{0}}^\dagger, \rho_0(\tau) a_{\mathbf{0}}^\dagger] F(\mathbf{k}) (1 + \theta_{\mathbf{q}}) \\
& \quad + \sum_{\mathbf{q}} f(-\mathbf{q}, \mathbf{q}, \mathbf{0})^* [a_{\mathbf{0}}^\dagger, \rho_0(\tau) a_{\mathbf{0}}^\dagger] F(\mathbf{q}) (1 + \theta_{\mathbf{q}}) \\
& \quad \equiv \\
& \quad \hat{I}_0 [a_{\mathbf{0}}^\dagger, \rho_0(\tau) a_{\mathbf{0}}] + \hat{I}_1 [a_{\mathbf{0}}, \rho_0(\tau) a_{\mathbf{0}}] + \hat{I}_2 [a_{\mathbf{0}}, \rho_0(\tau) a_{\mathbf{0}}] + \hat{I}_3 [a_{\mathbf{0}}^\dagger, \rho_0(\tau) a_{\mathbf{0}}^\dagger] + \hat{I}_4 [a_{\mathbf{0}}^\dagger, \rho_0(\tau) a_{\mathbf{0}}^\dagger]
\end{aligned} \tag{A.3}$$

The various variables introduced are F given by (2.51), f by

$$f(\mathbf{k}, \mathbf{q}, \mathbf{r}) \equiv \mathcal{U}(\mathbf{r}, \mathbf{q}) \mathcal{U}(\mathbf{k}, \mathbf{q})^* e^{\frac{i}{\hbar} \mathcal{E}_{\mathbf{r}, \mathbf{q}} t} e^{-\frac{i}{\hbar} \mathcal{E}_{\mathbf{k}, \mathbf{q}} \tau}, \tag{A.4}$$

and, as usual, $\theta_{\mathbf{q}} = \langle b_{\mathbf{q}}^\dagger b_{\mathbf{q}} \rangle$, in terms of which:

$$\begin{aligned}
I_0 &\equiv \sum_{\mathbf{q}} f(\mathbf{0}, \mathbf{q}, \mathbf{0}) (1 + n_{\mathbf{q}}) \theta_{\mathbf{q}}, & \hat{I}_0 &\equiv \sum_{\mathbf{q}} f(\mathbf{0}, \mathbf{q}, \mathbf{0})^* n_{\mathbf{q}} (1 + \theta_{\mathbf{q}}) \\
I_1 &\equiv \sum_{\mathbf{q}} f(\mathbf{0}, \mathbf{q}, -\mathbf{q}) F^*(\mathbf{q}) \theta_{\mathbf{q}}, & \hat{I}_1 &\equiv \sum_{\mathbf{q}} f(\mathbf{0}, \mathbf{q}, -\mathbf{q})^* F^*(\mathbf{q}) (1 + \theta_{\mathbf{q}}) \\
I_2 &\equiv \sum_{\mathbf{q}} f(\mathbf{0}, -\mathbf{q}, \mathbf{q}) F^*(\mathbf{q}) \theta_{\mathbf{q}}, & \hat{I}_2 &\equiv \sum_{\mathbf{q}} f(\mathbf{0}, -\mathbf{q}, \mathbf{q})^* F^*(\mathbf{q}) (1 + \theta_{\mathbf{q}}) \\
I_3 &\equiv \sum_{\mathbf{q}} f(\mathbf{q}, -\mathbf{q}, \mathbf{0}) F(\mathbf{q}) \theta_{\mathbf{q}}, & \hat{I}_3 &\equiv \sum_{\mathbf{q}} f(\mathbf{q}, -\mathbf{q}, \mathbf{0})^* F(\mathbf{q}) (1 + \theta_{\mathbf{q}}) \\
I_4 &\equiv \sum_{\mathbf{q}} f(-\mathbf{q}, \mathbf{q}, \mathbf{0}) F(\mathbf{q}) \theta_{\mathbf{q}}, & \hat{I}_4 &\equiv \sum_{\mathbf{q}} f(-\mathbf{q}, \mathbf{q}, \mathbf{0})^* F(\mathbf{q}) (1 + \theta_{\mathbf{q}})
\end{aligned} \tag{A.5}$$

The combinations of non-vanishing terms has been readily exhausted in the case of phonon-mediated interactions,

k	0	0	k	0	0	k	-q
q	0	q	0	q	-r	-k	q
r	r	0	0	-q	r	0	0

(A.6)

for instance, third entry selects $\mathbf{k} = \mathbf{r} = \mathbf{0}$ and lets \mathbf{q} runs free over all lattice vectors; this is the case which yield “normal correlations” (particle numbers).

Each I defines its time-integrated counterpart \mathcal{I} (times $-1/\hbar^2$) as follows:

$$\mathcal{I}_k \equiv -\frac{1}{\hbar^2} \int_{-\infty}^t I_k(\tau) d\tau \quad (\text{A.7})$$

the time dependencies in (A.5) are in $n_{\mathbf{q}}$ and $F_{\mathbf{q}}$, which arise from Markov approximation. The two last variables needed for the text are:

$$\mathcal{I} = \mathcal{I}_1 + \mathcal{I}_2 - \hat{\mathcal{I}}_3 - \hat{\mathcal{I}}_4 \quad (\text{A.8a})$$

$$\mathcal{I}' = \mathcal{I}_3 + \mathcal{I}_4 - \hat{\mathcal{I}}_1 - \hat{\mathcal{I}}_2. \quad (\text{A.8b})$$

A.2 Brute Force Verification of the Fokker-Planck Equation

We prove that (2.44) is solution to eq. (2.43):

$$\partial_t P = \frac{1}{2}(W_{\text{out}} - W_{\text{in}})(\partial_{\alpha}\alpha + \partial_{\alpha^*}\alpha^*)P + W_{\text{in}}\partial_{\alpha,\alpha^*}^2 P \quad (\text{2.43})$$

The solution is well known when $W_{\text{out}}, W_{\text{in}}$ are time independent (see for instance Mandel & Wolf (1995)):

$$P = \frac{1}{\pi m(t)} e^{-\frac{|\alpha - G(t)\alpha_0|^2}{m(t)}} \quad (\text{2.44})$$

with

$$G(t) = e^{\frac{1}{2}(W_{\text{in}} - W_{\text{out}})t}, \quad m(t) = \frac{W_{\text{in}}}{W_{\text{in}} - W_{\text{out}}} (e^{(W_{\text{in}} - W_{\text{out}})t} + 1). \quad (\text{A.9})$$

In our case, $W_{\text{in}}, W_{\text{out}}$ are time dependent scattering rates computed by solving numerically Boltzmann equations. The solution in this case remains (2.44), but (A.9) should now be replaced with

$$G(t) \equiv \exp\left[\frac{1}{2} \int_0^t (W_{\text{in}}(\tau) - W_{\text{out}}(\tau)) d\tau\right], \quad m(t) \equiv G(t)^2 \int_0^t \frac{W_{\text{in}}(\tau)}{G(\tau)^2} d\tau. \quad (\text{2.42})$$

This can be deduced from the operator solution (2.41), or checking the result by explicitly carrying out the algebra as follows. Since $\partial_{\alpha}\alpha P = P + \alpha\partial_{\alpha}P$ (likewise for α^*) we compute directly:

$$\begin{aligned} \partial_{\alpha}P &= -P \frac{\alpha^* - G\alpha_0^*}{m} \\ \partial_{\alpha^*}P &= -P \frac{\alpha - G\alpha_0}{m} \\ \partial_{\alpha,\alpha^*}^2 P &= P \frac{|\alpha - G\alpha_0|^2 - m}{m^2} \end{aligned} \quad (\text{A.10})$$

so that rhs of (2.43) evaluates to:

$$\left[\frac{W_{\text{out}} - W_{\text{in}}}{2} \left(2 - \frac{2|\alpha|^2 - G\alpha\alpha_0^* - G\alpha^*\alpha_0}{m} \right) + W_{\text{in}} \frac{|\alpha - G\alpha_0|^2 - m}{m^2} \right] P \quad (\text{A.11})$$

as for $\partial_t P$, we will need the following:

$$\begin{aligned} \partial_t G &= \frac{1}{2} G (W_{\text{in}} - W_{\text{out}}) \\ \partial_t m &= (W_{\text{in}} - W_{\text{out}})m + W_{\text{in}} \end{aligned} \quad (\text{A.12})$$

the latter coming from $\partial_t m = 2G(\partial_t G) \int_0^t \frac{W_{\text{in}}(\tau)}{G(\tau)^2} d\tau + W_{\text{in}}$ from direct derivation, then $\partial_t m = G^2(W_{\text{in}} - W_{\text{out}}) \int_0^t \frac{W_{\text{in}}(\tau)}{G(\tau)^2} d\tau + W_{\text{in}}$ substituting for $\partial_t G$ leading to the result, remembering the expression for G .

Time derivation is the most challenging. We find by direct computation and substitution:

$$\begin{aligned} \partial_t P &= -\frac{\partial_t m}{m} P - \frac{(-\partial_t G\alpha^*\alpha_0 - \partial_t G\alpha\alpha_0^* + 2G\partial_t G|\alpha_0|^2)m - |\alpha - G\alpha_0|^2 \partial_t m}{m^2} P \\ &= \frac{1}{m^2} \left[-(W_{\text{in}} - W_{\text{out}})m^2 - W_{\text{in}}m + \frac{1}{2}G(W_{\text{in}} - W_{\text{out}})\alpha^*\alpha_0m + \right. \\ &\quad \left. + \frac{1}{2}G(W_{\text{in}} - W_{\text{out}})\alpha\alpha_0^*m - G^2(W_{\text{in}} - W_{\text{out}})|\alpha_0|^2m + |\alpha - G\alpha_0|^2((W_{\text{in}} - W_{\text{out}})m + W_{\text{in}}) \right] P \\ &= \frac{(W_{\text{in}} - W_{\text{out}})(-m^2 + \frac{1}{2}G\alpha^*\alpha_0m + \frac{1}{2}G\alpha\alpha_0^*m - G^2|\alpha_0|^2m + |\alpha - G\alpha_0|^2m) + W_{\text{in}}(-m + |\alpha - G\alpha_0|^2)}{m^2} P \end{aligned}$$

which simplifies readily to (A.11), achieving the proof that time dependency of (2.42) is the one needed for (2.44) to be the solution of (2.43).

A.3 Derivation of the Analytical Expression for the Pseudospin

We detail the derivation of eq. (3.44) needed for the computation of $\langle S(t) \rangle$:

$$\begin{aligned} \langle n, \theta, \phi | e^{-iVt/\hbar} \exp\left(\frac{iVt}{\hbar}(a_{\downarrow}^{\dagger}a_{\downarrow} - a_{\uparrow}^{\dagger}a_{\uparrow})\right) S(0) | n', \theta, \phi \rangle &= \frac{e^{-iVt/\hbar}}{n!} \left[\langle 0, 0 | \sum_{\mu=0}^n \binom{n}{\mu} \alpha^{\mu} \beta^{*(n-\mu)} a_{\uparrow}^{\mu} a_{\downarrow}^{n-\mu} \right] \\ &\quad \exp\left(\frac{iVt}{\hbar}(a_{\downarrow}^{\dagger}a_{\downarrow} - a_{\uparrow}^{\dagger}a_{\uparrow})\right) a_{\uparrow} a_{\downarrow}^{\dagger} \left[\sum_{\nu=0}^{n'} \binom{n'}{\nu} \alpha^{\nu} \beta^{n'-\nu} a_{\uparrow}^{\nu} a_{\downarrow}^{\dagger n'-\nu} | 0, 0 \rangle \right] \end{aligned} \quad (\text{A.13})$$

where we introduced $\alpha \equiv \cos \theta$ and $\beta \equiv e^{i\phi} \sin \theta$ as shortcuts and reverted to explicit expression (3.42) for $|n, \theta, \phi\rangle$. Thus, in the spin-up/down polaritons basis:

$$\begin{aligned} &= \frac{e^{-iVt/\hbar}}{n!} \left[\sum_{\mu=0}^n \binom{n}{\mu} \alpha^{\mu} \beta^{*(n-\mu)} \sqrt{\mu!(n-\mu)!} \langle n - \mu, \mu | \right] \\ &\quad \exp\left(\frac{iVt}{\hbar}(a_{\downarrow}^{\dagger}a_{\downarrow} - a_{\uparrow}^{\dagger}a_{\uparrow})\right) a_{\uparrow} a_{\downarrow}^{\dagger} \left[\sum_{\nu=0}^{n'} \binom{n'}{\nu} \alpha^{\nu} \beta^{n'-\nu} \sqrt{\nu!(n'-\nu)!} | \nu, n' - \nu \rangle \right] \end{aligned} \quad (\text{A.14})$$

We can now evaluate the operator, say, on the right expression:

$$\begin{aligned}
&= \frac{e^{-iVt/\hbar}}{n!} \left[\sum_{\mu=0}^n \binom{n}{\mu} \alpha^\mu \beta^{*(n-\mu)} \sqrt{\mu!(n-\mu)!} \langle n-\mu, \mu | \right] \\
&\left[\sum_{\nu=0}^{n'} \binom{n'}{\nu} \alpha^\nu \beta^{n'-\nu} \exp\left(\frac{iVt}{\hbar}(n'-2\nu+2)\right) \sqrt{\nu!(n'-\nu)!} \sqrt{\nu(n'-\nu+1)} | \nu-1, n'-\nu+1 \rangle \right]
\end{aligned} \tag{A.15}$$

Since $\langle n-\mu, \mu | \nu-1, n'-\nu+1 \rangle = \delta_{\mu, \nu-1} \delta_{n, n'}$, summing over ν yields

$$= \frac{e^{-iVt/\hbar}}{n!} \frac{\alpha}{\beta} \sum_{\mu=0}^{n-1} \binom{n}{\mu} \binom{n}{\mu+1} \alpha^{2\mu} |\beta|^{2(n-\mu)} (\mu+1)! (n-\mu)! e^{iVt(n-2\mu)/\hbar} \tag{A.16}$$

$$= e^{iVt(n-1)/\hbar} \frac{\alpha}{\beta} \sum_{\mu=0}^{n-1} \frac{n!}{\mu!(n-\mu-1)!} \alpha^{2\mu} |\beta|^{2(n-\mu)} e^{-2iVt\mu/\hbar} \tag{A.17}$$

the sum can be computed exactly by the usual method of integration and derivation with respect to β to recover the coefficients in the binomial expansion. This way we evaluate the sum to $\beta^2(e^{-2iVt/\hbar}\alpha^2 + |\beta|^2)^{n-1}n$, so that with the prefactor, the expression simplifies to:

$$n \cos \theta \sin \theta e^{i\phi} (e^{-iVt/\hbar} \cos^2 \theta + e^{iVt/\hbar} \sin^2 \theta)^{n-1} \tag{A.18}$$

which is the expression of the text, eq. (3.46).

Publications

1. A. Kavokin, G. Malpuech and **F. P. Laussy**, *Polariton laser and polariton superfluidity in microcavities*, Phys. Lett. A, **306** 187, January 2003.
2. G. Malpuech, A. Kavokin and **F. P. Laussy**, *Polariton bose condensation in microcavities*, Phys. Stat. Sol. A, **195** 568, February 2003.
3. I. A. Shelykh, A. V. Kavokin, G. Malpuech, P. Bigenwald and **F. Laussy**, *Polarization beats in emission from polariton lasers*, Phys. Rev. B, **68** 085311, August 2003.
4. **F. P. Laussy**, Y. G. Rubo, G. Malpuech, A. Kavokin and P. Bigenwald, *Dissipative quantum theory of polariton lasers*, Phys. Stat. Sol. C, **0** 1476, August 2003.
5. G. Malpuech, Y. G. Rubo, **F. P. Laussy**, P. Bigenwald and A. V. Kavokin. *Polariton laser: thermodynamics and quantum kinetic theory*. Semicond. Sci. Technol., **18** S395, October 2003.
6. Y. G. Rubo, **F. P. Laussy**, G. Malpuech, A. Kavokin, and P. Bigenwald, *Dynamical theory of polariton amplifiers*. Phys. Rev. Lett., **91** 156403, October 2003.
7. **F. P. Laussy**, G. Malpuech and A. Kavokin, *Spontaneous coherence buildup in a polariton laser*, Phys. Stat. Sol. C, **1** 1339, February 2004.
8. **F. P. Laussy**, G. Malpuech, A. V. Kavokin and P. Bigenwald, *Coherence dynamics in microcavities and polariton lasers*, J. Phys.: Condens. Matter, **16** S3665, August 2004.
9. **F. P. Laussy**, G. Malpuech, A. Kavokin and P. Bigenwald, *Spontaneous coherence buildup in a polariton laser*. Phys. Rev. Lett., **93** 016402, June 2004.
10. **F. P. Laussy**, G. Malpuech, A. Kavokin and P. Bigenwald, *Spontaneous coherence buildup in polariton lasers*. Solid State Commun., **134** 121, April 2005

Bibliography

- Agranovich, V. (1959). Dispersion of electromagnetic waves in crystals, *Zh. Eksp. Teoret. Fiz. [JETP]* **37**: 430.
- Agranovich, V. & Ginsburg, V. L. (1966). *Spatial Dispersion in Crystal Optics and the Theory of Excitons*, Interscience Publ., London.
- Alexandrou, A., Bianchi, G., Péronned, E., Hallé, B., Boeuf, F., André, R., Romestain, R. & Le Si Dang, D. (2001). Stimulated scattering and its dynamics in semiconductor microcavities at 80 K under nonresonant excitation conditions, *Phys. Rev. B* **64**: 233318.
- Alferov, Z. (2000). Double heterostructure concept and its applications in physics, electronics and technology, Nobel lecture.
- Anderson, M., Ensher, J., Matthews, M., Wieman, C. & Cornell, E. (1995). Observation of Bose-Einstein condensation in a dilute atomic vapor, *Science* **269**: 198.
- Antoine-Vincent, N., Natali, F., Byrne, D., Vasson, A., Disseix, P., Leymarie, J., Leroux, M., Semond, F. & Massies, J. (2003). Observation of Rabi splitting in a bulk GaN microcavity grown on silicon, *Phys. Rev. B* **68**: 153313.
- Banyai, L. & Gartner, P. (2002). Real-time Bose-Einstein condensation in a finite volume with a discrete spectrum, *Phys. Rev. Lett.* **88**: 210404.
- Binder, R. & Koch, S. W. (1995). Nonequilibrium semiconductor dynamics, *Prog. in Quantum Electron.* **19**: 307.
- Boeuf, F., André, R., Romestain, R. & Le Si Dang, D. (2000). Evidence of polariton stimulation in semiconductor microcavities, *Phys. Rev. B* **62**: R2279.
- Cao, H., Pau, S., Jacobson, J. M., Björk, G., Yamamoto, Y. & Īmamoġlu, A. (1997). Transition from a microcavity exciton polariton to a photon laser, *Phys. Rev. A* **55**: 4632.
- Cao, H., Pau, S., Yamamoto, Y. & Björk, G. (1996). Exciton-polariton ladder in a semiconductor microcavity, *Phys. Rev. B* **54**: 8083.
- Cao, H. T., Doan, T. D., Thoai, D. B. T. & Haug, H. (2004). Condensation kinetics of cavity polaritons interacting with a thermal phonon bath, *Phys. Rev. B* **69**: 245325.
- Ciuti, C. (2004). Branch-entangled polariton pairs in planar microcavities and photonic wires, *Phys. Rev. B* **69**: 245304.

- Ciuti, C., Savona, V., Piermarocchi, C., Quattropani, A. & Schwendimann, P. (1998). Role of the exchange of carriers in elastic exciton-exciton scattering in quantum wells, *Phys. Rev. B* **58**: 7926.
- Ciuti, C., Schwendimann, P. & Quattropani, A. (2001). Parametric luminescence of microcavity polaritons, *Phys. Rev. B* **63**: 041303.
- Cohen-Tannoudji, C., Dupont-Roc, J. & Grynberg, G. (2001). *Photons et atomes*, EDP Sciences.
- Combescot, M. & Betbeder-Matibet, O. (2002). Effective bosonic hamiltonian for excitons: A too naive concept, *Europhys. Lett.* **59**: 579.
- Cornell, E. A. & Wieman, C. E. (2001). Bose–Einstein condensation in a dilute gas; the first 70 years and some recent experiments, Nobel lecture.
- D’Andrea, A. & Sole, R. D. (1990). Excitons in semiconductor confined systems, *Solid State Commun.* **74**: 1121.
- Davis, K. B., Mewes, M.-O., Andrews, M. R., van Druten, N. J., Durfee, D. S., Kurn, D. M. & Ketterle, W. (1995). Bose-Einstein condensation in a gas of sodium atoms, *Phys. Rev. Lett.* **75**: 3969.
- Deng, H., Weihs, G., Santori, C., Bloch, J. & Yamamoto, Y. (2002). Condensation of semiconductor microcavity exciton polaritons, *Science* **298**: 199.
- Dicke, R. H. (1954). Coherence in spontaneous radiation processes, *Phys. Rev.* **93**: 99.
- Dirac, P. A. M. (1927). The quantum theory of the emission and absorption of radiation, *Proc. Roy. Soc. London A* **114**: 243.
- Dirac, P. A. M. (1967). *The Principles of Quantum Mechanics*, 4th (rev.) edn, Oxford Science Publications.
- Efros, A. L., Rosen, M., Kuno, M., Nirmal, M., Norris, D. J. & Bawendi, M. (1996). Band-edge exciton in quantum dots of semiconductors with a degenerate valence band: Dark and bright exciton states, *Phys. Rev. B* **54**: 4843.
- Einstein, A. (1925). Quantentheorie des einatomigen idealen Gases. Zweite Abhandlung, *Sitzungber. Preuss. Akad. Wiss.* **1925**: 3.
- Fano, U. (1956). Atomic theory of electromagnetic interactions in dense materials, *Phys. Rev.* **103**: 1202.
- Fermi, E. (1932). Quantum theory of radiation, *Rev. Mod. Phys.* **4**: 87.
- Fernández-Rossier, J. & Tejedor, C. (1997). Spin degree of freedom in two dimensional exciton condensates, *Phys. Rev. B* **78**: 4809.
- Gardiner, C. W. & Zoller, P. (1997). Quantum kinetic theory: A quantum kinetic master equation for condensation of a weakly interacting Bose gas without a trapping potential, *Phys. Rev. A* **55**: 2902.

- Glauber, R. J. (1962). Photon correlations, *Phys. Rev. Lett.* **10**: 84.
- Glauber, R. J. (1963). The quantum theory of optical coherence, *Phys. Rev. Lett.* **130**: 2529.
- Glazov, M., Shelykh, I., Malpuech, G., Kavokin, K., Kavokin, A. & Solnyshkov, D. (2005). Anisotropic polariton scattering and spin dynamics of cavity polaritons, *Solid State Commun.* **134**: 117.
- Griffin, A., Snoke, D. W. & Stringari, S. (eds) (1996). *Bose–Einstein Condensation*, Cambridge University Press.
- Hanbury Brown, R. & Twiss, R. (1957). Interferometry of the intensity fluctuations in light. I. Basic theory of the correlation between photons in coherent beams of radiation, *Proc. Roy. Soc A* **242**: 300.
- Haug, H. & Koch, S. W. (1990). *Quantum Theory of the Optical and Electronic Properties of Semiconductors*, World Scientific.
- Hawrylak, P. (1999). Excitonic artificial atoms: Engineering optical properties of quantum dots, *Phys. Rev. B* **60**: 5597.
- Holland, M., Burnett, K., Gardiner, C., Cirac, J. I. & Zoller, P. (1996). Theory of an atom laser, *Phys. Rev. A* **54**: R1757.
- Hopfield, J. J. (1958). Theory of the contribution of excitons to the complex dielectric constant of crystals, *Phys. Rev.* **112**: 1555.
- Houdré, R., Stanley, R. P., Oesterle, U., Ilegems, M. & Weisbuch, C. (1994). Room-temperature cavity polaritons in a semiconductor microcavity, *Phys. Rev. B* **49**: 16761.
- Houdré, R., Weisbuch, C., Stanley, R. P., Oesterle, U., Pellandin, P. & Ilegems, M. (1994). Measurement of cavity-polariton dispersion curve from angle-resolved photoluminescence experiments, *Phys. Rev. Lett.* **73**: 2043.
- Hu, Y. Z., Koch, S. W., Lindberg, M., Peyghambarian, N., Pollock, E. L. & Abraham, F. F. (1990). Biexcitons in semiconductor quantum dots, *Phys. Rev. Lett.* **64**: 1805.
- Huang, R., Tassone, F. & Yamamoto, Y. (1999). Stimulated scattering of excitons into microcavity polaritons, *Microelectron. Eng.* **1947**: 325.
- Huang, R., Tassone, F. & Yamamoto, Y. (2000). Experimental evidence of stimulated scattering of excitons into microcavity polaritons, *Phys. Rev. B* **61**: R7854.
- Ilinskaia, A. V. & Ilinski, K. N. (1996). Generalization of the agranovich-toshich transformation and a constraint free bosonic representation for systems of truncated oscillators, *J. Phys. A: Math. Gen.* **29**: L23.
- İmamoğlu, A. (2002). Cavity-QED using quantum dots, *Optics & Photonics News* p. 25.
- İmamoğlu, A. & Ram, R. J. (1996). Quantum dynamics of exciton lasers, *Physics Letter A* **214**: 193.

- İmamoğlu, A., Ram, R. J., Pau, S. & Yamamoto, Y. (1996). Nonequilibrium condensates and lasers without inversion: Exciton-polariton lasers, *Phys. Rev. A* **53**: 4250.
- Jackson, J. D. (1975). *Classical Electrodynamics*, 2nd edn, Wiley.
- Jacobson, J., Pau, S., Cao, H., Björk, G. & Yamamoto, Y. (1995). Observation of exciton-polariton oscillating emission in a single-quantum-well semiconductor microcavity, *Phys. Rev. A* **51**: 2542.
- Jaksch, D., Gardiner, C. W. & Zoller, P. (1997). Quantum kinetic theory. II. Simulation of the quantum boltzmann master equation, *Phys. Rev. A* **56**: 575.
- Jaynes, E. & Cummings, F. (1963). -, *Proc IEEE* **51**: 89.
- Karr, J. P., Baas, A., Houdré, R. & Giacobino, E. (2004). Squeezing in semiconductor microcavities in the strong-coupling regime, *Phys. Rev. A* **69**: R031802.
- Kavokin, A., Lagoudakis, P. G., Malpuech, G. & Baumberg, J. J. (2003). Polarization rotation in parametric scattering of polaritons in semiconductor microcavities, *Phys. Rev. B* **67**: 195321.
- Kavokin, A. & Malpuech, G. (2003). *Cavity Polaritons*, Vol. 32 of *Thin Films and Nanostructures*, Elsevier.
- Kavokin, K., Renucci, P., Amand, T., Marie, X., Senellart, P., Bloch, J. & Sermage, B. (2005). Linear polarisation inversion: A signature of coulomb scattering of cavity polaritons with opposite spins, *Phys. Stat. Sol. C* **2**: 763.
- Kavokin, K. V., Shelykh, I. A., Kavokin, A. V., Malpuech, G. & Bigenwald, P. (2004). Quantum theory of spin dynamics of exciton-polaritons in microcavities, *Phys. Rev. Lett.* **92**: 017401.
- Keeling, J., Eastham, P. R., Szymanska, M. H. & Littlewood, P. B. (2004). Polariton condensation with localized excitons and propagating photons, *Phys. Rev. Lett.* **93**: 226403.
- Ketterle, W. (2001). When atoms behave as waves: Bose-Einstein condensation and the atom laser, Nobel lecture.
- Khitrova, G., Gibbs, H. M., Jahnke, F., Kira, M. & Koch, S. W. (1999). Nonlinear optics of normal-mode-coupling semiconductor microcavities, *Rev. Mod. Phys* **71**: 1591.
- Kira, M., Jahnke, F., Koch, S. W., Berger, J., Wick, D., Nelson Jr., T. R., Khitrova, G. & Gibbs, H. M. (1997). Quantum theory of nonlinear semiconductor microcavity luminescence explaining “Boser” experiments, *Phys. Rev. Lett.* **79**: 5170.
- Kittel, C. (1996). *Introduction to Solid State Physics*, 11th edn, Wiley.
- Laussy, F. P., Malpuech, G. & Kavokin, A. (2004). Spontaneous coherence buildup in a polariton laser, *Phys. Stat. Sol. C* **1**: 1339.
- Laussy, F. P., Malpuech, G., Kavokin, A. & Bigenwald, P. (2004a). Spontaneous coherence buildup in a polariton laser, *Phys. Rev. Lett.* **93**: 016402.

- Laussy, F. P., Malpuech, G., Kavokin, A. & Bigenwald, P. (2005). Spontaneous coherence buildup in polariton lasers, *Solid State Commun.* **134**: 121.
- Laussy, F. P., Malpuech, G., Kavokin, A. V. & Bigenwald, P. (2004b). Coherence dynamics in microcavities and polariton lasers, *J. Phys.: Condens. Matter* **16**: S3665.
- Laussy, F. P., Rubo, Y. G., Malpuech, G., Kavokin, A. & Bigenwald, P. (2003). Dissipative quantum theory of polariton lasers, *Phys. Stat. Sol. C* **0**: 1476.
- Le Si Dang, D., Heger, D., André, R., Boeuf, F. & Romestain, R. (1998). Stimulation of polariton photoluminescence in semiconductor microcavity, *Phys. Rev. Lett.* **81**: 3920.
- Loudon, R. (2000). *The Quantum Theory of Light*, 3rd edn, Oxford Science Publications.
- Malpuech, G., Di Carlo, A., Kavokin, A., Baumberg, J. J., Zamfirescu, M. & Lugli, P. (2002). Room-temperature polariton lasers based on gan microcavities, *Appl. Phys. Lett.* **81**: 412.
- Malpuech, G., Kavokin, A., Di Carlo, A. & Baumberg, J. J. (2002). Polariton lasing by exciton-electron scattering in semiconductor microcavities, *Phys. Rev. B* **65**: 153310.
- Mandel, L. & Wolf, E. (1995). *Optical coherence and quantum optics*, Cambridge University Press.
- Martin, M. D., Aichmayr, G., Viña, L. & André, R. (2002). Polarization control of the nonlinear emission of semiconductor microcavities, *Phys. Rev. Lett.* **89**: 077402.
- Maxwell, J. C. (1865). A dynamical theory of the electromagnetic field, *Philosophical Transactions of the Royal Society of London* **155**: 459.
- Merzbacher, E. (1998). *Quantum Mechanics*, 3rd edn, John Wiley & sons, Inc.
- Messin, G., Karr, J. P., Baas, A., Khitrova, G., Houdré, R., Stanley, R. P., Oesterle, U. & Giacobino, E. (2001). Parametric polariton amplification in semiconductor microcavities, *Phys. Rev. Lett.* **87**: 127403.
- Millikan, R. A. (1924). The electron and the light-quant from the experimental point of view, Nobel Lecture.
- Mollow, B. R. (1969). Power spectrum of light scattered by two-level systems, *Phys. Rev.* **188**: 1969.
- Moskalenko, S. & Snoke, D. (2000). *Bose-Einstein Condensation of Excitons and Biexcitons*, Cambridge University Press.
- Müller, M., Bleuse, J. & André, R. (2000). Dynamics of the cavity polariton in cdte-based semiconductor microcavities: Evidence for a relaxation edge, *Phys. Rev. B* **62**: 16886.
- Norris, T., Rhee, J.-K., Sung, C.-Y., Arakawa, Y., Nishioka, M. & Weisbuch, C. (1994). Time-resolved vacuum Rabi oscillations in a semiconductor quantum microcavity, *Phys. Rev. B* **50**: 14663.

- Pau, S., Cao, H., Jacobson, J., Björk, G., Yamamoto, Y. & Īmamođlu, A. (1996). Observation of a laserlike transition in a microcavity exciton polariton system, *Phys. Rev. A* **54**: R1789.
- Peter, E., Senellart, P., Martrou, D., Lemaître, A., Hours, J., Gérard, J. M. & Bloch, J. (2005). Exciton-photon strong-coupling regime for a single quantum dot embedded in a microcavity, *Phys. Rev. Lett.* **95**: 067401.
- Piermarocchi, C., Tassone, F., Savona, V., Quattropani, A. & Schwendimann, P. (1997). Exciton formation rates in GaAs/Al_xGa_{1-x}As quantum wells, *Phys. Rev. B* **55**: 1333.
- Pitaevskii, L. & Stringari, S. (2003). *Bose-Einstein Condensation*, Oxford University Press.
- Porras, D., Ciuti, C., Baumberg, J. J. & Tejedor, C. (2002). Polariton dynamics and Bose-Einstein condensation in semiconductor microcavities, *Phys. Rev. B* **66**: 085304.
- Purcell, E. M. (1946). Spontaneous emission probabilities at radio frequencies, *Phys. Rev.* **69**: 681.
- Purcell, E. M., Torrey, H. C. & Pound, R. V. (1946). Resonance absorption by nuclear magnetic moments in a solid, *Phys. Rev.* **69**: 37.
- Que, W. (1992). Excitons in quantum dots with parabolic confinement, *Phys. Rev. B* **45**: 11036.
- Raizen, M. G., Thompson, R. J., Brecha, R. J., Kimble, H. J. & Carmichael, H. J. (1989). Normal-mode splitting and linewidth averaging for two-state atoms in an optical cavity, *Phys. Rev. Lett.* **63**: 240.
- Reithmaier, J. P., Sek, G., Löffler, A., Hofmann, C., Kuhn, S., Reitzenstein, S., Keldysh, L. V., Kulakovskii, V. D., Reinecker, T. L. & Forchel, A. (2004). Strong coupling in a single quantum dot–semiconductor microcavity system, *Nature* **432**: 197.
- Rubo, Y. G., Laussy, F. P., Malpuech, G., Kavokin, A. & Bigenwald, P. (2003). Dynamical theory of polariton amplifiers, *Phys. Rev. Lett.* **91**: 156403.
- Sanchez-Mondragon, J. J., Narozhny, N. B. & Eberly, J. H. (1983). Theory of spontaneous-emission line shape in an ideal cavity, *Phys. Rev. Lett.* **51**: 550.
- Sarchi, D. & Savona, V. (2004). Dynamical condensation of polaritons.
- Savasta, S., Stefano, O. D. & Girlanda, R. (2003). Many-body and correlation effects on parametric polariton amplification in semiconductor microcavities, *Phys. Rev. Lett.* **90**: 096403.
- Savona, V., Piermarocchi, C., Quattropani, A., Schwendimann, P. & Tassone, F. (1998). Optical properties of microcavity polaritons, *Phase Transitions* **68**: 169.
- Savvidis, P. G., Baumberg, J. J., Porras, D., Whittaker, D. M., Skolnick, M. S. & Roberts, J. S. (2002). Ring emission and exciton-pair scattering in semiconductor microcavities, *Phys. Rev. B* **65**: 073309.
- Savvidis, P. G., Baumberg, J. J., Stevenson, R. M., Skolnick, M. S., Whittaker, D. M. & Roberts, J. S. (2000). Angle-resonant stimulated polariton amplifier, *Phys. Rev. Lett.* **84**: 1547.

- Schrödinger, E. (1926). Quantisation as a problem of characteristic values, *Ann. d. Phys.* **79**: 361.
- Senellart, P. & Bloch, J. (1999). Nonlinear emission of microcavity polaritons in the low density regime, *Phys. Rev. Lett.* **82**: 1233.
- Senellart, P., Bloch, J., Sermage, B. & Marzin, J. Y. (2000). Microcavity polariton depopulation as evidence for stimulated scattering, *Phys. Rev. B* **62**: R16263.
- Sermage, B., Long, S., Abram, I., Marzin, J. Y., Bloch, J., Planel, R. & Thierry-Mieg, V. (1996). Time-resolved spontaneous emission of excitons in a microcavity: Behavior of the individual exciton-photon mixed states, *Phys. Rev. B* **53**: 16516.
- Shelykh, I., Kavokin, K. V., Kavokin, A. V., Malpuech, G., Bigenwald, P., Deng, H., Weihs, G. & Yamamoto, Y. (2004). Semiconductor microcavity as a spin-dependent optoelectronic device, *Phys. Rev. B* **70**: 035320.
- Shelykh, I., Malpuech, G., Kavokin, K. V., Kavokin, A. V. & Bigenwald, P. (2004). Spin dynamics of interacting exciton polaritons in microcavities, *Phys. Rev. B* **70**: 115301.
- Skolnick, M. S., Fisher, T. A. & Whittaker, D. M. (1998). Strong coupling phenomena in quantum microcavity structures, *Semicond. Sci. Technol.* **13**: 645.
- Stanley, R. P., Houdré, R., Weisbuch, C., Oesterle, U. & Ilegems, M. (1996). Cavity-polariton photoluminescence in semiconductor microcavities: Experimental evidence, *Phys. Rev. B* **53**: 10995.
- Stenius, P. (1999). Quantum theory of an exciton condensate subject to radiative decay, *Phys. Rev. B* **60**: 14072.
- Stenius, P. & Ivanov, A. L. (1998). Relaxation kinetics of quasi two-dimensional excitons coupled to a bath of bulk acoustic phonons, *Solid State Commun.* **108**: 117.
- Tartakovskii, A. I., Emam-Ismaïl, M., Stevenson, R. M., Skolnick, M. S., Astratov, V. N., Whittaker, D. M., Baumberg, J. J. & Roberts, J. S. (2000). Relaxation bottleneck and its suppression in semiconductor microcavities, *Phys. Rev. B* **62**: R2283.
- Tassone, F., Piermarocchi, C., Savona, V., Quattropani, A. & Schwendimann, P. (1997). Bottleneck effects in the relaxation and photoluminescence of microcavity polaritons, *Phys. Rev. B* **56**: 7554.
- Tassone, F. & Yamamoto, Y. (1999). Exciton-exciton scattering dynamics in a semiconductor microcavity and stimulated scattering into polaritons, *Phys. Rev. B* **59**: 10830.
- Tassone, F. & Yamamoto, Y. (2000). Lasing and squeezing of composite bosons in a semiconductor microcavity, *Phys. Rev. A* **62**: 063809.
- Tawara, T., Gotoh, H., Akasaka, T., Kobayashi, N. & Saitoh, T. (2004). Cavity polaritons in InGaN microcavities at room temperature, *Phys. Rev. Lett.* **92**.

- Weisbuch, C., Nishioka, M., Ishikawa, A. & Arakawa, Y. (1992). Observation of the coupled exciton-photon mode splitting in a semiconductor quantum microcavity, *Phys. Rev. Lett.* **69**: 3314.
- Wiseman, H. M. & Collett, M. J. (1995). An atom laser based on dark-state cooling, *Phys. Lett. A* **202**: 246.
- Yamamoto, Y. & Īmamoġlu, A. (1999). *Mesoscopic Quantum Optics*, John Wiley & Sons, inc.
- Yamamoto, Y., Machida, S. & Bjork, B. (1992). -, *Optical and Quant. Elec.* **24**: S209.
- Yamamoto, Y., Tassone, F. & Cao, H. (2000). *Semiconductor Cavity Quantum Electrodynamics*, Springer.
- Yoshie, T., Scherer, A., Heindrickson, J., Khitrova, G., Gibbs, H. M., Rupper, G., Ell, C., Shchekin, O. B. & Deppe, D. G. (2004). Vacuum Rabi splitting with a single quantum dot in a photonic crystal nanocavity, *Nature* **432**: 200.
- Zamfirescu, M., Kavokin, A., Gil, B., Malpuech, G. & Kaliteevski, M. (2002). ZnO as a material mostly adapted for the realization of room-temperature polariton lasers, *Phys. Rev. B* **65**: R161205.
- Zhu, Y., Gauthier, D. J., Morin, S. E., Wu, Q., Carmichael, H. J. & Mossberg, T. W. (1990). Vacuum Rabi splitting as a feature of linear-dispersion theory: Analysis and experimental observations, *Phys. Rev. Lett.* **64**: 2499.

Abstract

The field of microcavity polaritons studies the strong-coupling of light with matter in heterostructures of semiconductors. Polaritons appear to be good bosons but with a short lifetime, so that an out-of-equilibrium description is required. Possibility of their Bose condensation has been sought essentially through Boltzmann equations. In this work, these equations are extended and solved analytically on a simple model and numerically for realistic cases, first with a ground state density matrix then with a quantum Boltzmann master equation. Spontaneous buildup of coherence is obtained. Polarisation of the system is studied in connection with condensation and a link is established between phase and linear polarisation, making polarisation an order parameter for condensation of particles with finite lifetime and spin degeneracy. Finally, strong coupling in quantum dots is compared with the atomic case.

Keywords

Microcavity Exciton-Polariton (Polariton), Bose-Einstein Condensation (BEC), Order Parameter, Coherence, Dynamics of Quantum Systems.

Résumé

La physique des polaritons de microcavité étudie le couplage fort lumière/matière dans les hétérostructures de semiconducteurs. Les polaritons apparaissent comme de “bons” bosons mais avec un temps de vie court nécessitant une étude hors-équilibre. La possibilité de leur condensation de Bose a été recherchée essentiellement via les équations de Boltzmann. Dans ce travail, ces équations sont étendues et résolues analytiquement sur un modèle simplifié et numériquement pour des structures réalistes, par le biais de la matrice densité de l'état fondamental puis avec une équation de Boltzmann pilote. La formation spontanée de la cohérence est obtenue. La polarisation du système est étudiée en rapport avec la condensation et un lien est établi entre phase et polarisation linéaire, faisant de la polarisation un paramètre d'ordre pour la condensation de particule de temps de vie fini avec dégénérescence de spin. Finalement, le couplage fort dans les puits quantiques est comparé au cas atomique.

Mots clefs

Exciton-Polariton de Microcavité (Polariton), Condensation de Bose-Einstein, Paramètre d'ordre, Cohérence, Dynamique des Systèmes Quantiques.